



**HAL**  
open science

# OH reactivity measurements in the Mediterranean region

Nora Zannoni

► **To cite this version:**

Nora Zannoni. OH reactivity measurements in the Mediterranean region. Analytical chemistry. Université Paris Saclay (COMUE), 2015. English. NNT : 2015SACLS163 . tel-01407352

**HAL Id: tel-01407352**

**<https://theses.hal.science/tel-01407352v1>**

Submitted on 2 Dec 2016

**HAL** is a multi-disciplinary open access archive for the deposit and dissemination of scientific research documents, whether they are published or not. The documents may come from teaching and research institutions in France or abroad, or from public or private research centers.

L'archive ouverte pluridisciplinaire **HAL**, est destinée au dépôt et à la diffusion de documents scientifiques de niveau recherche, publiés ou non, émanant des établissements d'enseignement et de recherche français ou étrangers, des laboratoires publics ou privés.

NNT : 2015SACLS163

THESE DE DOCTORAT  
DE  
L'UNIVERSITE PARIS-SACLAY  
PREPAREE A  
"UNIVERSITE PARIS-SUD "

ECOLE DOCTORALE N° 579  
Sciences mécaniques et énergétiques, matériaux, géosciences

Spécialité de doctorat : Chimie atmosphérique

Par

**Nora Zannoni**

Titre de la thèse

**OH reactivity measurements  
in the Mediterranean region**

**Thèse présentée et soutenue à Gif sur Yvette, le 30/11/2015:**

**Composition du Jury :**

Prof. Dr. Laurent Salmon  
Dr. Coralie Schoemaeker  
Dr. Silvano Fares  
Dr. Matthias Beekmann  
Prof. Dr. Nadine Locoge  
Dr. Valerie Gros  
Dr. Bernard Bonsang

Université Paris-Sud  
Université Lille  
CRA-RPS  
LISA  
Mines Douai  
LSCE  
LSCE

Président  
Rapporteur  
Rapporteur  
Examinateur  
Examinatrice  
Directeur de thèse  
Co-directeur de thèse

# OH reactivity measurements in the Mediterranean region

A dissertation submitted to  
Université Paris-Saclay

for the degree of  
Doctor of Chemistry

presented by  
NORA ZANNONI

Laboratoire des Sciences du Climat et de l'Environnement  
UMR 8212 CEA/CNRS/UVSQ

supervisor: Dr. Valerie Gros

co-supervisor: Dr. Bernard Bonsang

reviewers: Dr. Nadine Locoge, Dr. Matthias Beekmann

examiners: Dr. Coralie Schoemaeker, Dr. Silvano Fares, Dr. Laurent Salmon

September 2015



# Contents

<b>Abstract</b>	<b>xv</b>
<b>Résumé</b>	<b>xvii</b>
<b>1 Introduction to total OH reactivity</b>	<b>1</b>
1.1 Theoretical background on tropospheric chemical processes and reactive constituents . . . . .	1
1.1.1 Atmospheric relevance of reactive gases . . . . .	2
1.1.2 The hydroxyl radical and other atmospheric oxidants . . . . .	3
1.1.3 Nitrogen Oxides . . . . .	5
1.1.4 Volatile Organic Compounds (VOCs) . . . . .	6
1.2 Total OH reactivity: a change in philosophy . . . . .	15
1.2.1 OH reactivity relevance . . . . .	16
1.2.2 Measuring the OH reactivity . . . . .	18
1.2.3 OH reactivity in the world . . . . .	20
1.2.4 The missing OH reactivity . . . . .	23
1.3 The Mediterranean basin . . . . .	24
1.3.1 General aspects . . . . .	24
1.3.2 Natural and anthropogenic local emissions . . . . .	25
1.3.3 A hotspot for climate change . . . . .	28
1.4 Thesis objectives . . . . .	30

<b>2</b>	<b>Experimental</b>	<b>33</b>
2.1	Proton Transfer Reaction-Mass Spectrometer (PTR-MS)	33
2.1.1	Applications in atmospheric sciences	33
2.1.2	Instrumental operation	34
2.1.3	Compounds sensitivity and volume mixing ratio	36
2.2	Comparative Reactivity Method for OH reactivity studies	37
2.2.1	General principle	37
2.2.2	Derivation of the basic equation for CRM	38
2.2.3	The reactor	39
2.2.4	The detector	40
2.2.5	Method calibration	41
2.2.6	Interferences	42
2.2.7	Data processing	44
2.2.8	Limit of detection and measurement uncertainties	49
2.3	CRM-LSCE	49
2.3.1	Optimization of the Comparative Reactivity Method at LSCE	49
2.3.2	CRM-LSCE performance	53
2.3.3	CRM-LSCE: field deployment	56
<b>3</b>	<b>Intercomparison of two comparative reactivity method instruments in the Mediterranean basin during summer 2013</b>	<b>61</b>
3.1	Introduction	62
3.2	Experimental	65
3.2.1	The comparative reactivity method	65
3.2.2	Data processing	67
3.2.3	Comparative Reactivity Method set up	70
3.2.4	Description of the field site and experiments	74
3.3	Results and discussion	75
3.3.1	C1 acquired with the conventional and scavenger approaches	76

3.3.2	Assessment of the correction for humidity differences between C2 and C3 . . . . .	78
3.3.3	Assessment of the correction for the kinetics regime . . . . .	79
3.3.4	Correction for dilution . . . . .	81
3.3.5	Measurement uncertainty . . . . .	83
3.3.6	Intercomparison of OH reactivity results . . . . .	83
3.4	Summary and conclusions . . . . .	86
<b>4</b>	<b>OH reactivity and concentrations of Biogenic Volatile Organic Compounds in a Mediterranean forest of downy oak trees</b>	<b>89</b>
4.1	Introduction . . . . .	90
4.2	Methodology . . . . .	93
4.2.1	Description of the field site . . . . .	93
4.2.2	Ambient air sampling . . . . .	94
4.2.3	Comparative Reactivity Method and instrument performance . . .	95
4.2.4	Complementary measurements at the field site . . . . .	97
4.2.4.1	Proton Transfer Reaction-Mass Spectrometer . . . . .	97
4.2.4.2	Gas chromatography-flame ionization detector . . . . .	99
4.2.4.3	Formaldehyde analyzer . . . . .	100
4.2.4.4	NO <sub>x</sub> analyzer . . . . .	101
4.2.4.5	GC-MS offline analysis . . . . .	101
4.2.4.6	O <sub>3</sub> , CH <sub>4</sub> , CO . . . . .	101
4.2.4.7	Meteorological parameters . . . . .	101
4.3	Results . . . . .	102
4.3.1	Trace gases profiles and atmospheric regime . . . . .	102
4.3.2	Total OH reactivity . . . . .	105
4.3.3	Measured and calculated OH reactivity . . . . .	106
4.3.4	Nighttime missing reactivity . . . . .	109
4.3.5	OH reactivity at other biogenic sites . . . . .	112
4.4	Summary and conclusion . . . . .	114

<b>5</b>	<b>Total OH reactivity at a receptor coastal site in the Mediterranean basin during summer 2013</b>	<b>117</b>
5.1	Introduction . . . . .	118
5.2	Field site . . . . .	119
5.3	Methods . . . . .	120
5.3.1	Comparative Reactivity Method . . . . .	120
5.3.2	Ancillary measurements at the field site . . . . .	123
5.3.2.1	Proton Transfer Reaction-Mass Spectrometry . . . . .	123
5.3.2.2	Online Chromatography . . . . .	125
5.3.2.3	Offline Chromatography . . . . .	126
5.3.2.4	Hantzsch method for the analysis of formaldehyde . . . . .	126
5.3.2.5	Chemiluminescence for the analysis of NO <sub>x</sub> . . . . .	127
5.3.2.6	Wavelength-scanned cavity ring down spectrometry (WS-CRDS) . . . . .	127
5.3.3	Box model for mixing ratios and OH reactivity evaluation . . . . .	128
5.4	Results . . . . .	130
5.4.1	Air masses regime . . . . .	130
5.4.2	Total measured OH reactivity . . . . .	131
5.4.3	Calculated OH reactivity and importance of biogenic VOCs at the measuring site . . . . .	132
5.4.3.1	Long-term variability . . . . .	132
5.4.3.2	Contributions from different classes of compounds . . . . .	133
5.4.3.3	Impact of biogenic VOCs . . . . .	135
5.4.4	Comparison between measured and calculated reactivity . . . . .	137
5.4.5	Clues on the missing OH reactivity: a mix of primary emission and secondary production . . . . .	138
5.4.5.1	Unmeasured terpenes . . . . .	138
5.4.5.2	estimated reactivity of the unmeasured terpenes . . . . .	139
5.4.5.3	unmeasured secondary products . . . . .	140
5.4.6	Modeled OH reactivity . . . . .	142



5.4.6.1	Model inputs . . . . .	142
5.4.6.2	Model results and sensitivity . . . . .	143
5.4.6.3	Contributions to the modelled OH reactivity . . . . .	145
5.5	Conclusions . . . . .	146
5.6	Acknowledgments . . . . .	147
<b>6</b>	<b>Conclusion and future research</b>	<b>149</b>
<b>A</b>	<b>Rate coefficients of reaction with OH for selected atmospheric compounds</b>	<b>155</b>
<b>B</b>	<b>Selected Poster Presentations</b>	<b>157</b>
	<b>List of Tables</b>	<b>161</b>
	<b>List of Figures</b>	<b>163</b>
	<b>Bibliography</b>	<b>167</b>







# Preface

This thesis describes the work I have done during my PhD studies at Laboratoire des Sciences du Climat et de l'Environnement (LSCE) between November 2012 and October 2015.

The project concerns the technical optimization of the Comparative Reactivity Method (CRM) for measuring the total OH reactivity and field measurements of OH reactivity at targeted sites in the Mediterranean region.

The findings discussed in this thesis are the results of an experimental work conducted in the laboratory of LSCE for building and testing the technique of the CRM and of an experimental field work. The field work was performed during two main campaigns: ChArMEx (the Chemistry-Aerosol in a Mediterranean Experiment), during summer 2013 and CANOPEE (Biosphere-atmosphere exchange of organic compounds: impact of intra-canopy processes), during spring 2014. Field measurements were conducted for determining the total loading of reactants and our level of understanding of the reactive composition of the air masses influencing the sites.

The project is part of the European Marie Curie Innovative Training Network "PIMMS" (Proton Ionization Molecular Mass Spectrometry) which aims at developing molecular mass spectrometry techniques in different field of sciences, including environmental, food and medical sciences. This thesis project was funded through PIMMS because of the use of proton ionization mass spectrometry for measuring the OH reactivity. The PIMMS network provided me and this project the tools and means to improve the quality of this work, including visits to IISER Mohali, India to discuss about the CRM with Dr. Vinayak Sinha; Ionicon, Austria, to develop my knowledge on proton transfer molecular mass spectrometry; Juelich, Germany to participate to a field campaign on aerosols formation at the atmospheric chamber SAPHIR.

This thesis consists of six chapters. The first chapter provides an introduction to the concept and importance of OH reactivity. It is composed by four sections, i.e., background to tropospheric processes and composition, OH reactivity, the Mediterranean basin, and

the thesis goal. The first section discusses in detail the main players in tropospheric reactions, i.e., the hydroxyl radical, nitrogen oxides and volatile organic compounds and reactions they undergo. The second section describes the originality of the concept of OH reactivity and the need of developing it. It provides an overview of the methods currently existing for measuring the OH reactivity and values of OH reactivity observed from ground-state field measurements at different point sources in the world. Finally it reports the main findings on the missing reactivity, which is now a topic of great interest in atmospheric sciences. The third section introduces the Mediterranean basin as a region of great interest for atmospheric chemistry studies. It explains the main sources of pollution and why measurements of reactivity are needed in this part of the world. Finally, the last section describes specifically the goal and research questions that this project addresses. The research questions are answered specifically in the chapters 3, 4 and 5.

The second chapter is divided into three sections. The first two sections provide the theoretical background of the two main methodologies applied in this project: Proton Transfer Reaction-Mass Spectrometry (PTR-MS) and the Comparative Reactivity Method (CRM). The section of the CRM describes in detail the updated theory of the method, and includes its concept, operational settings and data processing. The third section focuses on the progresses made during this PhD project in our laboratory. It includes technical improvements for increasing the sensitivity of the method and improvements to reduce the stated interferences. It gives an overview of the performance of our instrument, here referred as CRM-LSCE and the performance of our instrument during the two field campaigns whose results are described in the following chapters.

The third chapter presents the findings of an intercomparison exercise run between CRM-LSCE and the instrument built at Mines Douai, France (CRM-MD) published as Zannoni et al., (2015a) on Atmospheric Measurements and Techniques. It includes a detailed description on the way to assess the corrections of the raw data and the way to process them on ambient raw data of reactivity. It shows the results of the tests and ambient measurements of reactivity run during July 2013 on the field in Corsica, France. It shows how the different corrections impact the raw data for each instrument and how the final processed data correlate well between them over the range of reactivity of 0-300 s<sup>-1</sup>. It highlights the importance of conducting a detailed experimental characterization of each CRM instrument and of extending intercomparison practices to more instruments using different techniques.

The fourth chapter presents the results of a field campaign conducted in the forest of downy oaks of Observatoire de Haute Provence (OHP) where the concentration of volatile organic compounds and OH reactivity were simultaneously measured. The results are shown in

the form of the article, published on Atmospheric Chemistry and Physics Discussions as Zannoni et al., (2015b). Here, the total loading and distribution of reactants at two heights of the forest: inside the canopy (i.e. 2 m) and above the canopy (i.e. 10 m) are presented. Comparison between the measured and calculated reactivity reported no difference during daytime observations, while large gaps were observed during nighttime. Finally, the chapter gives a perspective on values of OH reactivity measured in different forests of the world. It shows that the Mediterranean forest of OHP emits large amounts of reactive species, only comparable to tropical forests.

The fifth chapter is a preliminary draft of an article I wrote describing the main findings obtained from the measurements of OH reactivity during the field campaign ChArMEX. This draft includes the work of other scientists from LSCE (France), the laboratory of Mines Douai (France), LamP, Clermont Ferrant (France), which are not specifically mentioned as the draft was not distributed before this thesis submission. This chapter includes a description of the time series and diurnal profile of the OH reactivity measured during summer 2013 at the receptor field site of Ersa, Corsica, France. It includes a comparison between the measured reactivity and the one calculated from the species measured in the gas-phase. It provides some hypothesis on the discrepancy observed between these two parameters during one week of measurements. Finally, it provides the preliminary results of a chemical model used to determine the oxidation products of the biogenic compounds measured at the site and their contribution to the OH reactivity. The simulations were run by Dr. Sophie Szopa (LSCE) and aim at providing an idea of the type of information that can be obtained by combining the results from the measurements with a modelling approach.

Finally, chapter 6 is the outlook and conclusions of this PhD project, including some suggestions for further research.





# Abstract

The hydroxyl radical,  $\cdot\text{OH}$ , is the dominant oxidant in the atmosphere: it can initiate most of the oxidation reactions involving volatile organic compounds and leading to the formation of ozone and aerosols; with adverse effects on the air quality and climate.

There are many uncertainties associated to the total sink of the OH radical, because it is difficult to characterize all the reactive species responsible for its loss in the atmosphere.

The total OH reactivity is defined as the total first order loss rate of OH due to the atmospheric reactive gases and represents the total sink of OH. This parameter directly provides the total loading of reactive gases in ambient air and indicates the frequency of the oxidation reactions involving OH and reactive molecules.

Measurements of OH reactivity have many utilities, among them, they can be compared to the OH reactivity calculated from simultaneous measurements of reactive gases and highlight whether all these gases are measured and known or not. Several studies using such approach have highlighted that a significant fraction of reactive gases is not measured and possibly unknown. Especially, larger fractions of *missing reactivity* have been reported in forests and in those environments characterized by larger loadings of secondary or higher generation oxidation products.

In this thesis, the Comparative Reactivity Method (CRM) for measuring the total OH reactivity is deployed in an intercomparison exercise and at two targeted sites in the Mediterranean basin.

I here report a detailed characterization of a comparative reactivity method instrument built in our institute (Laboratoire des Sciences du Climat et de l'Environnement) and explain the technical improvements conducted during my PhD project. The instrument was constructed and characterized to specifically measure the OH reactivity at two sites exposed to different field constraints. In addition, the instrument performance was compared to the one of another CRM instrument built in another laboratory (Mines Douai, France). The intercomparison exercise highlighted that our measurements were reproducible in a range of reactivity between the instrument limit of detection and  $300\text{ s}^{-1}$  and

that a precise characterization of each CRM is needed.

Ambient OH reactivity was measured at two sites: at a receptor site in Corsica (field campaign ChArMEx, summer 2013) and in a forest of downy oaks in Provence, in the south of France (field campaign Canopee, spring 2014).

Both field studies highlighted two main points : (i) the targeted sites in the Mediterranean basin are both exposed to large loadings of reactive molecules, (ii) a detailed characterization of the atmospheric composition, including the products formed by oxidation reactions, is still challenging. Deploying the OH reactivity tool at other field sites and in laboratory studies would be of great benefit to better understand atmospheric processes, especially focusing on plants emissions and chemical transformation. Investigating more field sites in the Mediterranean region is also recommended to have a greater picture on the loading of reactants in this area.

# Résumé

Les radicaux hydroxyles (OH) sont les oxydants majeurs de notre atmosphère. Ils interviennent dans les processus d'oxydation de nombreux polluants atmosphériques, et notamment des composés organiques volatils (COV), et conduisent à la formation d'ozone et d'aérosols organiques ; ces derniers ayant des effets adverses sur la qualité de l'air et le climat. De nombreuses incertitudes existent quant à l'estimation du puit total des radicaux OH, en raison de la difficulté que représente la caractérisation expérimentale de l'ensemble des composés qui contribuent à leur consommation dans l'atmosphère. En effet, les COV représentent une famille de plusieurs centaines de molécules, présents dans l'air à l'état de traces mais fortement réactifs vis à vis des radicaux OH et autres oxydants atmosphériques. Ainsi, la quantification directe de l'ensemble de la fraction organique réactive dans l'atmosphère est à ce jour encore pratiquement irréalisable.

La réactivité atmosphérique totale OH est définie comme étant le taux de perte de premier ordre des radicaux OH liée à la présence de composés réactifs. Elle permet d'estimer de manière indirecte la charge totale de composés réactifs dans l'air et nous renseigne sur la fréquence des processus d'oxydation mettant en jeu les radicaux OH. La mesure expérimentale de la réactivité OH apporte de nombreuses informations quant à la composition de l'atmosphère. Elle permet notamment, après comparaison avec la réactivité OH calculée à partir des composés gazeux mesurés dans l'atmosphère, d'évaluer l'importance des espèces non-mesurées (et éventuellement inconnues) dans les processus chimiques qui régissent notre atmosphère. Il s'est avéré par le passé, que la réactivité mesurée était souvent plus élevée que la réactivité calculée. Cette réactivité manquante s'est montrée particulièrement élevée dans certaines forêts ainsi que des environnements caractérisés par la présence de nombreux produits d'oxydation intervenant loin dans les chaînes d'oxydation des COV.

Dans cette thèse, la Méthode de la Réactivité Comparative (CRM) pour la mesure directe de la réactivité OH a été mise en œuvre. La CRM est une méthode récente et prometteuse, mais nécessitant des améliorations de nature technique, et également dans l'interprétation des données. Ainsi, dans un premier temps, un exercice d'inter-comparaison a été effectué

pour l'optimisation et l'évaluation analytique de la méthode. La caractérisation détaillée de l'instrument CRM développé au sein de notre institut (Laboratoire des Sciences, du Climat et de l'Environnement) et les progrès techniques apportés durant mon travail de thèse sont présentés dans ce manuscrit. L'instrument a été construit et optimisé afin de permettre la mesure de la réactivité OH dans deux sites avec des régimes et conditions atmosphériques contrastés. De plus, la performance de notre instrument a été comparé à celui d'un second instrument CRM construit dans le laboratoire des Mines de Douai (France). Cet exercice d'inter comparaison a mis en évidence la bonne reproductibilité des mesures pour des niveaux de réactivité entre la limite de détection de l'appareil et  $300 \text{ s}^{-1}$ . La réactivité OH atmosphérique a été mesurée dans deux sites: dans un site récepteur en Corse (campagne ChArMEx, été 2013) et dans une forêt de chênes pubescents en Provence (campagne CANOPEE, été 2014).

Les deux études de terrain mènent à deux conclusions principales: (i) les sites situés dans le bassin Méditerranéen sont tous les deux exposés à d'importants apports de molécules réactives, (ii) la caractérisation détaillée de la composition de l'atmosphère, incluant les produits formés par réactions d'oxydation, reste compliquée. L'utilisation de l'outil de réactivité OH dans d'autres sites naturels ou en laboratoire serait très utile pour mieux comprendre les processus atmosphériques, en particulier si l'on s'intéresse aux émissions des plantes et aux transformations chimiques. L'étude d'autres sites de la région Méditerranéenne est aussi conseillée pour avoir une meilleure image de l'apport de réactifs dans cette région.

## Chapter 1

# Introduction to total OH reactivity

## 1.1 Theoretical background on tropospheric chemical processes and reactive constituents

The troposphere is the lowest layer of the atmosphere. It extends from the Earth's surface up to the tropopause for about 10-15 km in altitude, depending on the latitude and time of the year. It is characterized by decreasing temperature with height and rapid vertical mixing. Indeed, the name troposphere derives from the Greek word *tropos*, which means turning, since this is a region characterized by turbulence and mixing. Besides, it contains also almost all of the atmosphere's water vapor, and 80% of the total atmospheric mass, behaving in this way like a chemical reservoir. In this layer the transport of species to the stratosphere is much slower than internal mixing. All the species emitted by the Earth's surface, with a chemical lifetime shorter than a year, are removed from the troposphere before reaching the stratosphere. Light of sufficiently energetic wavelengths can also penetrate the troposphere and promote important photochemical reactions.

Here, almost the total of the whole atmospheric mass partitions into different phases: the gas phase and the particle phase or aerosols (solid, liquid, amorphous phase dispersed in the gas phase).

The main constituents of the gas phase are N<sub>2</sub> (78%), O<sub>2</sub> (21%), H<sub>2</sub>O vapor (<1%), Ar (<1%) and a fraction of less than 1% which contains all the remaining species, usually regarded as trace components. Trace gases include CO<sub>2</sub> (~345 ppmv), CH<sub>4</sub> (~1700 ppbv), O<sub>3</sub> (~20-80 ppbv), N<sub>2</sub>O (~320 ppbv), halogenated compounds (ppbv-pptv), and Volatile Organic Compounds (VOCs, ppbv-pptv). Although they form less than 1% by volume of the total atmospheric constituents, they play a major role in tropospheric processes since they can alter significantly the air quality, the weather and the climate.

### 1.1.1 Atmospheric relevance of reactive gases

Volatile organic compounds are key species in tropospheric processes since they can ultimately generate  $O_3$  and secondary organic aerosols (SOA), which have adverse effects on human health, air pollution and climate.

Ground level ozone is formed from the oxidation of VOCs in the presence of  $NO$ . Secondary Organic Aerosols (SOA) are formed in the atmosphere by the mass transfer to the aerosol phase of low vapor pressure products resulting from the oxidation of organic gaseous precursors. The ability of a given VOC to produce SOA from its oxidation depends on: (i) the volatility of its oxidation products, (ii) its atmospheric abundance, (iii) its chemical reactivity. Highly substituted species resulting from VOCs oxidation have lower volatility compared to their organic parent.

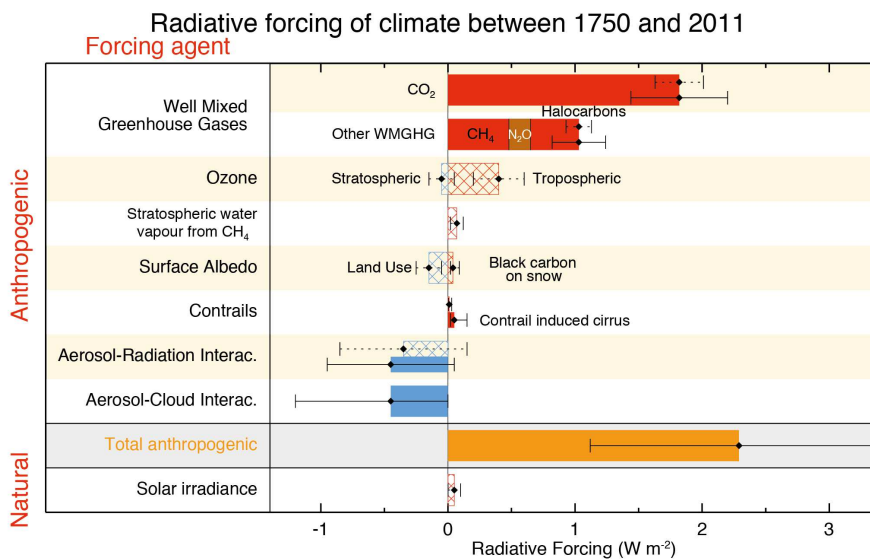


**Figure 1.1:** Assessed anthropogenic radiative forcing between 1750 to 2011 (IPCC, 2013).

Air quality effects include ozone's damages on the ecosystem and particle's reducing visibility.  $O_3$  and SOA are opposite climate forcers. Ozone acts as a greenhouse gas, while SOA can scatter and absorb the solar incoming radiation, as well as modify both the microphysical and properties of clouds. The Intergovernmental Panel on Climate Change 5th assessment report has published in 2013 the updated mean positive and negative radiative forcing resulting from anthropogenic emissions from 1750 (Fig. 1.1) for VOCs,  $O_3$  and SOA. Radiative forcings are changes in the energy fluxes of solar radiation and terrestrial radiation in the atmosphere, induced by anthropogenic or natural changes in the atmosphere composition. The total anthropogenic radiative forcing (RF) assessed in 2011 has a

---

net increase from 1750, on average it is  $2.29 \text{ W m}^{-2}$ , it has doubled from 1980 and has a large uncertainty associated. The major drivers are  $\text{CO}_2$  and  $\text{CH}_4$ ; VOCs,  $\text{O}_3$  and SOA participate at different levels with uncertainties of different magnitudes. VOCs, and by consequence  $\text{CO}_2$ ,  $\text{CH}_4$  and  $\text{O}_3$  produce a net positive RF of  $0.1 \text{ W m}^{-2}$ ;  $\text{O}_3$  is associated to several emitted compounds, overall resulting in a net positive RF. In contrast, aerosols produce a net negative RF. The level of scientific confidence on these results is still poor, and emphasizes the need to especially better understand atmospheric processes linked to aerosols formation.

### 1.1.2 The hydroxyl radical and other atmospheric oxidants

The hydroxyl radical ( $\cdot\text{OH}$ , referred throughout the manuscript as OH) is the key player in tropospheric chemistry, as it can initiate most of the oxidation reactions occurring in the troposphere. It was known for a long time that OH could react rapidly with hydrocarbons, but only in 1969 came the first hint of its fundamental role in tropospheric processes. In 1969 it was deduced that CO had a lifetime of 0.1 year, far smaller than what believed by that time (Weinstock, 1969). A likely removal of CO is the conversion to  $\text{CO}_2$ , through reaction with OH, which implies a fast mechanism of regeneration of OH, not known until then. In 1971 Levy showed that even a small fraction of excited atomic oxygen  $\text{O}(^1\text{D})$  produced by photodissociation of  $\text{O}_3$  was enough to maintain OH radicals in the atmosphere at the rate of  $10^6 \text{ molecules cm}^{-3} \text{ s}^{-1}$ , making OH the main tropospheric oxidant (Levy, 1971). Once produced, it is capable to react with the vast majority of atmospheric constituents. Interestingly, the most abundant oxidants in the atmosphere are  $\text{O}_2$  and  $\text{O}_3$ , but they have larger bond energies compared to OH. OH cannot react with the most abundant constituents, such as  $\text{N}_2$ ,  $\text{O}_2$ ,  $\text{CO}_2$  or  $\text{H}_2\text{O}$ . However, its significant concentration and high reactivity towards other molecules make it regarded as the most important atmospheric oxidant, and the "atmospheric cleansing agent". OH concentration is sustained, since when it undergoes reactions with ambient molecules, it is also regenerated from catalytic cycles, which maintain a concentration of  $10^6 \text{ molecules cm}^{-3}$  during daytime. The mechanism of formation of OH starts from  $\text{O}_3$  photodissociation (wavelengths  $< 319 \text{ nm}$ ) and passes through collisions with water molecules R 1-R 5:



Reactions R1-R2 produce both ground state oxygen and excited singlet oxygen atoms. While ground state oxygen recombines rapidly to form  $\text{O}_3$ , the excited singlet oxygen atom is quenched to the ground state by any atmospheric species (most likely it is  $\text{N}_2$  or  $\text{O}_2$ ) by R4. Both R3 and R4 are null cycles. Occasionally, the excited oxygen singlet atom collides with water molecules and produces 2 OH radicals (R5).

Both  $\text{O}_3$  and  $\text{H}_2\text{O}$  are needed to produce OH. Therefore higher OH levels are encountered in areas exposed to strong actinic fluxes and higher humidity, i.e. the tropics. Other sources of OH are formaldehyde (HCHO) and nitrous acid (HONO), reaction of alkenes with ozone, and recycling from peroxyradicals in low  $\text{NO}_x$  ( $\text{NO}+\text{NO}_2$ ) environments (Paulson et al., 1999; Hofzumahaus et al., 2009; Fuchs et al., 2013).

OH sinks are generally uncertain. Since the radical is capable of reacting with the large majority of the atmospheric species, knowing precisely its sinks means knowing with high precision the composition of the atmosphere. Indeed, it can undergo fast reactions with organic as well as inorganic trace gases. The reaction rate coefficients of OH with some inorganic and organic compounds are reported in the appendix.

There are other important oxidizing agents in the atmosphere, such as:  $\text{O}_3$ , the  $\text{NO}_3$  radical (only during nighttime), and Cl atoms to minor extents (important close to coastal areas).  $\text{O}_3$  is present in the troposphere as a result of: (i) diffusion of molecules from the stratosphere to the troposphere (net flux of  $\text{O}_3$  from the stratosphere to the troposphere estimated to be  $1\text{-}2 \cdot 10^{13}$  mol  $\text{O}_3/\text{year}$ ); (ii) in situ production of molecules into the troposphere. Mainly,  $\text{O}_3$  is formed in situ from oxidation reactions of VOCs with nitrogen oxides  $\text{NO}_x$  ( $\text{NO}+\text{NO}_2$ ), in the presence of sunlight. Atmospheric mixing ratio of  $\text{O}_3$  varies between 10-40 ppbv for unpolluted environments up to 100 ppbv for polluted areas.

$\text{NO}_3$  radicals are formed from the oxidation of NO into  $\text{NO}_2$ , followed by the oxidation reaction of  $\text{NO}_2$  into  $\text{NO}_3$ :





Since  $\text{NO}_3$  photolyses very fast (lifetime of about 5 s) and can rapidly react with NO,  $\text{NO}_3$  daytime levels are usually very small. On the other hand,  $\text{NO}_3$  concentration by night can be quite high (in the order of  $10^8$  molecules  $\text{cm}^{-3}$ , thus making this species regarded as the strongest oxidant during nighttime.

### 1.1.3 Nitrogen Oxides

Nitrogen oxides, also referred as  $\text{NO}_x$  ( $\text{NO} + \text{NO}_2$ ) undergo fast reaction with the hydroxyl radical. When present in large amount, their contribution to the OH chemistry is significant.  $\text{NO}_x$  global emissions estimates are illustrated in table 1.1. The largest source of  $\text{NO}_x$  is fossil fuel combustion, which explains why these species are more abundant in urban environments. Atmospheric levels of  $\text{NO}_x$  range from few pptv ( $\sim 20$  pptv) in remote areas, such as marine areas and tropical forests, to hundreds of ppbv in polluted urban areas. In rural environments their concentration ranges typically between 0.2 and 10 ppbv (Seinfeld and Pandis, 2006). Nitrogen oxides have a major role in tropospheric processes, which is determining whether VOCs oxidation reactions produce  $\text{O}_3$  or deplete it. Indeed, depending on the amount of NO present in the atmosphere, the oxidation reactions of VOCs can follow two pathways. In remote environments, where NO concentration is usually below 50 pptv,  $\text{O}_3$  is net depleted. When NO is available, like in polluted areas, where NO concentration can be about 100 ppbv,  $\text{O}_3$  is formed.

**Table 1.1:** Estimate of Global Tropospheric  $\text{NO}_x$  Emissions in  $\text{Tg N yr}^{-1}$  for Year 2000. Adapted from Seinfeld and Pandis (2006).

Sources	Emissions $\text{Tg N yr}^{-1}$
Fossil fuel combustion	33.0
Aircraft	0.7
Biomass burning	7.1
Soils	5.6
$\text{NH}_3$ oxidation	—
Lightning	5.0
Stratosphere	< 0.5
Total	51.9

### 1.1.4 Volatile Organic Compounds (VOCs)

The term VOCs refers to the total organic volatile fraction, excluding CO, CO<sub>2</sub> and CH<sub>4</sub>. It includes thousands of different compounds, an unspecified number estimated to be around 10<sup>4</sup>- 10<sup>5</sup>. Their abundance has largely and rapidly increased over the past 200 years, mainly due to human activities, as combustion of fossil fuels, biomass burning, industrial and agricultural activities and deforestation. Determining the exact composition and atmospheric abundance of this fraction of compounds are main challenges in atmospheric science because of their amount in traces and fast reaction rates towards the atmospheric oxidants. This section aims at providing some general information on the sources and sinks of these compounds.

#### Sources

Organic compounds are released into the atmosphere through processes associated with life, such as the growth, maintenance and decay of plants, animals and microbes. The combustion of living and dead organisms, such as fossil-fuel combustion and biomass burning are also sources of VOCs.

Organic compounds enter directly the atmosphere through natural and anthropogenic activities. In this way, VOCs are regarded as biogenic VOCs (BVOCs) and anthropogenic VOCs (AVOCs). There is also another important class of VOCs, regarded as oxygenated VOCs (OVOCs), which includes compounds having an oxygen atom in their structure. They can be of both natural and anthropogenic origin, and can enter the atmosphere directly through primary emission or because they are generated from oxidation reactions occurring in the atmosphere, hence secondary produced.

Natural activities are responsible of the emission of the largest majority of VOCs on a global scale (90%), while anthropogenic activities account only for a minor part of these emissions (10%). Globally, anthropogenic activities account for approximately 100 TgC/year of emissions, (Singh and Zimmermann, 1992). Regionally the proportions can be different, for example European anthropogenic and biogenic VOCs are more comparable in magnitude: biogenic emissions are estimated at ~14 TgC/year, and man-made around 24 TgC/year (Simpson et al., 1999).

Among the anthropogenic sources, road transport, wood burning and solvent use account for 36 TgC/year, 25 TgC/year and 20 TgC/year globally respectively (see table 1.2).

Anthropogenic VOCs include alcohols, short and long chain alkanes, alkenes, dienes, alkynes, aromatics, substituted aromatics, esters, ethers, aldehydes, ketones, acids and others (see Fig. 1.2). Industrial emissions for instance are mainly composed by short and long chain alkanes, alkenes and aromatics. On the other hand, biomass burning emissions

**Table 1.2:** Estimated global emissions of VOCs (TgC/year) for different anthropogenic sources (adapted from Middleton et al., (1995))

Activity	Emissions (Tg yr <sup>-1</sup> )
<i>Fuel Production / Distribution</i>	
Petroleum	8
Natural gas	2
Oil refining	5
Gasline distribution	2.5
<i>Fuel consumption</i>	
Coal	3.5
Wood	25
Crop residues (including waste)	14.5
Charcoal	2.5
Dung cakes	3
Road transport	36
Chemical industry	2
Solvent use	20
Uncontrolled waste burning	8
<i>Other</i>	10
<i>Total</i>	142

are mainly composed by alkenes, aromatics and acids.

On the other hand, major sources of biogenic VOCs are forests (821 TgC/year), crops (120 TgC/year), shrubs (194 TgC/year), oceans (5 TgC/year) and others (9 TgC/year), accounting for a total estimate of emissions of 1150 TgC/year (Guenther et al., 1995).

Plants emit BVOCs for many reasons; e.g. to protect against oxidative stress, to protect against bacteria, as a blossom hormone, for thermotolerance, to defend against herbivores attacks, as antioxidant when exposed to high ozone levels, for signaling (Kesselmeier et al., 1998 ; Laothawornkitkul et al., 2009). Figure 1.3 gives to the reader an idea of the number and type of VOCs and the origin of their emission from plants.

Biogenic VOCs include isoprenoids (isoprene, monoterpenes, sesquiterpenes etc.), alkanes, alkenes, alcohols, carbonyls, esters, ethers and acids (Kesselmeier and Staudt, 1999). Isoprenoids are composed by carbon skeletons of C<sub>5</sub> units, depending on the number of units

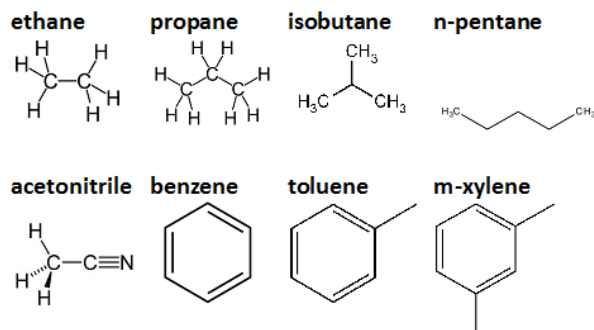


**Figure 1.2:** Chemical structures of some common anthropogenic VOCs.

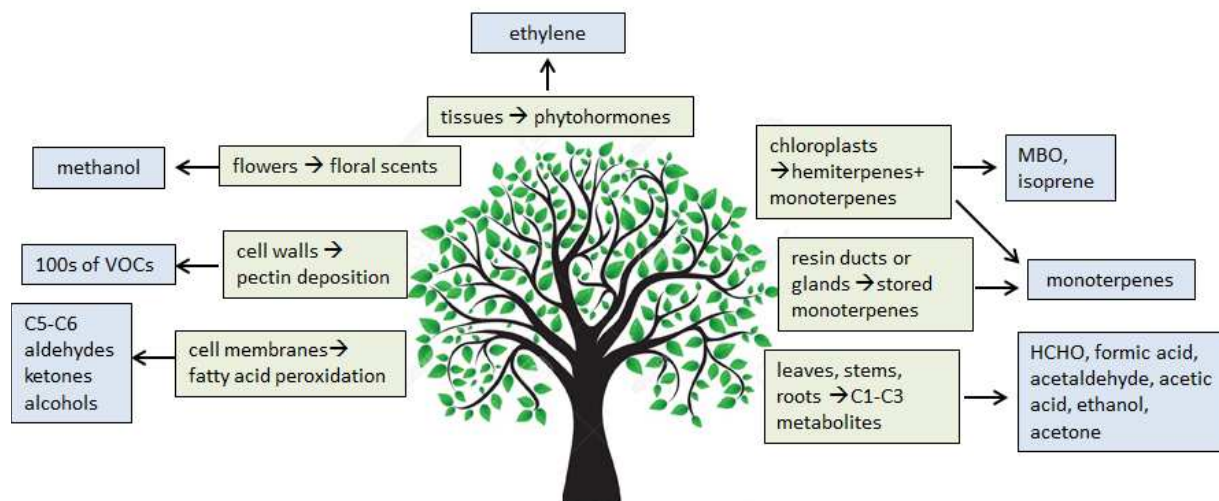


**Figure 1.3:** Simplified schematic of biogenic VOCs emissions pathways (adapted from Fall et al., (1999))

they are classified into hemiterpenes (like isoprene  $C_5H_8$ ), monoterpenes ( $C_{10}$ , like pinenes, terpinenes, limonene), sesquiterpenes ( $C_{15}$ , like caryophyllene), up to polyterpenes with more than  $C_{45}$  units. Figure 1.4 shows the chemical structure of a number of different isoprenoids.

Isoprene ( $C_5H_8$ , upper left) is quite unique among all the BVOCs for its dependence to photosynthetic activity in a plant. It is emitted from a large variety of deciduous plants when photosynthetically active radiation is present, and increases when air temperature also increases. On the other hand, terpenes emissions are linked to the biophysical processes associated with the amount of material stored in leaf oils and resins and the vapor pressure of the compound itself. Therefore, terpenes emissions do not strongly depend on light and can continue overnight, but they strongly vary with air temperature. Interest-

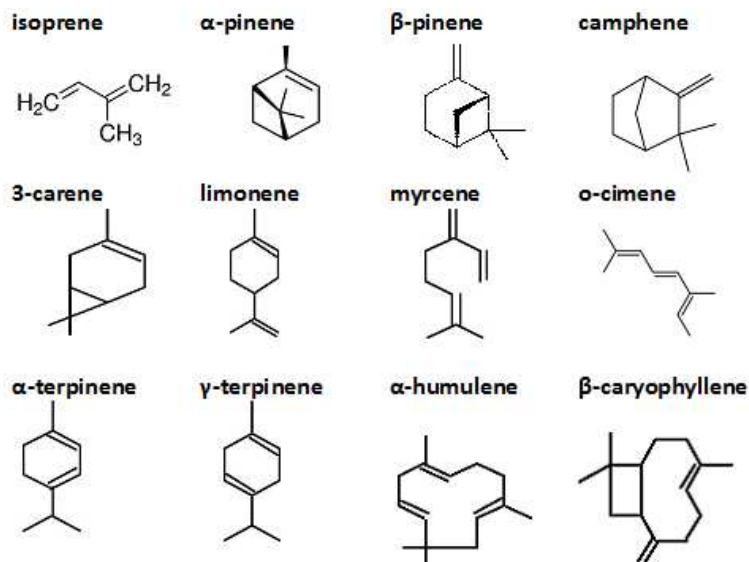


**Figure 1.4:** Chemical structures of some common biogenic VOCs.

ingly, every plant species emits its characteristics BVOCs: for instance two species of the oak family, *Quercus pubescens* and *Quercus Ilex* are respectively a strong isoprene emitter and a terpenes emitter (Kesselmeier et al., 1998). This species-dependent behavior adds additional challenges for estimating BVOCs emissions into the atmosphere. Estimates can be obtained for instance considering the source of emission (Leaf Area Index of the vegetation), the meteorological parameters activating the emissions and species composition (Megan v.2.1, Guenther et al., 2012).

Isoprene alone is estimated to make almost the half of the total BVOCs emitted (about 594 TgC/year, varying between 520-672 TgC/year), followed by methanol ( $130 \pm 4$  TgC/year), monoterpenes ( $95 \pm 3$  TgC/year), acetone ( $37 \pm 1$  TgC/year), sesquiterpenes ( $20 \pm 1$  TgC/year) and other reactive VOCs (96 TgC/year) (Sindelarova et al., 2014).

Global estimates of isoprene have been provided through several approaches, including inverse modelling from transport models and satellite data of formaldehyde, formaldehyde measurements and bottom-up emissions calculated from detailed regional vegetation descriptions. Within the same approach, based on bottom-up emissions, a factor 3 of difference exists for Europe. When more than an approach is also included, estimates are constrained within 400 and 700 Tg/year. Such result highlights that our current understanding on the emission of the most abundant VOC is still very poor (see Sindelarova et al., (2014)).

## Sinks

**Table 1.3:** Estimated global emissions of some common biogenic VOCs (adapted from Sindelarova et al., (2014))

Global total species	mean TgC yr <sup>-1</sup>
isoprene	594±34
sum of monoterpenes	95±3
α-pinene	32±1
β-pinene	16.7±0.6
sesquiterpenes	20±1
methanol	139±4
acetone	37±1
ethanol	19±1
acetaldehyde	19±1
erbene	18.1±0.5
propene	15.0±0.4
formaldehyde	4.6±0.2
formic acid	3.5±0.2
acetic acid	3.5±0.2
2-methyl-3-buten-2-ol	1.6±0.1
toluene	1.5±0.1
other VOC species	8.5±0.3
CO	90±4

The processes of removal of VOCs from the atmosphere include chemical and physical processes and their rate of efficiency depends on the physico-chemical properties of the specific chemical compound. Assuming an air parcel containing a generic compound, this organic compound can be simultaneously affected by the following removal processes: (i) oxidation reaction with any of the atmospheric major oxidants, (ii) photolysis by solar radiation, (iii) transport to the stratosphere, (iv) deposition onto surfaces, (v) partitioning into the particle phase. The average of the life histories of all molecules of the mentioned compound yields an average lifetime or the so-called averaged residence time of the compound.

For instance, from



where A is a generic VOC and  $k$  is the rate coefficient of the oxidation reaction with OH,

we can derive

$$\begin{aligned}\tau_{OH} &= \frac{[A]}{k[OH][A]} \\ &= \frac{1}{k[OH]}\end{aligned}\tag{1.1}$$

Considering all the processes affecting the removal of a species in the atmosphere the residence time can be quantified as:

$$\tau = \frac{1}{k_c + k_{ph} + k_t + k_d + k_{pa}}\tag{1.2}$$

With  $k_c$ ,  $k_{ph}$ ,  $k_t$ ,  $k_d$ ,  $k_{pa}$  being the first order loss rate of A due to chemical reactions, photolysis, transport, deposition and partitioning into the particle phase. The importance of one removal process compared to one another depends on many factors, included the physico-chemical properties of the considered species, e.g. its rate constant of reaction with one oxidant, its vapor pressure, and its absorbance of UV and visible light. Generally, oxidation reactions constitute the most important sink for VOCs. For instance, BVOCs are all highly reactive compounds towards all the mentioned atmospheric oxidants since they are all characterized by olefinic double bonds in their chemical structures (Fig. 1.4).

Table 1.4 reports a summary of the residence times for BVOCs as proposed in the review of Atkinson and Arey (2003), where calculations are performed for  $[OH]=2 \cdot 10^6$  molecules  $\text{cm}^{-3}$   $[O_3]=7 \cdot 10^{11}$  molecules  $\text{cm}^{-3}$  and  $[NO_3]=2.5 \cdot 10^8$  molecules  $\text{cm}^{-3}$ . The lifetimes reported here are only indicative in order to show a ranking of reactivity of the BVOCs. There are indeed many other factors influencing such reactions: time of the day, season, latitude, cloud cover, and the chemical composition of the air mass containing the BVOCs.

Isoprene lifetime towards OH is estimated to be only 1.4 hours, while methanol is more stable in the atmosphere and its estimated lifetime with OH is about 12 days. Some monoterpenes and sesquiterpenes, for instance have a residence time of only a few minutes ( $\alpha$ -terpinene has 0.5 min lifetime with  $NO_3$  and 1 min lifetime with  $O_3$ ,  $\beta$ -caryophyllene has 2 min lifetime with  $O_3$ ) therefore their measure in the atmosphere can result very challenging.

In contrast, the atmospheric lifetime of AVOCs is more variable and usually longer compared to the biogenic counterpart. Table 1.5 shows a summary of estimated lifetimes for AVOCs as reported in the review of Atkinson, 2000. Estimates were obtained from  $[OH]=2 \cdot 10^6$  molecules  $\text{cm}^{-3}$   $[O_3]=7 \cdot 10^{11}$  molecules  $\text{cm}^{-3}$  and  $[NO_3]=5 \cdot 10^8$  molecules  $\text{cm}^{-3}$ . For instance, propane lifetime is calculated to be 10 days with OH, while acetone needs 53 days before it is removed by OH.

**Table 1.4:** Calculated atmospheric lifetimes for some common biogenic volatile organic compounds (BVOCs). Calculations were performed for  $[\text{OH}] = 2 \cdot 10^6 \text{ molecules cm}^{-3}$   $[\text{O}_3] = 7 \cdot 10^{11} \text{ molecules cm}^{-3}$  and  $[\text{NO}_3] = 2.5 \cdot 10^8 \text{ molecules cm}^{-3}$ . Adapted from Atkinson and Arey (2003).

Organic	Lifetime due to		
	OH	O <sub>3</sub>	NO <sub>3</sub>
Isoprene	1.4 h	1.3 day	1.6 h
<i>Monoterpenes</i>			
Camphene	2.6 h	18 day	1.7 h
2-Carene	1.7 h	1.7 h	4 min
3-Carene	1.6 h	11 h	7 min
Limonene	49 min	2.0 h	5 min
Myrcene	39 min	50 min	6 min
$\alpha$ -Pinene	2.6 h	4.6 h	11 min
$\beta$ -Pinene	1.8 h	1.1 day	27 min
$\alpha$ -Terpinene	23 min	1 min	0.5 min
$\gamma$ -Terpinene	47 min	2.8 h	2 min
<i>Sesquiterpenes</i>			
$\beta$ -Caryophyllene	42 min	2 min	3 min
$\alpha$ -Humulene	28 min	2 min	2 min
<i>Oxygenates</i>			
Acetone	61 day	>4.5 yr	>8 yr
Camphor	2.5 day	>235 day	>300 day
Linealool	52 min	55 min	6 min
Methanol	12 day	>4.5 yr	2.0 yr

How strong is the reaction towards one specific oxidant compared to one other is again strictly species dependent (see Atkinson and Arey (2003) and Mogensen et al., (2015)). For instance, isoprene is more reactive towards OH, followed by its reaction with NO<sub>3</sub> and finally by O<sub>3</sub>. In contrast, monoterpenes are highly reactive with all the three oxidants, whereas sesquiterpenes favor the reaction with O<sub>3</sub> compared to OH. For the AVOCs counterpart, Formaldehyde needs 1.2 day to be removed by OH and more than 4 years to react with ozone. Propane lifetime with the three oxidants varies even more: it reacts with OH in 10 days, with NO<sub>3</sub> it needs around 7 years and with O<sub>3</sub> it is estimated to react in more than 4500 years.

By considering both classes of compounds, BVOCs and AVOCs, as well as the most



**Table 1.5:** Calculated lifetimes for some anthropogenic volatile organic compounds (AVOCs). Estimates were obtained from  $[\text{OH}]=2 \cdot 10^6$  molecules  $\text{cm}^{-3}$   $[\text{O}_3]=7 \cdot 10^{11}$  molecules  $\text{cm}^{-3}$  and  $[\text{NO}_3]=5 \cdot 10^8$  molecules  $\text{cm}^{-3}$ . Adapted from Atkinson (2000).

Organic	Lifetime due to			
	OH	NO <sub>3</sub>	O <sub>3</sub>	Photolysis
Propane	10 day	≈ 7 yr	>4500 yr	
<i>n</i> -Butane	4.7 day	2.8 yr	>4500 yr	
Ethene	1.4 day	225 day	10 day	
Propene	5.3 h	4.9 day	1.6 day	
Benzene	9.4 day	>4 yr	>4.5 yr	
Toluene	1.9 day	1.9 yr	> 4.5 yr	
<i>m</i> -Xylene	5.9 h	200 day	> 4.5 yr	
Styrene	2.4 h	3.7 h	1.0 day	
Phenol	5.3 h	9 min		
Formaldehyde	1.2 day	80 day	> 4.5 yr	4 h
Acetaldehyde	8.8 h	17 day	> 4.5 yr	6 day
Acetone	53 day	yr>11 day		≈60 day

abundant VOCs, for instance isoprene on a regional and global scale, emerges that OH, compared to O<sub>3</sub> and NO<sub>3</sub>, is by far the dominant oxidant.

Oxidation reactions of VOCs usually follow two pathways: (a) addition of the OH radical, NO<sub>3</sub> radical and O<sub>3</sub> to the C=C double bonds, (b) H-abstraction from C-H bonds (and to a lesser extent from O-H bond) by OH radicals and NO<sub>3</sub> radicals. Biogenics having C=C double bonds usually react by addition of the oxidants to the double bonds, while H-abstraction occurs from various C-H bonds of alkanes, ethers, alcohols, carbonyls and esters. The latter is also important for aldehydes, as methacrolein, one of the oxidation products resulting from the oxidation of isoprene.

Figure 1.5 shows a simplified schematic of the oxidation reaction of a VOC with any of the three atmospheric oxidants. When the VOC reacts with OH and NO<sub>3</sub>, an alkyl radical (R·) is formed. Then, R· reacts with oxygen forming organic peroxyradicals (RO<sub>2</sub>) and alkoxyradicals (RO·). The latter can decompose, isomerise, and react with O<sub>2</sub> in the atmosphere.

Oxidation of VOCs leads to a multitude of different chemical species, whose physico-chemical properties can differ much when compared to their primary precursors. As example, Fig. 1.6 provides the carbon mass balance calculations of the oxidation of six

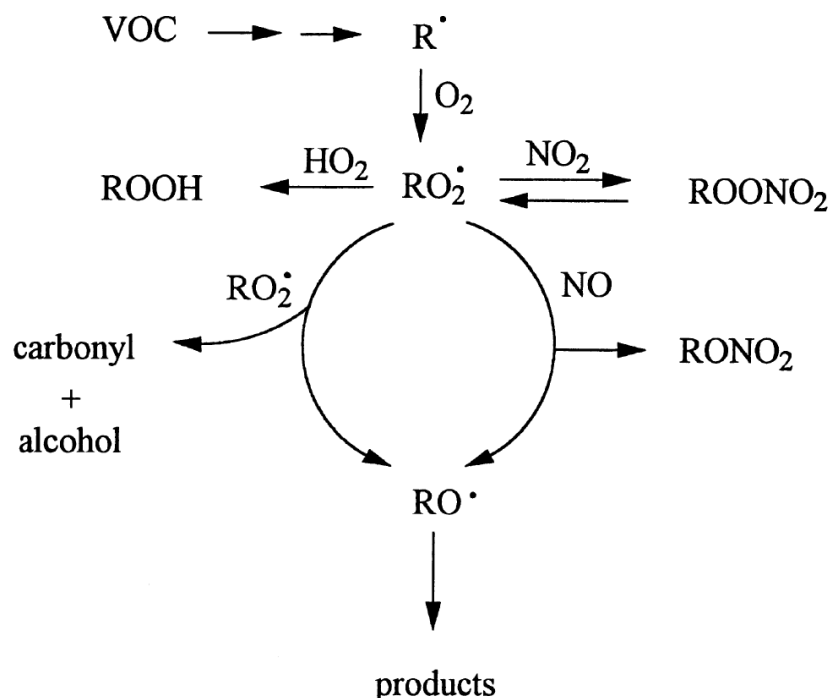


**Figure 1.5:** Simplified schematic of a volatile organic compound. Adapted from Atkinson (2000).

biogenic compounds (Goldstein and Galbally, 2007). Isoprene oxidation products include: formaldehyde, formic acid, acetic acid, acetaldehyde, MVK+MACR, methylfuran, a smaller percentage ends up in the particle phase, while a portion of gaseous products was not identified. This portion refers to a group of masses observed from mass spectrometry analysis which could not be properly identified.

As described in this section, there is a general lack of understanding linked to VOCs processes. Uncertainties are associated to their emissions and functioning, their atmospheric abundance and composition, the transformation as well as the removal of these species from the atmosphere. Considering just isoprene: it is the largest emitted and most studied non-methane hydrocarbon, it is extremely active in the atmosphere since it can fast react with OH, but estimates on its global emission provided during the last decade are poorly in agreement among them. Measurements of VOCs in ambient air are performed to better elucidate the atmospheric composition and concentration of different environments. However, many challenges arise when measuring VOCs concentration. First, they are a multitude of different species. Recent estimates have reported a large number of different organics present in nature, something around  $10^4$ - $10^5$  (Goldstein and Galbally (2007)). Then, organic volatiles are present in the atmosphere in trace amounts and they are highly

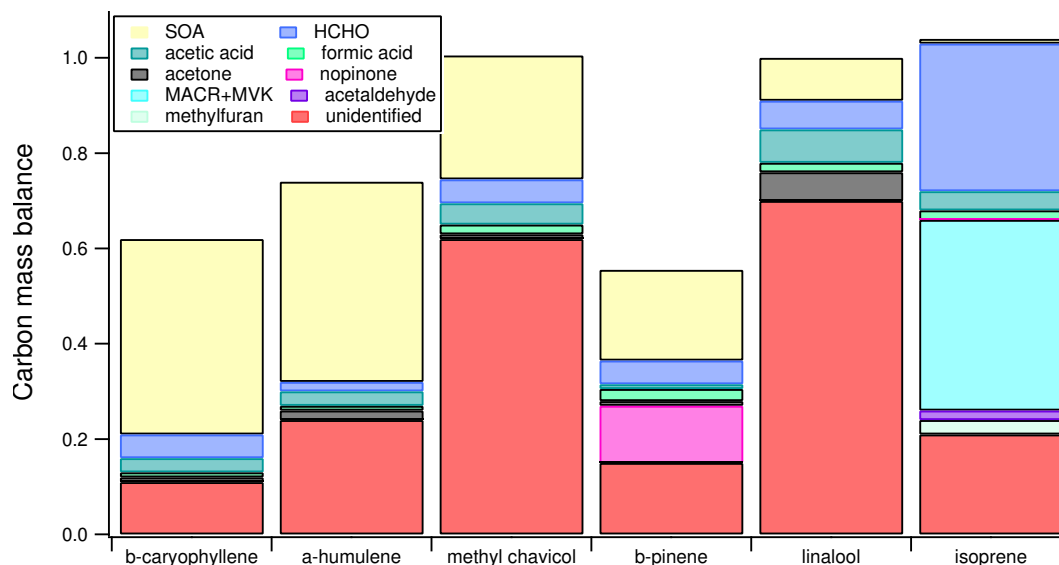


**Figure 1.6:** Carbon mass balance calculations for the oxidation products of six biogenic VOCs. Adapted from Goldstein and Galbally (2007).

reactive, meaning that some of these compounds can react fast with atmospheric oxidants and be completely or partially lost before they reach any detector. Consequently, a correct quantification of all these species results impracticable. For this reason, it is important to conceive a unique parameter which can directly quantify the total loading of these reactive atmospheric constituents. Interestingly, all these compounds have a common feature: reacting with the hydroxyl radical. It is exactly this natural process that all VOCs undergo to move towards the development of a new way of thinking in atmospheric sciences.

## 1.2 Total OH reactivity: a change in philosophy

A fundamental property of the atmosphere is the total OH reactivity, which is defined as the first order loss rate of reaction of the hydroxyl radical with the compounds present in ambient air and represents the inverse of the OH radical lifetime. OH reactivity indicates the frequency of the oxidation reactions involving the reactive atmospheric constituents and OH. Since OH is the main oxidant, OH reactivity also represents an estimate of the total loading of reactive molecules, those that actively participates in the tropospheric processes to form ozone and SOA altering the Earth's chemical and physical balances. First estimates of the total OH loss rate were obtained summing the concentration of the individual compounds measured multiplied by their rate coefficient of reaction with OH. This approach turned soon to be unfeasible. Indeed, before 1978, only 606 organic

compounds were identified in the atmosphere. This number increased to 2857 by 1986, with more advanced analytical technologies the number increased to  $10^4$ - $10^5$ , and it might be far smaller than the number of compounds which is actually present (Goldstein and Galbally, 2007). It turned soon essential to find an alternative approach to quantify such parameter independently from VOCs. Here is the novelty of the OH reactivity philosophy. It is not required measuring the composition of the atmosphere to the smallest detail when the total loading of active components in the air is known. This type of concept has also been extended to ozone production and SOA formation through parameters as ozone production rate (Cazorla and Brune, 2010) and Potential Aerosol Mass (Kang et al., 2007).

### 1.2.1 OH reactivity relevance

Measuring the total OH sink directly provides the information of the reactive components existing in ambient air, which, as described above, is an important atmospheric property. However, other important information can be obtained from the same measures of OH reactivity. Here below are summarized the main points that make such parameter essential to improve our current understanding of atmospheric chemistry:

#### (i) OH radical sources

Measures of the total OH sink (OH reactivity) are helpful to constrain the total OH source when the concentration of the hydroxyl radical is known:

$$[\text{OH}] = \frac{P_{\text{OH}}}{R_{\text{OH}}} \quad (1.3)$$

This approach was used by Whalley and coworkers (2011) for values of OH reactivity and OH concentration measured in the tropical rainforest of Borneo. In their work they stress the presence of an additional OH source when the OH production rates, sink and OH measurements are compared. They found that OH in the tropics is produced at a rate 10 times greater than the identified OH source. Predictions of OH concentration further highlighted that this parameter is underestimated by measures, with important consequences in the degradation of VOCs and methane lifetime over the tropics.

#### (ii) Unmeasured atmospheric constituents

Measures of OH reactivity can be performed together with measures of ambient air constituents. The former is generally regarded as "measured total OH reactivity", while the latter is used to calculate the OH reactivity from the summation of the concentration of the individual species multiplied by their rate coefficient with OH (eq. 1.4 and appendix for some references on reaction rate coefficients). The latter is therefore regarded

as "calculated OH reactivity".

$$R = \sum_i k_{i+OH} \cdot X_i \quad (1.4)$$

In an ideal environment where every single air component is known in detail the measured OH reactivity and the calculated OH reactivity are the same. If the calculated OH reactivity results smaller than the measured OH reactivity, then a fraction of the composition of the air results unidentified. This fraction is usually regarded as "missing OH reactivity". Missing OH reactivity was found to different extents in many environments where measures of OH reactivity were conducted (Di Carlo et al., 2004; Yoshino et al., 2006; Nölscher et al., 2012). This approach can be used to isolate different cases and improve our current understanding on environmental and atmospheric processes (see Sect. 1.2.4).

### (iii) Ozone production potential

Rate of instantaneous ozone production potential and regimes can be derived from measures of OH reactivity when associated to measurements of NO<sub>x</sub>, OH and peroxyradicals. Sinha and coworkers (2012) developed this type of approach to analyse the impact of point sources on regional ozone levels during a campaign in a coastal site in Spain. They found out that the ozone production potential was higher when the coastal site was more influenced by continental air masses. They also identified the point sources that were limiting such effect. Their findings demonstrate how significant could be to improve regional monitoring networks with OH reactivity measurements aside with measures of NO<sub>x</sub> and O<sub>3</sub>, in order to develop the right environmental policies to improve the air quality.

### (iv) Particles formation

OH reactivity offers a direct link between VOCs emission/production and particles formation. Mogensen et al. (2011) analysed the particles formation events occurred during one month of field campaign in the Finnish boreal forest with the measured data set of OH reactivity. They found out that the missing OH reactivity increased during the particle formation event. Correlations between measured and missing reactivity with the condensation sink confirmed that the missing reactivity could not be explained by OH loss on particles surface, but rather by OH oxidation with VOCs to form higher oxidized semivolatile compounds. Simultaneous measurements of gas phase chemical composition, particle phase chemical composition and OH reactivity would provide some hints to elucidate the process of particle formation.

## 1.2.2 Measuring the OH reactivity

In 1993, William H. Brune conceived for the first time the concept of total OH reactivity as the direct measure of OH loss rate. A few years later the first measurements of total OH reactivity were performed independently by two research groups in the laboratory based on LIDAR (Calpini et al., 1999) and in ambient air based on laser induced fluorescence for detecting OH (Kovacs and Brune, 2001).

Currently, the total OH reactivity can be measured directly using three different methods: (i) Total OH Loss Rate Measurement (TOLRM) (Kovacs and Brune, 2001; Mao et al., 2009; Hansen et al., 2014); Pump and probe technique (Calpini et al., 1999; Sadanaga et al., 2004; Yoshino et al., 2006; Ingham et al., 2009; Lou et al., 2010) and Comparative Reactivity Method (CRM) (Sinha et al., 2008; Nölscher et al., 2012a; Dolgorouky et al., 2012; Kim et al., 2011; Kumar and Sinha, 2014).

Total OH Loss Rate Measurement was first developed by Kovacs and Brune (2001). It consists of a flow tube used to sample ambient air at flow rates in the order of 50-400 sL min<sup>-1</sup>, wherein a large amount of OH is added through a movable injector. OH concentration is quantified at different reaction times using a FAGE apparatus (Fluorescence Assay by Gas Expansion, see Faloon et al., (2004) and Dusanter et al., (2009)) at the exit of the flow tube by moving the injector. A decay curve for OH is obtained due to a change in distance between the OH source and the OH detector.

The pump and probe technique was first pioneered by Calpini et al., (1999) and Jeanneret et al., (2001) and then adapted with some differences by other groups (Sadanaga et al., 2004, Yoshino et al., 2006; Ingham et al., 2009 and Lou et al., 2010). The instrument consists of three main parts: a flow tube to sample ambient air, a pulsed laser to generate OH in the sampling reactor, and a FAGE apparatus to quantify OH. The sampling flow is set around 10-20 sL min<sup>-1</sup> and assuming laminar flow the sample has about 1 s residence time for reaction with OH. The hydroxyl radical OH is generated inside the reactor from ozone photolysis. The decay of OH is measured considering the summed laser pulses using the FAGE instrument.

The Comparative Reactivity Method was more recently developed (Sinha et al., 2008) and then adopted by several research groups in the last decade (Kim et al., 2011; Dolgorouky et al., 2012; Michoud et al., 2015). The popularity of this method comes from the use of analytical techniques such as gas chromatography and mass spectrometry, already in use by many research groups working in the field of the atmospheric sciences. Indeed, in CRM a small glass flow reactor is coupled to a detector such a Proton Transfer Reaction Mass Spectrometer (PTR-MS) or a Gas Chromatography Photo-Ionization Detector (GC-PID).

The chosen detector monitors the concentration of a reference molecule, whose reactivity with OH is well known, throughout different experimental stages. The reference molecule, so far always pyrrole, is first diluted in clean air, then reacts with OH radicals generated inside the reactor, then competes for the OH radicals when ambient air is sampled. The competition between pyrrole and reactants in ambient air for OH is acquired in real time, while data processing produces raw data of reactivity with a time resolution of about 10 minutes. Since the CRM is the technique adopted for my PhD project, an exhaustive description of the method can be found in the experimental chapter of this thesis.

**Table 1.6:** Performance of instruments based on the three existing methods for measuring OH reactivity (modified from Nölscher et al., 2012).

Method	Uncertainty [%]	LoD [ $s^{-1}$ ]	Time resolution [s]	Sampling flow [ $sL \text{ min}^{-1}$ ]	Best application	main reference
TOLRM	10-12	1-2	30-180	50-400	Laboratory studies, permanent/longterm monitoring	Kovacs and Brune, (2001)
Pump and probe	16-25	1	210	10-20	Laboratory studies, permanent/longterm monitoring	Sadanaga et al., 2004
CRM	16-35	3-4	10-60	0.3	Forests, chamber studies	Sinha et al., 2008

Table 1.6 illustrates the differences among the three methods. A comparison of the methods is also provided in Nölscher et al., (2012a). The methods operating with a FAGE have a lower limit of detection (LoD) and report generally a lower uncertainty than CRM, but need larger sampling flows to operate. The CRM has the great advantage of a much smaller sampling flow needed, which broadens its application also to small chambers and branch enclosures experiments. Besides, it is designed to operate on the field. Its size is smaller and more portable than the two other instruments. In addition, it does not operate with a laser and lenses/mirrors that require additional time to be adjusted before performing well. Hence, the CRM can operate easily in the laboratory as on the field. The main drawback of the method consists in the intensive data processing for correcting the raw data for the interferences of the method. It results therefore less elaborated to operate the method in those environments where some of these corrections can be avoided, i.e. in forests for instance, where  $NO_x$  concentration is low. Furthermore, the CRM consists of a detector which is usually used to perform ambient measurements. An interesting approach

is to use the same instrument to perform both ambient gas phase measurements and OH reactivity (Kumar and Sinha (2014)).

### 1.2.3 OH reactivity in the world

Measurements of OH reactivity were performed so far at four different scales: (i) in branch enclosures/plant cuvettes (Kim et al., 2011; Nölscher et al., 2013); (ii) in flow tubes and environmental chambers (Nakashima et al., 2012; Nölscher et al., 2014); (iii) ground-based ambient measurements (e.g. Ren et al., 2003; Lee et al., 2010; Edwards et al., 2013) and (iv) airborne measurements (Mao et al., 2009).

Ground-based measures were conducted in different environments from different parts of the world. Fig. 1.7 illustrates the different sites in the world where the OH reactivity was measured. Green, gray and blue frames represent the type of environment where the measures were performed: i.e. forests, urban and coastal areas, respectively. Bold red font is used to highlight the sites where a maximum OH reactivity  $>50 \text{ s}^{-1}$  was observed. Finally the star indicates the measurements that were conducted with the Comparative Reactivity Method.

Different sites have been investigated so far: observations are reported for urban, forests, rural and remote environments. Forests of different climatic areas were analysed: boreal, temperate, mixed and tropical forests. Most of the measurements reported in literature were conducted, for logistical reasons, in northern hemisphere as can be seen in Fig. 1.7. However, measurements at tropical sites in Suriname and Borneo are also reported in literature (Sinha et al., 2008 and Edwards et al., 2013, respectively) and soon will be available the results of the first measures of OH reactivity in the pristine Amazonian rainforest.

Figure 1.7 permits to conclude:

- In only 15 years since the development of the first measurements of OH reactivity, a great effort for measuring this parameter and improving our understanding on atmospheric processes at different sides of the world has been made.
- Many interesting areas of the world are still unexplored: no measures of OH reactivity existed before my thesis project in the Mediterranean basin, no measures are reported in pristine areas of Asia and Africa, in the Siberian boreal forest, in densely populated urban areas as New Delhi, and in clean remote environments as the poles.
- The magnitude of OH reactivity does not depend on the method used to measure it. Highest values of OH reactivity were reported from measurements where the three



existing methods were applied (it is the case for the studies conducted in Mexico city and Paris, using respectively the TOLRM and CRM methods).

- Urban and forest sites are the environments better characterized. However, there is more variability in type of emission in forests than in urban sites, which means that we could explore more and more forested areas and still miss much information. Besides, unknowns on oxidation processes exist at different levels, generating more and more complex systems, e.g. primary reactants emitted from different plant species, secondary species formed from the primary biogenic precursors, interaction between biogenic precursors and anthropogenic components for the ecosystem influenced by pollution.
- Highest values of OH reactivity were reported in megacities and tropical forests (red highlighted sites). Despite being marked as a coastal area, maximum of OH reactivity at El Arenosillo (Spain) were observed when the site was influenced by continental pollution plumes from big cities as Madrid and Sevilla. Maximum values of OH reactivity observed in megacities are alarming:  $200 \text{ s}^{-1}$  in Mexico City during spring 2003 (Shirley et al., 2006);  $130 \text{ s}^{-1}$  in Paris during winter 2010 (Dolgorouky et al., 2012);  $100 \text{ s}^{-1}$  in Tokyo during autumn 2004, in New York City during winter 2004 and in Beijing during summer 2006 (Yoshino et al., 2006; Ren et al., 2006; Lu et al., 2013). In tropical forests local drivers as higher ambient temperature and solar radiation trigger the emissions of BVOCs, resulting in a more intense photochemistry, therefore higher OH reactivity compared to temperate environment.
- The magnitude of OH reactivity depends mainly on the type of environment but also on the season of measurements. Observations conducted in forested sites report a clear seasonal dependence, with the OH reactivity being larger in during spring and summer. Observations conducted in urban sites, as Tokyo, during all seasons provide an example: wintertime maximum OH reactivity was slightly below  $50 \text{ s}^{-1}$ , while during the other seasons was between  $80\text{-}100 \text{ s}^{-1}$ .

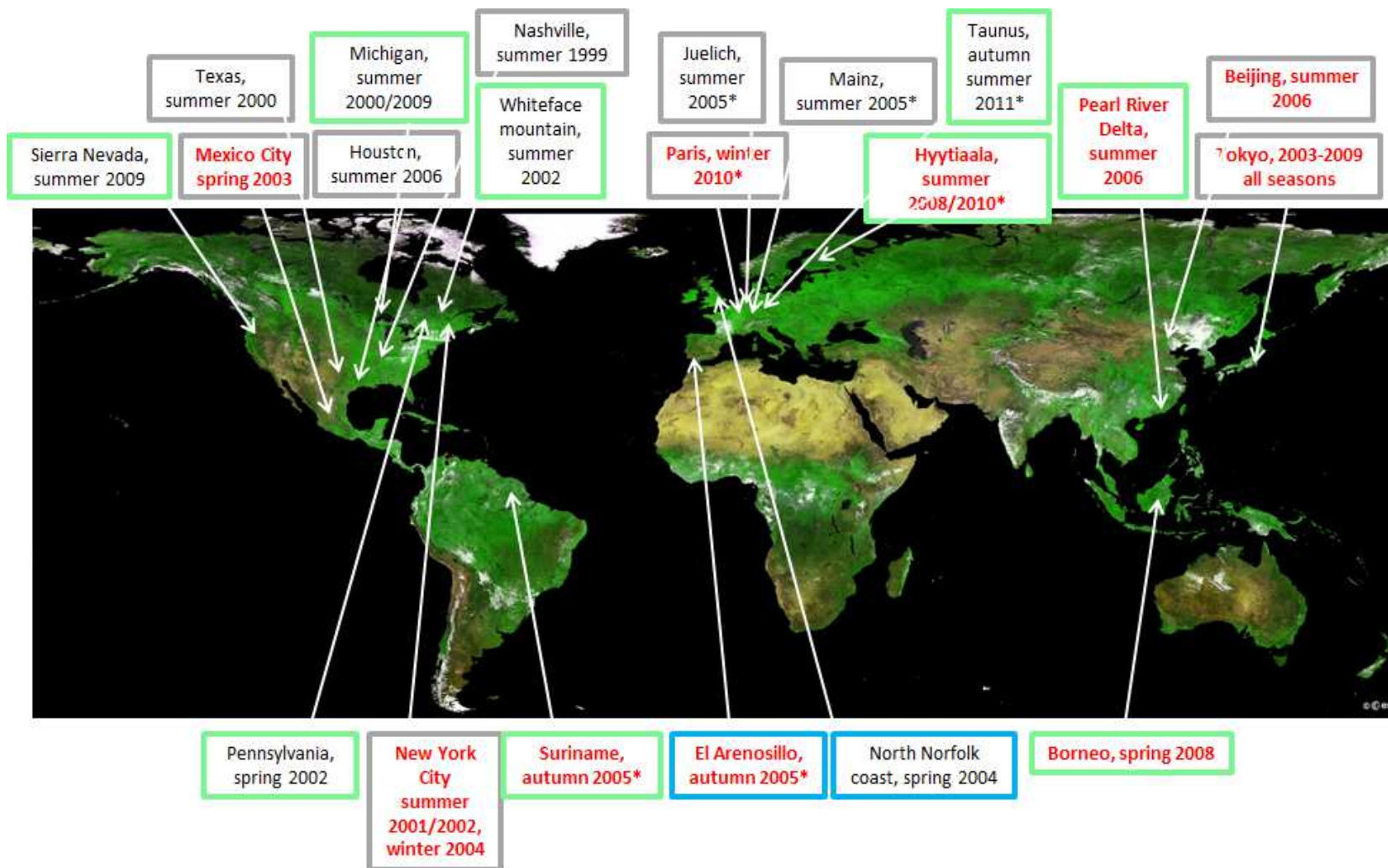


**Figure 1.7:** OH reactivity measurements world map. Arrows indicate the sites where measurements of OH reactivity using the three different experimental methods were conducted. Green, gray and blue frames refer to forested, urban and coastal sites. Red font indicates the sites where a maximum value of OH reactivity  $>50 \text{ s}^{-1}$  was reported. The star indicates the measurements carried out with the comparative reactivity method.

### 1.2.4 The missing OH reactivity

The missing OH reactivity is simply the fraction of reactivity which is not explained by the simultaneous measurements of concentration of gaseous atmospheric constituents. In other words, it corresponds to the unmeasured compounds in ambient air. These compounds can be unmeasured for three main reasons:

- (i) they are not measured because of the lack of an appropriate technique for measuring them;
- (ii) they are measured but their contribute to the OH reactivity is not known due to technical issues for identifying the species or to the not known kinetics of reaction;
- (iii) they are not measured because they are not known to exist.

It is especially this last hypothesis that has contributed considerably to pose the interest on the OH reactivity parameter. It is this last hypothesis to make us confident that there are more species in air than those measured or estimated to be (Goldstein and Galbally, 2007).

It is difficult to compare studies of OH reactivity using different methods, deployed by different operators while the suite of complementary measures available in the gas phase is different. Therefore comparisons among missing reactivity provided by different works have to be taken with caution. However, OH reactivity in forests have shown so far the largest gaps between OH reactivity measured and calculated. Those values are larger than in urban environments, for instance.

Di Carlo and coauthors (2004) were the first to show evidences for unknown reactive BVOCs in a temperate forest in Michigan. They showed that the missing reactivity in this forest had the same temperature dependency as terpenes and concluded that the unmeasured compounds were unknown terpene-like species. Kim et al. (2011) measured for the first time the OH reactivity in plant cuvettes. They isolated a few plant species to see if their emissions were completely characterized. Indeed plant cuvettes are perfect means to help disentangling the origin of the missing reactivity. They saw that the few plant species investigated were emitting compounds whose concentration was measured by their techniques. Hence they concluded that the missing OH reactivity has mainly a secondary origin. Nölscher et al., (2012) measured the OH reactivity in the Finnish boreal forest, during a warmer than usual summer. Their missing reactivity was almost 90% and they attributed it to species emitted as a consequence of heat stress on trees.

Holzinger et al., (2005) reported a broad suite of oxygenated compounds measured from a

Ponderosa pine forest in central California. These compounds were present at levels previously unreported, but none of the measured biogenic precursors was able to explain their amount. They back-calculated the amount of emissions needed to have such oxidation products and concluded that it was 6-30 times larger than the amount of monoterpenes they measured. Jud et al., (2015) recently reported that diterpenoid semivolatile compounds can react on plant surface to produce volatile carbonyls which are released in the atmosphere, but also that these compounds are not easy to measure.

On the urban side, larger missing gaps were found in the sites influenced by air masses significantly processed (Dolgorouky et al., 2012).

It looks like that the unknown species have therefore both primary and secondary origin. It seems that primary anthropogenic species are better characterized than primary biogenic species. At the same time it seems that the secondary products formed from reactions of anthropogenic and biogenic compounds are more difficult to measure: we miss the analytical means to measure them and we lack the theoretical knowledge of what is formed.

It is worth mentioning that a fraction of missing reactivity could be due also to the uncertainty associated to the rate constant of reactions between VOCs and OH. Mogensen et al., (2011) modelled the OH reactivity of the boreal forest from measurements conducted at Hyytiaala, Finland during August 2008. They pointed out that no experimental data of rate constants exist for many reactions of VOCs and OH, hence estimates of these values are rather used. They conducted a simple sensitivity study and highlighted that by multiplying the rate coefficients of a factor of 2, they were able to increase the modelled reactivity by 40%.

## 1.3 The Mediterranean basin

### 1.3.1 General aspects

The Mediterranean Basin derives its name from the latin word "*Mediterraneum*" which means "sea in the middle of land". Indeed the region consists of the area surrounding the Mediterranean Sea, which has a surface of 2.5 million km<sup>2</sup>. It includes 24 countries which are spread across three continents. From west to east the Mediterranean Basin stretches around 3,800 kilometres between Portugal and Lebanon, and around 1,000 kilometres from north to south, from Italy to Morocco and Libya. It also includes about 5,000 islands around the Mediterranean Sea and the Macaronesian islands in the North Atlantic Ocean. The Straits of Sicily divides the sea into two main bodies of water: western Mediterranean Basin, which is more under the influence of the Atlantic Ocean, and eastern Mediterranean

Basin.

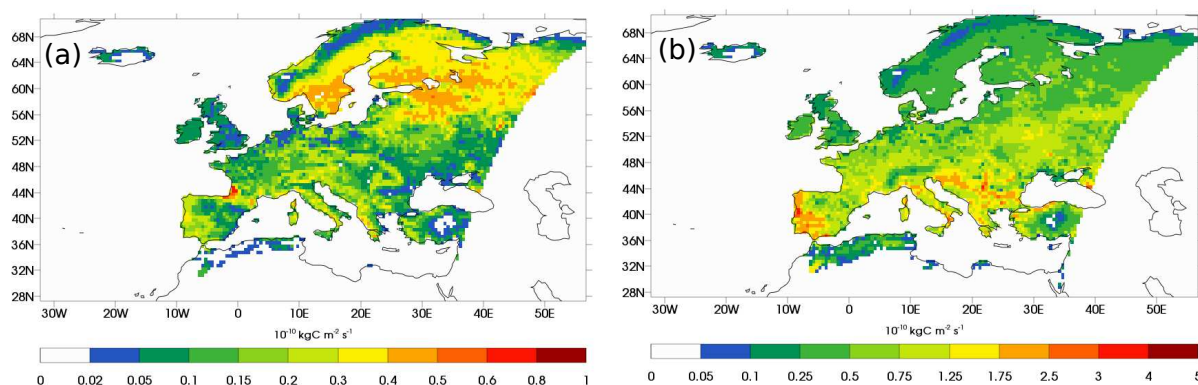
The Mediterranean Basin has the characteristic "Mediterranean climate", which describes the distinct, subtropical climate shared among other regions of the world such as, California, southwestern Oregon, western and southern Australia, South Africa, parts of Central Asia and central Chile; the Mediterranean Basin is the largest region among them. Summers are from hot to very hot and dry while winters are mild and wet. Temperature and rainfall can vary greatly throughout the region, with the mean annual rainfall ranging from as little as 100 mm in some areas to over 4,000 mm in others, usually heavier during wintertime. The climate is also generally considered to be harsher in the northern than in the southern shores of the Mediterranean Sea. Most of the regions of the basin experience average monthly temperature higher than 22°C during the warmest months, and on average between -3 and 18°C during the coldest ones. At least during four months the average monthly temperature is above 10°C. However, high temperatures during summers are generally not as high as those experienced in arid or semiarid climates due to the influence of the sea.

The atmospheric circulation over this region is also interesting. During summer, two semi-permanent weather systems located at each end of the Mediterranean dominate the whole basin: the Azores anticyclone (in the west) and a low pressure monsoon system which extends to the middle-east and southwestern Asia (in the east). Between the two weather systems the average air flow during summer is diverted from northern Europe and continental areas southwards towards northern Africa.

The climatic peculiarities make the Mediterranean region suitable for a wide range of vegetation types, and for this reason it has been ranked as the third richest hotspot in the world in terms of plants diversity. It is particularly known for the high level of endemism of the region: 52% of the 22500 plant species existing are found here and nowhere else in the world. There is a large variety of vegetation types including pine forests, mountain ranges up to 4,500 m high and floristic aromatic scrublands. Shrubs include olive trees, lavender, thyme, rosemary and many other aromatic plants. Forested areas include major vegetation types as oaks, conifers and deciduous forests, with about 290 tree species native to the Mediterranean basin, 201 of which are also endemic.

### 1.3.2 Natural and anthropogenic local emissions

The dense vegetation cover, rich biodiversity, high temperature and intense solar radiation make this area of the world a strong BVOCs emitter (Fig. 1.8 reports the estimated emissions of monoterpenes and isoprene in the Mediterranean and other European countries).



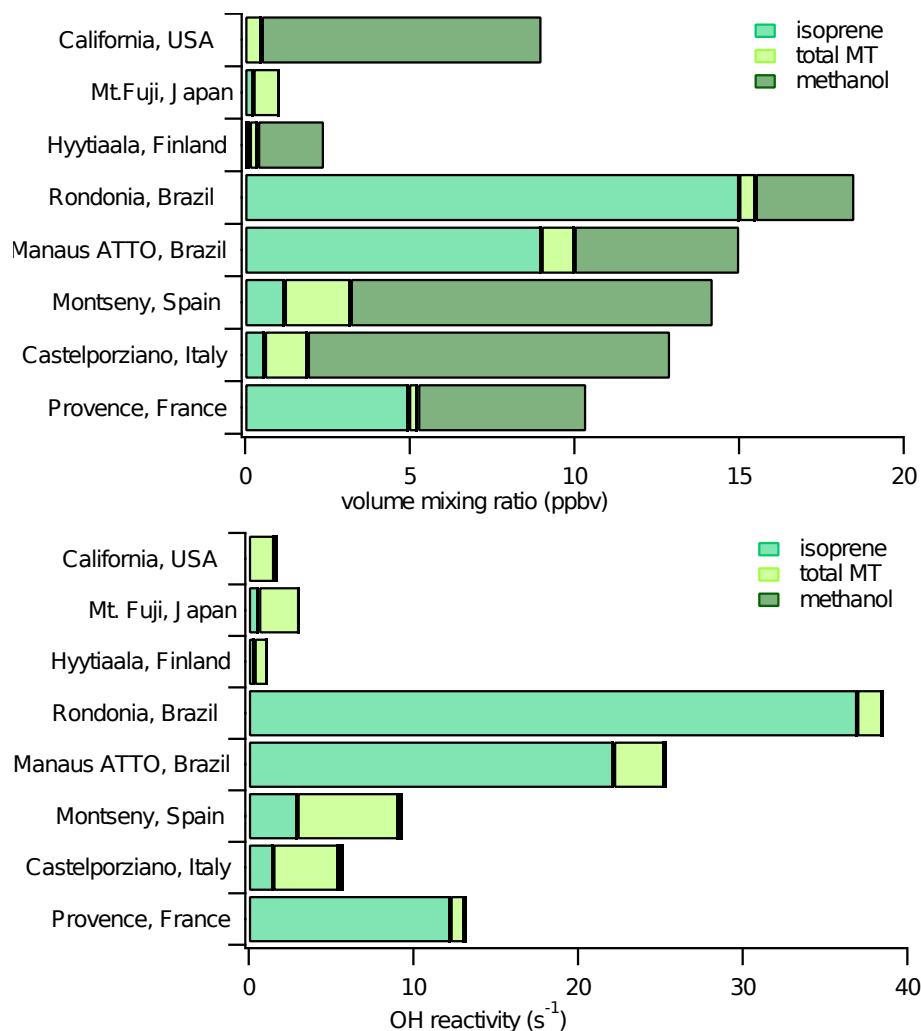
**Figure 1.8:** Present estimates of emissions of monoterpenes (a) and isoprene (b) for the Mediterranean and other European regions. Graphs courtesy of Palmira Messina.

Figure 1.9 illustrates a comparison among volume mixing ratios of three common BVOCs (methanol, isoprene, total monoterpenes) measured in different forests in the world. Although this comparison considers only a few studies reported in literature, it is interesting to notice that the levels of BVOCs observed in the Mediterranean are higher compared to those observed in a temperate forest in California, and higher than those reported in the Finnish boreal forest, but lower compared to the investigated tropical forested sites. Based on the mixing ratios reported in the top panel of fig. 1.9 a simple estimate of OH reactivity can be obtained, which is reported in the bottom panel of fig. 1.9. If we focus only on the measured reactive fraction of BVOCs, the difference among the Mediterranean, temperate forests and boreal forests is even larger. Indeed, the reactivity due to the biogenic fraction in forests of the Mediterranean basin is closer to the reactivity estimated in Amazonia.

Such similarity can be explained by the same levels of temperature and solar radiation registered in the two areas. Additionally, the presence of plants whose emission of isoprene is larger than the one of the more stable methanol for instance, seems to provide and added link.

As mentioned, BVOCs mixing ratios and reactivity can largely vary between seasons. Seco et al., (2011) reported volume mixing ratios of several VOCs during winter and summer 2009 measured in the forest of Montseny, Spain. For the same three VOCs it is possible to estimate a maximum OH reactivity of  $1.3 \text{ s}^{-1}$  in winter and a maximum OH reactivity of  $12 \text{ s}^{-1}$  during summertime.

Furthermore, there is a large variety in BVOCs emitted from Mediterranean plants. Owen et al., (2001) screened 40 native Mediterranean plant species and observed 32 compounds emitted from these plants. Considered that the reactivity towards OH is compound depen-



**Figure 1.9:** Mixing ratios of some biogenic VOCs (isoprene, total monoterpenes fraction and methanol) measured in selected temperate, boreal, tropical and Mediterranean forests (top panel). Estimated OH reactivity from exclusively the biogenic VOCs reported in the top panel for the same forested sites (bottom panel).

dent, we can expect a large variability between Mediterranean forests reactive loadings.

Beside the strong local emissions due to natural activity, the Mediterranean Basin has also been under human influence for far longer than any other biological hotspot. Indeed, it has been occupied by humans for about 8000 years, it is currently inhabited by 455 million people and an additional 246 million of tourists visit the area every year. Industrial and infrastructural development, transport, trades, deforestation, land use and other human practices expose the area to a strong local anthropogenic pollution. Table 1.7 illustrates, for example, the minimum and maximum values of some anthropogenic VOCs measured during winter and summer 2009 inside the urban area of Barcelona (Spain).

**Table 1.7:** Concentrations of anthropogenic VOCs during winter and summer 2009 inside the urban area of Barcelona, Spain (Seco et al., 2013)

Barcelona	Minimum (ppbv)	Maximum (ppbv)
acetone/propanal	1.45	4.52
acetaldehyde	1.11	4.06
acetic acid	1.24	2.63
benzene	0.30	1.76
toluene	0.86	7.58
C8 aromatics	0.87	12.27
acetonitrile	0.3	1.18

### 1.3.3 A hotspot for climate change

The Mediterranean represents therefore a crossroads of pollution: long-range transport from industrialized areas of northern Europe, pollution events from Asia, dust events from Africa; they all contribute in releasing high levels of contaminants over the basin (Lelieveld et al., 2002). Imported loadings mix with the local pollution providing a blend of emissions which is further oxidized initiating a complex chemistry. Berresheim et al. (2003) measured a midday maximum concentration of OH in Crete during summer 2001 of  $2 \cdot 10^7$  molecules  $\text{cm}^{-3}$ , higher than what is usually reported in other areas of the world. High levels of oxidants lead to an intense photochemistry which makes the Mediterranean region behaving like a natural photochemical reactor.

Atmospheric transport model simulations reported that summertime ozone values are exceeded throughout the Mediterranean, contributing to (i) the radiative forcing of climate; (ii) the quality of air over the region, which dramatically affects human health and the ecosystem (Lelieveld et al., 2002). It was found that 20-40% of ozone results from diffusion from the stratosphere, while the rest is produced within the troposphere and about half of this has anthropogenic origin. High values of ozone are formed in European air and then transported over the Mediterranean. Industrial activities along the coast add to the high background values, leading to high concentration of ozone over the whole region (60-70 ppbv measured in Crete during summer 2001, exceeding the European 8-hourly air pollution standard of 55 ppbv).

During the same study, the observations on aerosols showed that the fine mode is mostly composed by sulfates, organics, ammonium and black carbon, mostly from fossil fuel and biomass burning. Sulfates loadings were attributed to long range transport of pollutants over the area. Overall, it was found that about 80-90% of the fine aerosol fraction origi-



nates from anthropogenic activities. Aerosol radiative forcing is considered to be among the highest in the world during summertime in the Mediterranean. Atmospheric particles affect human health, visibility and furthermore influence the Mediterranean atmospheric energy budget by scattering and absorbing solar radiation. One consequence of the aerosol surface cooling is the reduction of evaporation and precipitation, resulting in strong perturbation to the hydrological cycle.

Experiencing such high levels of pollution, the Mediterranean is considered one of the world's major hotspots for climate change. Expected higher temperature levels and reduced precipitation will decrease the quality of air directly impacting the health of the inhabitants and the ecosystem.

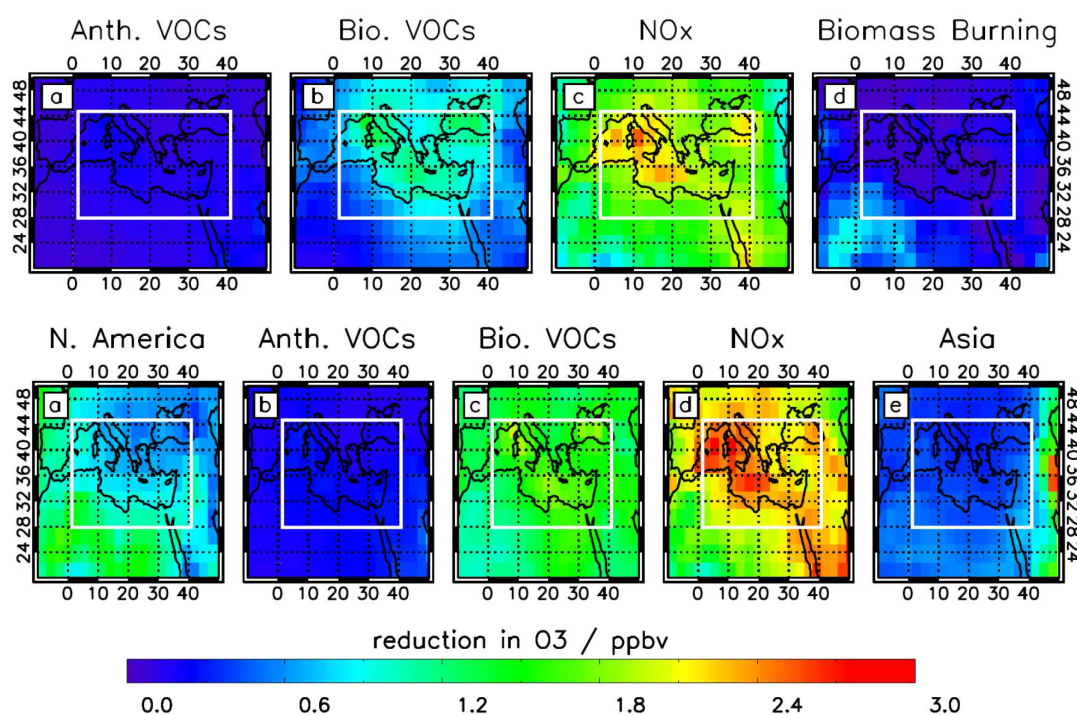


**Figure 1.10:** Reduction of surface mean ozone concentration (ppbv) due to 20% reduction of local emissions (top panel), global emissions (bottom panel). From Richards et al., 2013.

Figure 1.10 illustrates the effects on the mean surface ozone concentration over the Mediterranean region when local and global biogenic and natural emissions are reduced by 20%, (Richards et al., 2013). In particular, the top panel shows the ozone reduction (ppbv) when only a reduction on local sources is considered. Interestingly, the largest impact is observed when local anthropogenic NO<sub>x</sub> and local BVOCs are reduced by 20%, which amount respectively to 2.09 ppbv and 0.96 ppbv of reduction in concentration of ozone.

Among the global emissions (see Fig. 1.10 bottom panel), the largest impact is observed for global anthropogenic  $\text{NO}_x$  (2.49 ppbv of reduction of ozone), global biogenic VOCs (1.66 ppbv), all north American anthropogenic and biogenic emissions (0.94 ppbv), all Asian anthropogenic and natural emissions (0.46 ppbv).

It is recognized that few observations have been carried out in the Mediterranean until now, which adds further unknowns on the present and future state of this area (Mellouki and Ravishankara, 2007). Given the important role that reactive gases play in atmospheric processes, it is essential to conduct more efforts in providing observations of their loading in this region of the world.

## 1.4 Thesis objectives

In the previous sections I introduced which are the atmospheric reactive gases and the main processes they undergo. I underlined the atmospheric relevance of VOCs oxidation reactions and presented the utility of the OH reactivity parameter to better understand VOCs processes such as their emission and oxidation. Finally, the Mediterranean basin is presented as a reservoir of chemical pollutants where photochemistry is enhanced due to the particular solar conditions and higher temperature, resulting in this way as one of the major hotspots in the world for climate change.

In this context, the goal of this PhD work is to:

- Optimise the existing Comparative Reactivity Method (CRM) in order to conduct accurate measurements of OH reactivity
- Measure the OH reactivity at selected spots in the Mediterranean region exposed to different air masses regimes

More specifically, the scientific questions that this thesis work addresses are:

1. **Use of the Comparative Reactivity Method for measuring the OH reactivity on the field.** The CRM is only recently developed and the few existing publications available in literature show the promising results of applying this methodology on the field. However, they also highlight that the method has several interferences and that an intensive data processing is needed in order to obtain correct data of OH reactivity. The data processing includes corrections that account for the interferences of the method. Nevertheless, nobody reported so far how to assess these corrections and how to process the data in detail. Consequently, it is not available

either a standard protocol to process the data for comparing the results of reactivity acquired with different CRMs. Besides, no intercomparison exercises that compare the performances of different CRMs or between the CRM and other methods were reported in literature before this thesis project started (now it is possible to refer to Hansen et al. (2015) for a comparison between a CRM and pump and probe instruments). Building a CRM instrument and characterizing it in the laboratory and on the field allow to: *(i) understand the limitations of the instrument and conduct targeted technical improvements on it; (ii) prepare an instrument whose output is unambiguous.* The comparison of the performance of the CRM with another instrument through several tests and ambient measurements permits to assess *a common correct procedure to analyse the results and further characterize the instrumental and methodology advantages and limitations.*

2. **Understanding of the intra-canopy oxidation processes in a forest in the Mediterranean region influenced by isoprene emissions by using the OH reactivity tool.** Forests emit large quantities of organic volatiles whose composition, amount, and atmospheric effects are not well understood. During summertime the Mediterranean region experiences hot temperature and an intense solar radiation, which drives forests to release larger amounts of organic volatiles. However, it is not clear what is the fate of these species: whether they are removed or transformed by oxidation processes within the canopies, or they reach the atmosphere affecting its composition above forested areas. Measurements of OH reactivity and BVOCs concentrations inside and above a Mediterranean forest of oaks help assessing: *(i) the loading of reactive compounds inside and above the forest; (ii) whether the composition inside and above the forest is completely determined; (iii) better constrain atmospheric processes within a forest by using both the OH reactivity and missing reactivity.*
3. **Determination, with the OH reactivity, of the loadings of reactive compounds at a coastal receptor site in the western Mediterranean basin exposed to different air masses regimes.** The Mediterranean basin during summertime is exposed to high loadings of pollutants due to local anthropogenic and biogenic activities, intense atmospheric circulation and strong photochemistry. Only a few measurements have been conducted so far over the basin, and mainly focused on the eastern side. Such measurements highlighted the high levels of pollutants and stressed the need to conduct more intensive measurement campaigns over the area. In particular, it is hard to constrain precisely the total amount of reactive species due to the mix of primary reactants and imported processed reactive com-

pounds. Measuring the total OH reactivity and gaseous constituents at a receptor site located in the western basin permits to determine *the total loading of reactants and our level of understanding of the composition of the air masses imported from different sectors.*

## Chapter 2

# Experimental

## 2.1 Proton Transfer Reaction-Mass Spectrometer (PTR-MS)

### 2.1.1 Applications in atmospheric sciences

Proton Transfer Reaction Mass Spectrometry (PTR-MS) is a technique based on chemical ionization through proton transfer, developed for the detection of gaseous organic compounds in ambient air (Lindinger and Jordan, 1998; de Gouw and Warneke, 2007; Blake et al., 2009). It has been adopted as detector of choice for the analysis of volatiles in many different fields: from environmental research to food, medical, health analysis. The main applications of the PTR-MS in the atmospheric sciences field are:

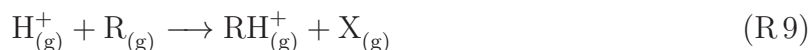
1. To measure atmospheric mixing ratio of VOCs. Atmospheric mixing ratios are then used to constrain chemical transport models and climate models and predict air pollution and climate effects.
2. To measure fluxes of VOCs. Since the atmospheric concentration of a reactive compound relies on too many degrees of freedom as emission, deposition, transport and chemistry, measuring the concentration of a species alone makes it hard to diagnose uncertainties in models (Karl et al., 2009). The direct measure of the flux of a reactive species helps to disentangle surface exchange from other processes affecting the chemical's atmospheric distribution. Eddy covariance is the most direct method to measure surface fluxes and relies on atmospheric turbulence measures, which require sampling at high temporal frequency, 10 Hz. PTR-MS is the suitable technique since its higher temporal resolution permits to conduct real-time eddy covariance fluxes.

3. To measure OH reactivity. The PTR-MS is often the detector of choice to conduct OH reactivity measures with the Comparative Reactivity Method. In this method, pyrrole, the reference molecule introduced into the system, is monitored unambiguously in real time throughout the experiment. Although using the PTR-MS to measure only one compound does not fully exploit its measuring capabilities; its robustness over time and high sensitivity makes this technique preferred to other existing methods. Additionally, the same instrument can be used to conduct both ambient mixing ratios and OH reactivity measures (Kumar and Sinha, 2014).
4. To measure the composition of atmospheric particles. State-of-the-art instruments that examine on-line the chemical composition of atmospheric particles are not able to speciate into the organic fraction, which is the most interesting and less understood fraction. New techniques that couple the PTR-MS to thermal desorption units have been recently developed with promising results for future applications in aerosol science (Holzinger et al., 2010; Eichler et al., 2015).

### 2.1.2 Instrumental operation

The PTR-MS is composed of three main parts: (i) the ion source, (ii) the drift tube, (iii) the ion detection system (Fig. 2.1). (i) The ion source consists of a hollow-cathode discharge source where water vapor generates  $\text{H}_2^+$ ,  $\text{H}^+$  and  $\text{O}^+$  ions which further react with water molecules to form  $\text{H}_3\text{O}^+$  with high efficiency (>99.5%). Other reagent gases despite water vapor can be used for such scope,  $\text{O}_2$  or  $\text{O}_2$  together with  $\text{N}_2$  for instance, can produce  $\text{O}_2^+$  and  $\text{NO}^+$  ions with slight less efficiency (90-95% and 95-99%, respectively). Typical count rates for  $\text{H}_3\text{O}^+$  are  $10^6$  cps.

(ii) The drift tube consists of a number of stainless steel rings, separated by Teflon rings which seal the vacuum and isolate the drift rings electrically. Precursor ions are extracted from the ion source to the drift tube, while the sampling gas flows into the tube through a separate inlet. In the drift tube, the reagent ions undergo many collisions with the molecules of the sample, but only a small number of collisions lead to proton transfer reactions (in the case of  $\text{H}_3\text{O}^+$  in the order of one percent), in the following way:



Proton affinities are commonly used to assess whether or not a proton transfer reaction is likely to be spontaneous. Molecules with a proton affinity larger than water ( $691 \pm 3$  kJ/mol), whereas this is used as reagent molecule, undergo exothermic hence spontaneous reactions. Most of volatile organic compounds have proton affinities slightly larger than

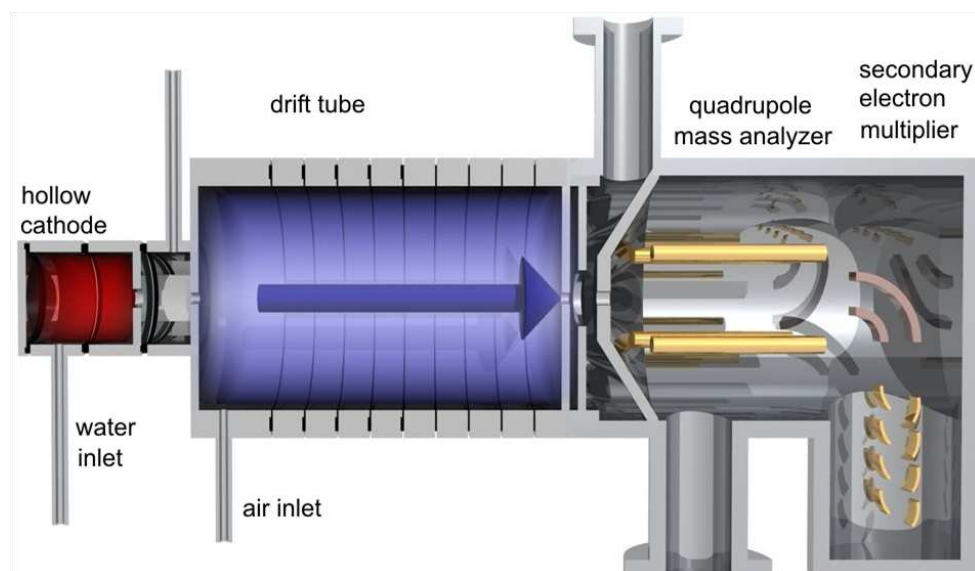


**Figure 2.1:** Schematic of the Proton Transfer Reaction-Mass Spectrometer with a quadrupole detector, showing the inlet for water and the air sample and the three sections: ion source, drift tube and detection module (adopted from M. Schwarzmann, 2001).

water, while inorganic molecules (i.e.  $O_2$ ,  $N_2$ ,  $CO_2$ ,  $O_3$ ,  $H_2O$ ) and methane, which make up the largest fraction of ambient air, possess smaller affinities hence they act as buffer thermalizing agents in the drift tube. Important consequences are: use of a short drift tube and no need to dilute the sample, hence shorter reaction time; ability in measuring only trace molecules; small enough excess energy released from transfer reactions to avoid extensive fragmentation of ions which makes proton transfer been regarded as a soft ionization method. In addition, a homogeneously increased voltage is applied to the rings of the drift tube, which generates a homogeneous electric field. The electric field is mostly responsible for the transport of ions along the tube, eliminating the need of a large pump. All these characteristics make PTR-MS a unique instrument with a high detection sensitivity (10 pptV) in a relatively compact size. Standard electric field applied, expressed as  $E/N$  are 120-140 Td (1 Td=10<sup>-17</sup> V cm<sup>2</sup>). Changing  $E/N$  and thus the mean collision energy in the drift tube allows to distinguish between product ions based on different fragmentation pathways (for instance between methacrolein and methyl vinyl ketone, the main oxidation products of isoprene which are usually measured together at the protonated mass  $m/z$  71).

(iii) The ion detection system can be either a quadrupole (QMS) or a time of flight mass spectrometer (TOF-MS). Our PTR-MS is equipped with a commercial quadrupole mass filter (Balzers QMG 421) and a SEM (secondary electron multiplier) for ion pulse counting detection. The ions exiting the drift tube are extracted into the quadrupole through a

sampling orifice while the buffer is pumped away. A quadrupole is composed of four parallel metallic rods between which is applied a tension generating an electron field that forces the ions to run under a different oscillating trajectory according to their mass-to-charge ( $m/z$ ) ratio. Ions with a selected  $m/z$  will travel along the quadrupole and reach the SEM where their signal will be converted into electrons and amplified in a current expressed as counts per seconds. In a TOF-MS ions are accelerated to the same kinetic energy by an applied electric field. A mass resolving power of about 5000 could be achieved, enough to separate most atmospheric relevant protonated VOCs and to identify the corresponding empirical ionic formulas. A full spectrum can be measured at once, every 0.1 s, corresponding to 400 mass peaks and 400 empirical formulas. The advantage of using a TOF-MS instead of a QMS is the higher resolution, compounds are separated according to their exact mass in the former, while compounds are separated according to their nominal mass in the latter. An unambiguous identification of the compounds is then possible with a TOF-MS.

### 2.1.3 Compounds sensitivity and volume mixing ratio

A Calibration of the PTR-MS for different molecules is conducted by measuring the response in normalized counts per second (ncps) of a standard gas molecule with a certified concentration. It is usually performed at different steps with variable concentration (typical range for calibrations is 0-20 ppbv) and repeated for different relative humidity values. Linear least squares fits of the ncps measured versus the ppbv injected for a specific molecule are used to determine the detector sensitivity to such molecule. Normalised sensitivities ( $S_{norm}$ ) and count rates ( $I(RH_i^+)$ ) are expressed as follows:

$$S_{norm} = \frac{I(RH_i^+)_{norm}}{VMR_{standar}} \quad (2.1)$$

$$I(RH_i^+)_{norm} = 10^6 \times \left( \frac{I(RH_i^+)}{m/z21 \times 500 + m/z37} - \frac{I(RH_i^+)_{zero}}{m/z21_{zero} \times 500 + m/z37_{zero}} \right) \quad (2.2)$$

Volume mixing ratios can be alternatively calculated through the transmission coefficients approach, in particular whereas a calibration for a specific molecule is not achievable:

$$VMR = \frac{I(RH_i^+)_{norm}}{S_{norm}} \quad (2.3)$$

$$I(RH_i^+)_{norm} = 10^6 \times \left( \frac{I(RH_i^+)}{m/z21 \times 500 + m/z37} - \frac{I(RH_i^+)_{zero}}{m/z21_{zero} \times 500 + m/z37_{zero}} \right) \quad (2.4)$$



The accuracy of the results is lower compared to the calibration with a gas standard, due to uncertainty in the reactions rate coefficients and relative transmission curve (de Gouw and Warneke, 2007; Taipale et al., 2008).

A measure of the concentration of molecules when only zero air is introduced inside the PTR-MS is useful to derive the background level for each species, which is therefore subtracted from the measured concentration to obtain the actual concentration level. The limit of detection (LoD) for each compound is usually calculated as  $3\sigma$  its background value.

## 2.2 Comparative Reactivity Method for OH reactivity studies

### 2.2.1 General principle

The Comparative Reactivity Method (CRM) is an indirect method for measuring the total OH reactivity in ambient air by using a reference molecule whose reaction rate with OH is well established (Sinha et al., 2008; Nölscher et al., 2012). The reference molecule is pyrrole ( $C_4H_5N$ ), which is usually not found in ambient air and can be easily detected through a PTR-MS at protonated ( $C_4H_5NH^+$ )  $m/z$  68 without any major interference. Pyrrole is diluted in a glass flow reactor with nitrogen and alternatively zero or ambient air and its concentration is monitored with a detector coupled to the reactor. Hydroxyl radicals are artificially produced inside the reactor from the photolysis of water vapor and pyrrole reacts with them once formed ([pyrrole] 60-70 ppbv, [OH] 40-50 ppbv). When ambient air flows inside the reactor, more molecules can react with OH, hence a competition with pyrrole for the generated OH starts.

A full experiment with the CRM is represented with the diagram in Fig. 2.2. In summary:

- Pyrrole diluted in dry nitrogen and dry zero air enters into the reactor and its concentration is monitored as C0;
- The UV lamp is switched on, pyrrole absorbs UV light and undergoes photolysis, its concentration decreases and is monitored as C1;
- The dry nitrogen flow passes through a bubbler containing milliq water, it is humidified and dilutes pyrrole with zero air. Water vapors photolysis with the UV lamp produces OH radicals, pyrrole reacts with OH, its concentration decreases and it is monitored as C2;
- Ambient air is sampled into the reactor. Ambient reactive gases compete with pyrrole

for the OH radicals and pyrrole concentration increases due to the competitive reaction. Pyrrole concentration is monitored as C3;  
 – Alternate switches between C2 and C3 make an accurate determination of the OH reactivity in ambient air possible.

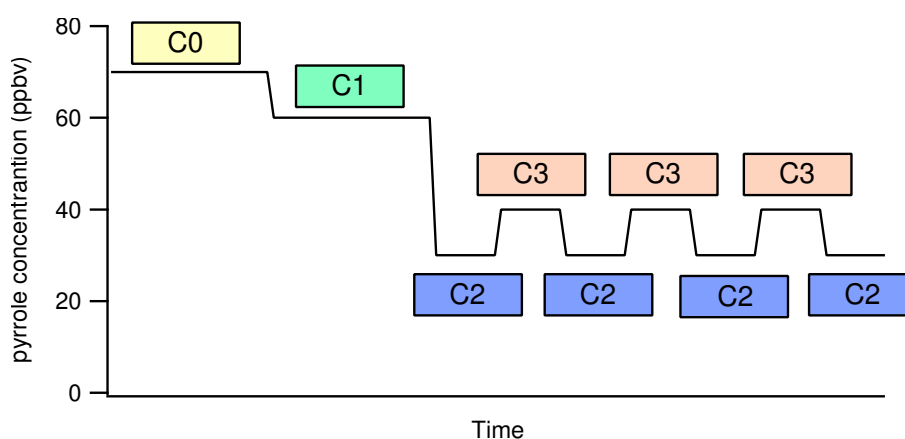


**Figure 2.2:** Example of experiment with the Comparative Reactivity Method instrument. Pyrrole initial concentration is recorded as C0; after lamp is switched on pyrrole concentration is measured as C1; OH are produced from photolysis of water vapor and concentration of pyrrole after reaction with OH is C2; ambient air is sampled and reactive molecules react with OH, pyrrole is measured as C3.

### 2.2.2 Derivation of the basic equation for CRM

The expression to determine the OH reactivity of the analysed sample is derived in terms of C1 (initial concentration of pyrrole), C2 (background concentration of pyrrole) and C3 (concentration of pyrrole after competition for air reactants), see Fig. 2.2.

The hydroxyl radical is lost in a two component mixture consisting of pyrrole and air in the following way:



leading to:

$$-\frac{d[\text{OH}]}{dt} = k_{\text{pyrrole}+\text{OH}}[\text{OH}] [\text{pyrrole}] + k_{\text{air}+\text{OH}}[\text{OH}] [\text{air}] \quad (2.5)$$

Where  $k_{pyrrole+OH}$  is the rate coefficient of the reaction of pyrrole with OH,  $k_{air+OH}$  is the rate coefficient of the reaction of all reactive components in air with OH and  $[air]$  is the summed concentration of all air components.

It is assumed that pyrrole reacts with OH following the pseudo first order reaction kinetics, hence  $[pyrrole] \gg [OH]$ , hence reaction of OH with pyrrole is given by eq. (2.6), and reaction of OH with air is given by eq. (2.7)

$$R_{pyrrole} = k_{pyrrole+OH}[pyrrole] \quad (2.6)$$

$$R_{air} = k_{air+OH}[air], \quad (2.7)$$

with  $R_{pyrrole} + R_{air}$  being the total loss rate of OH.

Considered that all OH is lost due to reactions with pyrrole and air, the change in pyrrole concentration (C1-C3) is calculated by eq. (2.8)

$$(C1 - C3) = \frac{R_{pyrrole}}{R_{pyrrole} + R_{air}}[OH] \quad (2.8)$$

Being  $[OH] = (C1 - C2)$  and  $[pyrrole] = C1$ , eq. (2.8) is rearranged to get:

$$k_{OH} = \frac{C3 - C2}{C1 - C3} k_{pyrrole+OH} C1 \quad (2.9)$$

With  $k_{OH}$  being the reactivity in ambient air ( $R_{air}$ ), C1, C2, C3 concentrations of pyrrole at different stages of the experiments.  $k_{pyrrole+OH}$  rate constant of the reaction between pyrrole and OH =  $(1.20 \pm 0.16) \times 10^{-10} \text{ cm}^3 \text{ molecule}^{-1} \text{ s}^{-1}$  (Atkinson et al., 1984; Dillon et al., 2012). Since concentrations have unit of molecules  $\text{cm}^{-3}$  and the rate constant of reaction of  $\text{cm}^3 \text{ molecules}^{-1} \text{ s}^{-1}$ ,  $k_{OH}$  has the unit  $\text{s}^{-1}$ , corresponding to the inverse of the lifetime of the OH radicals.

### 2.2.3 The reactor

Figure 2.3 shows a schematic of the glass flow reactor used for a CRM experiment. The length and volume of the glass reactor are approximately 14 cm and 94  $\text{cm}^3$ , respectively. The typical flow rate achieved inside the reactor ranges from 250 sccm to 350 sccm. Pyrrole gets mixed with zero/ambient air just before entering one arm of the reactor, while dry or humidified  $\text{N}_2$  enters from a second arm, leaving the other three arms to the UV lamp, an exhaust and the detecting module (Fig. 2.3). Nitrogen is dry at the first stages of the experiment (C0 and C1), when dry conditions are required to avoid OH radicals been

formed inside the reactor. Humidification of nitrogen is accomplished by passing gaseous nitrogen through a bubbler where ultrapure water is kept at room temperature. The lamp is a Pen ray spectral Hg vapour lamp (LOT Oriel, France) which emits at 184.9 nm, 253.6 nm, 312.5 nm, 365 nm and 435.8 nm; water vapour absorbs at 184.9 nm and dissociates to form OH radicals. The "wood's horn" shape opposite to the arm where the lamp is placed was designed in order to minimize reflection of the lamp and photochemical reactions along the length of the reactor. The total incoming flow rate is driven by the pump at the exhaust arm and the incoming flow at the detector. Flows are adjusted in a way that the total flow entering the reactor (pyrrole+ air+ N<sub>2</sub>) is slightly higher ( $\approx 10$ -20 sccm) than the total flow exiting the reactor (exhaust+ detector). This is achieved by using a mass flow controller for each component, except for the flow entering the detector, which is regulated through an inlet valve. The overflow ( $\approx 10$ -20 sccm) is monitored through a Tee-piece placed in line with the zero air gas line, before the mixing with pyrrole. Such opening is useful to monitor any change in flows occurring in the system and to prevent over-pressure building within the reactor, ensuring atmospheric pressure all times. Alternate measures of C2 and C3 (mixing pyrrole with zero air or ambient air, respectively) are achieved through a 4-way valve where zero air or ambient air is alternatively driven inside the reactor.

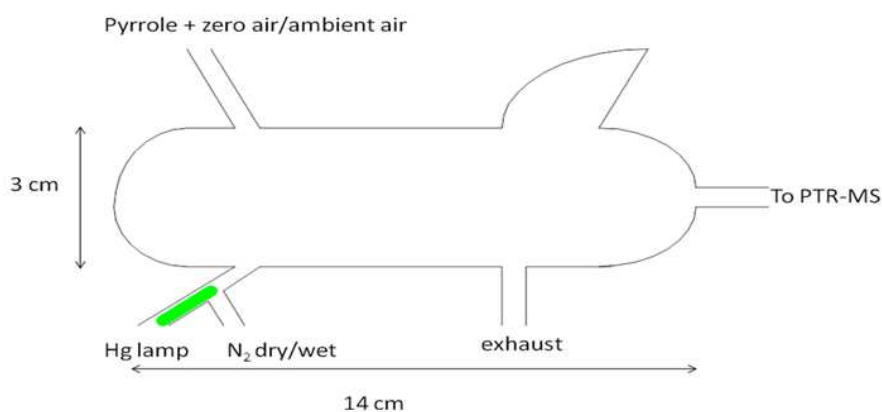


**Figure 2.3:** Simplified drawing of the flow reactor in the Comparative Reactivity Method instrument. Labels show the size of the reactor and the use of each arm. It is made out of glass with an inner coating in PTFE.

## 2.2.4 The detector

The detector is most of the cases a Proton Transfer Reaction-Mass Spectrometer (PTR-MS). This instrument has been extensively used to monitor volatiles concentration and is already described in Sect.2.1.1-2.1.3. Pyrrole is detectable with the PTR-MS since its

proton affinity is larger than water (209.2 kcal/mol and 165.2 kcal/mol respectively) and its signal can be easily monitored unambiguously at the protonated  $m/z$  68 ( $C_4H_5NH^+$ ) without any fragment. The protons and water clusters signals of PTR-MS at  $m/z$  21 (number of protons),  $m/z$  37 (first water cluster  $H_3O^+ \cdot H_2O$ ),  $m/z$  55 (second water cluster,  $H_3O^+ \cdot (H_2O)_2$ ) are also required to be monitored. Additionally, other molecules as methanol ( $m/z$  33), acetaldehyde ( $m/z$  45), acetone ( $m/z$  59) can be measured to trace any issue occurring inside the system, for instance the presence of a leakage or impurities. Recently, Kumar and Sinha (2014) presented an advantageous use of the same PTR-MS for detecting the OH reactivity with the CRM and measuring ambient volatiles concentration. The use of the same instrument for the two measures alternately permits to get crucial insights into the missing reactivity: it can measure the amount of a molecule in ambient air, and its amount after reaction with OH inside the reactor, which can be used to determine the rate coefficient of an "unknown" molecule with OH. Such application is still under study and looks promising for those groups whose PTR-MS has a high sensitivity also for larger masses. Alternatively, the CRM can also operate with a Gas Chromatography Photo Ionization Detector (GC-PID, Noelscher et al., 2012a). Such system is smaller (260x 160x 400 mm and 650x 1660x 550 mm), more portable (8 kg and 150 kg), less power consuming (50 W and 1500 W) and less expensive (18.000 euros and 180.000 euros) compared to the PTR-MS. In a GC-PID the air is drawn through a particle filter into the system. A short capillary column is used to separate the various VOCs and water from the sample matrix. The separated molecules are then selectively ionized by UV light in the detection cell. The formed ions are accelerated by an electric field to a collector module which gives a chromatogram whose peak area is off-line analysed to determine the mixing ratio of pyrrole. The disadvantages of this system are: possible interference of toluene, since its retention time overlaps with pyrrole (35-55 s); decrease in sensitivity over long operational time (less than 10% deviation in sensitivity over 5 days, 35% of deviation after 10 days); time resolution between 5-20 minutes. Pyrrole is calibrated for both detectors at dry and wet conditions. In both cases a good linearity is found and wet pyrrole usually shows a higher sensitivity compared to dry pyrrole (about 10% different for PTR-MS).

### 2.2.5 Method calibration

The CRM is calibrated using different reactive gas standards, whose concentration is known and their rate coefficient with OH well established. The measured reactivity calculated from eq. (2.9) is then compared to the injected, or theoretical reactivity, which is the one expected from the test gas used for calibrating the instrument. The injected

reactivity is calculated according to eq. (2.10):

$$R = k_{testgas+OH}X_{testgas}, \quad (2.10)$$

with  $k_{testgas+OH}$  being the rate coefficient of the reaction between the test gas and OH, and X the concentration of the test gas inside the reactor. Common test gases used to perform this test are propane ( $1.1 \cdot 10^{-12} \text{ cm}^3 \text{ molecules}^{-1} \text{ s}^{-1}$ ), ethane ( $2.4 \cdot 10^{-13} \text{ cm}^3 \text{ molecules}^{-1} \text{ s}^{-1}$ ), isoprene ( $1 \cdot 10^{-10} \text{ cm}^3 \text{ molecules}^{-1} \text{ s}^{-1}$ ) and mixtures of hydrocarbons (see for instance Kim et al., (2011)). Such molecules are chosen as proxies for atmospheric reactive gases. Test gases are mixed with zero air before entering the system, then the mixture test gas and zero air mixes with pyrrole and enters the reactor. Mixing can be achieved by using a simple tee-piece, or a mixing vessel where a higher surface/volume ratio is achieved. An excellent linearity and good accountability (slope of the linear regression of the measured vs. the injected reactivity) are usually found. Depending on the chosen test gas and concentration, different range of reactivity can be investigated. So far, an excellent linearity for the method has been reported until  $1200 \text{ s}^{-1}$  (Kim et al., 2011).

## 2.2.6 Interferences

The following possible interferences have been found for the Comparative Reactivity Method:

– Photolysis of pyrrole

Photolysis of water vapor by the UV Hg lamp is needed to produce OH radicals, but it also constitutes an instrumental interference for this technique. The pen ray Hg lamp (LOT Oriel, France) emits at 184.9 nm, 253.6 nm, 312.5 nm, 365 nm and 435.8 nm; pyrrole can absorb at the lamp emission lines therefore its initial concentration can be affected during an experiment. As already discussed in this chapter, pyrrole concentration is measured before (C0) and after photolysis (C1), with the latter being the one considered for calculations. Therefore, the experimental stage of C1 permits to exclude any photolysis interference for pyrrole.

– Differences in humidity among C2 and C3

One of the principal interferences identified for this method is the different humidity in the reactor when sampling ambient air (Sinha et al., 2008). Such differences are observed between the level C2 (background level of pyrrole when OH is produced in the reactor) and C3 (concentration of pyrrole after injection of ambient air inside the system) and often lead to an under or over estimation of the value of reactivity in ambient air. To track such changes we look at the  $m/z$  68 (pyrrole) and  $m/z$  37/ $m/z$  19 ratio (first water cluster

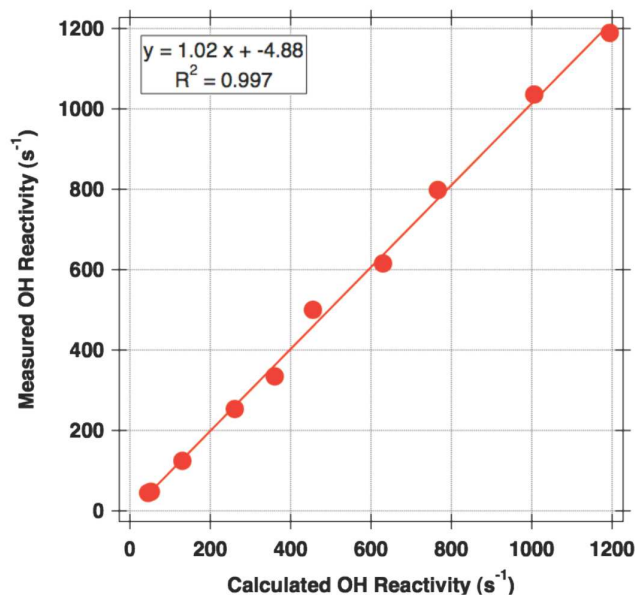


**Figure 2.4:** Measured OH reactivity vs Calculated OH reactivity reported by Kim et al., (2011). Results were obtained from laboratory calibrations and used to analyse the data collected during the CABINEX field campaign (Community Atmosphere-Biosphere INteractions Experiments) in 2009. A standard gas mixture including methanol, acetonitrile, acetaldehyde, acetone, isoprene, methyl vinyl ketone, benzene, toluene and camphene was used for the tests.

divided by the number of protons) in the PTR-MS during ambient measurements, and perform experiments to assess a correction factor to apply on the raw data of reactivity. The experiments are usually performed by varying the humidity of the C2 level and look at the dependency of pyrrole to such variation (Noelscher et al., 2012; Michoud et al., 2015 and Zannoni et al., 2015).

– OH recycling due to NO

When the UV lamp is switched on, photolysis of water vapor occurs according to the reaction R 12:



Leading to



When NO is present in ambient air it can react with HO<sub>2</sub> recycling OH radicals inside the reactor:



To determine the interference that NO has on the instrument, experiments with a standard gas of NO, and standards of reactive test gases (e.g. propane, ethane, isoprene) are performed and a correction for the data is obtained.

## 2.2.7 Data processing

Values of OH reactivity determined with eq. (2.9) are corrected for the interferences encountered in the set-up of the CRM and discussed in section 2.2.6. Corrections are performed at different steps and factors determined from empirical or theoretical tests conducted on the system over time are applied.

– Humidity differences between C2 and C3 correction:

The interference is monitored through m/z 68 and m/z 37/m/z 19 (Michoud et al., 2015 and Zannoni et al., 2015). The ratio m/z 37/m/z 19 is a measure of water content inside the PTR-MS, see also Ammann et al., (2006). When the ratio m/z 37/m/z 19 is smaller during the measure of C2 compared to the one during C3 (for instance when using synthetic dry clean air for C2), it will result in a smaller difference between C2 and C3 hence an underestimation of ambient OH reactivity. On the other hand, if the m/z 37/m/z 19 ratio is larger during C3 compared to the one during C2, then the ambient OH reactivity will be overestimated. Experiments are performed by introducing a known amount of zero air at different humidity inside the reactor while the instrument is measuring C2. The dependency of the difference in the observed C2 on the difference of m/z 37/m/z 19 is investigated and used to correct the ambient C2 value.

A linear least squares fit describes the dependency of C2 on m/z 37/m/z 19. The slope of the fit (coefficient p in eq. (2.11)) obtained from the experimental tests is then used to correct the C2 value during ambient measurements in the following way:

$$C2_{corrected} = C2 + p[(m/z37/m/z19)_{duringC3} - (m/z37/m/z19)_{duringC2}] \quad (2.11)$$

– NO interference correction:

The change in measured reactivity is determined from experiments conducted at different reactivity values under incremental additions of a NO gas standard into the system



(Fig. 2.5). Additions of NO are performed by diluting NO first with air, then with a test gas (for reactivity  $> 0 \text{ s}^{-1}$ ), then with pyrrole, before entering the reactor. When NO is added into the system, reactions R2, R3 and R4 occur, and OH recycling is evident by the decrease of pyrrole concentration measured by the detector (Fig. 2.5). NO is first added when the system is measuring C2, which corresponds to examine the effect of NO on  $0 \text{ s}^{-1}$  OH reactivity. Thereafter, the same incremental additions of NO are conducted while the system is measuring C3. For this purpose, a test gas standard can be used to reach higher values of reactivity and differences among the C2 level observed at  $0 \text{ s}^{-1}$  (Fig. 2.5) are added to the observed change on C3 to calculate the measured reactivity. The absolute value of reactivity (i.e. the change in C2 level due to successive additions of NO) has a positive linear dependency with the concentration of NO. Such dependency is affected by a change in slope at 20 ppbv of NO, reported by Dolgorouky et al., (2012) and confirmed by us using a different set-up (see section 2.3.2).

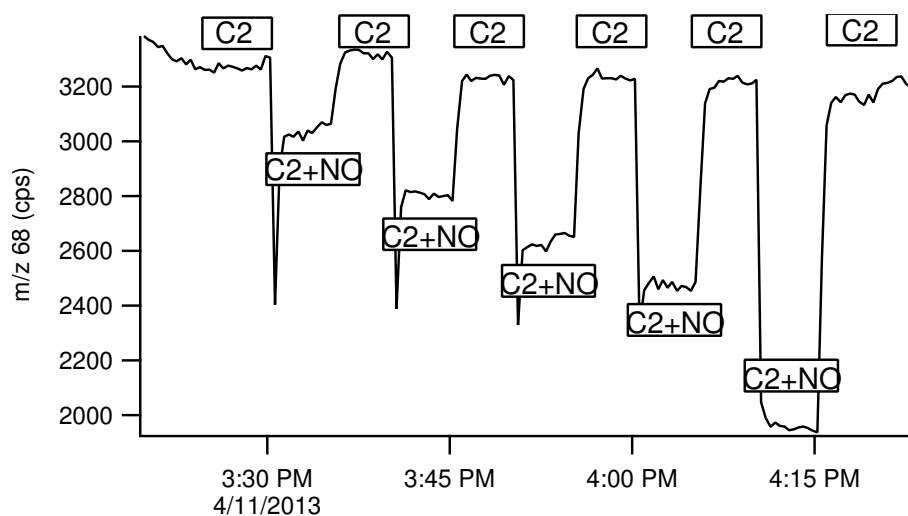


**Figure 2.5:** Pyrrole signal measured by the PTR-MS during an experiment for quantifying the NO interference on the CRM instrument. Consecutive additions of different and known amount of a NO standard lead to negative values of reactivity measured by the instrument (difference between C2+NO and C2 signals). In this example, NO additions are conducted on  $0 \text{ s}^{-1}$  OH reactivity, hence on the level C2.

Michoud and coauthors (2015) have reported a quadratic linear dependency of NO on different values of reactivity, which also depends on different kinetics regimes, i.e. pyrrole/OH ratio, in the system (Fig. 2.6). The difference between C3 measured and expected (decrease in reactivity) is higher for higher concentrations of NO introduced into the system and higher for higher pyrrole/OH. For 100 ppbv of NO inside the reactor they found an absolute change in reactivity of  $80 \text{ s}^{-1}$  at pyrrole/OH equal to 3.9, which is the double

observed for the same concentration of NO under pyrrole/OH of 1.6.

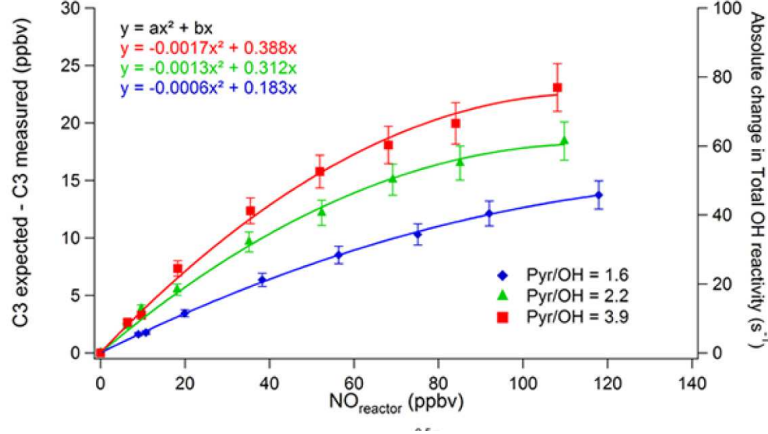


**Figure 2.6:** Detailed empirical investigations reported in Michoud et al., (2015) showing the NO interference on the reactivity and its dependency on the kinetics regime adopted inside the system. In the window of [pyrrole]/[OH] usually adopted for ambient measures of OH reactivity with the CRM it is reported a factor of 2 difference in the absolute change of reactivity for 100 ppbv of NO.

Therefore they derived the following expressions to correct for NO interferences:

$$C3_{corrected} = C3_{measured} + \Delta C3 \quad (2.12)$$

$$\Delta C3 = \left( a_1 \frac{[pyrrole]}{[OH]} + a_2 \right) [NO]^2 + \left( b_1 \frac{[pyrrole]}{[OH]} + b_2 \right) [NO] \quad (2.13)$$

NO<sub>2</sub> has a similar effect as NO, since it can be converted into NO which can lead again to OH recycling and interfere in the measures of OH reactivity. Although it would be easier thinking that NO is generated from the photolysis of NO<sub>2</sub>, Michoud et al., (2015) speculated that heterogeneous chemical processes on stainless steel pieces of the system might be the real cause of such conversion. The experimental tests conducted by Michoud et al., (2015) suggest an average conversion of NO<sub>2</sub> into NO of 24% ( $\pm 9\%$ ,  $1\sigma$ ). Using a similar approach as the one reported for NO, the correction for NO<sub>2</sub> interference is conducted on the level C3, using a quadratic regression from experimental calibrations with incremental additions of NO<sub>2</sub> into the reactor. It was found that the correction is independent on the [pyrrole]/[OH] and the magnitude for NO<sub>2</sub> correction is lower than the one for NO.

–pseudo-first-order kinetics assumption

Equation (2.5) is derived from the assumption that pyrrole reacts with OH according to the pseudo first order kinetics ( $[\text{pyrrole}] \ll [\text{OH}]$ ). However, the CRM is often operated in the  $[\text{pyrrole}]/[\text{OH}]$  regime between 1.2-3. Therefore, data of reactivity acquired at lower pyrrole/OH are corrected to be in the pseudo first order kinetics regime. Two approaches have been developed so far to correct the data: a theoretical approach, as reported by Sinha et al., (2008) and Noelscher et al., (2012), and an experimental approach, as reported by Michoud et al., (2015) and Zannoni et al., (2015). The theoretical correction is based on the FACSIMILE model which is built on simple numerical simulations where an initial concentration of OH is reacting first with pyrrole, and then with pyrrole and a hydrocarbon chosen as a proxy for ambient air (rate coefficient with OH  $\approx 2 \cdot 10^{-13}$ ) at different concentrations, for an OH reactivity in ambient air between 8 and  $300 \text{ s}^{-1}$ . However, the theoretical approach is based on simple simulations, where only one competition reaction is computed and other reactions, as radicals-radicals are not considered.

The experimental approach is based on the calibrations conducted on the CRM with different test gases. A known amount of an external gas standard whose reaction rate with OH is well established is mixed in line with zero air and is injected inside the reactor. The concentration of such gas in the reactor and its rate coefficient with OH permits to determine the injected OH reactivity with eq. (2.10). The calibrations are usually performed over a broad range of OH reactivity and for different  $[\text{pyrrole}]/[\text{OH}]$  ratio. Indeed the  $[\text{pyrrole}]/[\text{OH}]$  can vary over time due to: flows fluctuations affecting the dilution of pyrrole inside the instrument; humidity affecting the production of OH radicals in the system and lamp efficiency. Changes applied to these drivers permit to obtain different  $[\text{pyrrole}]/[\text{OH}]$  and investigate the response of the CRM under such changes. From these tests we can derive a correction factor used to process the data for each  $[\text{pyrrole}]/[\text{OH}]$  in the system. Figure 2.7 shows an example of plot where a correction factor (inverse of the slope of the regression analysis of measured reactivity/theoretical reactivity of the calibration) is represented versus the  $[\text{pyrrole}]/[\text{OH}]$ . The empirical determination of the correction to apply for the kinetics regime strictly depends on the reactor itself and operational settings deployed during the experiments. However, similar trends are always observed: the correction factor decreases for higher  $[\text{pyrrole}]/[\text{OH}]$ , when the regime is closer to pseudo-first-order conditions; larger differences among tests are usually seen for lower correction factor, when the regime is further from pseudo-first-order conditions. Since small differences among reactors (as lengths of the arms, pointing of the arms) can lead to slight different behaviors, it is important that each reactor is qualified experimentally in order to take such differences into account. The correction factor is then multiplied by the measured OH reactivity to obtain the corrected OH reactivity:

$$R_{corrected} = R_{measured} \times F, \quad (2.14)$$

With  $F$  being the correction factor determined as the slope (or a mean value) from the experimental calibrations.

– dilution inside the flow reactor

The dilution factor is given by the ratio between the sampling flow rate and the total flow rate inside the reactor (sum of flow rates of  $N_2$ , pyrrole and ambient air). This value is multiplied for the corrected OH reactivity to obtain the reactivity in ambient air.

Figure 2.7 provides an example of the different impacts of the above described corrections on the raw data of reactivity for ambient data collected during a field experiment. Corrections are cumulative and applied on the raw values of reactivity in the following order: (i) correction for humidity differences, (ii) correction for pseudo-first-order conditions and (iii) dilution (NO correction has not been considered for this specific case due to the low NO concentration observed in ambient air).

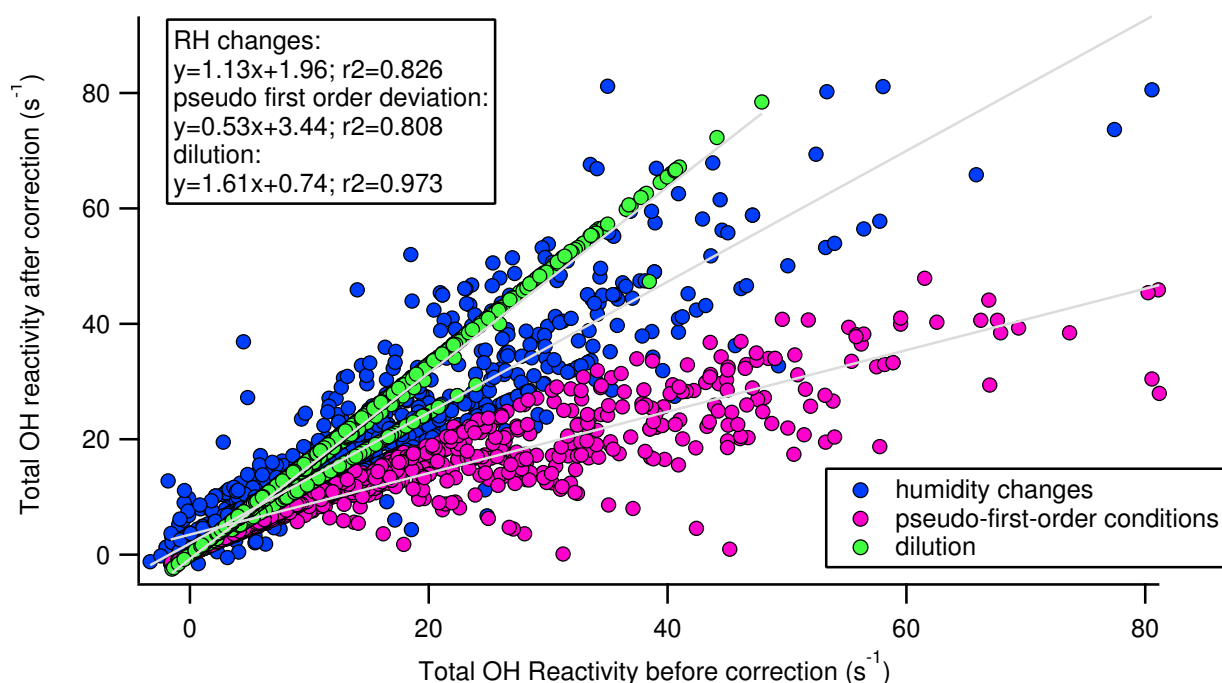


**Figure 2.7:** Weights of consecutive corrections applied to the raw data of OH reactivity for ambient measurements. The specific example shows the impact of the corrections on the data processed for the field campaign CANOPEE.

## 2.2.8 Limit of detection and measurement uncertainties

The limit of detection (LOD) for CRM measures corresponds to the least detectable difference between the two levels C2 and C3. It is calculated from a measure of C2 (longer than the usual 5 minutes C2), whose variability is considered as 1 standard deviation. Three times the standard deviation is then considered as C3 and the reactivity from eq. (2.5) is calculated for the given experimental C1, C2, and  $3\sigma$  the standard deviation of C2 as C3. A LOD around  $3 \text{ s}^{-1}$  is usually found for most CRM systems. The measurement uncertainty is calculated from the theory of the propagation of the errors and was found to be  $\approx 20\%$  by Sinha et al., (2008). Such uncertainty includes uncertainty in the pyrrole+OH rate coefficient of reaction  $(1.20 \pm 0.16) \times 10^{-10} \text{ cm}^3 \text{ molecules}^{-1} \text{ s}^{-1}$ , flow fluctuations (10%), uncertainty on the pyrrole standard (5%) and instrumental precision (6%). A detailed description of the calculations for the overall instrumental uncertainty (systematic+precision+ corrections of the data processing) is provided by Michoud et al., (2015). The largest source of uncertainty in such calculations is given by NO. For OH reactivity above  $15 \text{ s}^{-1}$  and NO below 30 ppbv the total uncertainty ranges between 17-25%, it increases up to 70% for NO below 80 ppbv and reaches 200% for NO larger than 80 ppbv. The instrumental precision depends on the OH reactivity value and ranges from 50% at low reactivity (around the LOD) to less than 4% for OH reactivity higher than  $50 \text{ s}^{-1}$ . When systematic errors are included the total uncertainty reaches about 20% for OH reactivity higher than  $15 \text{ s}^{-1}$ .

## 2.3 CRM-LSCE

### 2.3.1 Optimization of the Comparative Reactivity Method at LSCE

A Comparative Reactivity Method instrument was already existing in our laboratory and successfully deployed during the field work MEGAPOLI for measuring ambient OH reactivity in Paris (Dolgorouky et al., 2012). However, some improvements of the instrument were needed at that stage. Therefore, I built and qualified a new CRM at our institute during my PhD project. Since I was involved into two field works to deploy our CRM, I improved our instrument according to the field works constraints.

Below are summarized the main points that were achieved throughout these years, some of these points will be explained in more detail in chapter 3:

- (1) To improve the performance of the CRM:

– increase of the signal sensitivity

In order to conduct reactivity measurements at remote sites, where ambient OH reactivity can be close to the LoD of the instrument ( $3 \text{ s}^{-1}$ ,  $3\sigma$ ) such as the experience of the field campaign "ChArMEx", we carried out several tests on the instrument flows regime. Choosing the best "flows regime" is a matter of compromise to have a good sensitivity and reduced interferences. As a matter of fact, the lower is the signal of pyrrole the lower is its noise. Hence we considerably reduced the flow of pyrrole used in the previous set-up (to 2 sccm from 5 sccm for the same dilution). In addition we changed the proportions between the other flows entering the instrument and increased the final dilution of pyrrole. We also increased the dwell time of acquisition of pyrrole in the PTR-MS to 20 s. We obtained a very clean signal of pyrrole ( $1\sigma$  SD on C2  $\sim 0.3$  ppbv) which permitted to distinguish an OH reactivity down to  $3 \text{ s}^{-1}$ . It is important to notice that for very low levels of reactivity valves and pressure effects in the reactor when changing from C2 to C3 have greater effects resulting in higher difficulty in the data evaluation for data collected at remote sites. A further improvement would be to change the sampling time depending on the field sites.

– reduction of the temperature dependency

When the instrument was deployed on our first field work, probably due to the high ambient temperature reached during those days, we discovered that our system was very sensitive to temperature changes. Therefore, we equipped our system with a temperature regulated box set at  $25 \pm 2^\circ \text{ C}$ .

– flows fluctuations and monitoring

An opening for continuous flows check was realized in line with the zero air gas line to control any flow fluctuation or change in the system. Indeed at the opening we should always measure a flow corresponding to the difference between the total flow set to enter the reactor and the total flow set to exit the reactor. For extensive periods of operation of the instrument we observed some flow fluctuations. The reason for that was due to the use of pyrrole in the method, which can polymerize in the lines and clog at the PTR-MS first tee when the inlet line gets restricted to the capillary line. We did not solve this issue, unless doing a fast cleaning of the PTR-MS tee and capillary line as soon as we observed any change at the overflow rate. However, regulating the temperature of the instrument and insulating all lines of pyrrole seemed to reduce the effects of polymerization.

– automatic ambient measurements

The addition of a 4-ways automatic valve to the set-up permitted to conduct automatic ambient reactivity measurements. The valve operates in a way that the system is sampling either zero air (C2) while the sampling line is flushed by a second pump, either ambient

air (C3) while the pump flushes the line for zero air. The valve automation is programmed through the PTR-MS control software and the switching time between the two positions is usually conducted every five minutes (Fig. 2.8).

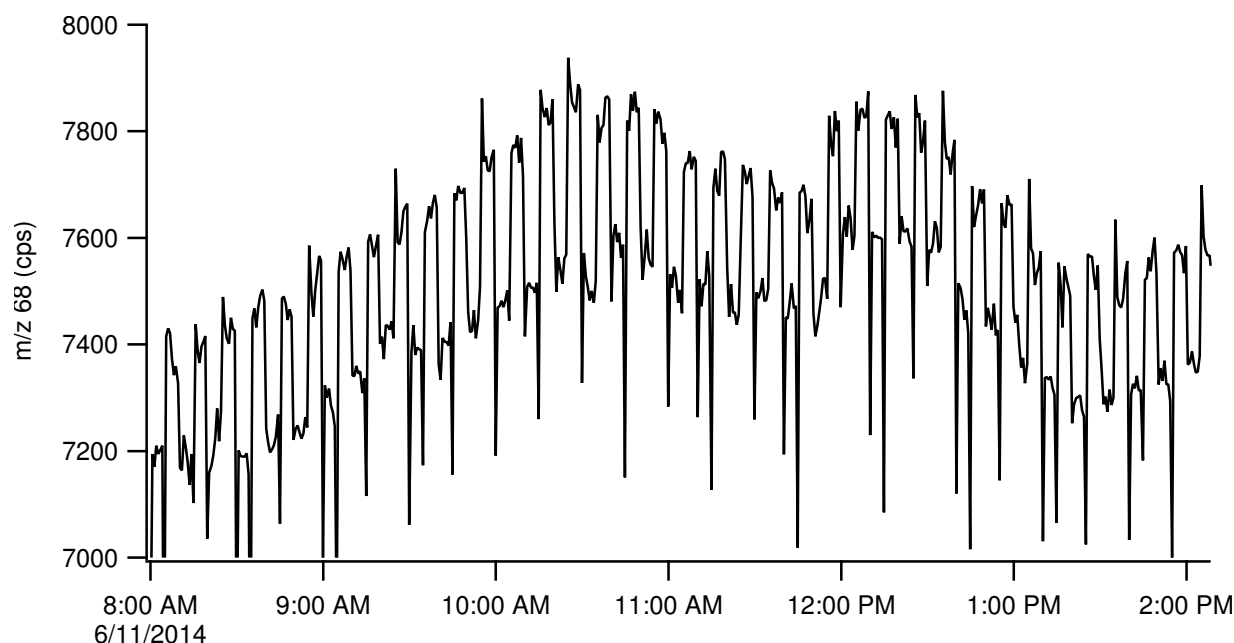


**Figure 2.8:** Automatic alternated switches between C2 and C3 to determine the total OH reactivity for ambient measures.

Before introducing a valve for automated measures, OH reactivity at LSCE was determined by interpolating over C2 background levels acquired 2-3 times per day, which brought an additional uncertainty of 15% on the final results of OH reactivity (Dolgorouky et al., 2012).

– reduction of the time constraints for measuring C1

During an intercomparison exercise carried out in summer 2013 at the field site of Ersa in Corsica, France with the help of Sebastien Dusanter from Mines Douai, we developed a way to conduct faster measures of C1 with the CRM. The time needed to acquire C1 (i.e. initial concentration of pyrrole after photolysis) is often challenged by the lamp warming up times and reactor dryness. Especially when checks are done after ambient observations, where the system has run for several days under very humid conditions, acquisition times for C1 can be extremely long (up to a day for the reactor of Mines Douai for instance). Basically, if the reactor has still some water vapor content and the lamp is on, even if the greater production of OH radicals is reduced, the acquisition of C1 will be still affected by the presence of OH radicals. With the scavenger method (on the field realized with methane (Zannoni et al., 2015), in the laboratory realized with propane as well (Michoud

et al., 2015)) a known amount of highly concentrated gas which cannot be measured by the PTR-MS (i.e. having a proton affinity smaller than water, see section 2.1.2) is introduced in the system while measuring C2. Methane will scavenge all the OH radicals present in the system, while this has not to be dried and pyrrole signal quickly reaches the C1 level.

– detailed protocol for deriving the corrections for the instrumental interferences

The intercomparison with the CRM constructed at Mines Douai was of great help to elucidate a common procedure to evaluate ambient reactivity data. As described in section 2.2.6 the data evaluation is a long process for the CRM technique. Qualifying the instrument and asses an experimental way to correct the data is almost half of the work to obtain results of OH reactivity. The qualification section (2.2.5) and data processing section (2.2.7) report extensively a procedure we adopted that was partly discussed during the intercomparison exercise (especially for what concerns the humidity changes and kinetics regime correction). More information about the intercomparison exercise, tests and ambient measurements can be found in Zannoni et al., (2015).

(2) To reduce the possible interferences found for CRM:

– reduced photolysis rate Photolysis of water vapor by the UV Hg lamp is needed to produce OH radicals, but it also constitutes an instrumental artifact for this technique. Pyrrole can absorb at the lamp emission lines therefore its initial concentration can be affected during an experiment. As already discussed in this chapter, pyrrole concentration is measured before (C0) and after photolysis (C1), with the latter being the one considered for calculations. The experimental stage of C1 permits to exclude any photolysis interference from the method. However, some ambient species may also absorb at the lamp emission lines, generating other species which can further react with OH. It is important therefore to keep the photolysis rate in the instrument low. From laboratory experiments we observed that to minimize photolysis we can play on some parameters, such as: (i) pyrrole concentration, the lower the concentration the lower its photolysis, (ii) lamp intensity, the lamp power supply permits to change between two different intensities (10 mA, 18 mA), (iii) the lamp position: the deeper it is placed into the reactor the higher is the photolysis. By working on these parameters we reduced the photolysis to 5% for some experiments, below 10% for all of them, from ~18-20% in the previous set-up.

– minimized changes in humidity differences between C2 and C3

To reduce changes between C2 and C3 we decided to use a catalytic converter to produce zero air. In such fashion, ambient air is scrubbed resulting in clean air (C2) with the same humidity of the sampled ambient air (C3). However, we still observe small changes in the humidity among C2 and C3, which explains why we are still correcting our data for such



changes. The best optimization would be therefore to humidify zero air to the exact value of humidity monitored in the sampled ambient air.

### 2.3.2 CRM-LSCE performance

Figure 2.9 shows the CRM built at LSCE during my PhD project. The instrument has been extensively qualified after its construction in the laboratory and on the field during the field works conducted in these three years. A full instrument qualification includes:

- calibration of pyrrole inside the CRM for dry and wet conditions.

A sensitivity around 10 ncps ppbv<sup>-1</sup> is found with the system being more sensitive for wet pyrrole than for dry pyrrole (in agreement with the trend reported by Sinha et al., (2009)).

- photolysis rate and [OH].

The photolysis rate is determined from the difference between the levels C0 and C1, while [OH] inside the reactor is given by the difference between C1 and C2. As already mentioned in this chapter, lamp intensity and position, dilution of pyrrole and nitrogen flow rate need to be adjusted to have a low enough photolysis rate and high enough [OH]. A compromise among these parameters is needed in order to reduce secondary photochemistry effects and measuring OH reactivity in environments with high loadings of reactive compounds. In CRM-LSCE photolysis of pyrrole is below 10% and [OH] between 40-50 ppbv.

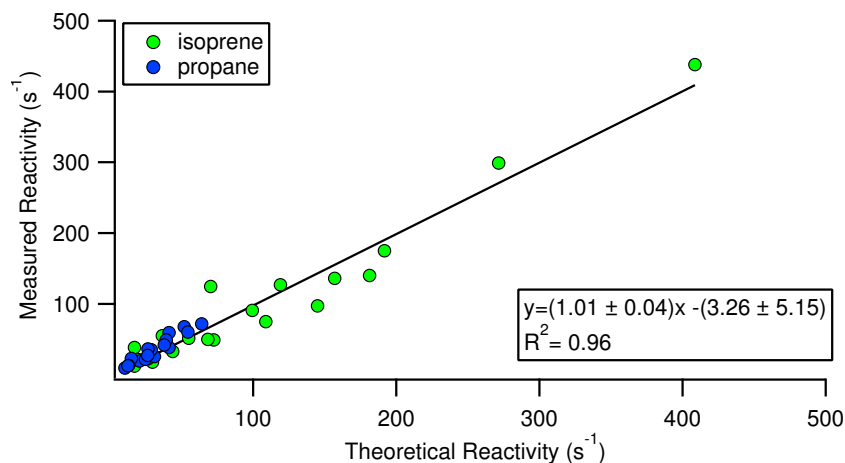
- Calibration of the CRM with test gases.

Figure 2.9 shows the calibration conducted with propane and isoprene as test gases for a large pyrrole/OH range, varying between 2 and 9. A linear dependency between the measured and injected reactivity is obtained for a range of reactivity between the LOD of our CRM (3 s<sup>-1</sup>) and 500 s<sup>-1</sup>. A good agreement (slope of 1.01) and good correlation (R<sup>2</sup>=0.96) is also obtained.

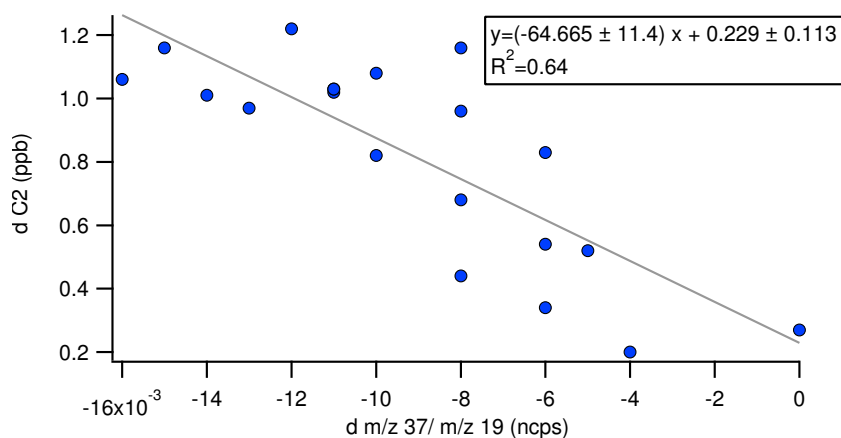
- Assess of the corrections for humidity and NO interferences, and pseudo first order kinetics deviation:

Figure 2.10 shows the variation of C2 according to different humidity changes in the sampled air. The slope of linear fit between dC2 and d m/z 37/m/z 19 is used in eq. (2.11) as the value p to correct for humidity changes.

Fig. 2.11 shows the changes in reactivity for increasing NO concentration. CRM-LSCE is sensitive to NO levels higher than 4 ppbv and shows a variation in reactivity of about 50 s<sup>-1</sup> when 50 ppbv of NO are introduced inside the reactor. The difference in slope for the



**Figure 2.9:** Linearity range of OH reactivity for CRM-LSCE. The calibrations were conducted with isoprene and propane over the reactivity range of 500 s<sup>-1</sup> and the pyrrole/OH varying between 2 and 9.



**Figure 2.10:** Humidity dependency on the C2 level. Difference between the C2 acquired when air is injected for an experiment and background C2 value reported versus the difference between m/z 37/m/z 19 when air is injected for an experiment and m/z 37/m/z 19 of background C2.

dependency of the absolute reactivity on NO observed in our instrument is in agreement with what reported in Dolgouroky et al., 2012. The interference of NO in our system has been investigated only until 50 ppbv of NO, this is because we have deployed our instrument only in unpolluted environments (remote site, forested site).

The correction factor for deviation from pseudo first order kinetics is obtained experimentally as described in section 2.2.7. Figure 2.12 shows that the correction factor linearly decreases for higher pyrrole/OH, towards the pseudo-first order kinetics conditions. A cor-

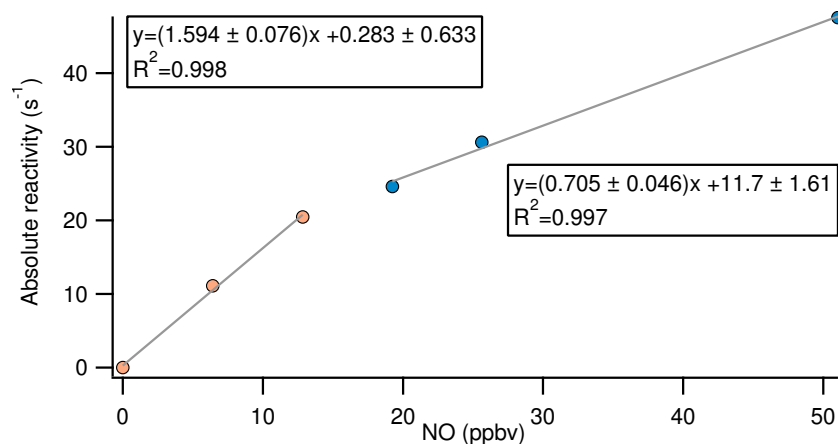


**Figure 2.11:** The absolute reactivity calculated from eq. (2.5) based on the signals of C2 and C2+NO reported in Fig. 2.6 is reported versus the concentration of NO present in the reactor. Linear least squares fits of the data show the same trend with different slopes below and above 20 ppbv of NO.

rection factor of 1 is reported for CRM-LSCE in the pyrrole/OH window of 3-4.5. Results in Fig. 2.9 were obtained with calibrations of CRM-LSCE with propane and isoprene.

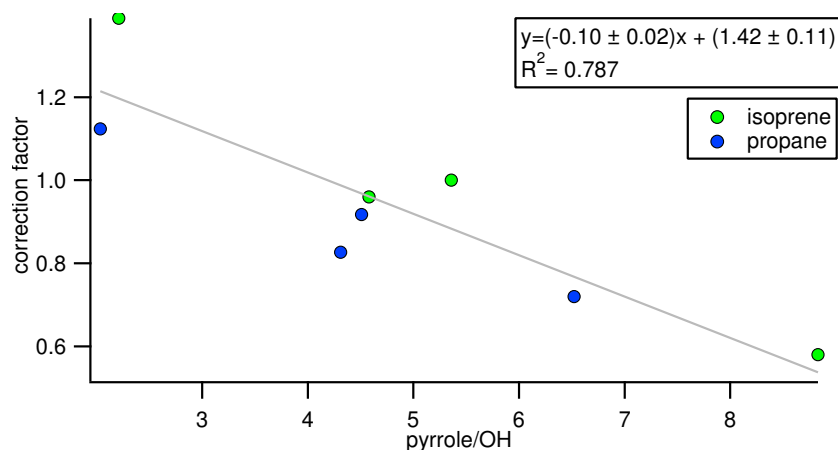


**Figure 2.12:** Correction factor represented in function of [pyrrole]/[OH] levels reached inside the instrument. Each data point corresponds to a different calibration performed with a test gas standard. The correction factor is calculated as the inverse of the slope of the regression analysis of the measured reactivity versus theoretical reactivity (see Fig. 2.4).

– LOD and uncertainty

CRM-LSCE has an LOD of  $3 \text{ s}^{-1}$  ( $3\sigma$ ). The total systematic uncertainty is 35%. It includes: uncertainty on the rate constant of reaction between pyrrole and OH, uncertainty associated to the concentration of the pyrrole standard, stability of the PTR-MS sensitivity

over time, humidity, pseudo first order kinetics and dilution corrections. For our system the largest sources of uncertainty are the stated concentration of the pyrrole standard from the producers (20%) and the correction for pseudo first order kinetics deviation (26%). The measures precision depends on the concentrations C1, C2, C3. Instrumental precision dominates in the low range of OH reactivity (below  $15 \text{ s}^{-1}$ ) while systematic errors are more influent for higher OH reactivity values. The overall uncertainty (systematic+ precision) is below 35% for OH reactivity higher than  $8 \text{ s}^{-1}$ , increases up to 50% for OH reactivity close to the instrumental LOD.

Figure 2.13 illustrates CRM-LSCE during the three years of my PhD project: in January 2013 (panel A) when it was built, in May 2013 (panel B) when it was used for the field work in Corsica, in April 2014 (panel C) during the field work in the forest of OHP, and finally in September 2015 (panel D) while I am writing this thesis.

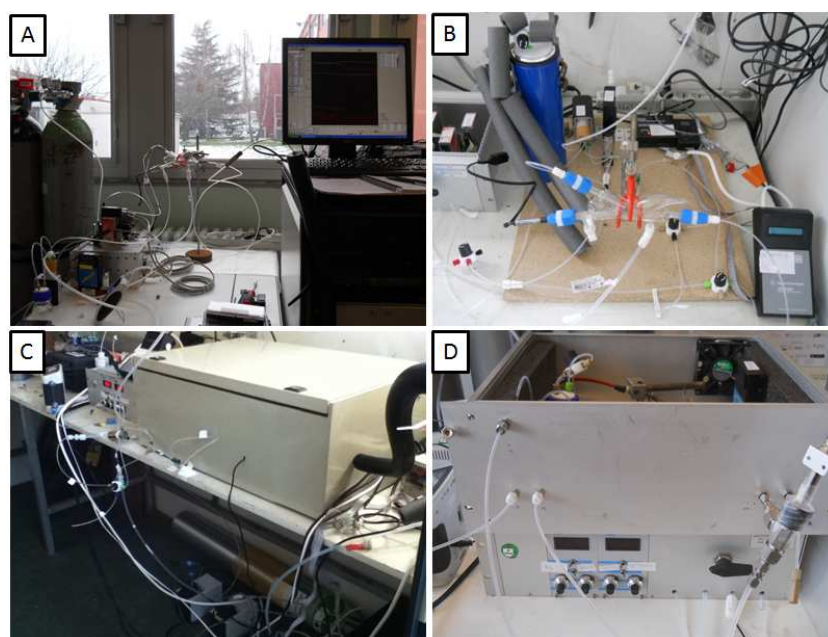


Figure 2.13: ...

### 2.3.3 CRM-LSCE: field deployment

We deployed our Comparative Reactivity Method instrument in the Mediterranean during one intercomparison exercise (Zannoni et al., 2015, see chapter 3) and two field campaigns (chapters 4 and 5) within the international projects ChArMEx (Chemistry-Aerosols in a Mediterranean Experiment) and Canopee (Biosphere-Atmosphere exchange of organic

compounds: impact of intra-canopy processes). We investigated two field sites, both located in the western Mediterranean basin, with different peculiarities and constraints.

The site chosen for the field work ChArMEx is located at Ersa, in the northern cape of Corsica. It is a receptor coastal site influenced by air masses coming from continental areas mainly enriched of anthropogenic pollutants and their oxidation products. It is also influenced by the dense Mediterranean maquis that surrounds the site, mainly composed by lower shrubs strong terpenes emitters. In this site I deployed our instrument during summer 2013, conducting both the intercomparison exercise with the instrument constructed at Mines Douai (CRM-MD) and the field campaign to elucidate the reactivity of the transported air masses. The main constraints of this site were: (i) the expected low OH reactivity since not close to a source of emissions; (ii) the large variability in humidity for being close to the sea; (iii) the elevated temperature for being in the Mediterranean during summertime; (iv) site logistics and power failures. Furthermore, our instrument was never tested before together with another instrument operating under the same conditions. Indeed my work during the first year mainly focused on the construction of a system able in detecting small differences between C2 and C3, i.e. with a signal of pyrrole affected by low noise, and with reduced humidity differences. I qualified the instrument for different flows regimes and chose the best compromise to have a low concentration of pyrrole and high enough production of OH. I equipped the instrument with a catalytic converter to reduce humidity differences between background pyrrole level and pyrrole diluted in ambient air. However, the main issues of our instrument were the extreme dependence to temperature of pyrrole and its enhanced polymerization in the PTR-MS lines. For these reasons the CRM was equipped with a temperature insulated box, and the pyrrole sensitivity to temperature immediately decreased. Main data gaps among our results were due to instrumental maintenance, controls, and power failures.

The site chosen for the field campaign Canopee is located at the Oak Observatory within the Observatoire de Haute Provence, in the south of France. It is a forested site influenced by biogenic VOCs directly emitted by trees and their higher generation oxidation products, with poor anthropogenic influence. It is dominated at 75% by the downy oak tree species. Downy oaks emit isoprene at 99%; being isoprene the largest emitted VOC globally, the Oak Observatory results in a quasi-homogeneous natural laboratory for focused studies on isoprene: from its emission, to its transformation and impact. In this site we deployed our CRM during spring 2014. The main constraints of this site were: (i) the high level of OH reactivity, since isoprene is one of the most reactive compounds towards OH and our measures were scaling from ambient to branch enclosure environments; (ii) instrumental accuracy for an environment dominated by isoprene; (iii) larger signal variability due to plants fast isoprene release and source proximity; (iv) elevated ambient temperature as for

the field work in Corsica. My main work during the second year of PhD focused indeed in accurately qualifying our CRM for a broader range of OH reactivity. The instrument was qualified to respond linearly over a range from the LOD to  $500 \text{ s}^{-1}$ . I tested it in the laboratory with several atmospheric gas proxies (propane, ethane, isoprene) and frequently repeated these tests on the field with isoprene and propane. We developed a sampling strategy to carry out simultaneous measures of trace gases and OH reactivity at two heights in the forest for better elucidating isoprene transformation from its emission. The residence time of ambient air in the two independent sampling lines was kept short and similar (13 s for CRM, 23 s for instruments for trace gases analysis) to avoid gas losses and prevent small differences in the comparison between measured and calculated reactivity. Furthermore the sampling lines were located close to perform collocated observations. To reduce the temperature sensitivity observed during the field work in Corsica I equipped the CRM with a temperature controlled box, kept at  $25 \pm 2^\circ \text{ C}$ . Main issues arose from the lamp loss of efficiency, hence a scarce production of OH radicals inside the reactor, and system quality check controls. Table 2.1 reports a comparison of the performance of our CRM between the two field works.

**Table 2.1:** Brief comparison of the performance of our CRM between the field works ChArMEx and Canopee. Differences are due to instrumental improvement with time.

	ChArMEx (Corsica, France, time of deployment: 24/06/2013–06/08/2013	Canopee (Provence, France time of deployment 23/05/2014–13/06/2014
Limit of Detection (LoD, $3\sigma$ )	$3 \text{ s}^{-1}$	$3 \text{ s}^{-1}$
Total systematic uncertainty	35%	35%
Detector sensitivity to pyrrole	Dry calibration: within 15% Wet calibration: within 5%	dry calibration: below 5% Wet calibration: below 5%
Flows stability	Lines clogging issue. PTR-MS sampling flow unstable over 3-4 days.	2%
C1	$72 \pm 4$ ppb	$50 \pm 10$ ppb
humidity correction test	linear correction, slope=33 (see Fig. 2.5)	linear correction, slope=65 (see Fig. 2.5)
Test with external gases	Linear response in the range: $3\text{-}70 \text{ s}^{-1}$ correlation: $y = (0.99 \pm 0.07)x + 4.55 \pm 2.18$ ; $R^2=0.786$ . Tests run with propane & ethane	Linear response in the range: $3\text{-}500 \text{ s}^{-1}$ correlation: $y = (1.01 \pm 0.04)x - 3.26 \pm 5.15$ ; $R^2= 0.96$ . Tests run with propane & isoprene
Magnitude of corrections (humidity and kinetics regime)	10% decrease, 2% decrease	13% decrease, 47% decrease





## Chapter 3

# Intercomparison of two comparative reactivity method instruments in the Mediterranean basin during summer 2013

*This chapter contains the article*

Zannoni, N., Dusanter, S., Gros, V., Sarda Esteve, R., Michoud, V., Sinha, V., Locoge, N., and Bonsang, B.: Intercomparison of two comparative reactivity method instruments in the Mediterranean basin during summer 2013, *Atmos. Meas. Tech.*, 8, 3851-3865, doi:10.5194/amt-8-3851-2015, 2015.

### **Abstract**

The hydroxyl radical (OH) plays a key role in the atmosphere, as it initiates most of the oxidation processes of volatile organic compounds (VOCs), and can ultimately lead to the formation of ozone and secondary organic aerosols (SOAs). There are still uncertainties associated with the OH budget assessed using current models of atmospheric chemistry and direct measurements of OH sources and sinks have proved to be valuable tools to improve our understanding of the OH chemistry.

The total first order loss rate of OH, or total OH reactivity, can be directly measured using

three different methods, such as the following: total OH loss rate measurement, laser-induced pump and probe technique and comparative reactivity method. Observations of total OH reactivity are usually coupled to individual measurements of reactive compounds in the gas phase, which are used to calculate the OH reactivity. Studies using the three methods have highlighted that a significant fraction of OH reactivity is often not explained by individually measured reactive compounds and could be associated to unmeasured or unknown chemical species. Therefore accurate and reproducible measurements of OH reactivity are required.

The comparative reactivity method (CRM) has demonstrated to be an advantageous technique with an extensive range of applications, and for this reason it has been adopted by several research groups since its development. However, this method also requires careful corrections to derive ambient OH reactivity.

Herein we present an intercomparison exercise of two CRM instruments, CRM-LSCE (Laboratoire des Sciences du Climat et de l'Environnement) and CRM-MD (Mines Douai), conducted during July 2013 at the Mediterranean site of Ersa, Cape Corsica, France. The intercomparison exercise included tests to assess the corrections needed by the two instruments to process the raw data sets as well as OH reactivity observations. The observation was divided in three parts: 2 days of plant emissions (8–9 July), 2 days of ambient measurements (10–11 July) and 2 days (12–13 July) of plant emissions. We discuss in detail the experimental approach adopted and how the data sets were processed for both instruments. Corrections required for the two instruments lead to higher values of reactivity in ambient air; overall 20% increase for CRM-MD and 49% for CRM-LSCE compared to the raw data. We show that ambient OH reactivity measured by the two instruments agrees very well (correlation described by a linear least squares fit with a slope of 1 and  $R^2$  of 0.75).

This study highlights that ambient measurements of OH reactivity with differently configured CRM instruments yield consistent results in a low  $\text{NO}_x$  ( $\text{NO} + \text{NO}_2$ ), terpene rich environment, despite differential corrections relevant to each instrument. Conducting more intercomparison exercises, involving more CRM instruments operated under different ambient and instrumental settings will help in assessing the variability induced due to instrument-specific corrections further.

## 3.1 Introduction

The hydroxyl radical (OH) is the main oxidizing agent in the atmosphere during daytime. It initiates the oxidation of most trace gases emitted by natural and anthropogenic sources

and participates in almost all the complex atmospheric chemical pathways. Oxidation of trace gases leads to the production of ozone ( $O_3$ ) and secondary organic aerosols (SOAs) which can impact air pollution and climate. With such a role, it is essential to accurately understand both sources and sinks of OH. The main sources of OH are the following: photolysis of  $O_3$ , formaldehyde (HCHO) and nitrous acid (HONO), reaction of alkenes with ozone, and recycling from peroxyradicals in low  $NO_x$  ( $NO + NO_2$ ) environments (Paulson et al., 1999; Hofzumahaus et al., 2009; Fuchs et al., 2013). Main sinks of OH are CO,  $CH_4$ ,  $NO_2$ , VOCs (volatile organic compounds) and radicals, mainly  $HO_2$ . Recent studies report that OH also reacts quickly with organic peroxy radicals such as  $CH_3O_2$ , and  $OH + RO_2$  reactions may be a significant sink of OH in pristine environments (Archibald et al., 2009; Fittschen et al., 2014).

Goldstein and Galbally (2007) have estimated the presence of  $10^4$ – $10^5$  different organics measured in the atmosphere, this number may be only a small part of the species actually present and makes exhaustive measurements of VOCs very challenging and unfeasible with current analytical techniques. In this context, several research groups in the past decade developed methods capable of measuring directly the total sink of OH, termed total OH reactivity.

Measurements of total OH reactivity present several advantages. The first one is to obtain direct information on the total OH sink term in a given environment without the need of measuring every species present in the gas phase. Secondly, since OH is in a steady state in the atmosphere the balance between OH production and loss rates can provide additional information on OH sources (Martinez, 2003; Hens et al., 2014). Moreover, OH reactivity measurements help to estimate instantaneous ozone production rates and regimes (Sinha et al., 2012). Finally, when mixing ratios of individual gaseous compounds are available at the same site under study, measured total OH reactivity can be used as a tool for chemical closure of the reactive carbon budget for that specific environment. In this case, we can determine the calculated OH reactivity as follows:

$$k_{OH} = \sum_i k_{i+OH} \cdot X_i, \quad (3.1)$$

with  $i$  any measured chemical in the gas phase,  $k_{i+OH}$  the rate coefficient of the reaction between  $i$  and OH, and  $X_i$  the measured concentration of  $i$ .

Several studies on simultaneous observations of total OH reactivity and gaseous compounds have highlighted discrepancies between the total measured OH reactivity and calculated reactivity, up to 90% in biogenic dominated environments e.g. Di Carlo et al. (2004); Nölscher et al. (2012b) and Hansen et al. (2014).

The difference between the total measured and the calculated OH reactivity has been

named missing OH reactivity and has been attributed to unmeasured primary and/or secondary compounds in the atmosphere (Di Carlo et al., 2004; Kim et al., 2011).

Currently, three methods exist to perform direct measurements of total OH reactivity, such as the total OH loss rate measurement (TOLRM) (Kovacs and Brune, 2001; Mao et al., 2009; Ingham et al., 2009; Hansen et al., 2014); Pump and probe technique (Calpini et al., 1999; Sadanaga et al., 2004; Yoshino et al., 2006; Lou et al., 2010) and the comparative reactivity method (CRM) (Sinha et al., 2008; Nölscher et al., 2012a; Dolgorouky et al., 2012; Kim et al., 2011; Kumar and Sinha, 2014). A detailed comparison of the three methods can be found in Nölscher et al. (2012a) and Hansen et al. (2015).

Total OH loss rate measurement consists of a flow tube used to sample ambient air at flow rates in the order of 50–400 sL min<sup>-1</sup>, wherein a large amount of OH is added through a movable injector. OH concentration is quantified at different reaction times using a FAGE apparatus (fluorescence assay by gas expansion, see Faloon et al. (2004) and Dusanter et al. (2009) at the exit of the flow tube by moving the injector, from which a decay curve is obtained due to a change in distance between the OH source and the OH detector.

The pump and probe technique was first pioneered by Calpini et al. (1999) and Jeanneret et al. (2001) and then adapted by other groups (Sadanaga et al., 2004, Yoshino et al., 2006 and Lou et al., 2010). The instrument consists of three main parts: a flow tube to sample ambient air, a pulsed laser to generate OH in the sampling reactor, and a FAGE apparatus to quantify OH. The sampling flow is set around 10–20 sL min<sup>-1</sup> and assuming laminar flow the sample has 1 s residence time for reaction with OH. The hydroxyl radical OH is generated by ozone photolysis within the reactor and is detected after each laser pulse using the FAGE apparatus to acquire time-resolved OH decay.

The comparative reactivity method was more recently developed (Sinha et al., 2008). It is an indirect method since OH is not directly monitored, based on the competition for synthetically generated OH radicals between a reference molecule, pyrrole, and reactive compounds in ambient air. This is realized in a glass flow reactor where ambient air ( $\approx 0.25$  sL min<sup>-1</sup>), pyrrole, and OH are continuously mixed in different stages, with the reactor coupled to a pyrrole detector, most of the time being a proton-transfer reaction mass spectrometer (PTR-MS). The reactivity is obtained from changes in pyrrole concentration as a result of the competition inside the reactor for OH radicals.

The comparative reactivity method exhibits several advantages compared to other existing methods. Among those, the smaller sampling flow needed to run it (since no FAGE apparatus is needed), which broadens the application of the technique to branch and plant enclosure studies for instance; the reader can refer to Kim et al. (2011) and Nölscher et al. (2013) for more information. In addition, several research groups have already a

PTR-MS for VOCs' measurements; FAGE instruments are more expensive and require highly skilled operators. These advantages have led to the construction of several CRM instruments throughout the world in the past few years.

Another existing version of the CRM consists of the glass reactor coupled to a Gas Chromatography- Photo Ionization Detector (GC-PID) (Nölscher et al., 2012a), this version is cheaper and more portable but has also demonstrated to be slightly less robust over time compared to the PTR-MS set-up.

On the other hand, processing of the raw data and corrections for measurements artifacts represent the main disadvantages of this technique. Previous studies (Sinha et al., 2008; Dolgorouky et al., 2012; Hansen et al., 2015; Michoud et al., 2015) stressed that careful corrections are necessary for CRM measurements and a standardized procedure for data processing has yet to be agreed by the community.

In this study, we present results of the first intercomparison experiment involving two Comparative Reactivity Method instruments, CRM-LSCE (Laboratoire des Sciences du Climat et de l'Environnement) and CRM-MD (Mines Douai) assembled in two different laboratories, run by different operators but working under similar settings. Our study was performed to test a clear and simple approach to process the raw data and accurately derive OH reactivity values. It aims at identifying potential limitations and getting insights into the robustness of the CRM. Our exercise includes a comparison of calibration factors, correction factors and measurements of OH reactivity conducted in ambient air (10–11 July) and from a plant enclosure (8–9 July and 12–13 July) to cover a broad range of OH reactivity (from the limit of detection, LOD, of the instruments up to  $300\text{ s}^{-1}$ ).

## 3.2 Experimental

### 3.2.1 The comparative reactivity method

The comparative reactivity method (CRM) relies on the competitive kinetics for OH radicals between a reference molecule not present in ambient air at normal conditions (i.e. pyrrole  $\text{C}_4\text{H}_5\text{N}$ ) and reactive species in ambient air. The experiment is conducted in a glass flow reactor coupled to a detector, in our case a proton transfer reaction mass spectrometer (PTR-MS) (Lindinger and Jordan, 1998). The glass reactor is equipped with a UV lamp and four arms for flows inlets and outlets; the PTR-MS monitors the concentration of the reference molecule, pyrrole, at any time during the experiment at protonated  $m/z$  68 ( $\text{C}_4\text{H}_5\text{NH}^+$ ). A detailed description of the reactor and method is available in the publications of Sinha et al. (2008); Nölscher et al. (2012a) and is displayed in Fig. 3.1.

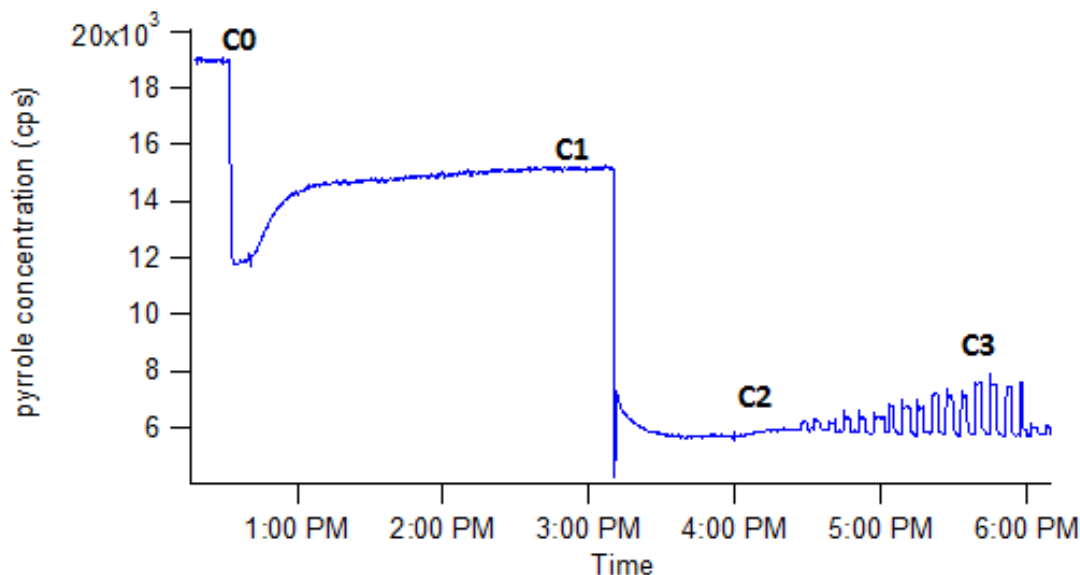


**Figure 3.1:** Pyrrole concentration detected by the PTR-MS during a typical OH reactivity experiment with CRM. C0, C1, C2, C3 are concentrations corresponding to different experimental stages. Technical improvements were done to minimize the difference between C0 and C1 reducing pyrrole loss for photolysis.

In brief: (i) a known amount of pyrrole is diluted in the glass reactor with zero air and dry  $N_2$ , and its concentration is measured with the PTR-MS (C0). Next, (ii) the UV lamp is switched on and photolysis of pyrrole occurs inside the reactor. This is considered our initial concentration of pyrrole and measured as C1. (iii) The flow of dry  $N_2$  is humidified through a bubbler containing high purity water and photolysis of water vapour at 184.9 nm takes place: at this stage we produce OH radicals in the system. The fraction of OH reacted with pyrrole is deduced from the difference between pyrrole initial concentration (C1) and pyrrole concentration when OH is formed (C2). C2 is the concentration of pyrrole after it has reacted with the OH produced, following the kinetic rate constant of  $1.2 \times 10^{-10} \text{ cm}^3 \text{ molecule}^{-1} \text{ s}^{-1}$  at 25 °C (Atkinson et al., 1984; Dillon et al., 2012). Finally, (iv) zero air is replaced by ambient air, and the competitive reaction for the OH radicals between pyrrole and ambient molecules starts. The level of pyrrole increases depending on the reactivity of OH reactants in ambient air and pyrrole concentration is recorded as C3. The higher the concentration and number of reactive species in ambient air, the larger is the reactivity, and broader the difference between C2 and C3. Regular switches between C2 and C3 permit to determine the total OH reactivity in ambient air using Eq. (3.2):

$$k_{\text{OH}} = \frac{(C3 - C2)}{(C1 - C3)} \cdot k_{\text{pyrrole+OH}} \cdot C1, \quad (3.2)$$

with  $k_{\text{pyrrole}+\text{OH}}$  the rate constant of the reaction between pyrrole and OH. For the derivation of this equation the reader can refer to Sinha et al. (2008).

In this expression it is assumed that the reaction between pyrrole and OH follows the pseudo first order kinetics, thus  $[\text{pyrrole}] > [\text{OH}]$ .

Measurements of OH reactivity with this method are usually conducted with the instrument recording alternatively C2 and C3 levels, while C1 can be monitored less often.

We automatically acquire C2 and C3 by using solenoid valves, which permit fast switches between zero air and ambient air to dilute pyrrole inside the reactor. In the tests reported herein we switch between the two levels every 5 min, to monitor the competition for OH radicals only and exclude interferences from possible fast humidity changes in ambient air, which can lead to OH field variations inside the reactor.

Measuring C1 usually takes a longer time, because of lamp warming up when switching from C0, and mainly because of the time required to dry the reactor completely. For this reason, we tested a new approach on both CRM systems which represents an alternative method to measure the initial concentration of pyrrole (C1). This approach is based on introducing a concentrated reactive molecule into the reactor, with the aim of minimizing pyrrole consumption due to OH reaction to a negligible fraction. The OH-scavenger has to exhibit a proton affinity lower than water to avoid a consumption of  $\text{H}_3\text{O}^+$  inside the PTR-MS, since a large amount of this species is needed to scavenge OH. Tests performed using methane at 30 000 ppmv are discussed in Sect. 3.3.1. This new approach showed to be an excellent alternative since it allows recording C1 more precisely in only a few minutes compared to hours with the usual method.

### 3.2.2 Data processing

To process data of OH reactivity we correct the values obtained from Eq. (3.1) as follows (see also Hansen et al., 2015; Michoud et al., 2015):

- i. correction on C2 to account for potential differences in humidity between C2 and C3 levels;
- ii. correction on C3 to account for some secondary chemistry ( $\text{HO}_2+\text{NO}\rightarrow\text{OH}$ ) which can lead to a significant production of OH inside the reactor;
- iii. correction on reactivity from Eq. (3.1) to consider deviation from pseudo first order kinetics (Sinha et al., 2008);
- iv. dilution of ambient air inside the reactor.

(i) Zero air and ambient air at different humidity used to dilute pyrrole and acquire respectively C2 and C3 lead to different water content and OH levels inside the reactor which can produce differences in the two levels and cause an under or overestimation of the reactivity in ambient air. To reduce humidity differences between C2 and C3 we equipped the CRM with a catalytic converter to generate zero air to acquire C2. The catalytic converter of CRM-LSCE is made of Pt- Pd pellets heated up to 350 °C, while the one of CRM-MD has Pt wool also held at 350 °C. However, humidity changes between C2 and C3 are still observed and corrections of the raw data of reactivity are often needed.

To look at humidity changes it is useful to monitor the ratio between  $m/z$  37 and  $m/z$  19 (here referred as  $m37/m19$ ) which corresponds to the protonated mass of the first water cluster normalized for the number of primary ions inside the PTR-MS (see Ammann et al., 2006 and Sinha et al., 2009) and depends on the absolute humidity of the air sampled. For instance, if zero air has a lower humidity than ambient air, the ratio  $m37/m19$  will be smaller for C2 compared to C3, which will result in a smaller difference between C2 and C3 and an underestimation of the reactivity in ambient air. In addition, humidity differences can also vary in opposite directions (C2 can have lower humidity than C3 and vice versa).

To quantify this type of correction we inject in the reactor a known amount of dry clean air and produce in this way a C2 level that differs from the actual C2 only for a different humidity (referred in this study as C2\*). Levels of C2 are plotted vs.  $m37/m19$  ratio recorded during C2 (see Fig. 3.2).

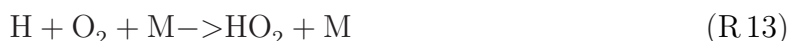
We correct therefore the measured C2 by applying Eq. (3.3):

$$C2_{\text{corrected}} = C2 + p \cdot [(m/z37/m/z19)_{\text{duringC3}} - (m/z37/m/z19)_{\text{duringC2}}], \quad (3.3)$$

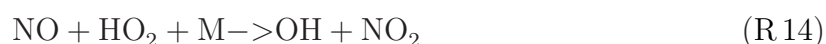
where  $p$  corresponds to a mean value of the slopes from the linear least squares fits obtained from different tests on the field and represented in Fig. 3.2. A comparison on the humidity correction for the two CRMs will be presented in Sect. 3.3.3 (ii) When the UV lamp is switched on, photolysis of water vapour at 184.9 nm occurs as follows:



H recombines with  $\text{O}_2$  present in zero air to rapidly generate  $\text{HO}_2$ :



$\text{HO}_2$  can react with NO, if this is present in the sampled air, to generate OH:





This secondary source of OH leads to a lower level of C3, the magnitude of which depends on the amount of ambient NO. This artifact leads to an underestimation of the OH reactivity in ambient air and can even result in negative values. A detailed description on how to assess the sensitivity of the CRM to NO and how to quantify the correction for this artifact is described elsewhere (Dolgorouky et al., 2012; Hansen et al., 2015; Michoud et al., 2015). During our intercomparison exercise the level of NO in ambient air reached a maximum of 1 ppbv, which resulted in negligible secondary formation of OH inside our two systems, therefore no corrections were warranted here. (iii) It is assumed in Eq. (3.1) that reactions of OH with pyrrole and ambient trace gases proceed through first order kinetics, i.e. pyrrole and trace gas concentrations are higher than OH concentration. However, CRM instruments are operated with OH concentrations on the same order of magnitude than pyrrole ([pyrrole]  $\sim$  60–70 ppbv, [OH]  $\sim$  40–50 ppbv) and a correction must be applied to account for a deviation from first order kinetics. A correction factor  $F$  can be obtained theoretically (Sinha et al., 2008) or experimentally (as in this study and in Hansen et al., 2015; Michoud et al., 2015) and used to process reactivity data already corrected for humidity changes and secondary OH formation as follows:

$$k_{\text{OH}_{\text{corrected}}} = k_{\text{OH}_{\text{measured}}} \cdot F. \quad (3.4)$$

Previous studies used simple numerical simulations to determine such correction factor. Simulations were run at pyrrole-to-OH ratio of 10, near pseudo first order condition, and 1.22, experimental conditions, for more information see Sinha et al. (2008). A fitting function is obtained from simulations in the experimental conditions which showed that if a correction is not taken into account, measurements of OH reactivity can be overestimated for low values of pyrrole-to-OH ratio.

In our study, we use an experimental approach to correct for deviations from first order kinetics, which can be more representative of the complex chemistry occurring inside the reactor.

To do so, we introduce inside the reactor a known amount of a standard gas whose reactivity with OH is well determined and reported in literature. We test the instrument response over a broad range of reactivity, for instance from the LOD to  $300 \text{ s}^{-1}$ , for different standard gases and different pyrrole-to-OH ratios. From each test a linear least squares fit for the measured OH reactivity vs. the injected reactivity is obtained, and the inverse of the slope is then reported for every pyrrole-to-OH ratio investigated. In such way, we obtain a correction factor which is instrument specific for the experimental conditions adopted.

In our intercomparison exercise we used as test gases propane and ethane, with ethane being the same standard gas for both instruments. Results of these tests are shown in Sect. 3.3.4 (iv) OH reactivity values obtained from Eq. (3.1) and corrected for humidity

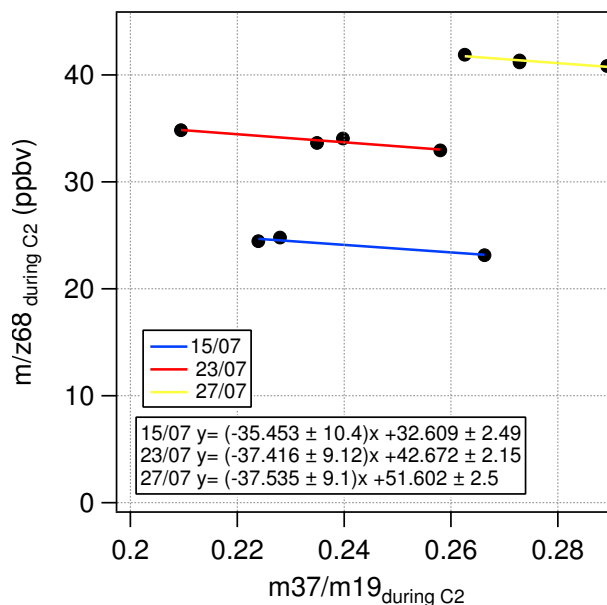


**Figure 3.2:** Linear least squares fit of  $m/z$  68 during C2 vs.  $m_{37}/m_{19}$  during C2 for the tests conducted on the field to assess the correction for humidity differences between C2 and C3 for CRM-LSCE. Equation coefficients are reported with one standard deviation. Differences in the intercepts are due to a less efficient tracking of absolute humidity from  $m_{37}/m_{19}$  on a longer time scale.

changes, secondary OH formation, and deviation from first order kinetics, are then corrected for the dilution of ambient air sampled inside the reactor. The dilution factor is calculated as the ratio between the sampling flow rate and the total flow rate inside the reactor (sum of flow rates of  $N_2$ , pyrrole and ambient air).

### 3.2.3 Comparative Reactivity Method set up

A description of the two CRM instruments used in this study, including operating conditions, is given below. It is illustrated by a detailed description of the instrument constructed at LSCE (Laboratoire des Sciences du Climat et de l'Environnement) in Fig. 3.3 and differences with the one from MD (Mines Douai) are reported in Tab. 3.1 and discussed below.

The comparative reactivity method instrument assembled at LSCE is a modified version of the CRM used during the MEGAPOLI field campaign and presented in Dolgorouky et al. (2012). Briefly, pyrrole (Westfalen, Germany, 10.2 ppmv in  $N_2$ , 20 % uncertainty), zero air (Messer standard mixture) and  $N_2$  (Messer, purity 99.9999 %) are injected in a glass flow reactor (same shape and size as the one described by Sinha et al., 2008) and pyrrole

concentration is monitored with a PTR-MS (High sensitivity quadrupole, from IONICON Analytic GmbH, Innsbruck, Austria). Zero air is obtained from synthetic air to achieve dry conditions for the acquisition of C1 and from sampling ambient air through a catalytic converter to generate zero air at ambient RH when measuring C2. A pump is placed at the exhaust of the cell, therefore the total flow is driven inside the reactor by the pump at the exhaust and the PTR-MS sampling. A UV pen ray Hg lamp (Lot Oriel, France) emitting at 184.9 nm is used to produce hydroxyl radicals. The total flow rate inside the reactor is usually kept around  $0.3 \text{ sL min}^{-1}$ , with a concentration of pyrrole in the range of 20–30 ppbv in the C2 level, C1 of  $65 \pm 5.8 \text{ ppbv}$  ( $1\sigma$ ) and pyrrole-to-OH ratio ranging from 1.2 to 2.6.

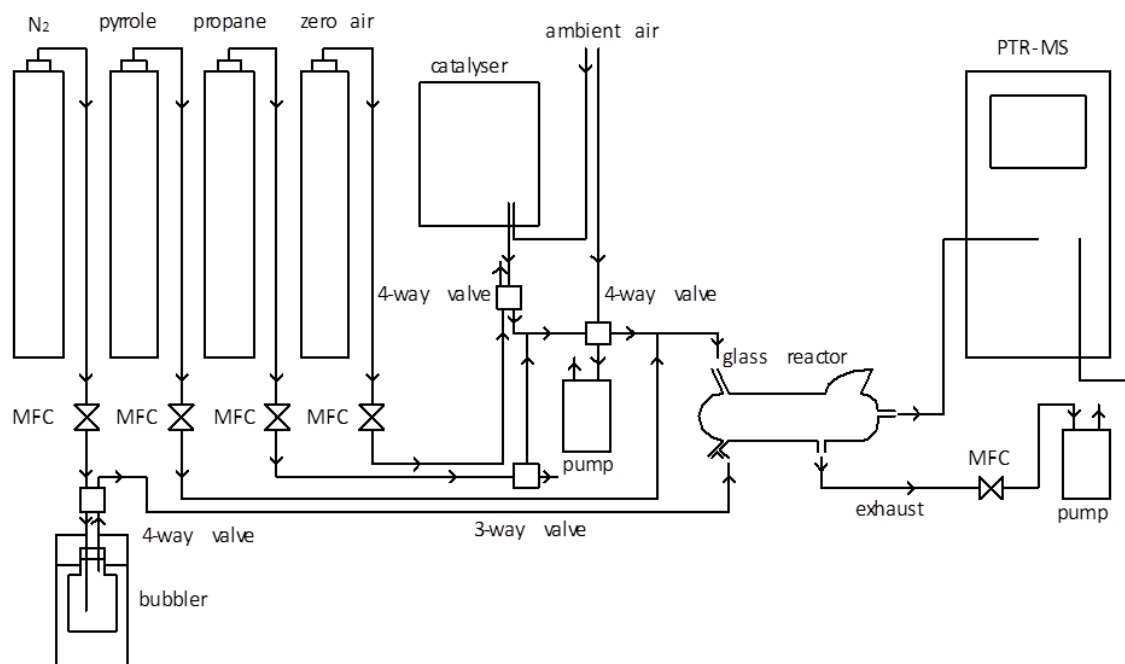


**Figure 3.3:** Simplified not-to-scale schematic of the comparative reactivity method instrument of LSCE. Known flows of pyrrole,  $\text{N}_2$ , and zero air are injected into a glass flow reactor. A four-way manual valve is used to humidify the flow of nitrogen, when OH radicals production is required. A four-way automatic valve allows for fast switches between C2 and C3 stages. A known amount of an external standard (in this case, propane) can be injected in the reactor to calibrate the instrument through a three-way valve.

A three-way valve is used to inject an external gas standard inside the sampling line. Additions of a standard test gas permit to derive the correction for a deviation from first order kinetics (see Sect. 3.3.4). A four-way valve is used to switch automatically every 5 min between C2 (zero air from the catalytic converter) and C3 (ambient air).

## 72 Chapter 3. Intercomparison of two comparative reactivity method instruments

**Table 3.1:** Technical parts and operational settings of CRM LSCE and CRM MD during the intercomparison exercise. MPI stands for Max Planck Institute (chemistry division, Mainz, Germany).

	CRM-LSCE	CRM-MD
Reactor	glass reactor from MPI	glass reactor from MPI
Detection system	PTR-QMS (from IONICON, Innsbruck, Austria)	PTR-ToFMS (second generation, Kore Technology Ltd, Ely, UK)
Sampling for KOH in ambient air		
-line OD /length (inches, m)	1/8"/3	1/4"/30
-flow rate (sL min <sup>-1</sup> )	0.25	2
-residence time (s)	~ 3	~ 3
Sampling for KOH plant enclosure		
-line OD /length (inches/m)	1/8"/3 + 1/4"/2.5	1/4"/30
-flow rate (sL min <sup>-1</sup> )	~ 14	~ 16
-residence time (s)		
Sampling set up	no pump before sampling, PTFE filter at the inlet	Teflon pump between sampling line and reactor, no filter at the inlet
Total flow inside reactor (sL min <sup>-1</sup> )	~ 0.33	~ 0.355
Photolysis rate (%)	~ 5	~ 2
C1 value (ppbv)	interpolated over the measured C1 dry 65 ± 5.8 (1σ)	from methane test 61.4 ± 0.6 (1σ)
Systematic uncertainty (%)	35	18
LOD (s <sup>-1</sup> ) (3σ)	3	3

An additional pump is used to either flush the sampling line with ambient air while the system is measuring C2 or to flush the catalytic converter while the system is measuring C3. Sampling lines for the reactor and the catalytic converter are collocated to reduce

humidity variations when measuring C2 and C3. Although the humidity difference between C2 and C3 is reduced with a catalytic converter, we still observe differences between the two levels; therefore, we correct the raw data as reported in the data processing section.

Five mass flow controllers are used to control the flow rates, including pyrrole, synthetic air, N<sub>2</sub>, external standard (for instance propane), and the flow rate at the exhaust to ensure a constant and precise dilution of pyrrole and ambient air during the measurements. An opening for an overflow is placed before the mixing of zero air with the external standard and is kept around 0.01–0.02 sL min<sup>-1</sup>, to avoid any pressure build up in the system and to provide an outlet to check flows stability at any time. CRM-LSCE measures total OH reactivity automatically, except for manual quality check controls (external standard injection), and C1 acquisition.

The dwell time for the acquisition of  $m/z$  68 is 20 s, and C2-C3 switches are performed every 5 min, leading to OH reactivity measurements every 10 min. The LOD of LSCE-CRM is  $\sim 3 \text{ s}^{-1}$  ( $3\sigma$ ) and the systematic uncertainty is  $\sim 35 \%$  ( $1\sigma$ ), including uncertainties on the rate coefficient between pyrrole and OH (8%), detector sensitivity changes and pyrrole standard concentration (22%), correction factor for kinetic regime (26%) and flows fluctuations (2%).

Potential measurement artifacts discussed in Sinha et al. (2008) are either corrected for the CRM-LSCE system or negligible under characteristic ambient conditions of the measuring site. In particular, photolysis is quantified to be  $\sim 5 \%$ ; humidity changes are corrected as reported in the data processing section and OH formation by HO<sub>2</sub>+NO is negligible.

The CRM-MD instrument is described elsewhere (Hansen et al. 2015; Michoud et al., 2015). For this study, several improvements were performed compared to the instrument described in Hansen et al. (2015), to achieve a lower pyrrole photolysis in the reactor ( $< 5 \%$ ), and by consequence, to reduce the potential photolysis of other trace gases. The CRM-MD instrument was operated under the same conditions of flow rates, pyrrole concentration, and pyrrole-to-OH ratios as the LSCE instrument to allow an assessment of the reproducibility of OH reactivity measurements using the CRM technique. CRM-MD exhibits similar figures of merit than CRM-LSCE, including a detection limit ( $3\sigma$ ) of  $3 \text{ s}^{-1}$  and a systematic error quantified to be  $\sim 18 \%$  ( $1\sigma$ ). Differences in uncertainty between the two instruments can be explained by different uncertainties ( $1\sigma$ ) on the concentration of the pyrrole standard used (20% for CRM-LSCE and 5% for CRM-MD) and uncertainties in the correction factors applied for deviations from first order kinetics (26% for CRM-LSCE while 9% for CRM-MD).

The main differences between both instruments are listed in Tab. 3.1 and are discussed below:

- i. Choice of the detector; both have a proton transfer reaction mass spectrometer: quadrupole from IONICON Analytik, Austria for LSCE and Time of Flight from KORE Technology, UK for MD.
- ii. The sampling point during the ambient kOH experiment: the sampling lines of the two instruments were placed on top of each trailer, about 30 m far from each other, and 2 m different in height. The length of the sampling lines was the same, while the outer diameter size and sampling flow rates differ to have a similar residence time of the sample in the lines of about 3 s.
- iii. The length of the sampling line during the enclosure kOH experiment: approximately 30 m for CRM-MD and 5.5 m for CRM-LSCE. A longer sampling line was used for CRM-MD to perform collocated measurements with CRM-LSCE. However, the sampling flow rate was adjusted to  $2 \text{ L min}^{-1}$  to get similar residence times in the sampling lines of the two instruments (approximately 14 and 16 s for CRM-LSCE and CRM-MD, respectively).
- iv. The sampling strategy: CRM-MD is equipped with a Teflon pump between the sampling line and the reactor while CRM-LSCE has the sampling line directly connected to the reactor, without any pump. The extra flow from the pump is vented through an open T-connector and similar sampling flow rates are achieved for both instruments. In addition, the sampling line of CRM-LSCE has a PTFE filter at the inlet to exclude particles with a diameter larger than  $0.25 \mu$  entering the reactor, while CRM-MD has no filters at the inlet.

In addition, each instrument uses a different pyrrole standard, i.e. from Westfalen, Germany (10.2 ppmv in  $\text{N}_2$ , 20 % uncertainty,  $1\sigma$ ) for CRM-LSCE and from PRAXAIR Inc., France (10.1 ppmv in  $\text{N}_2$ , 5 % uncertainty,  $1\sigma$ ) for CRM-MD. There are legitimate concerns that differences in the OH reactivity measurements could be due to the pyrrole standard since this type of gas cylinder is not common. In order to estimate the impact of using two different standards on the intercomparison results, the standard from Mines Douai was tested on the LSCE instrument, which instead was calibrated using the LSCE standard. The concentration of pyrrole measured in the MD cylinder was  $9170 \pm 272$  ppbv, which is less than 10 % different of the certified concentration of 10.1 ppmv.

### 3.2.4 Description of the field site and experiments

The two CRM instruments were deployed from the 8–13 July 2013 at a remote site, Ersa, Cape Corsica, France ( $42.97^\circ \text{ N}$ ,  $9.38^\circ \text{ E}$ , alt 533 m). The site was chosen for intensive

monitoring of atmospheric trace gases and aerosols under the ChArMEX project (Chemistry and Aerosols in a Mediterranean Experiment), an international program of field monitoring and modelling of atmospheric properties and climate interactions over the Mediterranean basin (<https://charmex.lsce.ipsl.fr/>). OH reactivity was measured as part of the 2013 CARBOSOR (CARBON within continental pollution plumes: SOURces and Reactivity) field campaign by CRM-LSCE from the 16 July–5 August.

The field site is located in the northern part of cape Corsica on the top of a hill facing the Mediterranean sea (533 m a.s.l.) and a few km away from the coast (2.5, 4.5, and 6 km from the west, north and east side respectively). The site is characterized by an intense Maquis shrubland, including characteristic plant species of the Mediterranean ecosystem as *Pistacia Lentiscus*, *Myrtus Communis*, *Cistus Monspeliensis*, *Rosmarinus Officinalis*, *Genisteae*, *Hellebores* and others. The closest anthropogenic source is the city of Bastia, second largest city and main harbour of the island, 50 km southern the monitoring site.

The intercomparison exercise consisted of three periods of collocated measurements of OH reactivity (between 8 and 9 July, between 10 and 11 July and during 12–13 July) and tests to evaluate the data processing using a common procedure.

During these days, ambient reactivity was close to the LOD of the systems; therefore we decided to measure the reactivity of a plant species close to our trailers and known to emit highly reactive compounds as monoterpenes (Bracho-Nunez et al., 2011). The plant we chose is a *Rosmarinus officinalis*, commonly known as rosemary, found in low shrubs with evergreen needle-like leaves and native to the Mediterranean region.

For this experiment, we placed our inlets in a small enclosure constructed from a PET flask and showed to not interfere with ambient measurements. We chose it to prevent the sampling lines from rain and wind exposure and concentrate the emissions from the plant. From time to time we induced higher emissions by applying some mechanical stress (for instance by scraping or cutting some small branches); hence the results reported in the next section are not indicative for the plant's natural emissions. Figure 3.4 shows a top view of the field site and respective position of the two instruments.

### 3.3 Results and discussion

In the following section we present results of the intercomparison exercise and tests run on the two instruments to define a common and consistent approach to evaluate the data of OH reactivity. Tests include measurement of C1 according to the conventional approach presented in the experimental section and reported by Sinha et al. (2008) as well

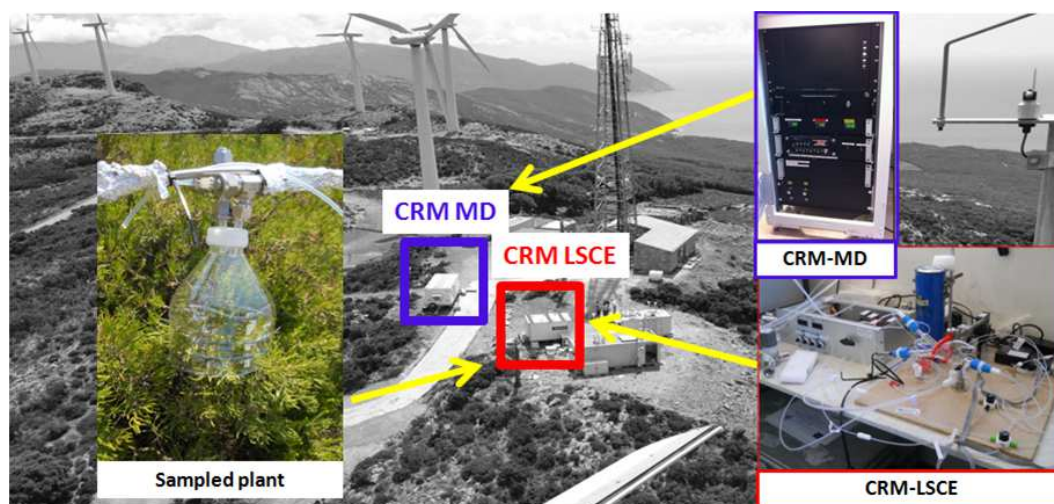


**Figure 3.4:** Top view of the field site at Cape Corsica. Relative distances between the trailers containing the instruments, details of the instruments and sampled plant species are provided.

as measurement of C1 according to a new approach based on the use of an OH scavenger. We show results from collocated measurements of OH reactivity and the corrections needed for both instruments, and how corrections influence the correlation of the results of the two instruments.

### 3.3.1 C1 acquired with the conventional and scavenger approaches

The initial concentration of pyrrole, named C1, is usually measured when pyrrole is mixed with dry zero air and dry nitrogen, with the mercury lamp on. However, switching from humid to dry air to get a complete drying of the reactor can often be time consuming, especially when the instrument is operating on the field.

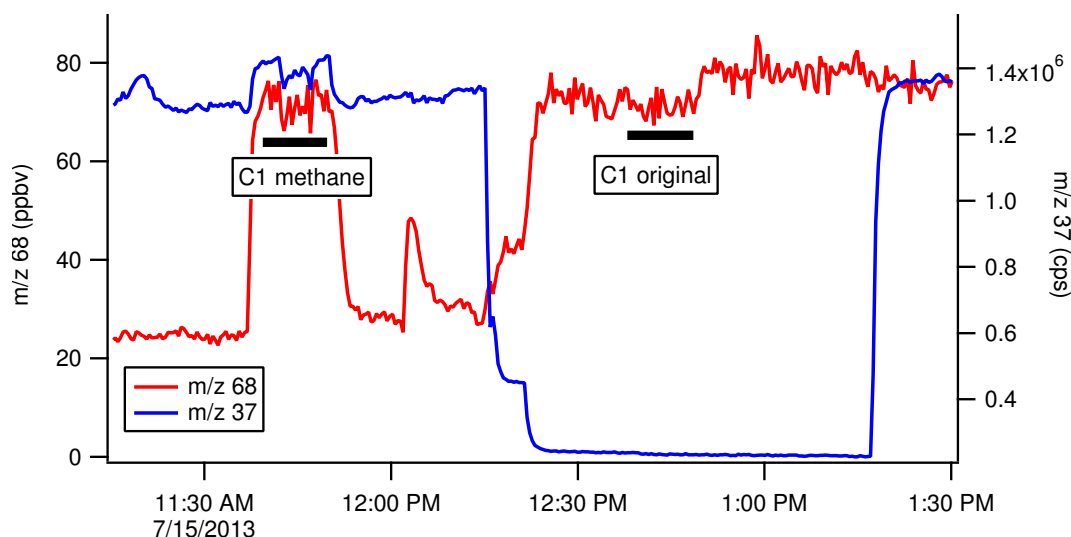
For this reason we conducted the experiment to inject a known amount of a scavenger molecule, in this case methane, into the CRM reactors to reach a mixing ratio of approximately 3% by volume.

Figure 3.5 shows three measurements of C1 performed with CRM-LSCE at flow rates of 12, 8, and 0.014 sL min<sup>-1</sup> of methane mixed in a total flow of about 0.330 sL min<sup>-1</sup>, leading to CH<sub>4</sub> mixing ratios of 3.4, 2.3 and 4.0% respectively. At 11:30 (CEST), the PTR-MS was measuring C2, the cell was wet, pyrrole mixing ratio was 24.3 ± 0.4 ppbv and *m/z* 37 signal was 1.25 × 10<sup>6</sup> cps. At 11:40 we injected methane at the three flow rates indicated above and pyrrole mixing ratio increased to 73.5 ± 0.6, 71 ± 0.5 and 72.6 ± 2.9 ppbv inside the cell. It can be noticed, that we measured the same concentration of pyrrole when different



flow rates of methane were added into the reactor, suggesting that only a negligible fraction of OH reacts with pyrrole and most of OH is scavenged by methane.

C1 was then also acquired under dry conditions, with  $m/z$  37 being  $2.35 \times 10^5$  cps, i.e. 1 order of magnitude lower than under wet conditions, at time 12.30. In this case, the pyrrole mixing ratio reached  $73.8 \pm 2.9$  ppbv, which is not significantly different from the concentration measured using the scavenger approach. In this specific experiment, the acquisition of C1 with the usual approach took approximately 20 min, this time can vary to hours depending on the reactor design and coating.



**Figure 3.5:** Comparison between C1 acquired with the OH scavenger approach and with the original approach. Values of  $m/z$  37 refer to the protonated first water cluster which is used as tracer for absolute humidity in the system and depends on PTR-MS operational conditions, in our case  $E/N = 120$  Td.

For the CRM-LSCE instrument, similar values of C1 were found using both methodologies, highlighting the feasibility of the scavenger approach. Similar tests performed on the CRM-MD instrument showed significant differences in C1 values measured using the two approaches, with higher C1 values when the scavenger was used. This disagreement is likely due to difficulties to completely dry the reactor for the CRM-MD instrument, leading to the formation of OH from the photolysis of residual water molecules, which in turn leads to an underestimation of C1. The scavenger approach appeared to give a more robust determination of C1 for this instrument. Similar tests were also conducted in the laboratory after the ChArMEx field campaign using propane as a scavenger (at approximately 900 ppmv), showing consistent results with field observations.

The scavenger approach appears to be more suitable for field deployments than the conven-

tional approach for CRM instruments, where drying requires more than an hour, since it allows faster C1 measurements (response in a few minutes against hours depending on the reactor's conditions), allowing more frequent checks of pyrrole stability without impairing ambient measurements of OH reactivity.

### 3.3.2 Assessment of the correction for humidity differences between C2 and C3

As mentioned in Sect. 3.2.2, the correction on the C2 measurement aims at reducing artifacts due to different humidity levels between C2 and C3 measurements. While differences in humidity are already reduced using a catalytic converter to generate zero air from ambient air, small differences are still observed on the  $m37/m19$  ratio, which in turn can lead to significant errors in OH reactivity measurements if C2 is not corrected.

Both CRM instruments were characterized in the laboratory and several times during the field experiment to quantify the C2-dependence on humidity.

Calibrations for humidity consist of modulating the humidity of wet zero air flowing inside the reactor while recording C2 by mixing the wet zero air with dry zero air at different ratios inside the reactor. In this way, we monitor C2 (ambient humidity) and C2\* (ambient humidity mixed with dry synthetic air) signals, and alternate rapidly between them to avoid any interference from local ambient humidity changes. Values of C2 acquired in this way are plotted vs. the normalized counts of the first water cluster ( $m37/m19$ ) during C2 as shown in Fig. 3.2. A linear least squares fit of  $m/z$  68 (during C2) vs.  $m37/m19$  (during C2) provide the equation used to correct C2 as described in Sect. 3.2.2.

We performed simultaneous measurements of OH reactivity during 8–13 July 2013 and processed the raw data as reported in Sect. 3.2.2. We found that the correction for humidity differences applied to the raw data sets has an average impact of 12 % for CRM-LSCE and 4 % for CRM-MD (see Tab. 3.2). Interestingly, these corrections resulted in an increase of the CRM-LSCE measurements and in a decrease of the CRM-MD measurements. We believe that this opposite behaviour was due to a difference we had in the sampling set-up. CRM-LSCE usually operates with a PTFE filter at the inlet of the sampling line to prevent atmospheric particles entering the reactor; while CRM-MD did not use any filter for the intercomparison exercise. The PTFE filter might have act as water reservoir; retaining water vapours when the air was very humid and releasing water vapours when the air was dry. Therefore, using a filter at the inlet leads to both C2 drier or more humid than C3, depending on atmospheric conditions; while C2 of CRM-MD was always more humid than ambient air.

### 3.3.3 Assessment of the correction for the kinetics regime

As mentioned in Sect. 3.2.2, we use an experimental approach to estimate the correction factor that is needed to account for the deviation from pseudo first order kinetics during ambient measurements of OH reactivity. We introduced a known amount of OH reactivity produced by different gas standards in the reactors, including ethane and propane for both CRM instruments during the intercomparison on the field. Additional gases were also used during laboratory testing, before or after the field intercomparison, including isoprene for CRM-LSCE and ethene, propene, and isoprene for CRM-MD. These standards are intended to be representative for the range of reactivity of ambient trace gases with OH (bimolecular rate constants in the range  $10^{-13}$ – $10^{-10}$   $\text{cm}^3 \text{molecule}^{-1} \text{s}^{-1}$ ). Moreover, the standard of ethane used in the field and during laboratory tests was the same one for both instruments.

Tests made with gas standards covered a range of OH reactivity from the LOD ( $\approx 3 \text{s}^{-1}$ ,  $3\sigma$ ) up to  $300 \text{s}^{-1}$ . A smaller range of OH reactivity was investigated on CRM-MD with values ranging from the LOD ( $\approx 3 \text{s}^{-1}$ ,  $3\sigma$ ) up to  $65 \text{s}^{-1}$ . However, tests performed in the laboratory using complex mixtures of NHMCs (non-methane hydrocarbons) and OVOCs (oxygenated volatile organic compounds) (see supplementary material of Michoud et al., 2015) showed that CRM-MD correctly measures higher OH reactivity values, with a linear response of the instrument up to approximately  $900 \text{s}^{-1}$ . The range of pyrrole-to-OH ratios investigated during these tests ranges from 1.2 to 2.6, which is within the range of pyrrole-to-OH ratios observed during ambient measurements at Cape Corsica (1.2–2.6 for CRM-LSCE and 1.5–2.1 for CRM-MD).

Figure 3.6 shows results from the calibrations made for both CRMs on the field, using ethane (hollow circles) and propane (full circles) as gas standards. It is interesting to notice that the correction factor for both instruments seems to follow a linear dependency with the pyrrole-to-OH ratio inside the reactor. In particular, the correction factor decreases when higher ratios are achieved inside the reactor. This behaviour was shown to be reasonably well reproduced by modelling the chemistry inside the CRM (Michoud et al., 2015). Moreover, calibrations on CRM-LSCE reveal that a correction factor of 1 is reached for a pyrrole-to-OH ratio of 1.86, while CRM-MD reaches 1 at a ratio of 1.56. However, for pyrrole-to-OH in the range 1.2–2.6 as the one of this study and showed in Fig. 3.6, such linear dependency seems to be fairly significant only for CRM-MD ( $R^2 = 0.546$ ), while it is not relevant for CRM-LSCE ( $R^2 = 0.206$ ). Therefore the data set from CRM-MD was corrected with the equation from the linear fit reported on Fig. 3.6 while the data set from CRM-LSCE was corrected with a mean value of the correction factors obtained from the experiments conducted on the field. Since we obtained close corrections for our

**Table 3.2:** Summary of correction stages applied to raw reactivity data for CRM-LSCE and CRM-MD. Correction coefficients are obtained from experiments as described in the section data analysis.

Correction	CRM-LSCE	CRM-MD
Humidity	12 %	4 %
Kinetics	Correction factor = 1.71– $0.38 \times \text{Pyr}/\text{OH}$ (1 @ $\text{pyr}/\text{OH}=1.86$ ), constant factor of 0.98 applied	Correction factor = 1.28– $0.18 \times \text{Pyr}/\text{OH}$ (1 @ $\text{pyr}/\text{OH}=1.56$ )
Dilution	1.36	1.31
Overall increase of raw data due to corrections	49 %	20 %

data sets (0.98 correction factor for CRM-LSCE, 0.97 for CRM-MD on average), this data processing did not substantially influence the correlation between the results from the two instruments. Table 3.2 reports a summary of the corrections resulting from our tests and their impact on the measures.

The second important point to notice from Fig. 3.6 is the larger variability in correction factors from the experiments observed for CRM-LSCE compared to CRM-MD ( $1\sigma$  on the correction factor equals to 0.22 for CRM-LSCE and 0.07 for CRM-MD). We think that the main difference is attributable to a possible different mixing efficiency occurring inside the reactors where the two arms for air and nitrogen/OH are pointing. Although our reactors have the same shape, covering material and same flow rates injected, we suspect that even small differences in the length and pointing of the injection arms inside the reactor might provoke a different mixing and hence radical segregation inside the two systems. These differences in radical segregation could lead to differences in kinetics inside the two reactors. We need to further investigate different reactors to actually verify this hypothesis. To prevent that such small differences determine a wrong interpretation of the measured reactivity we consider therefore important that each CRM undergoes the experimental quantification of this correction factor; not only to assess the right correction for the kinetics regime but also to determine the specific reactor performance. Propane

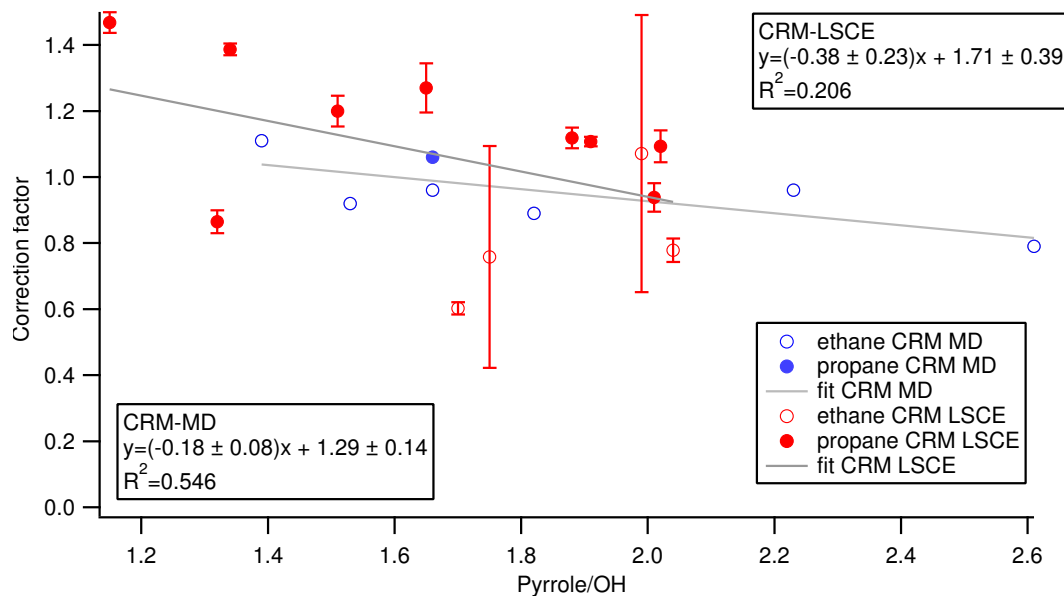


**Figure 3.6:** Correction factor of reactivity for the kinetics regime reported vs. pyrrole-to-OH ratio in the reactors. Correction for CRM-LSCE is represented in red while correction for CRM-MD is represented in blue. Full circles refer to the experiments conducted with propane while hollow circles refer to the experiments with ethane as gas standard. Linear fits include coefficient values  $\pm 1\sigma$ .

and ethane also showed slightly different behaviour when used as test gases for the CRM calibration. Different rate coefficients with OH could explain this behaviour, since for the same injected reactivity different concentration of the selected test gas are needed, hence the higher the concentration the closer the system is in the pseudo first order kinetics assumption. Additional experimental tests performed in the laboratory with a more reactive test gas as isoprene, and by modelled results of compounds with different reactivity conducted in the same pyrrole/OH range and discussed in the paper of Michoud et al. (2015), supported this hypothesis. However, the larger variability in the correction factors from all experimental field tests (propane and ethane) makes differences among test gases behaviour not significant in the evaluated range of pyrrole/OH, hence a mean value or a linear fit including all experimental results is suitable to correct the reactivity.

### 3.3.4 Correction for dilution

After corrections on C2 for changes in humidity between C2 and C3, and on the reactivity for deviations from the pseudo first order kinetics, we accounted for the dilution of the sampled air inside our reactors to determine the reactivity in ambient air. As mentioned in

Sect. 3.2.2, such correction is calculated from the sampled flow rate of ambient air and the total flow rate within the reactor. Factors of 1.36 and 1.31 were calculated for CRM-LSCE and CRM-MD respectively, and a similar increase of our final data is therefore obtained.

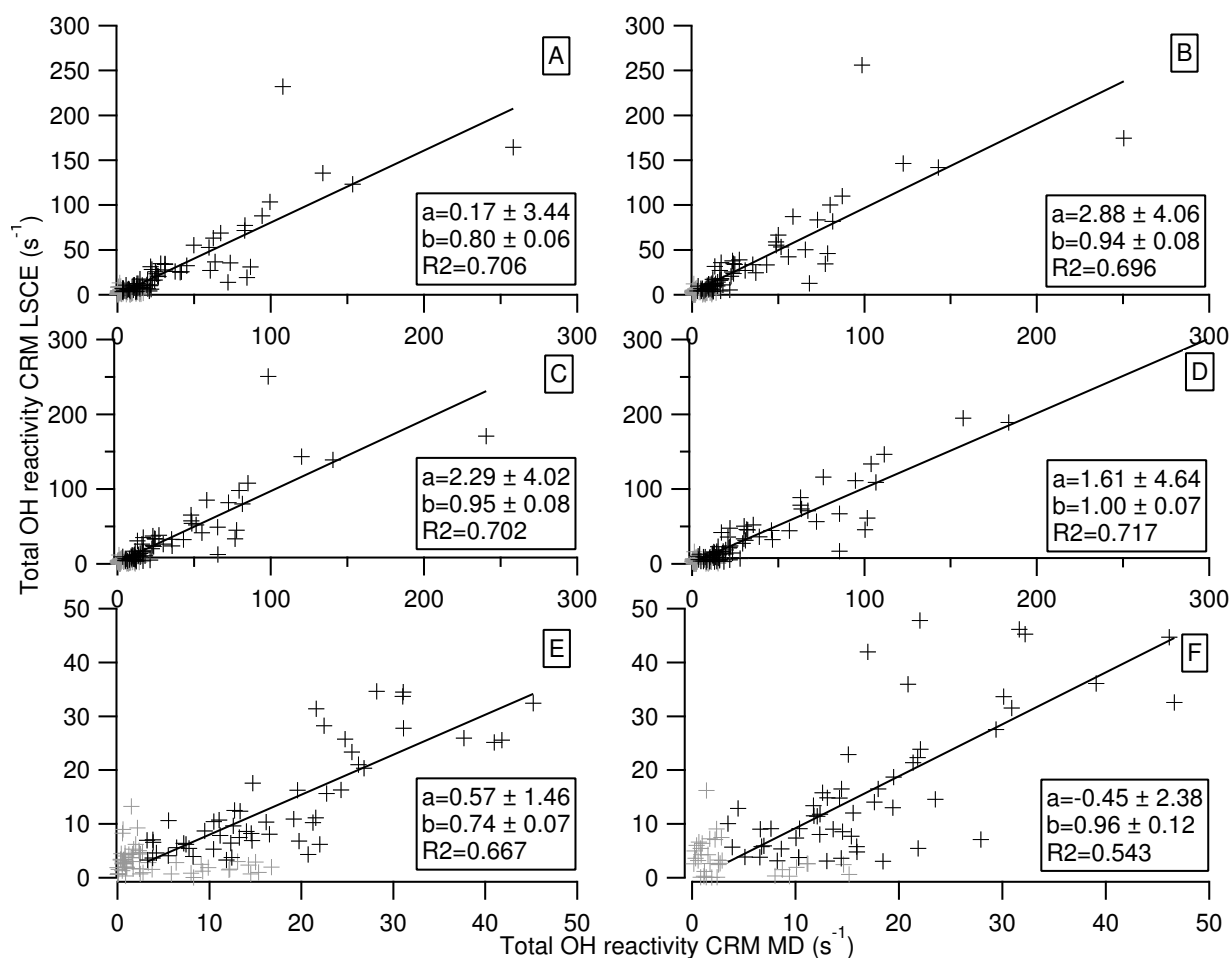


**Figure 3.7:** Linear least squares fits of total OH reactivity measured by CRM-LSCE vs. Total OH reactivity measured by CRM-MD. Panels from top left to bottom right show: correlation among raw results (a); correlation among data corrected for humidity (b); correlation among data corrected for humidity and deviation from pseudo first order kinetics (c); correlation among data corrected for humidity; kinetics regime and dilution inside the reactor (d); correlation among raw values in the range 0–50 s<sup>-1</sup> (e); correlation among final values in the range 0–50 s<sup>-1</sup>. (f). Coefficient values are extracted from the equation: OH reactivity CRM-LSCE =  $b$ (OH reactivity CRM-MD) +  $a$  and report 1 $\sigma$  standard deviation. The regressions are applied to the values above the instrumental LOD only.

### 3.3.5 Measurement uncertainty

Processed reactivity data are subject to three types of corrections, which impact the final result by 49 % for CRM-LSCE and 20 % by CRM-MD (Tab. 3.2). Among the discussed corrections, humidity differences play a more important role for CRM-LSCE while the other corrections influence the measurements from both instruments in a similar manner due to similar operating conditions.

Overall uncertainties include systematic errors and precision and were estimated according to the calculation described by Michoud et al. (2015). Systematic errors originates from the uncertainty on the rate coefficient between pyrrole and OH,  $k_{\text{pyrrole+OH}}$ , the uncertainty associated to the pyrrole standard, the stability of the PTR-MS sensitivity over time, the humidity and pseudo first order corrections described above and the correction for dilution. Such uncertainty is estimated to be 35 % for CRM-LSCE and 18 % for CRM-MD. Differences between instruments are due to the different uncertainties on the concentration of pyrrole in the standard cylinder (20 % for CRM-LSCE while 5 % for CRM-MD) and on the correction factor assessed for the kinetics regime (26 % for CRM-LSCE while 9 % for CRM-MD). The measurement precision depends on the concentration levels C1, C2, C3. The random error from precision dominates in the low range of OH reactivity (below  $15 \text{ s}^{-1}$ ) while systematic errors dominates for higher OH reactivity values. Overall uncertainty (systematic and precision) for this specific experiment, were estimated to be below 35 % on average for CRM-LSCE for OH reactivity values higher than  $8 \text{ s}^{-1}$  and approximately 18 % for CRM-MD when OH reactivity values are higher than  $15 \text{ s}^{-1}$ . For lower OH reactivity the overall uncertainty increases up to 50 % at the LOD of  $3 \text{ s}^{-1}$  ( $3\sigma$ ) for both instruments (Michoud et al., 2015).

### 3.3.6 Intercomparison of OH reactivity results

Simultaneous measurements of OH reactivity with CRM-LSCE and CRM-MD were conducted between the 8 and 13 July, 2013; the processing of the raw data was discussed in Sects. 3.2.2–3.2.4.

Figure 3.7 shows the correlation between reactivity data collected by CRM-LSCE ( $y$  axes) and CRM-MD ( $x$  axes) from their sampling (panel a, raw data) throughout their processing (panel b and c, respectively data corrected for humidity differences and data corrected for deviation from the assumed kinetics) to the final results (panel d, reactivity in ambient air). Data points include three different sampling periods: a first plant enclosure test during 8–9 July, ambient measurements between 10–11 July, and a second plant enclosure test between 12 and 13 July. As previously mentioned, to produce higher reactivity than

ambient levels and extend our range of values for comparison we applied some stress on the plant to induce the emission of high levels of reactive compounds. In turn, our instruments responded to these high levels with small delays, and data acquisition was not perfectly synchronized, despite the fact that we achieved a residence time in the sampling lines on the same order of magnitude (12 s for CRM-LSCE and 13 s for CRM-MD). By consequence, small delays resulted in significant differences for high values of OH reactivity. We smoothed such differences considering thirty minutes averages of the measurements. Scatter plots therefore report all the data points obtained from our intercomparison experiment (190 points) and the agreement is quantified using linear least squares fit according to

$$k_{\text{OH}_{\text{CRM-LSCE}}} = b \cdot k_{\text{OH}_{\text{CRM-MD}}} + a. \quad (3.5)$$

Text boxes in Fig. 3.7 report an equation for each correlation plot,  $1\sigma$  standard deviation on the equation coefficients and the determination coefficients  $R^2$  for the proportion of variability in the data sets.

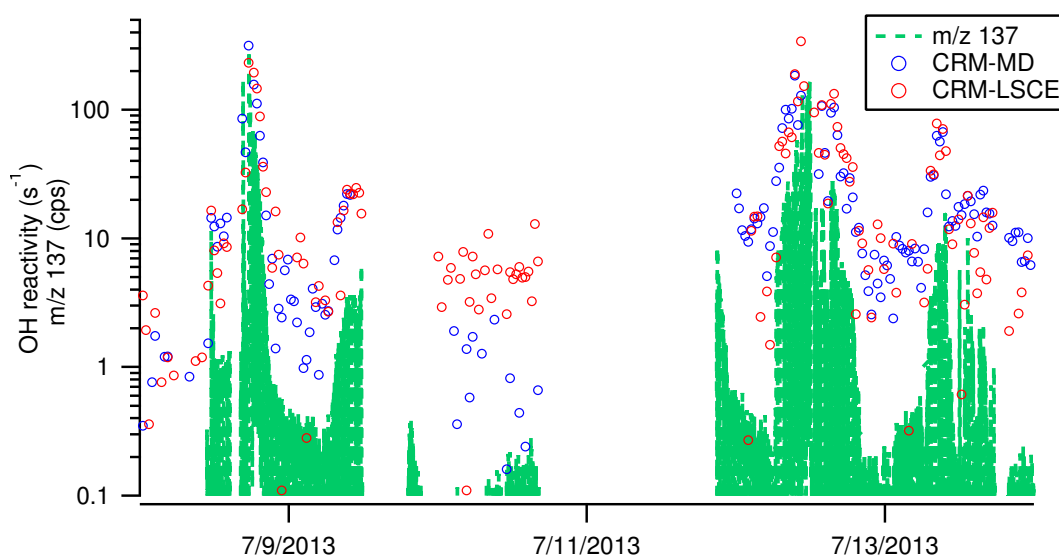
These panels show a stepwise (A→D) increase in the level of correlation and a slight decrease in variability among data sets from the two instruments when each correction is subsequently applied. During the sampling, CRM-LSCE measured a lower reactivity compared to CRM-MD (19 % lower for the whole raw data set). Corrections for humidity changes and deviation from pseudo first order kinetics brought the results closer, with a difference of only 4 %. Finally, panel d shows that the correlation between the two data sets when the correction for ambient air dilution is applied is described by a slope of 1 and a coefficient  $R^2$  of 0.75; which demonstrates that the results from the two instruments agree very well within the instrumental uncertainty. A linear least squares fit is also applied to the same data sets in a narrower range of reactivity values between 0 and  $50 \text{ s}^{-1}$  which is more relevant for the ambient OH reactivity values at the field site. For this range of values the variability among data is higher compared to the data points in the range  $0\text{--}300 \text{ s}^{-1}$  ( $R^2$  from 0.667 to 0.543 vs.  $R^2$  from 0.706 to 0.717). However, the agreement among CRM-LSCE and CRM-MD reactivity data sets also increases with the corrections applied when the  $0\text{--}50 \text{ s}^{-1}$  range is considered. From the raw data to the final corrected reactivity in the interval  $0\text{--}50 \text{ s}^{-1}$  the slope of the fits varies from 0.74 (raw data), 0.93 (humidity corrected data), 0.92 (kinetics corrected data) to 0.96 (dilution corrected, final result). Therefore the two data sets show a good agreement, within the instrumental uncertainties, also for reactivity values below  $50 \text{ s}^{-1}$ .

Figure 3.8 shows the time series of ambient OH reactivity measured by CRM-LSCE (red data points) and CRM-MD (blue data points). Data points refer to fully corrected results from the three periods of exercise including plant enclosure and ambient air measurements.



The signal measured by the PTR-MS of CRM-LSCE at  $m/z$  137, which corresponds to the unfragmented protonated mass of total monoterpenes, is also reported as a reference for reactive biogenic VOCs, in particular for the plant enclosure test. Peaks emerging during the plant enclosure tests were obtained from induced plant emissions (8–9 July and 12–13 July). As Fig. 3.8 shows, OH reactivity peaked when  $m/z$  137 peaked and signals from CRM-LSCE, CRM-MD and PTR-MS during the whole test exhibit the same variability. The method also demonstrated the real time quick response to the induced plant emissions.

It is worth noticing that this exercise was run on only two instruments which were also operated under similar conditions. It would be therefore very interesting to conduct this type of exercises on a larger number of CRMs, operated with different settings and in various environments. This would allow determining work cases when different corrections need to be applied and getting more insights on the impact they have on reactivity. However, intercomparison exercises for CRM instruments alone cannot help identifying specific and still unknown analytical issues for this technique. Therefore, experiments involving CRM and other techniques would be of greater interest.



**Figure 3.8:** Time series of enclosure kOH (8–9 July), ambient kOH (10–11 July), enclosure kOH (12–13 July) measured by CRM-LSCE (red) and CRM-MD (blue). Total monoterpenes signal measured by CRM-LSCE as protonated unfragmented  $m/z$  137 is reported with the green line.

### 3.4 Summary and conclusions

Our study presents results of the first intercomparison exercise reported on two Comparative Reactivity Method instruments assembled in different laboratories and used under similar operating conditions at the field site of Ersa, Cape Corsica, France. The two instruments discussed here are CRM-LSCE and CRM-MD, from the laboratories LSCE (Laboratoire des Sciences du Climat et de l' Environnement) and MD (Mines de Douai) where they were assembled. The intercomparison took place during early July 2013 in the frame of the ChArMEx project (Chemistry and Aerosols in a Mediterranean Experiment). It consisted of different calibration and validation tests of the instruments as well as simultaneous measurements of OH reactivity.

We here present for the first time an alternative approach to rapidly measure the initial concentration of pyrrole (C1) without perturbing the system. The method consists in introducing an OH scavenger in the reactor, when the system is measuring C2 under wet conditions. The scavenger, methane in this study, reacts with most of the OH radicals available for reaction with pyrrole and/or any other ambient molecule. Therefore, even if the cell is wet, and OH radicals are produced, the amount of pyrrole reacting with OH is negligible, and its actual level would be C1. The main advantage of this alternative approach is a substantial reduction in the conditioning time from several 10s of minutes to a few minutes. Such improvement is particularly useful during field works.

We document in detail the corrections needed to treat a data set of reactivity measured by CRM and use an alternative experimental approach to correct for deviations from first order kinetics. Humidity differences between C2 and C3 arise even when using a catalytic converter to generate zero air. The corrections applied for humidity influence the raw data of 4% (CRM-MD) and 12% (CRM-LSCE) on average. We showed how the instruments response changed by introducing known amounts of reactivity in the kinetics regime of pyrrole-to-OH ratios ranging from 1.2–2.6. In particular, we saw that the correction factor needed to account for a deviation from pseudo first order conditions is close to unity.

When the three corrections for humidity differences, deviations from first order kinetics, and dilution are applied they have an average impact on the two data sets of 20% for CRM-MD and 49% for CRM-LSCE.

We also tested the ability of the two instruments in measuring OH reactivity over a broad range of values from the instruments LOD ( $3\text{ s}^{-1}$ ) to approximately  $300\text{ s}^{-1}$ . Correlations between 30 min averaged data resulted in CRM LSCE measurements being extremely close to CRM MD measurements, a correlation described by a linear least squares fit with a slope of 1 and a  $R^2$  of 0.75. This excellent agreement among our results consolidates the

robustness of the comparative reactivity method to measure OH reactivity. Our study also stresses out the intensive data processing for this method and the importance of a proper determination of each correction needed to process the data for each instrument.

Finally, more intercomparison exercises among CRM instruments, and among different methods used to measure OH reactivity would be of great interest to evaluate the limitations and strengths of this technique.

**Acknowledgments** This study was supported by the European Commission’s 7th Framework Programme under grant agreement number 287382 “PIMMS” and under grant agreement number 293897, “DEFIVOC”. Financial support was also received from ChArMEx, PRIMEQUAL CARBO-SOR, CNRS, CEA, and the CaPPA project (chemical and physical properties of atmosphere), which is funded by the French National Research Agency (ANR) through PIA (Programme d’Investissement d’Avenir) under contract ANR-11-LABX-0005-01 and by the Regional Council Nord-Pas de Calais and the European Funds for Regional Economic Development (FEDER). We thank F. Dulac, E. Hamonou for managing the ChArMEx project and A. Borbon for the CARBO-SOR project, as well as all the scientists, engineers and students involved in the field campaign at Cape Corsica for their support. We acknowledge J. Williams and his group at MPIC for providing the glass reactors for our instruments.



## Chapter 4

# OH reactivity and concentrations of Biogenic Volatile Organic Compounds in a Mediterranean forest of downy oak trees

*This chapter contains the article*

Zannoni, N., Gros, V., Lanza, M., Sarda, R., Bonsang, B., Kalogridis, C., Preunkert, S., Legrand, M., Jambert, C., Boissard, C., and Lathiere, J.: OH reactivity and concentrations of Biogenic Volatile Organic Compounds in a Mediterranean forest of downy oak trees, *Atmos. Chem. Phys. Discuss.*, 15, 22047-22095, doi:10.5194/acpd-15-22047-2015, 2015.

### **Abstract**

Understanding the processes between the biosphere and the atmosphere is challenged by the difficulty to determine with enough accuracy the composition of the atmosphere.

Total OH reactivity, which is defined as the total loss of the hydroxyl radical in the atmosphere, has proved to be an excellent tool to identify indirectly the important reactive species in ambient air. High levels of unknown reactivity were found in several forests worldwide and were often higher than at urban sites. Such results demonstrated the importance of OH reactivity for characterizing two of the major unknowns currently present

associated to forests: the set of primary emissions from the canopy to the atmosphere and biogenic compounds oxidation pathways. Previous studies also highlighted the need to quantify OH reactivity and missing OH reactivity at more forested sites.

Our study presents results of a field experiment conducted during late spring 2014 at the forest site at the Observatoire de Haute Provence, OHP, France. The forest is mainly composed of downy oak trees, a deciduous tree species characteristic of the Mediterranean region. We deployed the Comparative Reactivity Method and a set of state-of-the-art techniques such as Proton Transfer Reaction-Mass Spectrometry and Gas Chromatography to measure the total OH reactivity, the concentration of volatile organic compounds and main atmospheric constituents at the site. We sampled the air masses at two heights: 2 m, i.e. inside the canopy, and 10 m, i.e. above the canopy, where the mean canopy height is 5 m. We found that the OH reactivity at the site mainly depended on the main primary biogenic species emitted by the forest, which was isoprene and to a lesser extent by its degradation products and long lived atmospheric compounds (up to 26 % during daytime). We determined that the daytime total measured reactivity equaled the calculated reactivity obtained from the concentrations of the compounds measured at the site. Hence, no significant missing reactivity is reported in this specific site, neither inside, nor above the canopy. However, during two nights we reported a missing fraction of OH reactivity up to 50 %, possibly due to unmeasured oxidation products.

Our results confirm the weak intra canopy oxidation, already suggested in a previous study focused on isoprene fluxes. They also demonstrate how helpful can be the OH reactivity as a tool to clearly characterize the suite of species present in the atmosphere. We show that our result of reactivity is among the highest reported in forests worldwide and stress the importance to quantify OH reactivity at more and diverse Mediterranean forests.

## 4.1 Introduction

Biogenic Volatile Organic Compounds (BVOCs) are the most important class of reactive organic compounds in the troposphere, once emitted they can be rapidly oxidized into other forms which have important feedbacks on air quality and climate.

The dominant source of BVOCs is the foliage of terrestrial vegetation (Steiner and Goldstein, 2007), above all, trees provide the largest portion of emitted BVOCs (75 %, Wiedinmyer et al., 2004), followed by shrubs and grasslands and minor sources such as oceans and soils (Bonsang et al., 1992; Guenther et al., 1995; Schade and Goldstein, 2001; Williams et al., 2004). Biogenic VOCs include isoprenoids (isoprene, monoterpenes, sesquiterpenes etc.), alkanes, alkenes, alcohols, carbonyls, esters, ethers and acids (Kesselmeier

and Staudt, 1999). Among the biogenic compounds isoprene and monoterpenes are the most studied, with a number of publications covering their synthesis and emission factors (Laothawornkitkul et al., 2009), canopy fluxes (Rinne et al., 2002; Karl et al., 2007), atmospheric mixing ratios (de Gouw and Warneke, 2007; Yáñez-Serrano et al., 2015), and atmospheric role (Atkinson and Arey, 1998; Fuentes et al., 2000; Whalley et al., 2014) currently available.

Isoprene alone makes up half of all biogenic compounds emitted, and the largest single source of VOCs in the atmosphere, with a current global estimate of about 500 TgC per year (Guenther et al., 2006) and large uncertainties still associated (Sindelarova et al., 2014).

When isoprene is released into the atmosphere, it is rapidly oxidized by the hydroxyl radical (OH), by ozone ( $O_3$ ), by the nitrate radical ( $NO_3$ ) during nighttime and occasionally by chlorine atoms. What determines its high reactivity as molecule is the presence, position and number of the double bonds. Atkinson and Arey (2003), have estimated lifetimes for isoprene ranging from a few hours with OH and  $NO_3$  to a few days with  $O_3$ , while monoterpenes and sesquiterpenes lifetimes can range from few minutes to hours with OH,  $NO_3$  and  $O_3$  (with mean concentrations of oxidants equal to  $2 \times 10^6$  molecules  $cm^{-3}$  for OH,  $7 \times 10^{11}$  molecules  $cm^{-3}$  for ozone and  $2.5 \times 10^8$  molecules  $cm^{-3}$  for  $NO_3$ ). By comparison, anthropogenic emitted molecules have lifetimes that vary between hours to years (Atkinson, 2000) which make biogenic compounds playing a dominant role in the lower troposphere and atmospheric boundary layer.

Isoprene dominant loss is the oxidation reaction with the OH radical, which involves the formation of six isomeric peroxyradicals which in unpolluted environments (under low  $NO_x$  regime) further react forming methyl vinyl ketone (MVK), methacrolein (MACR) and formaldehyde (HCHO) as primary products in the highest yields (Jenkin et al., 1998). Other product intermediates and secondary products in its oxidation pathway include hydroperoxides, hydroxyacetone, glyoxal, methylglyoxal, 3-methylfuran, acetic acid, glycolaldehyde and formic acid. Reactions with OH finally lead to the production of carbon dioxide and water, including formation of ozone and low volatile products which can partition to the particle phase. Significant production of ground level ozone on the regional scale were reported by Hirsch et al. (1996); Tsigaridis and Kanakidou (2002) for northeastern USA and Europe, while production of Secondary Organic Aerosols was demonstrated by Claeys et al. (2004).

Furthermore, isoprene and BVOCs emissions influence the oxidative capacity of the atmosphere, impacting the lifetime of many species including long-lived species such as methane and hydrofluorocarbons which are commonly depleted by OH.

Total OH reactivity is defined as the total loss of the hydroxyl radical due to reaction with ambient reactive molecules. It has demonstrated to be an excellent tool to provide indirect evidence of the importance of reactive molecules in ambient air. In addition, when OH reactivity is measured together with the concentration of trace compounds, it is possible to evaluate whether all the reactive components in the studied environment are identified or not. Missing reactivity, which is the fraction of measured OH reactivity not explained by complementary gas phase measurements, has been already reported in several forested sites (di Carlo et al., 2004; Sinha et al., 2010; Nölscher et al., 2013), up to almost 90% (Nölscher et al., 2012a) and usually higher than most of the urban sites investigated (Ren, 2003; Yoshino et al., 2006). Di Carlo and co-workers were the first to report evidences of a missing biogenic source in a forest in Michigan, probably associated to terpene-like emissions and not accounted from trace gases analysis. Their work pioneered and motivated the following studies of OH reactivity at other forested sites, including boreal forests (Sinha et al., 2010; Nölscher et al., 2012a; Mogensen et al., 2011), temperate mixed forests (Ren et al., 2006; Mao et al., 2012; Nölscher et al., 2013; Hansen et al., 2014 and Nakashima et al., 2014), and tropical forests (Sinha et al., 2008; Ingham et al., 2009 and Edwards et al., 2013).

The Mediterranean alone emits about  $40 \text{ t km}^{-2} \text{ year}^{-1}$  of BVOCs, (as country specific emission density considered for Portugal, Cyprus, Spain, Greece, Albania, Slovenia, Italy, Croatia and Bosnia-Herzegovina, (Rainer Steinbrecher 2009), its warm temperature and sunny conditions trigger emissions of BVOCs, which have a clear light and temperature dependence. Global warming is expected to impact the Mediterranean more than other areas in the world (Mellouki and Ravishankara, 2007). Model predictions have shown that this area will be characterized by higher temperatures, extended drought periods, enhanced ozone and particles levels (Giorgi, 2006; Giorgi and Lionello, 2008; Giorgi et al., 2011) which will all influence BVOCs emissions in strength and pattern (Laothawornkitkul et al., 2009). Such findings pose the attention on the importance of conducting more, intense and long-term field studies in the Mediterranean region.

Our study represents the first and only available to date study of OH reactivity in a Mediterranean forest. It shows results of total OH reactivity and BVOCs concentration from a field experiment conducted at two heights in the forest of the Observatoire de Haute Provence, France during late spring 2014.

The site at Observatoire de Haute Provence (OHP) is a special forest in the Mediterranean basin, located in the south east of France, poorly influenced by anthropogenic pollution and known for being almost homogeneous in BVOCs emissions. The dominant tree species at the site is the downy oak (*Quercus pubescens Willd.*), which has demonstrated to emit



nearly exclusively isoprene in large quantities (Kesselmeier et al., 1998; Genard-Zielinski et al., 2015). Recent studies at OHP have shown evidences for large tree specific intra variability in emission strength (Genard-Zielinski et al., 2015) strong isoprene fluxes to the atmosphere (up  $10.1 \text{ mg m}^{-2} \text{ h}^{-1}$  during summer 2010 (Baghi et al., 2012) and up to  $9.7 \text{ mg m}^{-2} \text{ h}^{-1}$  during spring 2012 (Kalogridis et al., 2014) and low intracanopy oxidation processes (Kalogridis et al., 2014).

OH reactivity was used as a tool to close the reactive carbon budget, and help assessing the oxidative processes occurring through the canopy. We measured total OH reactivity with the Comparative Reactivity Method (CRM, Sinha et al., 2008) and used complementary measurements of trace gases concentration to elucidate any missing reactivity pattern. We sampled OH reactivity and trace gases concentration at the same time, and investigated two canopy heights, one inside the forest at 2 m, a second one above the forest at 10 m.

## 4.2 Methodology

### 4.2.1 Description of the field site

We measured total OH reactivity and atmospheric gases concentrations at the oak observatory of the field site of Observatoire de Haute Provence **OHP**, as part of the **CANOPEE** project. Observatoire de Haute Provence is located in the Mediterranean region, south east of France ( $5^{\circ}42'44'' \text{ E}$ ,  $43^{\circ}55'54'' \text{ N}$ , 650 m a.s.l.), with Marseille the closest largest city about 100 km south, and Manosque the closest town about 18 km south from the site (Fig. 4.1).

The oak observatory (O3HP, <https://o3hp.obs-hp.fr>) was installed in 2009 within the OHP site in order to conduct field studies in ecology, plant phenology, microbiology and the atmosphere related to the third most abundant tree species in the French Mediterranean region. A geophysical sciences station (Gerard Megie) and an ICOS tower (Integrated Carbon Observation System, operative from 11 July 2014) also operate at OHP. The oak observatory is about 95 ha large and extends throughout a deciduous ecosystem dominated by downy oaks (*Quercus pubescens* Willd.) and Montpellier maple (*Acer monspessulanum* L.) which represent the 75 and 25 % respectively of the overstorey canopy. Smokey bushes (*Cotinus coggygria* Scop.) and other grass species constitute the understorey canopy. The whole canopy is about 5 m high with an average leaf area index (LAI) measured during August 2010 of 2.4 (LAI-2000, Li-Cor, Lincoln, NE, USA). The climate at the site is typical of the Mediterranean area, with dry and hot summers and humid cool winters.

Downy oak is a tree species known to emit almost exclusively isoprene (about 99 %, see

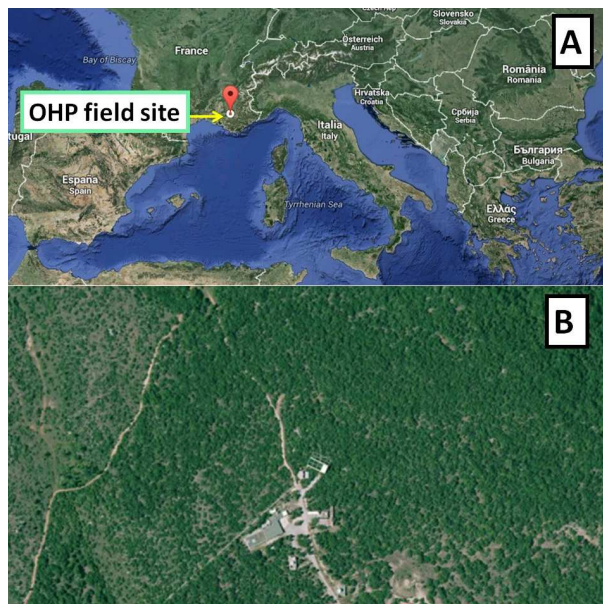


**Figure 4.1:** Site of Observatoire de Haute Provence (OHP) in the European map (a) and seen from above (b).

Genard-Zielinski et al. (2015) and for its dominance in this forest it makes OHP a natural laboratory for focused studies on isoprene.

Our field work took place during 29 May 2014–12 June 2014, as a follow up experimental study of the works conducted during spring 2012 and published by Kalogridis et al. (2014) and Genard-Zielinski et al. (2015).

### 4.2.2 Ambient air sampling

We measured the total OH reactivity together with the concentrations of BVOCs emitted by the forest, their oxidation products and main atmospheric constituents. For these measurements we deployed the Comparative Reactivity Method (CRM, home built), a Proton Transfer Reaction Mass-Spectrometer (PTR-MS, Ionicon Analytik GmbH, Austria), a Gas Chromatography Flame Ionization Detector (GC-FID, Chromatotech, France), a formaldehyde analyzer through the Hantzsch reaction (Aero-Laser GmbH, Germany), off-line analysis of sampling tubes through Gas Chromatography Mass Spectrometry (GC-MS, 3800/2200 ion trap MS, Varian, USA) and a  $\text{NO}_x$  detector (Thermo Scientific, USA). We sampled simultaneously OH reactivity and VOCs levels through two PFA sampling lines (OD 3/8") collocated on a mast. Measurements were performed sequentially at two heights inside and above the canopy (respectively 2 and 10 m), during 29 May 2014–12 June 2014. With an average canopy height of 5 m, air collection conducted at 2 and 10 m at OHP was

used to elucidate the composition and reactivity of air masses inside and above the whole forest. The sampling lines were insulated with black tubing and slightly heated with a thermocouple type K (1 °C above ambient temperature) to prevent losses along the tubes. Ambient air sampled from the two lines was directed to the two main trailers where the instruments were placed. Ambient air from sampling line A was divided through a manifold into four lines, directed respectively to PTR-MS, GC-FID, an HCHO analyzer and a main driving pump. Sampling line B was used for OH reactivity measurements and the manifold separated the flows to measure C2 (background pyrrole signal for OH reactivity), C3 (ambient air signal for OH reactivity) and a second driving pump. Flows to the main pumps were adjusted to achieve residence times differing about 10s maximum between the two sampling lines (residence time for CRM of 13s and for the other instruments of 23s).

An autosampler (Sypac V2, Tera Environnement, France) was used to adsorb air on packed sampling tubes in stainless steel with Tenax TA and Carbopack X as sorbent, for GC-MS offline analysis of monoterpenes levels. In this case we used an independent extra line that was placed at middle height on the mast. Sampling was performed every three hours on specific days and relative speciation among the detected monoterpenes ( $\alpha$ -pinene,  $\beta$ -pinene, myrcene, limonene) was used to determine the monoterpenes specific abundance and infer their amount from the total monoterpenes concentration, which instead was measured by PTR-MS every 5 min.

In addition,  $\text{NO}_x$  ( $\text{NO} + \text{NO}_2$ ) were monitored from sampling through an independent extra line placed 15 m away from the main sampling site. Ozone was monitored by the regional air quality network and its sampling line was placed a few hundred meters away the main sampling site.

### 4.2.3 Comparative Reactivity Method and instrument performance

Measurements of total OH reactivity were performed with a Comparative Reactivity Method instrument (home built CRM, see Sinha et al. (2008) and Nölscher et al. (2012b) for more details on the CRM).

A CRM instrument consists of a glass flow reactor and a detector, in our case a commercial Proton Transfer Reaction-Mass Spectrometer (PTR-MS quadrupole, Ionicon Analytik GmbH, Innsbruck, Austria). The concept of CRM is to produce a competition between a reference molecule, pyrrole ( $\text{C}_4\text{H}_5\text{N}$ ) and reactive molecules in ambient air to take up OH radicals generated inside the glass reactor. OH radicals are obtained from photolysis

of water vapor with a pen ray Hg lamp which emits at 184.9 nm placed inside one of the reactor arms. Pyrrole is first diluted in zero air and dry nitrogen, and its concentration is monitored on the PTR-MS at the protonated  $m/z$  68 (C0). When the Hg lamp is switched on, pyrrole concentration decreases due to photolysis and its concentration is monitored as C1. Then, the flow of nitrogen passes through a bubbler and water vapors are transported to the lamp to achieve photolysis and production of OH; in this stage pyrrole reacts with OH (rate coefficient =  $1.2 \times 10^{-10} \text{ cm}^3 \text{ molecule}^{-1} \text{ s}^{-1}$  at 25 °C, (Atkinson et al., 1984) and (Dillon et al., 2012) and C2 is monitored. A 4-way valve permits fast switches between zero air and ambient air, when the latter dilutes pyrrole the competition for OH radicals takes place and C3 is the measured concentration of pyrrole. C3 differs from C2 depending on the amount and type of reactive molecules present in ambient air. Differences between C2 and C3 are used to determine the total OH reactivity from the following equation:

$$R_{\text{air}} = \frac{(C3 - C2)}{(C1 - C3)} \cdot k_{\text{pyrrole+OH}} \cdot C1 \quad (4.1)$$

Equation (4.1) assumes that the reaction between pyrrole and OH is in the pseudo first order kinetics, i.e.  $[\text{pyrrole}] \gg [\text{OH}]$ .

Reactivity in ambient air is obtained every 10 min and raw values are corrected for humidity differences between the levels C2 and C3, deviation from first order kinetics, and dilution inside the reactor (Zannoni et al., 2015).

We qualified the performance of the CRM before and during the field campaign through injections of a known amount of reactivity generated by external gas standards. For this purpose, we used a standard of propane, which has a medium reactivity towards OH ( $k_{\text{propane+OH}} = 1.1 \times 10^{-12} \text{ cm}^3 \text{ molecule}^{-1} \text{ s}^{-1}$ , (Atkinson et al., 1997) and can therefore represent a proxy of an unknown air matrix; and isoprene, which instead is very reactive towards OH ( $k_{\text{isoprene+OH}} = 1 \times 10^{-10} \text{ cm}^3 \text{ molecule}^{-1} \text{ s}^{-1}$ , (Atkinson, 1986) and represents the main component of the air parcels sampled in this specific forest. Injections were performed over a range of pyrrole/OH between 2 and 9, with 9 being the closest to pseudo first order kinetics regime. The reactivity measured plotted versus the reactivity injected with the two mentioned standards gave a slope of  $1.01 \pm 0.04$  ( $1\sigma$ ) and an  $R^2$  of 0.96 up to reactivity values of  $500 \text{ s}^{-1}$ . The correction factor (slope of injected reactivity versus measured reactivity) is plotted versus the pyrrole-to-OH ratio and used to correct the raw reactivity for deviations in the kinetics regime. Corrections for humidity were obtained by averaging the results of three main tests conducted during the field campaign and were comparable to the results obtained in the laboratory (19% standard deviation among results). Calibrations of the PTR-MS for pyrrole dry and wet were carried out at the beginning and end of the field campaign and showed a very good agreement between each

other (difference within 1 % for the dry calibration factor and 4 % for the wet calibration factor).

During the days dedicated to the sampling of trace gases, we measured OH reactivity only for five days (three days inside the canopy and two days above the canopy) due to time needed to accurately qualify the performance of our instrument on the field, settings adjustment and tests needed to process the raw data.

Our instrument performs measurements between the limit of detection, LoD, of the instrument ( $3 \text{ s}^{-1}$ ,  $3\sigma$ ) up to  $500 \text{ s}^{-1}$  with an overall systematic uncertainty of 35 % ( $1\sigma$ ). More information on our instrument can be found in Zannoni et al. (2015).

#### 4.2.4 Complementary measurements at the field site

We measured the concentration of BVOCs emitted from the forest, their oxidation products and main atmospheric constituents. Concentrations are used to calculate the OH reactivity at the site with Eq. (4.2) and the species specific relative contribution.

$$R = \sum_i k_{i+\text{OH}} \cdot X_i \quad (4.2)$$

with  $i$  any measured compound listed in Tab. 4.1.

##### 4.2.4.1 Proton Transfer Reaction-Mass Spectrometer

We used a Proton Transfer Reaction-Quadrupole Mass Spectrometer (PTR-QMS, Ionicon Analytik, Austria) operated under standard conditions ( $p_{\text{drift}} = 2.2 \text{ mbar}$ ,  $E/N = 130 \text{ Td}$  ( $1 \text{ Td} = 10^{-17} \text{ V cm}^{-1}$ ),  $T_{\text{inlet}} = 60^\circ\text{C}$ ) to record the concentrations of trace gases at the site, (Lindinger and Jordan, 1998). We sampled the air masses in the scan mode, and inspected all species with protonated mass from  $m/z$  21 to  $m/z$  138 with cycles of 5 min each. Sampling in the scan mode procedure revealed to be a convenient way for analyzing unknown air parcels.

We calibrated the instrument using a gas calibration unit (GCU, Ionicon Analytik, Austria) with a standard gas mixture (GCU, Ionicon Analytik, Austria) containing: methanol ( $m/z$  33), acetonitrile ( $m/z$  42), acetaldehyde ( $m/z$  45), acrolein ( $m/z$  57), acetone ( $m/z$  59), isoprene ( $m/z$  69), crotonaldehyde ( $m/z$  71), methyl ethyl ketone ( $m/z$  73), benzene ( $m/z$  79), toluene ( $m/z$  93),  $\alpha$ -pinene ( $m/z$  137); see Tab. 4.2 for the list of compounds, their protonated mass, mean sensitivity from field calibrations and masses LoD. Calibrations were run over the range 0–20 ppbv at the beginning and at the end of the field campaign, with no significant change in the detector sensitivity (differences up to 10 %

**Table 4.1:** Measured species (except for CO and methane whose concentrations were assumed) used for calculating OH reactivity.

Family group	Species name
alkanes	methane; ethane; propane; n-butane; i-butane; n-pentane; i-pentane; 2,2-dimethylbutane; cyclohexane; hexane
alkenes	ethylene; propene; 1-butene; i-butene; cis-2-butene; 1,3-butadiene; trans-2-pentene; 1-pentene; cis-2-pentene; trans-2-butene
alkynes	acetylene
aromatics	benzene; toluene
biogenics	isoprene; MVK+MACR+ISOPOOH; $\alpha$ -pinene; $\beta$ -pinene; myrcene; limonene
oxygenates	formaldehyde; acetaldehyde; methanol; acetone; methyl ethyl ketone
inorganics	CO; NO; NO <sub>2</sub>

and for most species within 5 %) therefore we used a mean calibration factor for the whole campaign.

Volume mixing ratios for the calibrated species were obtained following the procedure of Taipale et al. (2008). Mixing ratios for the non-calibrated species were obtained from the transmission curve of the instrument and the species specific transmission coefficient. Correlations within mixing ratios obtained from calibration and transmission coefficients for calibrated species showed a good/fair agreement ( $R^2$  for  $m/z$  33,  $m/z$  45 and  $m/z$  69 respectively 0.81, 0.86 and 0.43).

We used a Gas Chromatography-Flame Ionization Detector to cross validate the concentration obtained for isoprene, which is the dominant compound at the site, usually measured at the protonated  $m/z$  69 with the PTR-MS but often prone to fragmentation in the drift tube (see Sect. 4.2.4.2). All the measured species, except isoprene, were not cross validated, and their mass identification was conducted based on the existing literature at similar sites, e.g. Kalogridis et al. (2014); Holzinger et al. (2002); Warneke et al. (2001). This is the case in particular for masses  $m/z$  71 and  $m/z$  73. Previous studies highlighted the presence of isoprene hydroperoxides (ISOPOOH) fragmenting at  $m/z$  71 in the PTR-MS, and representing a major yield from isoprene oxidation for low NO<sub>x</sub> environments, such as our case study (Liu et al., 2013 and Rivera-Rios et al., 2014). Since we did not separate between these compounds, we will therefore refer hereinafter to  $m/z$  71

**Table 4.2:** Name and mass of VOCs included in the standard mixture used for calibrating the PTR-MS. Reported sensitivities correspond to mean values of calibrations performed during the campaign. Limit of detections (LoD) correspond to  $3\sigma$  of the standard deviation.

VOCs contained in the calibration gas standard			
$m/z$	Identified compound	$S_{\text{norm}}$ (ncps ppbv <sup>-1</sup> )	LoD (ppbv)
33	Methanol	11.0	0.72
42	Acenotrile	19.0	0.12
45	Acetaldehyde	16.5	0.26
57	Ethylketone	17.6	0.09
59	Acetone	20.9	0.15
69	Isoprene	6.6	0.19
71	Crotonaldehyde	21.0	0.22
73	MEK	18.6	0.11
79	Benzene	9.9	0.13
93	Toluene	10.5	0.08
137	$\alpha$ -pinene	2.7	0.08

as the sum of the isoprene oxidation products ISOP.OXs: methyl vinyl ketone (MVK) + methacrolein (MACR) + isoprene hydroperoxides (ISOPOOH). Mass-to-charge 73, here reported as MEK and calibrated as such, can have several interferences. Among the possible interferences we speculate the presence of methylglyoxal, a compound generated during the degradation path of isoprene, which is the most abundant compound measured at our site. A detailed discussion about this compound and possible interferences at our site will be available in Yanez-Serrano et al. (2015).

#### 4.2.4.2 Gas chromatography-flame ionization detector

A gas chromatograph equipped with a flame ionization detector (GC-FID, airmoVOC C2–C6, Chromatotec, Saint Antoine, France) was deployed to sample hydrocarbons in the fraction C2–C6, with a time resolution of 30 min (10 min sampling followed by 20 min analysis). The instrument sampled ambient air with a flow rate of 18 sccm via a stainless steel inlet. Ambient air passed through a Nafion dryer, then to a preconcentration trap cooled down to  $-8^{\circ}\text{C}$ , filled with Carboxen, Carboxen B and Carboxen C, and finally thermodesorbed at  $220^{\circ}\text{C}$  and injected on-column into a metal capillary column (Porous Layer Open Tubular Column PLOT,  $\text{Al}_2\text{O}_3/\text{KCl}$ ; 0.53 mm inner diameter and 25 m length,

Varian Inc., USA). Calibrations were performed twice per week with a certified standard VOCs mixture (National Physical Laboratory, UK). The overall uncertainty was estimated to be 15 % ( $1\sigma$ ). Correlation between isoprene measured by GC-FID and  $m/z$  69 identified as the protonated isoprene mass over thirty minutes averaged data showed differences within 14 % among the two instruments ( $\text{isoprene}_{\text{GC-FID}} = 0.86(\text{isoprene}_{\text{PTR-MS}})$ ,  $R^2 = 0.93$ ).

#### 4.2.4.3 Formaldehyde analyzer

Formaldehyde was measured with a commercial Aerolaser analyzer (AL-4021, Aero-Laser GmbH, Germany). The technique, a continuous liquid fluorimetry, has been described in detail elsewhere (Dasgupta et al., 1988). Briefly, gaseous HCHO was scrubbed into a diluted sulfuric acid solution in a stripping coil thermostated at +10 °C. A fluorescent compound was quantitatively produced at +70 °C by the reaction of the liquid solution with the Hantzsch reagent (i.e. a dilute mixture of acetyl acetone, acetic acid, and ammonium acetate) and subsequently detected at 510 nm.

The working conditions applied to the AL 4021 for this study were similar to those applied previously for the same device in two HCHO studies conducted in Antarctica (Preunkert and Legrand, 2013; Preunkert et al., 2015). In brief, liquid reagents were prepared from analytical grade chemicals (Merck, USA) and ultrapure water (18 MOhm, TOC < 1 ppbv, Elga Labwater); the air flow was kept at 1000 scm which ensured a stripping efficiency of more than 99 %. Raw data were collected with a time resolution of 30 s. Gas standard calibrations and background levels took 50 and 25 min and were performed every 12 and 3 h, respectively. A mean detection limit of  $42 \pm 16$  pptv is calculated as twice the standard deviation of the raw data (30 s) obtained during the 121 zero measurements made during the campaign, which was consistent with the typical LoD achieved ( $\sim 30$  pptv) with the same analyzer in the previous studies above cited.

To minimize the effects of temperature changes on the field (see details in Preunkert et al., 2013), the instrument was placed in a thermostated box at 24 °C. A Teflon filter (47 mm diameter) was placed on the sampling line between the manifold (see Sect. 4.2.2) and the HCHO analyzer to prevent large particles (e.g. plant debris) entering the instrument. A comparison conducted on the field between line A (see Sect. 4.2.2, including the Teflon filter) and a 3 m long PTFE line (OD 1/4") connected directly to the analyzer confirmed that no significant contamination or loss of HCHO was present with this set up.



#### 4.2.4.4 NO<sub>x</sub> analyzer

Nitrogen oxides were measured with a commercial instrument (17i model, Thermo Scientific, USA), based on chemiluminescence. Its calibration was performed after the field campaign, where a LoD of 0.3 ppbv ( $2\sigma$ ) and a precision of  $\pm 0.4$  ppbv were estimated.

Nitrogen oxides were sampled at 15 m from the main sampling site, hence we assumed that their concentration inside and above the canopy was not affected by any significant change.

#### 4.2.4.5 GC-MS offline analysis

Adsorbing sampling tubes in stainless steel with Tenax TA and Carbopack X as sorbents were used to sample monoterpenes as  $\alpha$ -pinene,  $\beta$ -pinene,  $\beta$ -myrcene and limonene for off-line analysis with a Gas Chromatograph-Mass Spectrometer (GC-MS, 3800/2200 ion trap MS, Varian, USA). Sampling was conducted at ambient temperature with an autosampler (Sypac V2, Tera Environnement, France) every three hours, tubes were then stored at 4°C and analyzed within one month in the laboratory. Concentrations of individual monoterpenes were then used to infer their relative abundance from the total monoterpenes concentration obtained with the PTR-MS and calculate their contribution to the OH reactivity.

#### 4.2.4.6 O<sub>3</sub>, CH<sub>4</sub>, CO

Ozone is constantly monitored at OHP from the regional Air quality network Air-Paca, France (<http://www.atmopaca.org/>). The monitor is placed in a container located a few hundred meters distant from the sampling site. Methane and carbon monoxide mean concentrations were derived based on measurements conducted during spring 2012 and considered to be 1900 and 180 ppbv respectively.

#### 4.2.4.7 Meteorological parameters

Meteorological parameters such as temperature, relative humidity (CS215, Campbell Scientific, UK), Photosynthetical Active Radiation (PAR) (LI-190, Li-Cor, Lincoln, NE, USA), wind speed and wind direction were acquired through sensors already available at the measurements site (O<sub>3</sub>HP website: <https://o3hp.obs-hp.fr/index.php/fr/>). In this work we used data collected at 2 m and at 6 m to help discussing results inside the canopy and above the canopy respectively.

## 4.3 Results

### 4.3.1 Trace gases profiles and atmospheric regime

During the first week of campaign we observed some peaks of contamination due to car exhaust for about one hour every morning. Such data points were filtered from the data sets that will be discussed in this section.

Figures 4.2 and 4.3 illustrate diurnal profiles and time series of  $m/z$  69, identified as isoprene, its main degradation products  $m/z$  71, identified as MVK+MACR+ISOPOOH and here referred as ISOP.OXs (isoprene oxidation products), and formaldehyde (HCHO), together with meteorological parameters as air temperature and PAR, at both sampling heights. Figure 4.2 shows that these compounds have clearly diurnal profiles, but while isoprene covariates perfectly with PAR and temperature, its degradation products tend to increase after isoprene increases, which confirms the main secondary origin of such species. Isoprene peaks when temperature is highest in both cases: during the afternoon inside the canopy (left panel), during the late afternoon above the canopy (right panel). Formaldehyde mixing ratios are higher than  $m/z$  71 for both the heights; inside the canopy its profile is clearly diurnal, while above the canopy it looks more stable, mostly because of the higher nighttime level reached on 8 June 2014, see Fig. 4.3.

Time series are reported in Fig. 4.3 for the whole campaign period, from 29 May 2014 to 12 June 2014, and distinguished between air masses sampled at 2 m (data reported with the green line), and at 10 m (data reported with the blue line), on different days. All species show a progressive increase towards the end of the field campaign, when air temperature at the site was higher compared to the first days of measures. Data collected between 7–12 June 2014 above and inside the canopy can be directly compared, based on similar conditions of temperature and solar radiation. Maximum values for isoprene inside and above the canopy are close (maximum at 10 m is 19 ppbv, maximum at 2 m is 23 ppbv) and small differences can be explained mainly on a dilution basis, a better mixing of air masses reached above the canopy height due to the sparse canopy structure. Interestingly, high levels of  $m/z$  71 and HCHO were recorded during the nights between 7 and 8 June and between 11 and 12 June. Such high nighttime concentrations are also observed for other chemical species (see text below). Figure 4.4 illustrates time series for masses  $m/z$  33,  $m/z$  45,  $m/z$  59,  $m/z$  73 and  $m/z$  137; identified respectively as methanol, acetaldehyde, acetone, methyl ethyl ketone and sum of monoterpenes. Monoterpenes are primary emitted biogenic compounds while the other species can have both primary and secondary origins (Jacob et al., 2002, 2005 and Millet et al., 2010). Methanol has a daily maximum of 14 ppbv (inside the canopy), which makes it the second most abundant com-

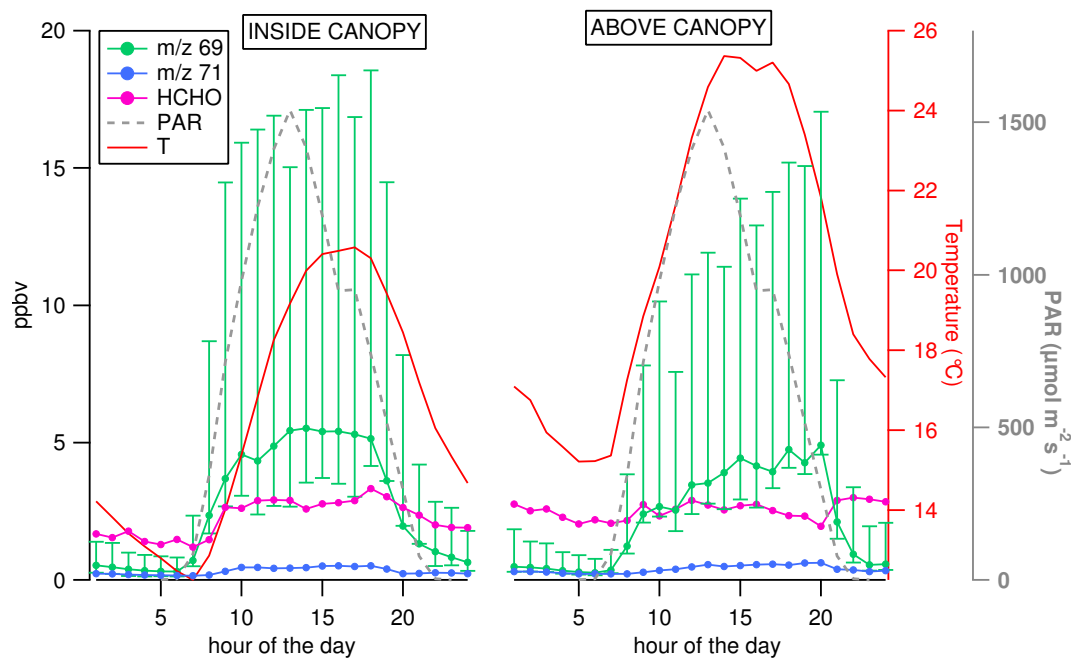


**Figure 4.2:** Diurnal profile of  $m/z$  69,  $m/z$  71, HCHO, temperature and PAR for days of measurements at 2 m (left panel) and at 10 m (right panel) of the field campaign. Bars on  $m/z$  69 correspond to  $\pm 1\sigma$  standard deviation. PAR data were collected at 6 m for both cases.

pound measured at OHP after isoprene (daily max inside the canopy 23 ppbv), followed by acetone, acetaldehyde, monoterpenes, ISOP.OXs, toluene and benzene, in order of abundance (Tab. 4.3). Based on a 24 h statistics, methanol is instead the first most abundant compound at OHP, followed by isoprene, acetone and acetaldehyde. Both methanol and isoprene have a diurnal profile, but methanol has a longer lifetime compared to isoprene (estimated to be 12 days and 1.4 h respectively, see Atkinson and Arey (2003) therefore over 24 h the former shows less variability in the atmosphere.

During the two nights mentioned above (8 and 12 June) the concentration of the oxygenated compounds was higher compared to the other nights. More discussion on this behaviour is provided in Sect. 4.3.4.

Anthropogenic hydrocarbons mixing ratios in the fraction C2–C6 were individually below 1.5 ppbv, with ethane the most abundant (mean over the campaign =  $0.9 \pm 0.2$  ppbv), followed by acetylene, ethylene and iso-pentane. Anthropogenic tracers measured by PTR-MS showed the same trend and confirmed the poor anthropogenic influence at this forested site: benzene maximum was 0.41 ppbv, with a 24 h statistics mean of 0.04 ppbv, toluene was maximum 0.69 ppbv and its mean over 24 h was 0.05 ppbv. Concentrations of NO and NO<sub>2</sub> were maximum 1.7 and 5 ppbv with a mean value of  $0.45 \pm 0.38$  and  $3.4 \pm 0.49$  ppbv

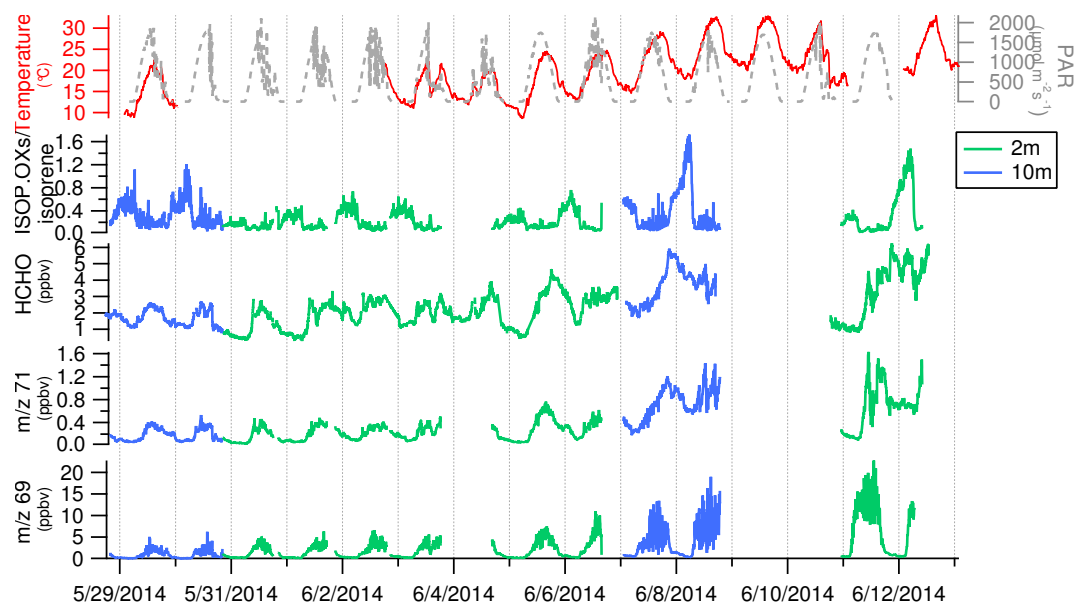


**Figure 4.3:** Time series of  $m/z$  69 (isoprene),  $m/z$  71 (ISOP.OXs=MVK+MACR+ISOPOOH), HCHO and ISOP.OXs/isoprene during the field campaign at OHP. Data were collected inside the canopy (2 m, green line) and above the canopy (10 m, blue line) on different days. Temperature and PAR measured at 6 m are reported as reference on the top panel.

**Table 4.3:** Volume mixing ratios inside and above the canopy of targeted molecules sampled with the PTR-MS.

$m/z$	Identified compound	Volume mixing ratios inside the canopy (2 m) (ppbv)				Volume mixing ratios above the canopy (10 m) (ppbv)			
		Mean 24 h statistics	Mean day (06:30–22:00)	Mean night (22:00–06:30)	Daily max	Mean 24 h statistics	Mean day (06:30–22:00)	Mean night (22:00–06:30)	Daily max
33	Methanol	5.41	5.35	4.44	2.80–13.51	5.47	5.72	4.81	7.87–11.16
45	Acetaldehyde	1.20	1.20	0.94	1.21–5.01	1.03	1.18	1	1.77–6.41
59	Acetone	2.39	2.37	2.20	2.33–10.03	2.08	2.04	2.06	2.02–7.12
69	Isoprene	2.54	3.54	0.47	1.17–22.77	2.26	2.80	0.42	5.11–19.02
71	ISOP.OXs	0.33	0.36	0.20	0.14–1.63	0.40	0.41	0.28	0.44–1.43
79	Benzene	0.04	0.04	0.03	0.12–0.36	0.07	0.11	0.07	0.14–0.41
93	Toluene	0.05	0.05	0.04	0.08–0.69	0.06	0.07	0.05	0.17–0.48
137	Monoterpenes	0.18	0.21	0.11	0.25–1.76	0.14	0.15	0.08	0.35–0.89

during the whole campaign, respectively. Ozone concentration ranged within 21–78 ppbv, with a mean value of  $47 \pm 10$  ppbv.

Values discussed herein can be compared to values measured during the field work conducted at OHP during spring 2012 (compare Tab. 4.3 in this work with Tab. 4.2 in Kalogridis et al., 2014). Both field works were conducted during the same time and season (late spring, beginning of June), with the site exposed to slightly different temperature levels (daily maximum in 2012 30°C, daily maximum in 2014 31.5°C), but the sampling was

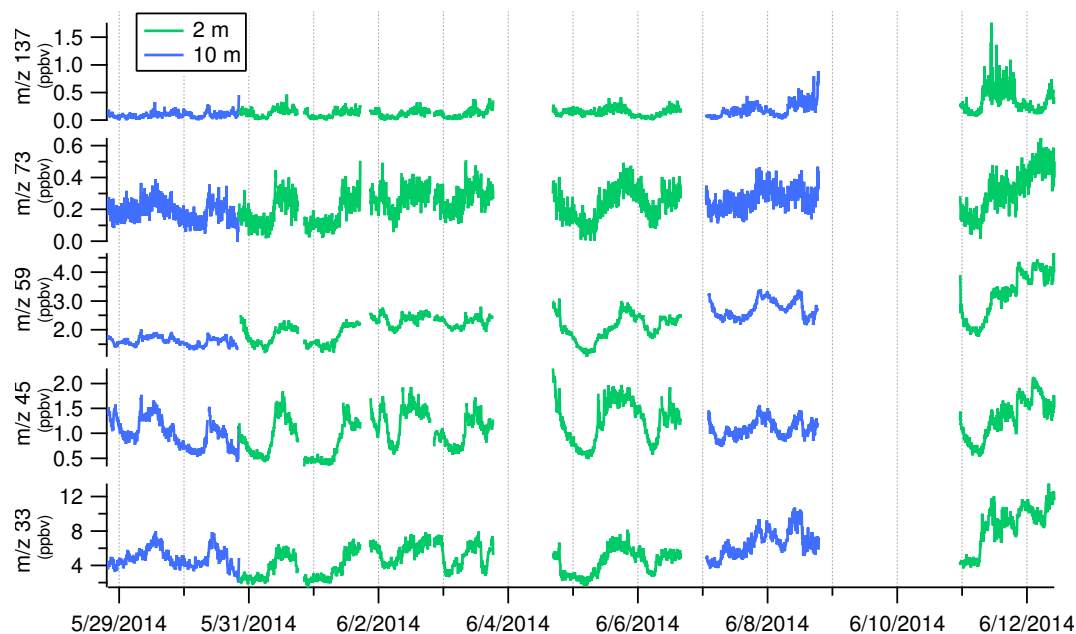


**Figure 4.4:** Time series of  $m/z$  33 (methanol),  $m/z$  45 (acetaldehyde),  $m/z$  59 (acetone),  $m/z$  73 (methyl ethyl ketone),  $m/z$  137 (monoterpenes) inside (2 m, green line) and above (10 m, blue line) the canopy at OHP.

performed at different portions of the forest, distant between each other a few hundreds of meters. It is interesting to notice that atmospheric levels of VOCs are close only for anthropogenic species while all biogenic species and oxygenated compounds have almost doubled from 2012 to 2014. The same isoprene-temperature dependence was achieved during the two experimental works, which demonstrates that the higher mean concentration of biogenic compounds observed in 2014 was probably due to the higher mean temperature during the second campaign.

### 4.3.2 Total OH reactivity

Figures 4.5 and 4.6 report thirty-minutes averaged values of total OH reactivity inside and above the canopy during 11–12 June 2014 and 7–8 June 2014 with the black line and associated error bars (overall uncertainty 35%,  $1\sigma$ ). At 2 m OH reactivity varied between the instrumental LoD up to  $69\text{ s}^{-1}$ , and was on average  $26 \pm 19\text{ s}^{-1}$ . At 10 m it varied between the LoD and a maximum of  $68\text{ s}^{-1}$  and was on average  $24 \pm 14\text{ s}^{-1}$ . OH reactivity had the same trend of temperature and PAR, with a diurnal profile that demonstrates its dependency on the emission and profile of biogenic compounds emitted by the forest, released when sunrise started and temperature increased. During 11 June 2014 OH reactivity started to increase at 6 a.m. (CEST) when the sun rose up and it

reached a maximum around 10:30 a.m., then again around 4 p.m., associated to more intense solar radiation. It decreased after sunset, at 8 p.m. when also temperature and light reduced. Reactivity sampled at 10 m had also a diurnal profile. On 7 June 2014 it started to increase at 6:30 a.m., had its maximum around 6:30 p.m. and decreased at 9:30 p.m. On 8 June 2014 it increased at 6:30 a.m. and reached its maximum at 2:15 p.m.

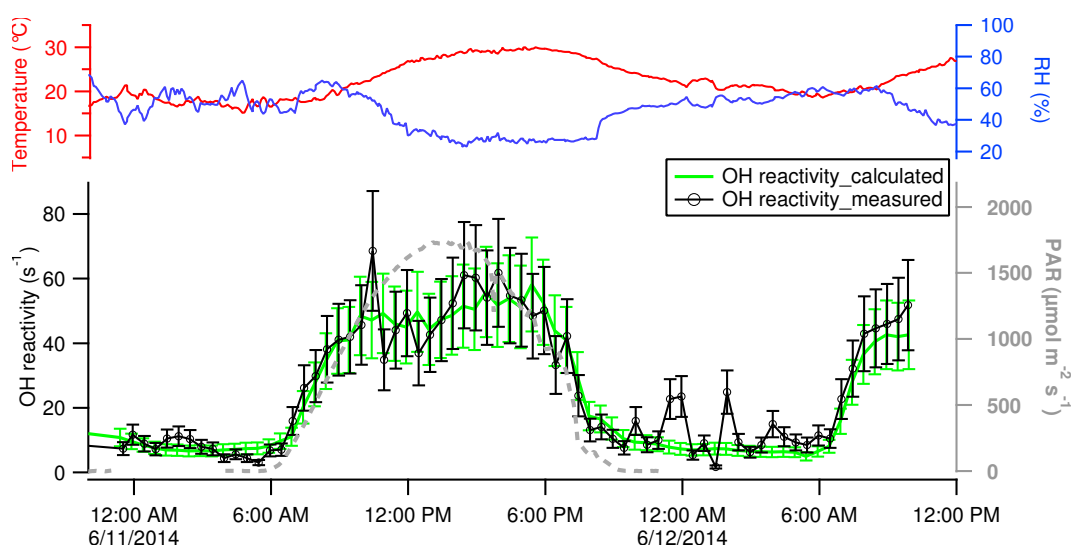


**Figure 4.5:** Total OH reactivity measured (black line and markers) with the Comparative Reactivity Method (CRM) and calculated OH reactivity from measured concentrations of trace gases (green line) on the left axes, Photosynthetic Active Radiation on the right axes (gray dashed line), temperature and Relative Humidity on the left and right upper axes (red and blue lines). Data points represent thirty minutes averages of the sampled data and error bars correspond to 35 and 25 % ( $1\sigma$ ) instrumental uncertainties. Data refer to air sampled inside the canopy at 2 m height.

### 4.3.3 Measured and calculated OH reactivity

We compared the total OH reactivity measured with the CRM instrument with the one calculated from the concentrations of the measured trace gases and their rate coefficients with OH. Tab. 4.1 illustrates the classes and species measured by ancillary methods on the field used to compute their relative contribution to the OH reactivity. It has to be noticed that due to instruments availability and the relative homogeneity of species emitted by the forest, only a few primary emitted compounds and main atmospheric species were measured and used to calculate the OH reactivity. For methane and carbon monoxide we derived a mean value from measurements run in 2012, respectively 1900 and 180 ppbv.

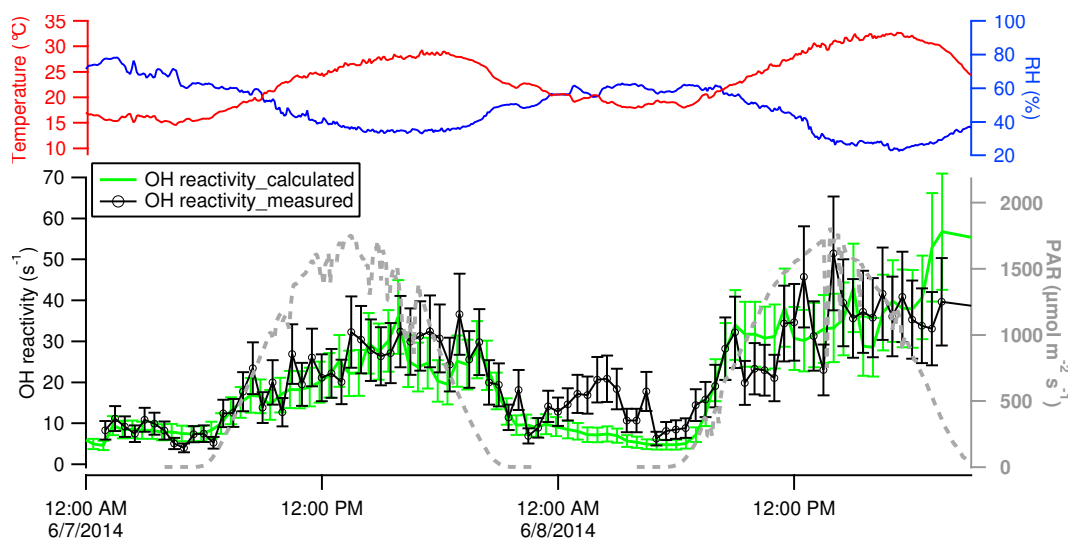


**Figure 4.6:** Total OH reactivity measured (black line and markers) and OH reactivity calculated (green line) above the canopy at 10 m height. Temperature (red line), RH (blue line) and PAR (gray dashed line) are reported for reference. Data points represent thirty minutes averages over the data collected. Uncertainties correspond to 35 and 25 % for the measured and calculated reactivity respectively ( $1\sigma$ ).

Isoprene oxidation products (ISOP.OXs) OH reactivity was calculated from their measured total concentration and the mean rate coefficient of the reaction of MVK and MACR with OH. Since we did not separate the different ISOP.OXs, we could not determine the exact fraction of MVK and MACR contributing to the OH reactivity, which leads to a slight overestimation of the calculated reactivity (Rivera-Rios et al., 2014); in our case such overestimation is not significant due to the higher abundance of isoprene.

Calculated OH reactivity was determined to be between 5 and  $58\text{ s}^{-1}$  and on average  $24 \pm 19\text{ s}^{-1}$  between 11–12 June 2014 at 2 m inside the canopy. At 10 m, above the canopy height, it varied between 3 and  $55\text{ s}^{-1}$ , being on average  $19 \pm 12\text{ s}^{-1}$ .

Figures 4.5 and 4.6 show the covariation between measured (black line) and calculated (green line) OH reactivity during 11–12 June 2014 at 2 m and during 7–8 June 2014 at 10 m, with associated error bars (35 % for the measured reactivity and 25 % for the calculated reactivity,  $1\sigma$ ).

For both time series, during daytime, inside and above the canopy height, the measured OH reactivity agreed very well with the calculated one within the instrumental uncertainties. Since there was not a significant difference between the two values we can conclude that no significant missing reactivity was observed in this specific ecosystem in the Mediterranean basin during our measurement campaign. In addition, the precise characterization of

the composition of air even at 10 m height corroborates the weak oxidation of primary compounds within the canopy.

Simultaneous ancillary measurements of trace gases permit to resolve the total OH reactivity into the relative contributions of the individual species. Figures 4.7 and 4.8 show the breakdown of OH reactivity into the main contributors during daytime and nighttime at the two heights considered. In all cases the dominant reactive species was isoprene. Isoprene is among the most reactive compounds towards OH, the most abundant compound in this forest and nearly the only compound emitted by downy oak trees which constitute the large majority of tree species accounted in this ecosystem. Hence, we expected its large contribution to the reactivity. Isoprene made up from 28 to 83% of the total OH reactivity during nighttime (total mean  $6\text{ s}^{-1}$ ) and daytime (total mean  $29\text{ s}^{-1}$ ) respectively at 2 m high. It made up from 24% during night to 74% during the day of the total reactivity (total means 6 and  $20\text{ s}^{-1}$  respectively) at 10 m. Assuming the same OH reactivity inside and above the canopy during those days of measurements ( $30^\circ$  temperature maximum at 2 m, and  $32^\circ$  maximum at 10 m) the weight of isoprene between the two heights differs only of 9 points percentage, considered that at 2 m data of alkanes+alkenes are missing, we can conclude that there was not a substantial difference between the two heights. Inside the canopy during daytime, all the measured species apart from isoprene, contributed in total about 17% to the OH reactivity. Carbon monoxide, HCHO and  $\text{NO}_2$  were the second important species accounting for 3 points percentage each, followed by acetaldehyde, MVK+MACR and monoterpenes with 2 points percentage each and all the other compounds less than this. During nighttime, the concentration of isoprene reduced to a few pptv and other species such as CO and methane which were more stable in the atmosphere became more important, contributing to 16 and 5% respectively. Formaldehyde,  $\text{NO}_2$ , acetaldehyde, MVK+MACR and monoterpenes made up respectively 11, 16, 8, 5 and 4%. Above the canopy during daytime the second most reactive species were CO,  $\text{NO}_2$ , HCHO and MVK+MACR (5, 5, 4 and 3%). Still above the canopy but during nighttime, CO,  $\text{NO}_2$ , HCHO, alkanes+alkenes, MVK+MACR, methane and acetaldehyde weighted respectively 17, 15, 14, 6, 5, 5 and 5%. Monoterpenes weighted about 2–1% during daytime and 4% during night in both cases. Monoterpenes are also very reactive BVOCs towards OH, when present they can definitely compete with isoprene in terms of reactivity. At OHP, monoterpenes mixing ratios were low (see Tab. 4.3), they did not constitute a major class of compounds of the area and by consequence their contribution to the OH reactivity was poor.



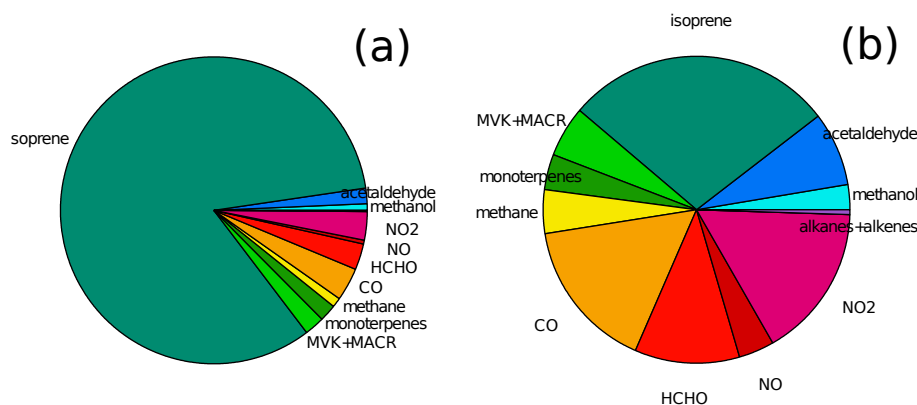


**Figure 4.7:** Total OH reactivity speciation inside the canopy (2 m height) during daytime (left pie chart **a**) and during nighttime (right pie chart **b**). Data refer to air masses sampled at OHP during 11–12 June 2014. Total OH reactivity was  $29 \text{ s}^{-1}$  (daytime mean value) and  $6 \text{ s}^{-1}$  (nighttime mean value). All compounds reported in Tab. 4.1 were used to calculate their relative contributions.

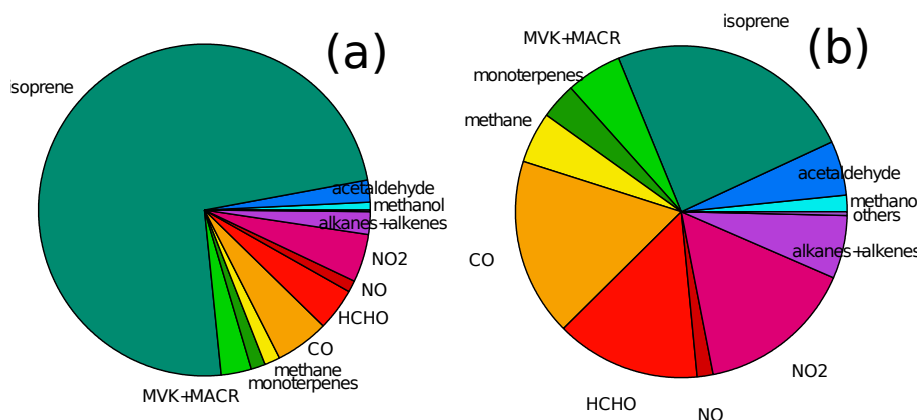


**Figure 4.8:** Total OH reactivity speciation above the canopy (10 m height) during daytime (left pie chart **a**) and during nighttime (right pie chart **b**). Data refer to air masses sampled at OHP during 7–8 June 2014. Total OH reactivity was  $20 \text{ s}^{-1}$  (daytime mean value) and  $6 \text{ s}^{-1}$  (nighttime mean value). All compounds reported in Tab. 4.1 were used to calculate their relative contributions. Others refer to the sum of the contributions of: acetonitrile, acetone, MEK, benzene and toluene.

#### 4.3.4 Nighttime missing reactivity

During the nights between 7 June 2014 and 8 June 2014 and between 11 June 2014 and 12 June 2014, the measured total OH reactivity and the calculated reactivity reported some discrepancies (Figs. 4.5 and 4.6). For the results above the canopy such discrepancy was visible around midnight, and significant differences were observed from 1 a.m. to 4:30

a.m. (Fig. 4.6). Inside the canopy, the signal of total OH reactivity started to scatter around 11:30 p.m., then again at 2 a.m. and flattered back to the signal of calculated OH reactivity around 4:30 a.m. (Fig. 4.5). Both differences were respectively  $13\text{--}14\text{ s}^{-1}$  and accounted for a fraction higher than 50% of missing OH reactivity. Such values of missing reactivity are comparable to values of total OH reactivity measured in boreal and temperate forests (Sinha et al., 2010; Ren et al., 2006).

To investigate the molecules responsible for the missing OH reactivity, we examined the variability of the calculated and measured OH reactivity, along with primary biogenic compounds, anthropogenic tracers, OVOCs and ozone concentrations, and ISOP.OXs / isoprene ratio. It is striking noticing that whereas isoprenoids exhibited a regular diurnal cycle, all OVOCs showed increased nighttime values (Figs. 4.3 and 4.4). Species profiles as reported in Fig. 4.3 show that on 7 June 2014 ISOP.OXs and HCHO started to increase during the day, around 1 p.m., reached a maximum around 7:30 p.m. and then decreased during the night. While isoprene concentration flattered much faster due to its higher reaction rate, its oxidation products reacted slower, which explains the higher ISOP.OXs / isoprene ratio observed. The ISOP.OXs / isoprene ratio had the same magnitude and trend for both missing reactivity events and reached a maximum during these two specific nights compared to the rest of the campaign period (Fig. 4.3). Interestingly, ISOP.OXs / isoprene well anticovariated with ozone's decrease (Figs. 4.9 and 4.10). Profiles of other measured OVOCs ( $m/z$  45,  $m/z$  59,  $m/z$  73, Fig. 4.4) show higher concentrations around the midnight of both nights, suggesting an accumulation of oxygenated compounds and an intense nighttime chemistry. Indeed, meteorological parameters as wind speed and wind direction for data collected at 10 m help noticing that during the night between 7 and 8 June 2014 the wind blew from the same direction with low speed, suggesting more stable meteorological conditions which could have favored some nighttime chemistry (Fig. 4.10). Daytime air temperature for these two days was also the highest registered over the whole measurement campaign (Fig. 4.3).

Several evidences make us believe that the production of OVOCs was linked to the oxidation of biogenic molecules. First, common anthropogenic tracers as acetonitrile and benzene did not show any special increase during these events, supporting the idea that such nighttime higher concentration of oxidized compounds in the atmosphere was associated to local drivers rather than transport. Secondly, we observed an increase of atmospheric levels of some masses measured by the PTR-MS and not used to calculate the OH reactivity before, such as:  $m/z$  47,  $m/z$  61,  $m/z$  75,  $m/z$  83,  $m/z$  87 and  $m/z$  101. These protonated masses can be identified as oxidation products resulting from the degradation of isoprene according to the existing literature and associated respectively to: formic acid, acetic acid, hydroxyacetone, 3-methylfuran and other unsaturated C5, methacrylic acid

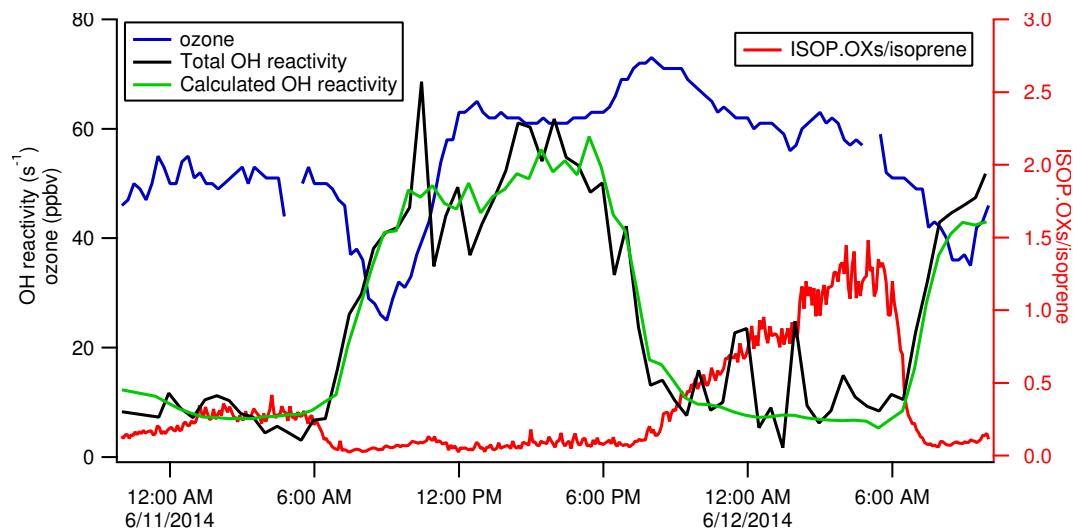


**Figure 4.9:** Total OH reactivity, calculated reactivity and ISOP.OXs / isoprene ratio at 2 m height. Ozone data were acquired a few hundred meters away from the sampling area.

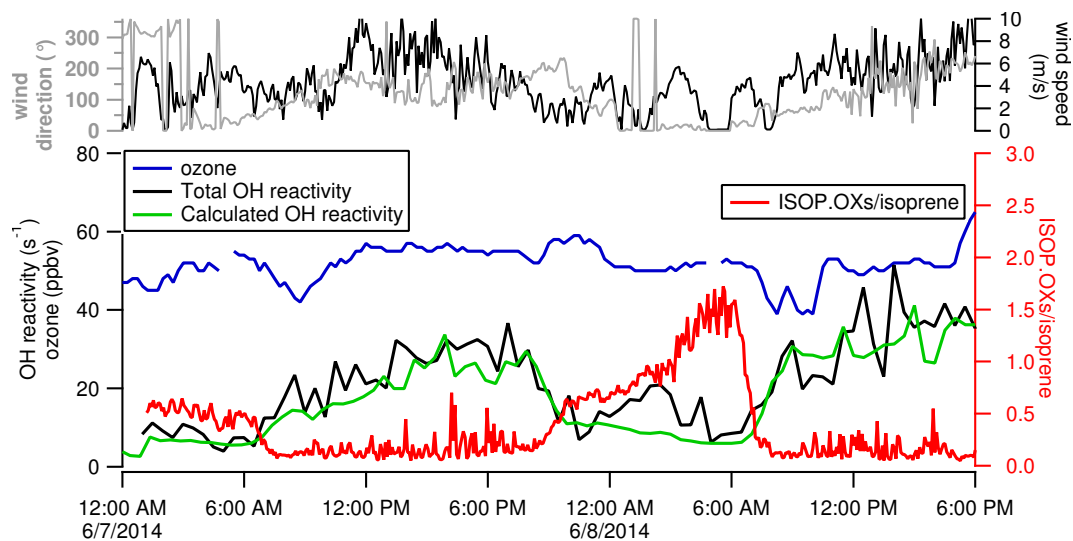


**Figure 4.10:** Total OH reactivity, calculated reactivity and ISOP.OXs / isoprene ratio at 10 m height. Ozone data were acquired a few hundred meters away from the sampling area. The upper panel shows wind direction and wind speed data.

and isoprene hydroperoxides (Warneke et al., 2001; Holzinger et al., 2002). We estimated roughly the contribution of such species to the calculated OH reactivity and found out that only a small fraction of the missing OH reactivity could be explained. Therefore there must be other unmeasured species that were formed locally, very likely OVOCs that were present during those nights.

Gas phase chemistry during nighttime is usually initiated by ozone and the nitrate radical.

The low levels of  $\text{NO}_x$  observed at the site (nighttime NO was maximum 0.8 ppbv and on average  $0.14 \pm 0.13$  ppbv) indicate that nitrate chemistry is not a probable source of such oxidized compounds; on the other hand ozone isoprene chemistry is slow and cannot explain alone their production in the gas phase (isoprene lifetime with nitrate is 1.6 h while with ozone is calculated to be 1.3 days (Atkinson and Arey, 2003)). If the unmeasured OVOCs were not generated exclusively from isoprene, neither had anthropogenic precursors, we speculate that they must have been a combination of higher generation products derived from isoprene oxidation and OVOCs resulting from reactive primary biogenic precursors, other than isoprene, and more reactive towards ozone. We can expect that these biogenic precursors were larger molecules that could not be measured with our means.

Holzinger et al. (2005) measured a whole class of oxidation products in a pine forest and suggested that they must have formed from reactions of ozone with very reactive terpene-like compounds. He estimated these compounds to be emitted about 6–30 times more the emission of the observed monoterpenes above his forest. Karl et al. (2005) have identified the same oxygenated compounds for different pine species and speculated their production at the leaf level, rather than in the gas phase. Recent experiments on leaves of tobacco plantations have identified the unsaturated semivolatile compounds undergoing leaves reactions (Hansel et al., oral presentation EGU 2015). Those compounds once deposited on the leaves quickly undergo surface oxidation reactions with ozone releasing volatile products into the gas phase. Oxidation reactions are favored by higher ambient RH, high ozone levels and can also occur when leaves stomata are closed. Measuring the species initiating these surface reactions is extremely difficult with the instruments we had on the field, therefore we do not have more clues to support this hypothesis nor exclude it has occurred in the forest of OHP. Focused studies on the leaves of downy oak trees with branch enclosure techniques would be of help to elucidate it.

### 4.3.5 OH reactivity at other biogenic sites

Our results of reactivity from OHP constitute the first data set of total OH reactivity measured in a Mediterranean forest. Nevertheless, several observations in other forested sites exist to date. Such environments constitute perfect laboratories to study the emissions from different plant species and their evolution due to natural factors such as light and air temperature. OH reactivity observations have been of great help in the years to elucidate the presence of unknown compounds and to eventually assess BVOCs oxidation patterns which were not before characterized (Nakashima et al., 2012; Nölscher et al., 2014). In addition, biogenic species constitute a class of compounds with the highest reactivity towards the hydroxyl radical. OH reactivity during springtime and summertime

in forests is usually higher than in metropolitan areas which are often polluted by less reactive hydrocarbons.

Figure 4.11 illustrates all the existing studies of OH reactivity conducted in biogenic environments with their corresponding references. Colored bars show the range of reactivity measured at the site; while colors refer to different type of climatic zones to which the studied forests belong. The reader has to notice that not all the studies were carried out with the same method (see figure's caption for more details).

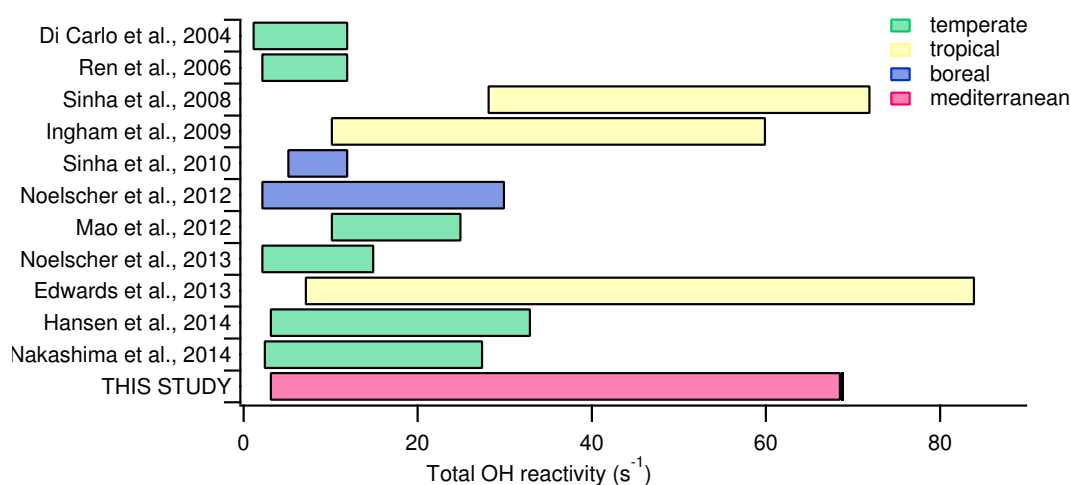


**Figure 4.11:** Total OH reactivity results from all the published experiments conducted worldwide at forested sites. Bars refer to the ranges observed between the minimum (often corresponding to the instrumental LoD) and the maximum values published. Studies were all conducted during spring- summer time. This study and those from Sinha and Noelscher adopted the Comparative Reactivity Method; while Di Carlo, Ren, Mao, Ingham, Edwards and Hansen used a Total OH Loss Rate Measurement based on Laser Induced Fluorescence; Nakashima deployed a Laser Induced Fluorescence Pump and Probe Technique (see references for instrumental details).

The forest at OHP is among the investigated biogenic sites producing the highest OH reactivity worldwide. The only two sites where a higher reactivity was reached is the tropical rainforest of Borneo (Edwards et al., 2013), where a maximum of  $84\text{s}^{-1}$  was reported and the tropical rainforest of Suriname with a maximum of  $72\text{s}^{-1}$  (Sinha et al., 2008). Tropical forests are usually more heterogeneous in plants species and BVOCs emission patterns compared to the forest at OHP, which is particularly homogeneous also compared to other Mediterranean forests. In Borneo, the dominant primary species to the OH reactivity was also isoprene (relative contribution of 36.8%), but terpenes made up 7% and the largest portion of reactivity was attributed to the oxidation products of BVOCs and products intermediates (47.1%). In conclusion, on one side the intense temperature

and solar radiation result in similar emission strength and reactivity, while on the other side, biodiversity and canopy structure draw the major differences between the two sites. Indeed, the forest at OHP besides being homogeneous is also shorter and sparser compared to tropical forests, such structure allows a better mixing of the air masses and a faster transport of the primary species to the atmosphere.

By comparison, the investigated mixed temperate forests and boreal forests produced lower OH reactivity, which can also be attributed to the lower temperature and less intense solar radiation leading to weaker emissions from the local canopies.

## 4.4 Summary and conclusion

During late spring 2014 at the downy oaks forest of the site Observatoire de Haute Provence we found that the total OH reactivity was maximum  $69\text{ s}^{-1}$  at 2 m (inside the canopy), and  $68\text{ s}^{-1}$  at 10 m (above the canopy). Interestingly, during daytime, at both heights the measured OH reactivity was in good agreement, within the measurements uncertainties, with the calculated OH reactivity obtained from the suite of measurements of trace gases concentration available during our field experiment. Hence, we did not observe any missing OH reactivity neither inside nor above the forest.

In addition, considering the homogeneity of the forest and strong reactivity of isoprene, we expected isoprene to be the species contributing mostly to the OH reactivity, at least for measurements at 2 m high. We found indeed that inside the canopy during daytime, isoprene contributed to the OH reactivity at the 83 %, followed by CO, NO<sub>2</sub> and HCHO. Above the canopy height, isoprene made up 74 %, followed by CO, NO<sub>2</sub>, HCHO and MVK+MACR. Such results indicate that there was not a significant difference in the speciation inside and above the canopy. During nighttime, when isoprene emissions are arrested and atmospheric concentrations were a few pptv, long lived species such as CO and methane contributed to about 16–17 and 5 % for both inside and above the canopy. Still, even by night, isoprene accounted for the largest portion of OH reactivity.

The low levels of isoprene oxidation products observed during the day indicate that the intracanopy oxidation is low, and almost all the isoprene emitted by the canopy is transported to the atmosphere, which confirms the previous experimental work on isoprene fluxes conducted during spring 2012. The fact that no missing OH reactivity was observed, especially above the canopy, additionally corroborates the fact that any unmeasured compound, product of the oxidation of isoprene was present.

During the nights between 7–8 June 2014 and 11–12 June 2014 from sampling above

and inside the canopy respectively, the total OH reactivity we measured was significantly higher compared to the calculated OH reactivity. Such missing reactivity accounted for more than 50 % and can be explained by locally produced unmeasured oxidation products. We speculate that unmeasured OVOCs represent a mixture of species including higher generation products resulting from isoprene oxidation and products of the reaction between reactive biogenic precursors and ozone.

Our work represents the first and unique data set to date of total OH reactivity measured in a Mediterranean forest. In a worldwide perspective, the investigated forest of downy oaks at OHP produces an OH reactivity among the highest measured. Remarkably, only tropical forests showed to be as much reactive as OHP. Lower OH reactivity was measured in boreal and mixed temperate forests, due to the lower temperature and solar radiation and possibly to the more heterogeneous-like forests (i.e. less abundance of isoprene).

The Mediterranean region is rich in biodiversity, and biogenic activity is enhanced by its characteristic climate. Out of 2 million km<sup>2</sup> of surface only about 100 thousands remain undisturbed by human activity. We expect therefore that OH reactivity in the Mediterranean can vary much depending on the type of vegetation, its extension and interaction with pollutants derived by human activity. In addition, the Mediterranean is also a hotspot for climate change. This issue will certainly impact the biogenic emissions strength and pattern which therefore will influence the total OH reactivity. We would therefore pose the interest with our work to persecute studies of OH reactivity and BVOCs levels at diverse biogenic sources in the Mediterranean area for extensive periods.

**Acknowledgments** This study was supported by European Commission's 7th Framework Programme under Grant Agreement Number 287382 "PIMMS", ANR-CANOPEE and ChArMEx, CEA and CNRS. We would like to thank N. Bonnaire for his work on the GC-MS analysis. We acknowledge J. P. Orts, I. Reiter, the staff at O<sub>3</sub>HP and at Gerard Megie, INERIS for logistical help. We thank F. Dulac and E. Hamonou for managing the ChArMEx project.





## Chapter 5

# Total OH reactivity at a receptor coastal site in the Mediterranean basin during summer 2013

*This chapter contains the draft of an article in preparation that is going to be submitted to Atmos. Chem. Phys., ChArMEx special issue. Several participants to the project ChArMEx are coauthors to this article.*

### **Abstract**

Total OH reactivity, the total first order loss rate of OH in ambient air directly provides the total reactive carbon loading in air. We measured the total OH reactivity for the first time in the western Mediterranean basin during summertime. Measurements were performed at the field site Ersa, in the northern cape of Corsica, France, during summer 2013 for the project CARBOSOR (CARBOn within continental pollution plumes: SOurces and Reactivity) under the project ChArMeX (Chemistry-Aerosols Mediterranean Experiment). Here, we compare the measured total OH reactivity with the OH reactivity calculated from the measured reactive gases. The difference among these two parameters is regarded as the missing reactivity, i.e. the fraction of reactivity due to the unmeasured species. The measured total OH reactivity at the site varied between the instrumental LoD ( $3 \text{ s}^{-1}$ ) to a maximum of  $17 \pm 6 \text{ s}^{-1}$  and was on average  $5 \pm 4 \text{ s}^{-1}$  ( $1\sigma$  standard deviation of the data). It covaried with air temperature and showed a diurnal profile similar to the one observed

for the atmospheric mixing ratio of the biogenic species measured at the site. During the period between 23-30/07 a significant fraction of missing OH reactivity was observed (56% on average of missing fraction). A set of tools, as air masses regime modelling and trace gases concentration were helpful to demonstrate the influence that secondary originated products have on the missing OH reactivity. In addition, box model simulations considering the oxidation of the primary biogenic compounds helped identifying the classes of unmeasured species.

## 5.1 Introduction

Atmospheric photochemical reactions are initiated by four main oxidants: the hydroxyl radical (OH), ozone (O<sub>3</sub>), the nitrate (NO<sub>3</sub>) and chlorine (Cl) atoms. Among those, the OH radical is by far the most important atmospheric oxidant, capable to react with the vast majority of chemical species in the troposphere (Levy, 1971). Photochemically initiated reactions are the most efficient cleansing process occurring in the atmosphere, and constitute an important sink for Volatile Organic Compounds and other atmospheric gases.

Total OH reactivity is the total hydroxyl radical rate loss in the atmosphere due to the presence of reactive species. It is a direct measure of the total sink of OH and an index of the total loading of reactants in ambient air, without considering the unfeasible task of measuring every single species present. Measurements of total OH reactivity in ambient air are often coupled to measurements of a limited number of trace gases. The latter permits to calculate the OH reactivity from the summation of the concentration multiplied by the rate coefficient of the measured species with OH. This is what is usually referred as calculated OH reactivity and comparison among the calculated and the total measured OH reactivity have reported discrepancies in various environments to different extents (Di Carlo et al., 2004; Dolgorouky et al., 2012; Nölscher et al., 2012a). The missing OH reactivity, the fraction of OH reactivity not explained by simultaneous measurements of reactive gases, has been associated to unmeasured primary compounds and/or secondary generated ones.

The Mediterranean basin stretches east to west from the tip of Portugal to the shores of Lebanon and north to south from Italy to Morocco and Libya; it comprises countries from three different continents and a population of 450 million inhabitants. The climate is characterized by humid-cool winters to hot-dry summers in which the area is usually exposed to an intense solar radiation and high temperature levels. Forests, woodlands and shrubs occupy large areas of the region, with a rich biodiversity and a high number of species

identified to exist here and nowhere else in the world. Moreover, the Mediterranean is also exposed to an intense atmospheric circulation and mixing of air masses at a larger scale. During summertime, the weather system is dominated from west by the Azores anticyclone and from east by a low pressure monsoon system. In this way, the average air flow is driven from north to south, exposing the basin to air masses coming from European mega cities and industrialized areas. In addition, the region also receives pollution events from Asia at higher altitude, and dust events from North Africa (Lelieveld, 2002). Transported pollution and an intense local anthropogenic and biogenic activity result in high loadings of atmospheric gases and particles and a complex chemistry.

Climate model predictions indicate that the Mediterranean will face unique impacts of climate change. Results show that the region will face higher temperatures and extended drought stress periods, which will affect the strength and type of emissions further impacting air quality and climate (Giorgi and Lionello, 2008). Besides this, it is proved that the Mediterranean lack of observations, and joint international efforts are needed (Mellouki and Ravishankara, 2007).

In this context, we measured the total OH reactivity at a receptor coastal site in the Mediterranean basin during summer 2013 within the ChArMEx project (Chemistry and Aerosols in a Mediterranean Experiment). Measurements were part of an intensive field work aimed at investigating sources and sinks of gaseous constituents in the area (CARBOSOR, CARBO<sub>N</sub> within continental pollution plumes: SO<sub>U</sub>RCES and REACTIVITY). Total OH reactivity was measured with the Comparative Reactivity Method during 16/07/2013-05/08/2013 at the monitoring station of Ersa, in the northern cape of the island Corsica, France. The field site was chosen for being: (i) free from local anthropogenic pollutants; (ii) exposed to air masses of different origin, including air masses enriched in processed compounds transported from continental areas. The utility of the OH reactivity was to measure the total loading of reactive molecules reaching the site, and investigate the completeness of the measurements conducted in the gas-phase. This study presents the first data set of measured OH reactivity obtained during summertime in a receptor site in the Mediterranean basin. It offers a comparison between the measured reactivity and the calculated reactivity from trace gases measures, providing crucial insights into the summertime reactive carbon budget in this area of the western basin.

## 5.2 Field site

Ersa windfarm (42.97°N, 9.38°E, altitude 533 m) is located in the northern cape of Corsica, France, in the western Mediterranean basin (Fig. 5.1). It is 2.5 km far from the

nearest coast (west side) and 50 km far from the largest closest city and harbour Bastia (south side). It is located on a hill (533 m a.s.l.) and surrounded by the Mediterranean sea on west, north and east sides. The site was chosen for its unique characteristics of receiving air masses from continental areas especially France and northern Italy, with the harbours of Marseille and Genoa about 300 km far, and the industrialized areas of Milan and the Po valley 400 km away. Furthermore, the whole measurement station is densely surrounded by the Mediterranean maquis, a shrubland biome typical of the whole Mediterranean region. The station consists of a long-term meteorology, aerosol size and composition monitoring laboratory (measurements run from 2012 to 2014), and temporary measurements of gases and aerosol properties over a total surface area of a few hundred square meters. Measurements of total OH reactivity and trace gases reported in this study were all performed within this area (see Fig. 5.1 for details on instruments allocation). We conducted our measurements of OH reactivity during two main phases: an intercomparison exercise with another instrument for measuring the OH reactivity between 8/07 and 13/07/2013 (see Zannoni et al., (2015)), the CARBOSOR (CARBON within continental pollution plumes: SOURces and Reactivity) ambient measurements campaign during 16/07-05/08/2013. Within this project, instruments for measuring gaseous constituents, including radicals, inorganic and organic compounds, aerosol chemical composition and physical properties, meteorology were simultaneously deployed. The next section will provide an overview of the methods used for this study.

## 5.3 Methods

### 5.3.1 Comparative Reactivity Method

We carried out measurements of total OH reactivity using a Comparative Reactivity Method instrument assembled in our laboratory (CRM-LSCE from Laboratoire des Sciences du Climat et de l'Environnement, see Zannoni et al., (2015)). In brief, the Comparative Reactivity Method (CRM) is based on the concept of producing a competition for in-situ generated OH radicals, between a reactive reference compound, in our case pyrrole ( $C_4H_5N$ ), and ambient reactive gases (Sinha et al., 2008). This is reproduced by introducing a known amount of pyrrole diluted in zero air and  $N_2$  in a flow reactor coupled to a Proton Transfer Reaction-Mass Spectrometer (PTR-MS, for more information about this technique please refer to the next section). Pyrrole is chosen as reference compound for its well characterized kinetics (Atkinson et al., 1984; Wallington, 1986; Dillon et al., 2012), for not being present in the atmosphere at normal conditions, and for being easily de-



**Figure 5.1:** Field site of Ersa windfarm ( $42.97^\circ$  N,  $9.38^\circ$  E, altitude 533 m) located in Corsica, France, where the ChArMEx-CARBOSOR campaign took place. Measures location: 1. Trace gases with PTR-MS, online and offline chromatography; 2. OH reactivity; 3.  $\text{NO}_x$ ,  $\text{O}_3$ , aerosols composition and black carbon; 4. Meteo and particles microphysics; 5. HCHO, trace gases and radicals; 6. CO,  $\text{CO}_2$ ,  $\text{CH}_4$ ; 7. Trace gases and particle filters; 8. Particles physics. The photo was taken before the start of the campaign (cars parked nearby).

tectable at the protonated  $m/z$  68 ( $\text{C}_4\text{H}_5\text{NH}^+$ ) with a PTR-MS without any interference. A Proton Transfer Reaction-Mass Spectrometer is the detector of choice for its real-time measurements capabilities and robustness over time (Nölscher et al., 2012b).

A usual experiment with a CRM includes in order: monitoring of C0 wet/dry, followed by C1 dry, C2 wet, and C3 ambient. With C0, C1, C2, C3 being in order the concentration of pyrrole detected with the PTR-MS: after injection (C0), when photolysis reaches the equilibrium (C1), after reaction with OH (C2), when ambient air is injected and the competition for OH radicals can start (C3). Alternated switches between C2 (background pyrrole in zero air) and C3 (pyrrole in ambient air) result in pyrrole signal modulations which are used to derive total OH reactivity values from the following equation:

$$R_{air} = \frac{C3 - C2}{C1 - C3} k_{pyrrole+[OH]} C1 \quad (5.1)$$

With  $k_{pyrrole+[OH]}$  rate constant of reaction between pyrrole and OH =  $(1.20 \pm 0.16) \times 10^{-10}$   $\text{cm}^3 \text{ molecule}^{-1} \text{ s}^{-1}$  (Atkinson et al., 1984, Dillon et al., 2012).

A detailed description of our instrument is available in Zannoni et al., 2015. Our instrument showed on the field an unexpected sensitivity on temperature changes. We speculate that this behaviour depends on: (i) the higher temperature of ambient air with respect to the one inside the van where the CRM was located and (ii) the "stickiness" of pyrrole. We

partly solved the problem by covering the lines where pyrrole was flowing with insulating coating foam, and by placing the whole CRM in a temperature insulated box.

During the whole campaign we run several quality controls on our system, to assure that none of the accounted variables could lead to any misleading result (see Tab. 5.1 for type and frequency of tests). We accounted for: flows of all species injected and coming out the reactor, pyrrole initial concentration (C1), response to a known injected OH reactivity (for instance with propane as test gas,  $k_{propane+OH} = (1.1 \pm 0.2) \times 10^{-12} \text{ cm}^3 \text{ molecule}^{-1} \text{ s}^{-1}$ , Atkinson et al., 2007), sensitivity of the PTR-MS towards  $m/z$  68.

**Table 5.1:** Quality check controls run on the CRM instrument and frequency during the field campaign.

Parameter	Problem	Frequency
Flows	Small fluctuations	Twice a day
C1 value	Flows fluctuations	~3 days
Injection of a known reactivity	CRM linearity	~2 days
PTR-MS flow	Clogging	Twice a day
Cleaning of peek line PTR-MS	Clogging	~5 days
Dry and wet calibration $m/z$ 68	PTR-MS sensitivity	Twice all campaign

We calibrated the PTR-MS for pyrrole twice during the whole campaign and took an average value from the two calibrations (within 15% difference for the dry calibration factors and within 5% difference for the wet calibration factors). In addition, every time a C1 was measured, we also measured C0 dry and wet which confirmed the previously determined dry and wet calibration factors.

The C1 value was on average  $72 \text{ pm}^4 \text{ ppbv}$ . Such variability was given by a systematic decrease of the flow entering the PTR-MS due to clogging of the inlet lines for pyrrole stickiness. For this reason, we decided to keep a regular maintenance of our PTR-MS and clean the lines when needed. To determine the most accurate result of reactivity we interpolated the measurements of C1 over those days where no control was run.

We performed a sensitivity study on the C1 value. Over our results of measured total OH reactivity, C1 changes due to small flows fluctuations do not affect the final result of reactivity. We did a sensitivity study also on temperature fluctuations inside our van (25-30°C), considering different rate constants for the reaction between pyrrole and OH (Wallington et al., 1986). We saw that also in this case, the final result was not affected by temperature changes (differences maximum of  $0.3 \text{ s}^{-1}$  of reactivity among values). We recorded PTR-MS data using a dwell time for pyrrole of 20 s, to assure a high sensitivity

in the measurement and be able to distinguish a variation between C2 and C3 values even at low reactivity. We had a full cycle of measurements every 30 s. We switched between C2 and C3 values every 5 minutes, resulting in a data point of reactivity every 10 minutes. Each data point of reactivity obtained from Eq. (5.1) was corrected for: (i) humidity changes between C2 and C3, (ii) deviation from pseudo first order kinetics between pyrrole and OH, (iii) dilution of ambient air reactivity inside the reactor. A detailed description on how the correction factors were obtained and how the raw data were processed can be found in the publication of Zannoni et al., (2015). Particularly, we did not account for NO recycling in our reactor since ambient NO was below 2 ppbv at the site, which is not enough to produce OH recycling in our system. The LoD of CRM-LSCE is  $\approx 3 \text{ s}^{-1}$  ( $3\sigma$ ) and the systematic uncertainty is  $\pm 35\%$  ( $1\sigma$ ), including uncertainties on the rate coefficient between pyrrole and OH (8%), detector sensitivity changes and pyrrole standard concentration (22%), correction factor for kinetic regime (26%) and flows fluctuations (2%).

### 5.3.2 Ancillary measurements at the field site

Gas-phase constituents were measured by combining a number of different techniques available at the site, including: Proton Transfer Reaction-Mass Spectrometry (PTR-MS), Gas Chromatography (GC), Liquid Chromatography (LC), formaldehyde analysis based on the Hantzsch reaction method and wavelength-scanned cavity ring down spectrometer (WS-CRDS). The measured concentration with the reaction rate coefficients with OH of each measured component were used to calculate the OH reactivity with the following equation:

$$R = \sum_i k_{i+\text{OH}} \cdot X_i \quad (5.2)$$

With  $i$  any measured compound listed in Tab. 5.2. In the following sections we present the mentioned techniques and Tab. 5.3 provides a summary of them.

#### 5.3.2.1 Proton Transfer Reaction-Mass Spectrometry

Proton Transfer Reaction Mass Spectrometry (PTR-MS) is a technique based on chemical ionization through proton transfer, initially developed for the detection of gaseous organic compounds in ambient air (Lindinger and Jordan, 1998) and extensively deployed for online atmospheric trace gases measurements (Holzinger et al., 2002; Karl et al., 2009). The PTR-MS deployed during the field work ChArMEx is a PTR-ToF-MS (Proton Transfer Reaction-Time of Flight-Mass Spectrometer) of second generation, from Kore Technology

**Table 5.2:** Measured compounds and group of reference reported over the manuscript to indicate the compounds concentration used to calculate the OH reactivity.

Species group	Species name
AVOCs (44)	methane, ethane, propane, n-butane, n-pentane, n-hexane, n-octane, n-nonane, n-undecane, n-dodecane, 2-methylpropane, 2-methylpentane, 2-methylhexane, 2,2- dimethylbutane, 2,2-dimethylpropane, 2,3- dimethylpentane, 2,4- dimethylpentane, 2,2,3-trimethylbutane, 2,2,4-trimethylpentane, 2,3,4- trimethylpentane, cyclohexane, ethylene, propylene, 1-butene, 2-methylpropene, 2-methyl-2-butene, 3-methyl-1-butene, 1,3-butadiene, trans-2-butene, cis-2-butene, 1-pentene, trans-2-pentene, cis-2-pentene, hexene, benzene, toluene, ethylbenzene, styrene, m-xylene, o-xylene, p-xylene, acetylene, 1-butyne, acetonitrile.
BVOCs (7)	isoprene, $\alpha$ -pinene, $\beta$ -pinene, limonene, $\alpha$ -terpinene, $\gamma$ -terpinene, camphene.
OVOCs (15)	acetaldehyde, formic acid, acetone, acetic acid, mglyox, methyl ethyl ketone, propionic acid, ethyl vinyl ketone, butiric acid, nopinone, pinonaldehyde, methacrolein, methyl vinyl ketone, formaldehyde, methanol.
Others (3)	NO, NO <sub>2</sub> , CO.

Ltd., UK. Sampling was conducted through a 5 m PFA sampling line, which was installed about 1.5 m above the trailer where the PTR-MS was placed, kept at 50°C, with a sampling flow rate of 1.2 sL min<sup>-1</sup> and a sample residence time of 4 s. The sampling flow of the PTR-MS was 0.15 sL min<sup>-1</sup>, hence an additional pump was installed in line with the PTR-MS in order to have a total sampling flow of 1.2 sL min<sup>-1</sup>. The conditions of operation of the PTR-MS were: drift tube pressure of 1.33 mbar and drift tube temperature of 40°C, for an E/N of 135 Td. Every hour the air sample passed automatically through a catalytic converter (stainless steel tubing filled with Pt wool held at 350°C) to obtain a background value for each investigated mass. We calibrated the PTR-MS every three days using a Gas Calibration Unit (GCU, Ionicon Analytik GmbH, Austria) to dilute and humidify the standard gas mixtures (15 VOCs mixture by Restek, France; 9 VOCs mixture by Praxair, ; 19 OVOCs mixture by Praxair, ) at 50% while the temperature was 20°C. The time resolution of each cycle was 10 minutes.

Finally, we calculated the volume mixing ratio of each component considering the signal of primary ions (H<sub>3</sub>O<sup>+</sup>) and first water cluster (H<sub>3</sub>O+(H<sub>2</sub>O)) according to:

$$[\text{RH}] = \frac{i_{RH_{net}}}{(i_{H_3O^+} + [X]_r i_{H_3O+(H_2O)})} \frac{150000}{R_f} \quad (5.3)$$



Where [RH] is the volume mixing ratio of a given VOC,  $i_{RH_{net}}$  the net signal of the VOC, the signal of  $H_3O^+$  ions, the signal of the first water cluster,  $X_r$  the factor obtained for the effect of humidity on the sensitivity of the PTR-MS (see de Gouw and Warneke, (2007)),  $R_f$  the sensitivity determined during calibrations and 150000 cps the corresponding number of primary  $H_3O^+$  ions in our PTR-MS.

### 5.3.2.2 Online Chromatography

Trace gases were sampled online with a Gas Chromatography-Flame Ionization Detector coupled to a second Flame Ionization detector (GC-FID/FID, Perkin Elmer, see Badol et al., (2004)) and with a Gas Chromatography/Flame Ionization Detector coupled to a Mass Spectrometer (GC-FID/MS, Perkin Elmer, see Roukos et al., (2009)).

For the GC-FID/FID, hydrocarbons in the fraction C<sub>2</sub>-C<sub>12</sub>, including alkanes, alkenes, alkynes and aromatics, were sampled at a flow rate of 0.015 sL min<sup>-1</sup> through a 5 m PFA 1/8" OD sampling line. First, the air passed through a Nafion membrane for drying, then was pre concentrated for 40 min on a cool sorbent trap (Carbopack B and Carbosieve SIII) which was held at -30° C by a Peltier cooling system. Compounds were thermodesorbed up to 300° C and injected into the Perkin Elmer GC system. Separation was achieved by switching between two capillary columns which reduce issues of co-elution resulting in a better separation. The first column was a CP Sil 5CB (50 m, 0.25 mm, 1 μm) and permits to separate the heavy fraction of hydrocarbons (C<sub>6</sub>-C<sub>12</sub>). The second column was a fused silica porous layer open tubular column, coated with Al<sub>2</sub>O<sub>3</sub>/Na<sub>2</sub>SO<sub>4</sub> (50 m, 0.32 mm, 5 μm) which enables to separate the light fraction of hydrocarbons (C<sub>2</sub>-C<sub>5</sub>). Compounds when eluted were detected by the FID detector. The total time resolution of the GC-FID/FID is 90 minutes, with the first 50 minutes dedicated to the elution of the compounds. This instrument was calibrated twice, before and after the field campaign, with a standard gas mixture from NPL, UK.

The GC-FID/MS measured online the oxygenated VOCs in the fraction C<sub>3</sub>-C<sub>7</sub>, including aldehydes, ketones, alcohols, ethers, esters, as well as primary VOCs, including BVOCs and aromatics. For this instrument, air was sampled via a 5 m PFA 1/8" OD sampling line at a sampling flow rate of 0.015 sL min<sup>-1</sup> by an Air server-unity (Markes International, UK) passing through a KI ozone scrubber. First it was diluted with dry zero air to keep its relative humidity below 50%; then it was collected on a cooled trap at 12.5° C consisting of a 1.9 mm ID quartz tube filled with two different sorbents (5 mg of Carbopack B and 75 mg of Carbopack X, Supelco, USA). Compounds were then thermodesorbed at 280° C, injected into the column and analyzed by the GC (Agilent Technologies, USA) equipped with a FID for detection and quantification and with a Mass Spectrometer (MS) to help

their identification. The column was a high polar CP-lowox column (30 m, 0.53 mm, 10  $\mu\text{m}$ ) (Varian Inc., USA). Also in this case the total time resolution was 90 minutes, with the sampling lasting 40 minutes and the analysis lasting 50 minutes. Calibrations were performed before and after the campaign, using a cylinder containing 29 different compounds (Praxair Inc., USA).

### 5.3.2.3 Offline Chromatography

Trace gases were also sampled through an Automatic Clean ROom Sampling System (ACROSS, TERA Environment) on sampling tubes and offline analysed in the laboratory by GC-FID and HPLC-UV (High Performance Liquid Chromatography-UV light detector). Sampling of trace gases on cartridges lasted three hours. For the GC-FID analysis the fraction C<sub>5</sub>-C<sub>16</sub> including alkanes, alkenes, aromatics and BVOCs and the fraction of C<sub>6</sub>-C<sub>12</sub> n-aldehydes were investigated. The sampling line and flow rate were respectively 3 m of  $\frac{1}{4}$ " OD PFA line and 0.2 sL min<sup>-1</sup>. Air passed through a MnO<sub>2</sub> ozone scrubber and a stainless-steel particle filter (excluding particles with Dp<sub>i</sub> 2 $\mu\text{m}$ ). Sampling tubes were composed of Carbopack C (200 mg) and Carbopack B (200 mg), pre conditioned with clean air at 250° C during 24 h. For more information about the sampling and the development on the field please refer to Detournay et al. (2011) and Ait-Helal et al., (2014).

With the HPLC-UV we investigated the fraction C<sub>1</sub>-C<sub>8</sub> of carbonyls. The same sample device was deployed, but this time trace gases were absorbed on cartridges composed of 2,4-Dinitrophenylhydrazine (DNPH). The air was sampled via a 3 m Teflon PFA line (1/4" OD) at 1.5 sL min<sup>-1</sup> and passed through a KI ozone scrubber and a stainless-steel particle filter (excluding particles with Dp<sub>i</sub> 2 $\mu\text{m}$ ). Concentrations of these species are available only for the 10 first days of the field work due to a leakage and contamination problem that occurred to the samples. The LoD (Limit of Detection) of all these trace molecules were determined as 3 $\sigma$  their background values and uncertainties were estimated based on the guidelines provided by the "Aerosols, Clouds, and Trace gases Research InfraStructure (ACTRIS)" network for uncertainty evaluation (ACTRIS Measurement Guideline VOC, 2012).

### 5.3.2.4 Hantzsch method for the analysis of formaldehyde

We measured formaldehyde with a commercial instrument based on the Hantzsch method (Model 4001, AERO-LASER GmbH, Garmisch-Partenkirchen, Germany). Gaseous HCHO is stripped into a slightly acidic solution, followed by reaction with the Hantzsch reagent,

i.e. a diluted mixture of acetyl acetone acetic acid and ammonium acetate. Such reaction produces a fluorescent compound which absorbs at 510 nm. Further details are available in Dasgupta et al., (1988); Junkermann, (2009) and Preunkert et al., (2013). Sampling was conducted through a 5 m long PTFE  $\frac{1}{4}$  OD line, with a 47 mm PFA in-line filter installed at the inlet and a flow rate of about 1 L min<sup>-1</sup>. The liquid reagents (stripping solution and Hantzsch reagent) were prepared from analytical grade chemicals and ultrapure water according to the composition given by Nash, (1953) and stored at 4° C on the field. The instrumental background was measured twice a day (using an external Hopcalite catalyst consisting of manganese and copper oxides) and calibrated three to four times a week using a liquid standard at 1.10<sup>-6</sup> mol L<sup>-1</sup>, corresponding to a volume mixing ratio in the gaseous phase of about 16 ppbv. The calibration points were interpolated linearly in order to correct from sensitivity fluctuations of the instrument. The limit of detection, defined here as two times the standard deviation of the background, was 130 pptv. The coefficient of variation, i.e the ratio of the standard deviation to the mean background value, was estimated to be 0.4 %. Measurements of HCHO ran smoothly from the beginning of the campaign until 11 AM of 28/07/2013 (CEST). At this time an instrument failure occurred and measurements were stopped.

### 5.3.2.5 Chemiluminescence for the analysis of NO<sub>x</sub>

Nitrous oxides (NO<sub>x</sub>=NO+NO<sub>2</sub>) were measured with a CRANOX instrument (Ecophysics, Switzerland). This instrument permits to measure both NO and NO<sub>2</sub> (after photolytic conversion) . It consists of a high performing two channel CLDs (Chemiluminescence Detectors) with pre-chambers for compensation of the background, an integrated powerful pump, a photolytic converter, an ozone instrument and a calibrator. An appropriate control software (Labview) handles and manages the different tasks. The detection limit is 50 pptv, for a 5 minutes time resolution.

### 5.3.2.6 Wavelength-scanned cavity ring down spectrometry (WS-CRDS)

The in-situ measurements of CO<sub>2</sub>, CH<sub>4</sub>, CO molar fractions at Ersa are part of the French monitoring network of greenhouse gases, integrated in the European Research Infrastructure ICOS. The air is sampled at the top of a 40 m high telecommunication tower (573 m), and is analyzed with a wavelength-scanned cavity ring down spectrometer (WS-CRDS, G2401 from Picarro, USA). The analyzer is calibrated every 3 weeks with a suite of four reference cylinders, whose molar fractions are linked to the WMO (World Meteorological Organization) scales through the LSCE (Laboratoire des Sciences du Climat et de

l'Environnement) reference scale. Measurements are corrected for H<sub>2</sub>O dilution to calculate the molar fractions in dry air.

**Table 5.3:** Summary of the experimental methods deployed during the field work and described in the methods section. LoD stands for Limit of Detection.

Technique	Compounds measured	LoD (pptv)
PTR-MS	16 VOCs	7-500
GC- FID/FID	22 NMHCs C2-C12	10-100
GC-FID/MS	22 NMHCs (OVOCs+ C3-C7)	5-100
HPLC	42 NMHCs (C1-C16)	5-40
Hantzsch reaction	HCHO	130
CLD	NO <sub>x</sub>	50

### 5.3.3 Box model for mixing ratios and OH reactivity evaluation

In order to get more insights from the comparison of the measured and calculated OH reactivity, we analysed numerical simulations of the photo-oxidative chemistry performed with a simplified model. The simulations permit to analyse the atmospheric mixing ratio of the reactive species and the OH reactivity. Particularly, the modelling aims at understanding the impact of the oxidative products resulting from the oxidation of the primary BVOCs. We chose therefore to use a two-layer box model where the gaseous chemistry is described by a simplified chemical scheme.

The model assumes that the concentration of the compounds varies over time according to the following processes: chemistry, deposition, advection and boundary layer height variability. Emissions are not considered. Particle formation and partitioning of chemical species between the gaseous and the particle phase is also not considered. The model set-up only includes realistic variations of physical parameters typical of a summer day, since capturing the real meteorology at the site is too complex for the site constraints (site located on a hilly cape, surrounded for three sides by the sea). The chemical compounds are exchanged between the two layers in order to represent the effect of the diel boundary layer height variability. The top of the lower layer varies from 150 m during the night to 1000 m in the afternoon. Gaussian diurnal variation of temperature and solar radiation are also considered. The reference case includes advection of air, assuming a turnover time of the air inside the box of 6 h. This time frame corresponds to the time in which the air inside the box would be completely replaced by clean air (assuming no chemical species

concentration is imposed and no emission occurs). A second case, without advection, is considered to test the hypothesis of the set up. Deposition velocities are computed using the model of Wesely (1989) for  $\text{SO}_2$ ,  $\text{O}_3$ ,  $\text{H}_2\text{O}_2$ ,  $\text{NO}_2$ ,  $\text{NO}$  and  $\text{HNO}_3$ , considering the deposition during midsummer on a surface covered by 60% of deciduous forests and 40% of crops corresponding approximately to the land coverage of eastern Corsica. Photolysis rates were calculated for  $45^\circ\text{N}$  under cloud-free conditions for a typical summer day.

We input the initial concentration of  $\text{H}_2\text{O}_2$ ,  $\text{SO}_2$ ,  $\text{CH}_4$ ,  $\text{CO}$ , PAN-like species and ozone for both layers, while the concentrations of BVOCs and  $\text{NO}_x$  are imposed during the whole simulations to match the levels observed on the field. We considered three groups of BVOCs to run the simulations: isoprene (iso),  $\alpha$ -pinene (apin), limonene (limo); according to their similar reactivity towards OH and available chemical mechanisms in literature. In these groups, the concentration profiles of all measured BVOCs were considered: isoprene stands alone,  $\alpha$ -pinene makes a group with  $\beta$ -pinene and camphene, while limonene is grouped with terpinenes. The initiation of the oxidation of limonene and  $\alpha$ -pinene is described according to the SAPRC99 mechanism while isoprene and the secondary products oxidation scheme is described according to Szopa et al. 2005 (updated with recent literature for inorganic chemistry and  $\text{CH}_4$  oxidation). The rate constant of the oxidation reactions of the biogenics with OH and ozone were updated according to SAPRC07. Specifically, the chemical scheme was developed to reproduce correctly the reactivity (particularly the production of ozone) in various scenarios, see Szopa et al., 2005. For this reason, the chemical scheme is reduced, the oxidation leads directly to stable products on one hand and artificial operators representing the  $\text{NO}/\text{NO}_2$  conversions involved into the peroxy/alkoxy chemistry on the other hand. Most of the compounds participating to the chemical scheme represent a group of compounds that belong to the same chemical class rather than an individual chemical species. Therefore, the model output does not provide the information of the individual secondary species contributing to the reactivity, while it can yield the relative contributions to the reactivity of the main chemical families.

The model output is the mixing ratio of reactive atmospheric constituents and surrogates chemical species. From the obtained mixing ratios we calculated the OH reactivity, namely modelled OH reactivity. Simulations were run over five days. Since successive diurnal cycles for key species (e.g.  $\text{O}_3$ ,  $\text{H}_2\text{O}_2$ , OH,  $\text{HO}_2$ ) are nearly identical from the first day, we will discuss the results of the diurnal profile of the first 24-h to avoid considering bias due to accumulation of reactive species.

## 5.4 Results

### 5.4.1 Air masses regime

We modelled the back-trajectories of 48 h, every 6 hours, that reached the monitoring site (coordinates 42.969° N, 9.380° E, alt: 600 m) for the whole campaign. The model we used is the online version of Hysplit (HYbrid Single-Particle Lagrangian Integrated Trajectory) developed by the National Oceanic and Atmosphere Administration (NOAA) Air Resources Laboratory (ARL) (Draxler and Hess, 1998; Stein et al., 2015).

We classified the obtained back-trajectories according to their origin, the altitude and wind speed. More information about the modelling of the back-trajectories and chemical processes of the air masses can be found in the article of Michoud et al., (in preparation).

Table 5.4 shows the classification of the air masses according to different origin and wind speed during the field work. The air masses regime is classified into 5 different clusters: 1, continental air masses from North East, including North of Italy and Europe; 2, marine air masses from West, including coastal areas of the South of France and East of Spain; 3, air masses coming from South, travelling over the islands Corsica and Sardinia; 4, continental air masses coming from North West, including the South East of France; 5, air masses mainly of local origin characterised by low wind speed.

The most abundant clusters are the second and fifth, i.e. the West and calm-low wind clusters, respectively, with 30% of recurrence. Afterwards, the first (NE), third (S) and fourth (NW) are present at 26%, 8% and 6%, respectively. The first four clusters are characterized by different time of travel, considering their last contamination from the time that the air mass left the continental coast. We observed that the air masses from the Marine-West cluster spent 36 to 48 h above the sea, while the air masses from North-East, and North-West clusters spent between 10-20 hours and 12-18 hours, respectively. Air masses reported for the South cluster had instead a transport time between 12-24 hours, which represents the time spent by the air masses above the continental areas (Corsica and Sardinia Islands). Different times of travel indicate different processing times for the air masses, with a possible longer processing time for the air masses belonging to the Marine-West cluster compared to the others. Finally, the fifth cluster groups the air masses characterized by short distances crossed in 48 h and therefore by calm situations with low wind speed.

**Table 5.4:** Air masses regime modeled with Hysplit. Five clusters are reported which correspond to different wind sectors and origin of the air masses: 1. North-East sector (North of Italy, Europe); 2. West (marine, South of France, North-East of Spain); 3. South (islands, Corsica and Sardinia); 4. North-West sector (South East of France); 5. Calm-low wind (local).

Time frame	Cluster- Wind Sector	Notes
15/07/2013-19/07/2013	5	calm-low
19/07/2013-20/07/2013	2 W	marine
20/07/2013	5	calm-low
21/07/2013-23/07/2013	1 NE	continental
23/07/2013	5	calm-low
23/07/2013-27/07/2013	2 W	marine
27/07/2013-29/07/2013	3 S	islands
29/07/2013	2 W	marine
29/07/2013-31/07/2013	4 NW	continental
31/07/2013-03/08/2013	1 NE	continental
03/08/2013-04/08/2013	5	calm-low
04/08/2013-05/08/2013	2 W	marine

### 5.4.2 Total measured OH reactivity

Figure 5.2 shows results of the measured total OH reactivity with temperature and relative humidity time series during the whole measurements campaign. Results of OH reactivity are reported with the black data points for 10 minutes frequency observations and with the black line for hourly averages of the raw data. Figure 5.2 reports all data measured during 16/07/2013- 05/08/2013; missing data are due to minor instrumental issues and instrumental quality controls. At this Mediterranean field site OH reactivity reached a maximum of  $22 \text{ s}^{-1}$  (10 minutes time resolution data) in the afternoon of 28/07/2013 and was on average  $5 \pm 4 \text{ s}^{-1}$ . It covaried with air temperature: over the measurements period higher values of reactivity are reached when higher air temperature and lower relative humidity are also observed (Fig. 5.2). Maximum values of measured OH reactivity are observed during between 26-28/07/2013 and 02-03/08/2013. Air masses during these periods have different origins: from the western to the southern and the northern-east sectors.

Total OH reactivity had a clear diurnal profile: background reactivity was  $4 \text{ s}^{-1}$  on average over the whole campaign, it increased at 8 h and reached a maximum at 11 h, started to

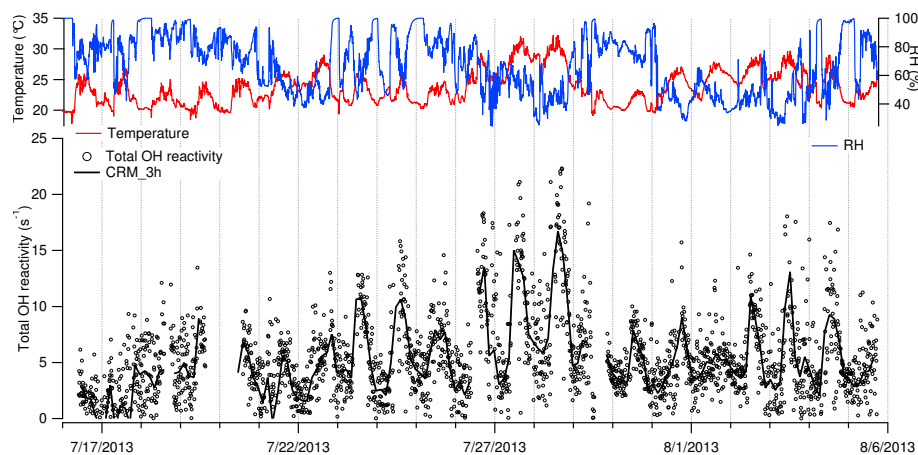


**Figure 5.2:** Total OH reactivity profile measured at Ersa, Corsica, France during July-August 2013. Data points have time resolution of 10 minutes, black line is the hourly average over these data. Air temperature and Relative Humidity (RH) are reported for reference.

decrease at 19 h and reached its background value at 22 h (Fig. 5.3, all times are given in local time, GMT/UTC+2 hours). Largest variability is observed at 11 h and 18 h in the 24 hours profile. Figures 5.3 and 5.4 offer a comparison between the diurnal profiles of OH reactivity and total concentration of Biogenic Volatile Organic Compounds (BVOCs) measured at the same site. The averaged 24 hours total mixing ratio of BVOCs (see Tab.5.2 for the measured BVOCs compounds) increased at 7 h, peaked at 12 h (whisker) and 14 h (average) started to decrease at 17h and went to the background value at 22 h. Remarkably, both profiles have the same shape, suggesting a close dependence of OH reactivity to the concentration of the biogenic compounds.

### 5.4.3 Calculated OH reactivity and importance of biogenic VOCs at the measuring site

#### 5.4.3.1 Long-term variability

All the chemical species reported in Tab.5.2 were measured at the site during the same period and their concentrations were input in Eq. (5.2) to determine the calculated OH reactivity. The calculated OH reactivity during the measuring campaign varied between  $0.6 \text{ s}^{-1}$  and  $11 \text{ s}^{-1}$ , was on average  $3 \pm 2 \text{ s}^{-1}$  ( $1\sigma$ ). As the measured reactivity, also the calculated reactivity had a distinct diurnal profile (Fig. 5.5).



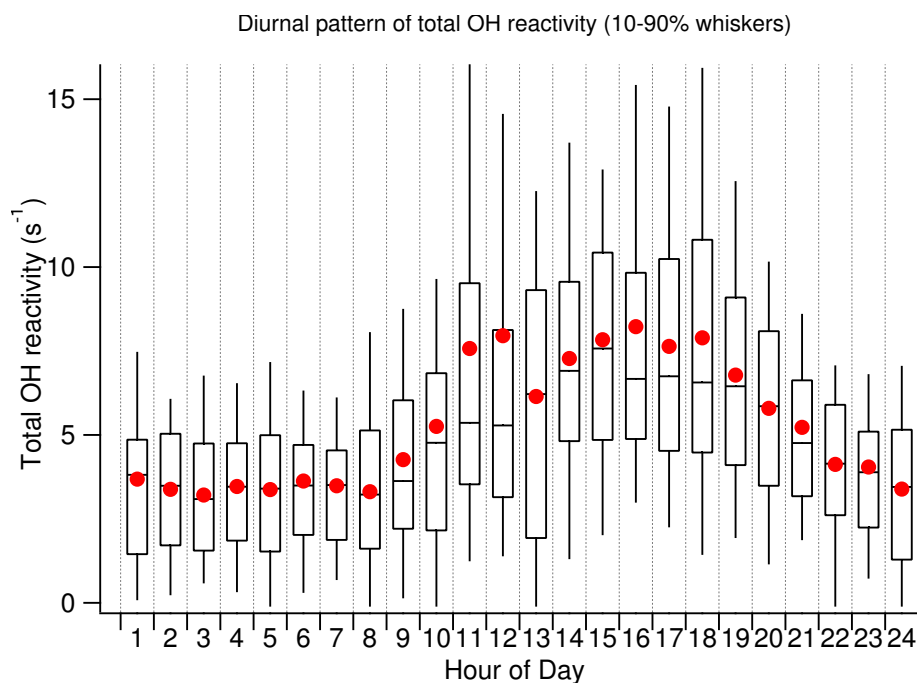


**Figure 5.3:** Diurnal pattern with 10-90% whiskers of the measured total OH reactivity.

#### 5.4.3.2 Contributions from different classes of compounds

A broad suite of complementary measurements were available at the site, to make it simple, we classified these species into four main groups: Anthropogenic Volatile Organic Compounds (AVOCs, 44 compounds measured), Biogenic Volatile Organic Compounds (BVOCs, 7 compounds), Oxygenated Volatile Organic Compounds (OVOCs, 15 compounds), others (3 inorganic species: CO, NO and NO<sub>2</sub>). A large interest of the project focused on anthropogenic compounds and their oxidation products, expecting major influences on the atmospheric composition from air masses coming from continental polluted areas. However, only weak pollution events reached the site during our measurements campaign. Figure 5.5 reports the mean daytime and nighttime contributions to the calculated OH reactivity at the site during the three weeks of measurements according to the four groups listed in Tab. 5.2 and mentioned above. Remarkably, during daytime only seven BVOCs contributed to the largest fraction of OH reactivity (39%), followed by inorganics (34%), OVOCs (16%) and finally AVOCs (11%). It means that, in terms of reactivity, seven measured BVOCs had a larger impact than the 44 measured AVOCs, which, under weak pollution events is expectable since BVOCs have generally shorter lifetimes with OH than AVOCs (Atkinson and Arey, 2003). Interestingly, BVOCs accounted only 10% of the total VOCs concentration measured during daytime during the same period, followed by OVOCs (67%) and AVOCs (23%). The larger BVOCs influence in reactivity is also cor-

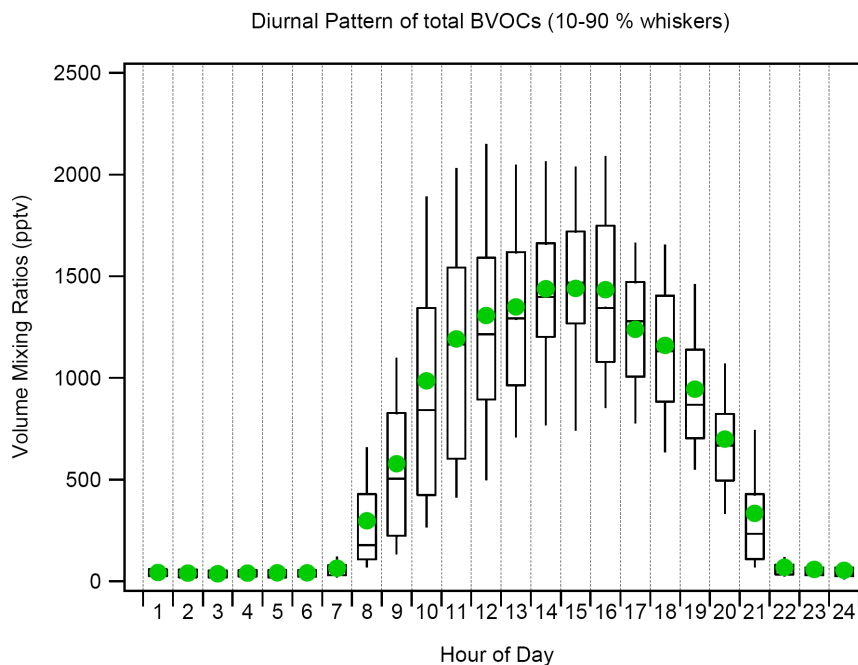


**Figure 5.4:** Total biogenic volatile organic compounds volume mixing ratio measured at Ersa during the whole campaign.

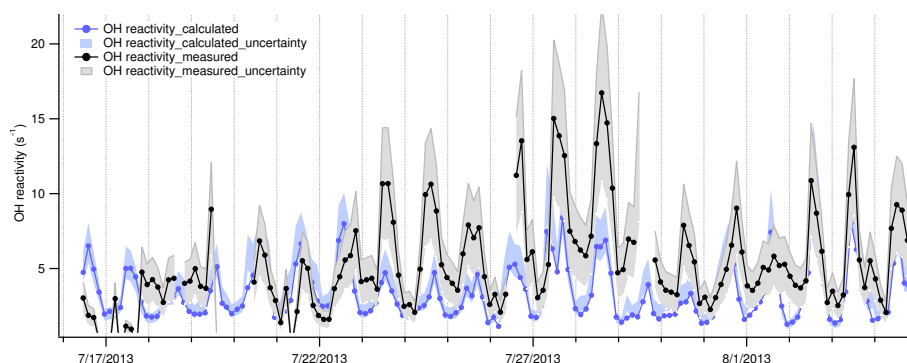


**Figure 5.5:** Total measured OH reactivity and calculated OH reactivity from the measured compounds in ambient air, with their relative uncertainty (35% for the measured OH reactivity, 20% for the calculated reactivity).

robored by the similarity already observed between the diurnal profile of OH reactivity and BVOCs at our site (Figs. 5.3 and 5.4). During nighttime BVOCs concentration decreased (Fig. 5.3) and inorganic species had the major impact (52%), followed by OVOCs (24%), AVOCs (21%) and BVOCs (4%). In particular, inorganic species and long lived OVOCs and AVOCs constituted a background reactivity of  $\sim 4 \text{ s}^{-1}$ , the same observed during nighttime in the diurnal profile reported in Fig. 5.3.

### 5.4.3.3 Impact of biogenic VOCs

Among the biogenic species measured at the site, the total fraction of monoterpenes contributed more than isoprene alone (black line compared with the red line in Fig. 5.5). During daytime the reactivity of monoterpenes with OH varied between 1.4 to 7.4 s<sup>-1</sup>, and it covaried with air temperature at the site. Isoprene absolute reactivity with OH, on the other side, varied between 0.3-2.3 s<sup>-1</sup> during daytime (minimum value during the day on 29/07/13 and maximum value during the day on 03/08/2013). In comparison with monoterpenes reactivity, the reactivity of isoprene covaried with both air temperature and solar irradiance. In terms of atmospheric mixing ratios, monoterpenes constituted 4% of the total VOCs concentration, while isoprene only 2.5%. Such result can be explained by the larger emission of monoterpenes compared to isoprene from the local vegetation, mainly composed by Mediterranean aromatic shrubs. Overall both monoterpenes and isoprene reactivity had the characteristic diurnal profile observed for their atmospheric concentration. Additionally, BVOCs reactivity increased when the wind speed measured at the site was lower (see Fig. 5.6), meaning that highest atmospheric mixing ratios are reached for calm meteorological conditions. This result suggests a larger local contribution of BVOCs, which can be expected from their known shorter lifetime compared to other atmospheric constituents.

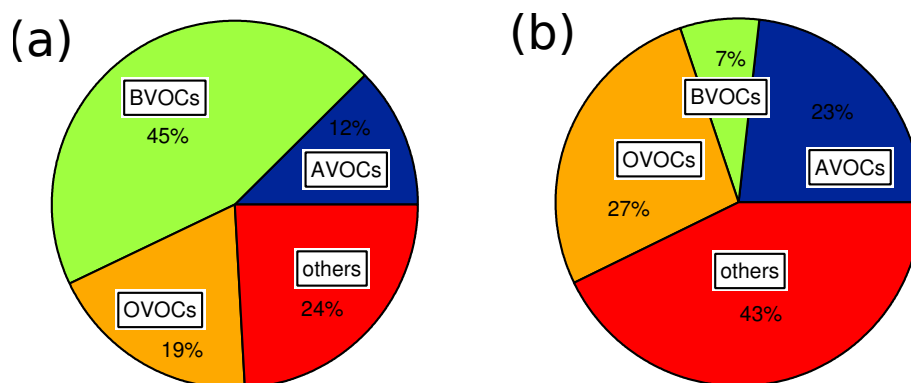


**Figure 5.6:** Daytime (left pie) and nighttime (right pie) contributions to the calculated OH reactivity for the measured compounds listed in Tab. 5.1. Total calculated OH reactivity during daytime was maximum 11 s<sup>-1</sup>, on average 4±2 s<sup>-1</sup>; while during nighttime it was maximum 3 s<sup>-1</sup>, on average 2±0.4 s<sup>-1</sup>.

The very reactive monoterpene  $\alpha$ -terpinene had the largest contribution among the measured BVOCs (31%), followed by isoprene (30%),  $\beta$ -pinene (17%), limonene (12%),  $\alpha$ -pinene (8%), camphene (2%) and  $\gamma$ -terpinene (1%), over a total BVOCs reactivity considered of 2±2 s<sup>-1</sup>, mean value over the field campaign. During the night monoterpenes had

overall a larger impact than isoprene, due to their known only-temperature dependency (Kesselmeier and Staudt, 1999). Also during nighttime, the largest impact was given by  $\alpha$ -terpinene, see Tab. 5.5.

In terms of absolute OH reactivity  $\alpha$ -terpinene had a maximum of  $5.3 \text{ s}^{-1}$  on 02/08/13 at 2 PM (CEST), which is also when the highest peak of OH reactivity due to BVOCs was observed during the field campaign. Remarkably, the mean concentration of this compound makes it the fourth largest BVOCs measured, with isoprene being the first (35%), followed by  $\beta$ -pinene (22%),  $\alpha$ -pinene (15%),  $\alpha$ -terpinene (13%), limonene (9%) and  $\gamma$ -terpinene (1%). It reached a maximum of 594 pptv, with an average value between 10 AM and 5 PM during the field campaign of  $131 \pm 110$  pptv. Hence, its short lifetime is due to the high rate coefficient towards OH reported in literature, which amounts to  $3.6 \cdot 10^{-10} \text{ cm}^3 \text{ molecules}^{-1} \text{ s}^{-1}$ , see Atkinson, (1986), higher than the one of the very reactive isoprene ( $k_{\text{isoprene}+\text{OH}} = 1 \cdot 10^{-10} \text{ cm}^3 \text{ molecules}^{-1} \text{ s}^{-1}$ , (Atkinson, 1986)) for instance.

Very little is reported in literature regarding the emission and ambient level of this compound in the Mediterranean region. Owen et al., (2001) measured  $\alpha$ -terpinene from a few Mediterranean tree species, including: *Juniperus phoenicea*, *Juniperus oxycedrus*, *Spartium junceum* L., and *Quercus ilex*. Ormeno et al., (2007) published a content of  $\alpha$ -terpinene of  $34.9 \pm 2.3 \text{ } \mu\text{g/gDM}$  in the leaves of *Rosmarinus officinalis*, whose shrubs were present in large quantity around our field site in Corsica.

**Table 5.5:** Relative contributions of speciated BVOCs to the total calculated OH reactivity BVOCs fraction. Daytime BVOCs OH reactivity accounted for maximum  $9 \text{ s}^{-1}$ , on average  $2 \pm 2 \text{ s}^{-1}$ , nighttime BVOCs OH reactivity fraction accounted for maximum 0.5, on average  $0.1 \text{ s}^{-1}$ .

BVOCs	Day (%)	Night (%)
$\alpha$ -pinene	7.69	20.73
$\beta$ -pinene	16.49	16.05
limonene	12.03	11.36
camphene	1.48	3.05
$\alpha$ -terpinene	31.08	31.33
$\gamma$ -terpinene	1.28	5.04
isoprene	29.96	12.45

#### 5.4.4 Comparison between measured and calculated reactivity

Figure 5.7 shows together the time series of total measured reactivity and calculated OH reactivity. Data points were averaged over three hours (longest time resolution achieved by the gas phase measurements) to allow a direct comparison between the measured and calculated reactivity. In addition Figure 5.7 also reports the uncertainties on the measured and calculated reactivity, to highlight periods where an agreement or a significant discrepancy exists. Such uncertainties were considered to be 35% and 20%, respectively. When instrumental uncertainties are considered, the time series report a good agreement during the periods 20-23/07 and 31/07-05/08. The air masses during these days carried to the field site anthropogenic pollutants from the north of Italy and the south-west of France. Interestingly, such good agreement suggest that the air masses were mainly composed by measured AVOCs while OVOCs were present in lower amount. In contrast, the largest significant discrepancy among the measured and calculated reactivity is noticeable between the 23/07 and 30/07. To help understanding the source of this missing reactivity fraction we combined the modeled air masses regime (discussed in section 4.1) with the atmospheric mixing ratio of some common atmospheric tracers. We used isoprene and pinenes for air masses enriched by species derived by natural activities, while propane and ethane were chosen for the air masses enriched in anthropogenic pollutants. The regime of the air masses was interestingly various: during our field work we received air masses from diverse sectors which offered the possibility to analyse different possible scenarios for a site located in the western Mediterranean basin. The atmospheric mixing ratio of anthropogenic pollutants increased when the air masses were coming from the North East sector: between the 21-23/07 and between 31/07-03/08. On the other side, the biogenic enrichment was independent to the origin of the air masses, while it showed a closer variability to local drivers, such as the air temperature and the solar radiation. Peaks of concentration of BVOCs in ambient air were registered for all the modeled clusters of the air masses classification reported in Tab. 5.4. Remarkably, during the field work the site received air masses from the same sector more than once, however it does not seem that the magnitude of difference between the measured and calculated reactivity is associated to the origin of the air masses (compare Tab. 5.4 to Fig. 5.7).

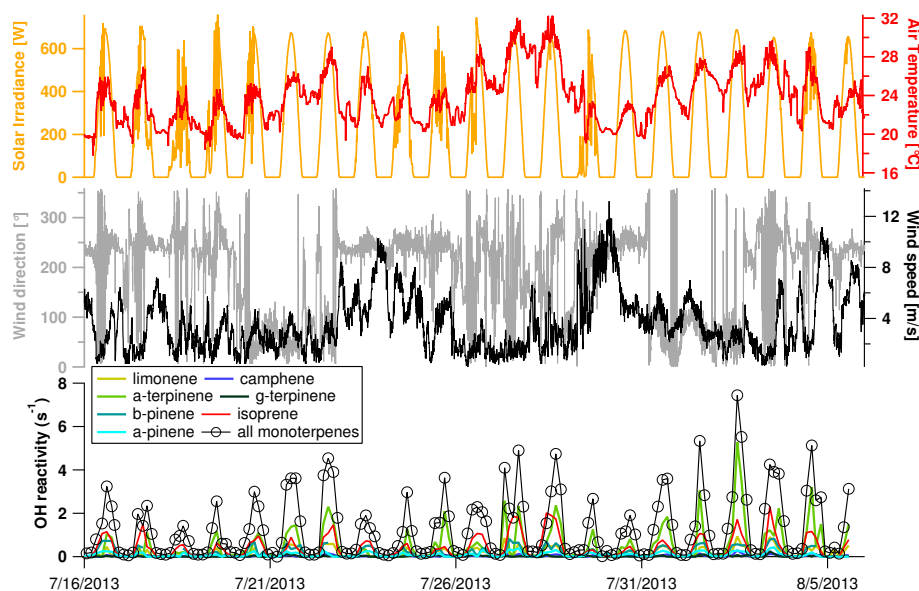


**Figure 5.7:** Absolute OH reactivity calculated for the measured biogenic compounds at the site during the period of the campaign. Higher panels show the profiles of wind direction, wind speed, solar irradiance, and air temperature measured at the same site during the same period.

## 5.4.5 Clues on the missing OH reactivity: a mix of primary emission and secondary production

### 5.4.5.1 Unmeasured terpenes

To get more insights into the source of our missing reactivity we need therefore to consider also the breakdown of the OH reactivity during these periods. Indeed, the highest contribution to the calculated OH reactivity during 23-27/07 was due to the OVOCs fraction, while during 27-30/07 the BVOCs explained the largest fraction of OH reactivity. We start hence to consider the emission of the primary species whose contribution to the OH reactivity was crucial at the site, thus the BVOCs. Some of them were sampled on-line through GC-FID, while others were first collected on sampling tubes and then off-line analysed in the laboratory through GC-MS (details about the methods were already provided in the methods section). The concentration obtained in these two ways was input for calculating the OH reactivity and their relative contribution. Speciated monoterpenes measured either by GC-FID or GC-MS were compared with the total monoterpenes concentration measured by PTR-MS. Proton Transfer Reaction-Mass Spectrometry cannot distinguish between structural isomers as monoterpenes, therefore its output is the sum of their individual concentrations. A comparison between the concentration of the to-

total fraction of monoterpenes obtained from the PTR-MS and the sum of the speciated monoterpenes acquired by gas chromatography showed indeed that between 0.2 and 0.6 ppbv of monoterpenes were not measured (Fig. 5.8), which is significant since uncertainties on GC and PTR-MS are quantified as 20% and 9% respectively. The unmeasured monoterpenes fraction can be due to monoterpenes not measured by GC methods (see Tab. 5.2 for the terpenes measured) or losses from sampling tubes prior to their analysis and of course can be subject to variation due to measurements uncertainty.

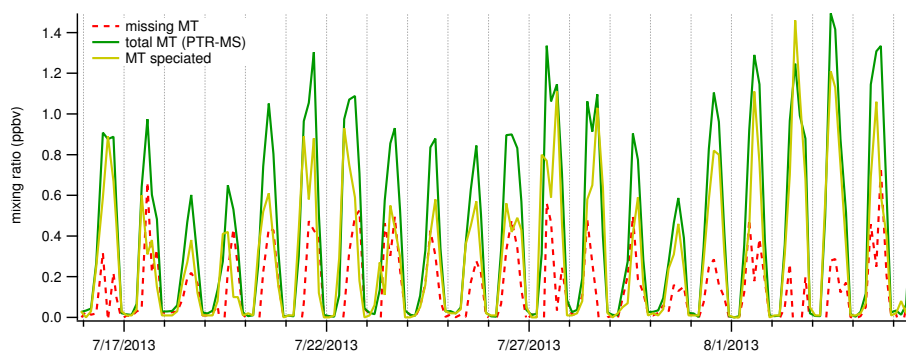


**Figure 5.8:** Total monoterpenes measured by PTR-MS compared to speciated monoterpenes measured off-line by GC-MS. Speciated monoterpenes were input for the calculation of the OH reactivity. The red dashed line refers to the difference between total measured and total speciated, here referred as "missing monoterpenes".

#### 5.4.5.2 estimated reactivity of the unmeasured terpenes

We input the missing concentration of terpenes with different species rate coefficients towards OH to estimate the terpenes impact to the calculated OH reactivity, i.e. whether the unmeasured monoterpenes fraction can explain alone the missing OH reactivity. Rate coefficients of a number of monoterpenes emitted by Mediterranean plant species were considered, for instance from a rosemary shrub since several plants of this species surrounded the monitoring station. Figure 5.9 displays the estimate of OH reactivity obtained from a number of monoterpenes, starting from the input of the missing monoterpenes concentration reported in Fig. 5.8. It has to be noticed that this is only a rough estimate of OH reactivity, since we do not know what was not measured, which is more likely to be the sum of different molecules rather than a single compound. Such compounds can actually explain a part of the missing reactivity over the whole measurements period (Fig. 5.9). However, it looks like to contribute only on minor levels to the whole missing fraction. This is especially evident when two cases are considered: the time period of significant missing reactivity (23-30/07), and the nighttime missing fraction. We need therefore to look into

the secondary products contribution to explain the missing fraction of OH reactivity.

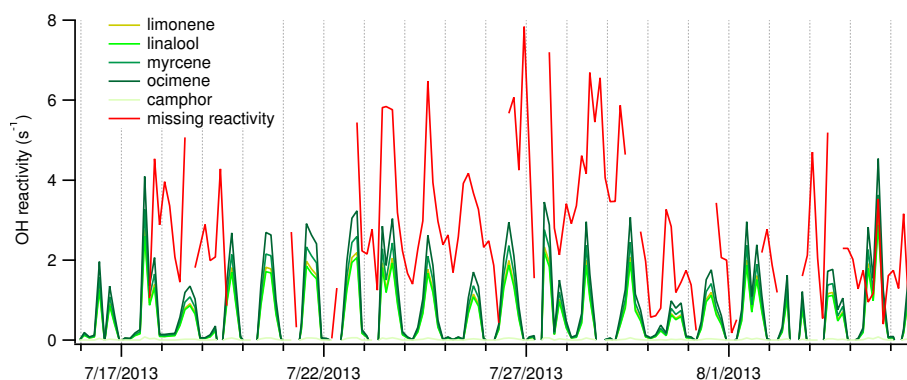


**Figure 5.9:** Calculated OH reactivity for different monoterpenes emitted by typical Mediterranean plants (Bracho-Nunez et al., 2011). The missing monoterpenes concentration reported in Fig. 8 was used as input, with the specific rate coefficient of the species with OH. Missing OH reactivity is reported as reference.

### 5.4.5.3 unmeasured secondary products

Evidences of a stronger oxidation of VOCs at the site were observed and will be available in two companion publications focusing on VOCs chemical aging and BVOCs profiles at the field site. Michoud et al., (now in preparation) found out that air masses transported from the west sector (during 23-27/07/2013) were processed over a longer period of time compared to the air masses coming from other wind sectors.

Figure 5.10 shows the variability of CO and ethyne as anthropogenic tracers. The largest difference among the two tracers is reported for the period between 23-27/07, suggesting that part of CO might originate by VOCs processing rather than primary emission. Kalogridis et al., (now in preparation) looked at the time series of acetone and CO to trace the source of oxidation of VOCs. Indeed, CO in our case is considered as a product obtained by the oxidation of anthropogenic species, due to its good covariance during the campaign with the anthropogenic black carbon and acetylene (here not shown). Acetone, on the other side, is here considered as an oxidation product from both sources: anthropogenic and biogenic. Whereas acetone exhibits a similar covariance with CO during most of the days, thus suggesting an anthropogenic origin, a larger discrepancy is observed between 27-30/07 when BVOCs were at their maximum levels, suggesting therefore an additional biogenic source (Fig. 5.11).

During the same period the relative individual contributions of BVOCs to the calculated OH reactivity of the total BVOCs are considered. Figure 5.12 shows that isoprene,  $\alpha$ -



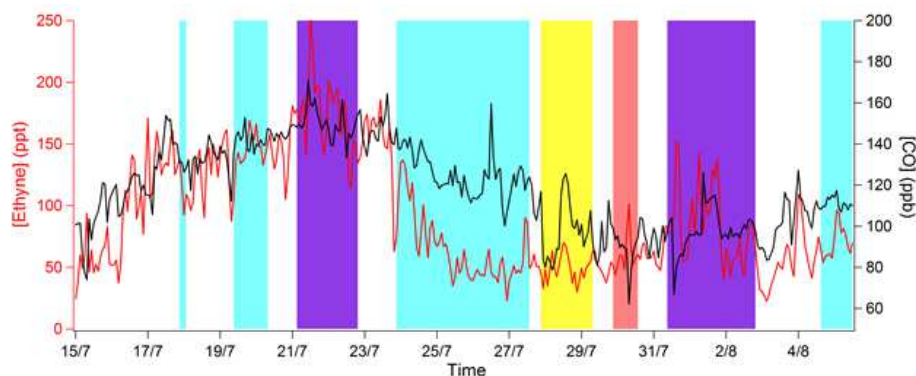


**Figure 5.10:** Ethyne and CO variability along the time of the field work. Colored bars highlight the different clusters identified with Hysplit. Between 23 and 30/07 is reported the largest difference among the two anthropogenic species, although the air masses have different origins, higher loadings of CO corroborate the hypothesis of stronger oxidation during those days. Graph courtesy of Vincent Michoud.

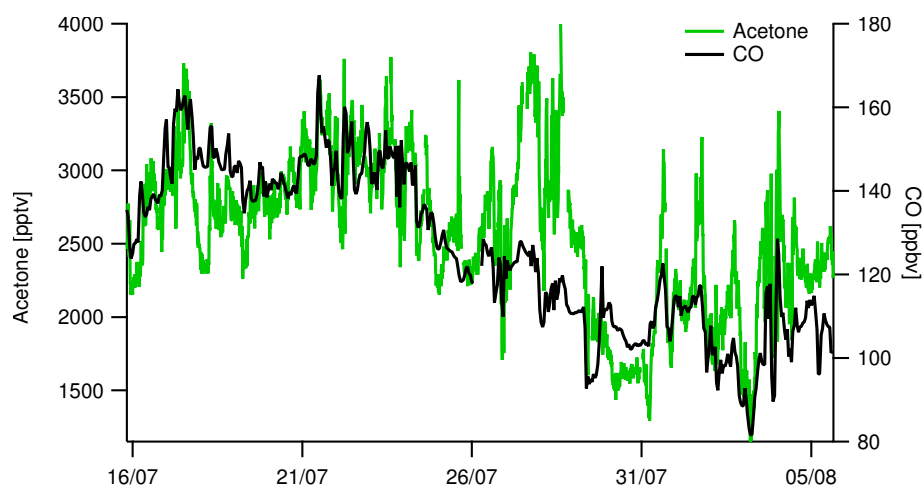


**Figure 5.11:** Acetone and CO variability along the time of the field work. Species are chosen as proxies of oxygenated products formed mainly by anthropogenic primary species (CO) and by anthropogenic and biogenic species (acetone). Graph courtesy of Cerise Kalogridis.

terpinene and limonene had a decisive impact in the OH reactivity. In particular, isoprene seems to have mostly a daytime impact while the monoterpenes had also a nighttime impact.

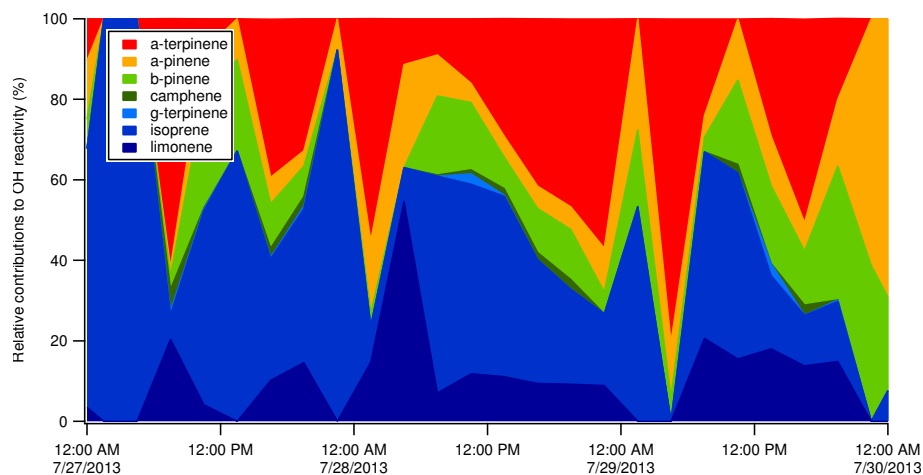


**Figure 5.12:** Relative contributions to the calculated OH reactivity among the measured biogenic volatile organic compounds during the period of highest missing OH reactivity and highest temperature.

## 5.4.6 Modeled OH reactivity

To get more insights into the OH reactivity of the secondary products generated from BVOCs oxidation we simulated their concentration with the model described in the methods section. From the concentration of these species we calculated what is referred in this section as modelled OH reactivity. In particular, we decided to look into the impact of the oxidation of the biogenic precursors measured at the site and see how much is their contribution in terms of reactivity. For this reason, we considered a two-layers box model with the chemical scheme as described in the methods section.

### 5.4.6.1 Model inputs

As input, we chose to use some of the physical and chemical conditions observed during the campaign. Since we are mainly interested to look at the effect of the BVOCs oxidation we focused on the period between 27/07/2013 and 30/07/2013 (see Figs. 5.7 and 5.12). During this period we observed the highest concentration of BVOCs (1134 pptv and 1335 pptv for isoprene and total monoterpenes, respectively), highest temperature (33° C), low wind speed (below 2 m/s) and significant missing OH reactivity (56% average missing fraction during this period). In addition, on the 28/07/2013 we registered the maximum values of concentration of BVOCs, OH reactivity ( $17 \pm 6 \text{ s}^{-1}$  and  $7 \pm 1 \text{ s}^{-1}$  measured and calculated respectively) and missing reactivity (59% average missing fraction) of the mentioned period. Therefore, the values measured on the 28/07/2013 were chosen as the initial concentration or imposed concentrations in our simulations. We input the

initial concentration of  $\text{H}_2\text{O}_2$  (1ppbv),  $\text{SO}_2$  (1 ppbv),  $\text{CH}_4$  (1840 ppbv), CO (100 ppbv), PAN-like species (affecting the reactivity but not the mass, 80 pptv) and ozone (60 ppbv) for both layers. These concentrations were chosen to represent typical rural concentrations (Sillman et al. 1990) for  $\text{H}_2\text{O}_2$ ,  $\text{SO}_2$  and PAN or based on concentrations typically observed during our campaign for CO,  $\text{CH}_4$  and  $\text{O}_3$ . The concentrations of BVOCs and  $\text{NO}_x$  are imposed during the whole simulations to match the levels observed on the field. Their profiles were prepared by interpolating the measurements run on 28/07/2013 (see Fig. 5.13a, b, c). Temperature, relative humidity, solar radiation and other physical parameters were obtained from the average of the observed values on 28/07/2013 and input in the model.

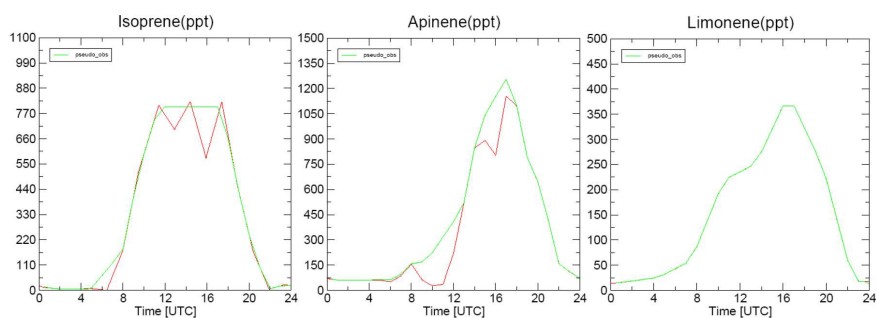


**Figure 5.13:** Observed (red line) and imposed (green line) atmospheric mixing ratios for isoprene (panel a), sum of pinenes and camphene (apinene, panel b), sum of limonene and terpinenes (limonene, panel c) during 28/07/2013.

#### 5.4.6.2 Model results and sensitivity

The modeled OH reactivity with the conditions of this day had a maximum at  $11.5 \text{ s}^{-1}$ . We evaluated the hypothesis used in our model with a sensitivity analysis of the parameters that were input. Table 5.6 shows the results of the sensitivity study for a case where advection is not considered and the modelled OH reactivity results  $12 \text{ s}^{-1}$ . This result is slightly higher than the modeled value with advection since here accumulation of reactants enhances the reactivity. In the sensitivity analysis all the variables input in the base case are kept constant to the base case, except for one that is varied. The chosen range of variability is within the limits of minimum and maximum values observed during the campaign, except for the cases of 20 ppbv for isoprene and 10-50 ppbv for  $\text{NO}_x$ .

The sensitivity analysis shows: (i) The model gives reasonable results, since for an input of isoprene of 20 ppbv (which is by far higher than the value measured in Corsica) results an OH reactivity of  $70 \text{ s}^{-1}$ . At the forest of OHP (Observatoire de Haute Provence), France, a

**Table 5.6:** Sensitivity study of the model for a base case of modelled OH reactivity of  $12 \text{ s}^{-1}$ 

Sensitivity Test	Lower	Normal Case	Higher
ISO	400 pptv <b>10.0</b>	800 pptv	1600 pptv 20 ppbv <b>15.7</b> <b>70</b>
APIN	625 pptv <b>10.5</b>	1250 pptv	2500 pptv <b>15.2</b>
LIMO	183 pptv <b>10.8</b>	366 pptv	733 pptv <b>14.6</b>
NO <sub>x</sub>	0.28 ppbv <b>11.5</b>	0.565 ppbv	1.13 ppbv 10 ppbv 50 ppbv <b>12.8</b> <b>15.4</b> <b>22.5</b>
O <sub>3</sub> fixed	40 ppbv <b>11.4</b>	50 ppbv <b>11.8</b>	60 ppbv <b>12.2</b>
OH fixed	$5 \times 10^6 \text{ molec.cm}^{-3}$ <b>12.0</b>	$1.2 \times 10^7 \text{ molec.cm}^{-3}$ <b>12.1</b>	$1.7 \times 10^7 \text{ molec.cm}^{-3}$ <b>12.1</b>
Temperature	18° C <b>11.5</b>	28° C	38° C <b>12.6</b>
Rel. Humidity	56.5% <b>11.8</b>	66.5%	76.5% <b>12.2</b>
Solar Radiation	45° lat 21/12 <b>9.8</b>	60° lat 21/07 <b>11.5</b>	30° lat 21/07 <b>12.2</b>

maximum measured value of isoprene of 20 ppbv was responsible, almost alone, of  $69 \text{ s}^{-1}$  of reactivity (see, Zannoni et al., 2015b). (ii) The result of reactivity is not much affected by OH concentration. Hence, an OH recycling due to isoprene and monoterpenes oxidation neglected by our model, could not be the main reason of discrepancy between model and measurements. (iii) Local drivers as temperature and solar radiation do not significantly affect the OH reactivity. They can instead directly affect the emissions of BVOCs, which are not included in the model. (iv) OH reactivity does not change significantly when NO<sub>x</sub> concentration is multiplied by a factor of 2. However, we can notice that the OH reactivity almost doubles for higher NO<sub>x</sub> concentration (50 ppbv input) which would be an important result in an urban environment, but not for our case study (NO<sub>x</sub> maximum concentration measured during CARBOSOR was 7 ppbv). (v) Primary BVOCs concentration seems to have a major impact on the resulting OH reactivity. Therefore, from the range of results obtained through the sensitivity study we can conclude that the modeled OH reactivity has an uncertainty of about  $\pm 2 \text{ s}^{-1}$ .

### 5.4.6.3 Contributions to the modelled OH reactivity

The contributions to the modelled OH reactivity are represented in Fig. 5.14. Here we can notice that half of the OH reactivity is represented by the measured primary BVOCs and inorganics. Besides them, aldehydes, ketones, carboxylic acids and hydroperoxides had the largest impact on the OH reactivity. Especially, a number of aldehydes that follow into the group of propionaldehyde ( $\text{CH}_3\text{CH}_2\text{CHO}$ ) had an impact to the total reactivity of 12%, almost as high as the primary measured isoprene (16%). In the specific, the acetaldehyde group of molecules ( $\text{CH}_3\text{CHO}$ ) weighted 7%, formaldehyde ( $\text{CH}_2\text{O}$ , here only as formaldehyde but measured during 28/07/2013 only until 11 AM) weighted 7%, followed by a group of ketones (MVKET, 5%), methylhydroperoxides ( $\text{CH}_3\text{OOH}$ , 4%), longer chain hydroperoxides ( $\text{CH}_3\text{CH}_2\text{CH}_2(\text{OOH})$ , 4%), other hydroperoxydes (3%) and methacrolein aldehydes (MEACR, 3%). Many of the species showed in Fig. 5.13 were not measured during the campaign, especially considered that most of these species represent more chemical compounds that fall into the named category. To compare the calculated and modelled OH reactivity we need to consider that half of the species reported in Fig. 5.13 were either not measured, either are surrogates including species measured and not measured. Therefore, we can only compare the absolute values obtained for the primary BVOCs and inorganics. The maximum calculated reactivity obtained for 28/07/2013 is  $7 \pm 1 \text{ s}^{-1}$ , while the modeled reactivity is  $11.5 \pm 2 \text{ s}^{-1}$ . Roughly, half of the species representing the modeled reactivity (BVOCs and inorganics) were also measured and amount to below  $6 \text{ s}^{-1}$ , the contribution of some secondary species also measured can easily reach the  $7 \pm 1 \text{ s}^{-1}$  calculated. The difference between 11.5 and 7 is likely to represent an additional contribute to the measured reactivity which is not accounted for in the calculated value.

The unmeasured organic products predicted by the model to be formed are indeed highly reactive and fall into two main categories: aldehydes and hydroperoxides. The model does not permit the further speciation of the groups into the individual produced compounds, however, it gives a direction that a major effort for measuring aldehydes and hydroperoxides should be done. The obtained modelled reactivity is still lower than the measured OH reactivity, even when uncertainties are considered (total measured OH reactivity of  $17 \pm 6 \text{ s}^{-1}$ , while modelled OH reactivity  $11.5 \pm 2 \text{ s}^{-1}$ ). Considered that our model only examines the oxidation of BVOCs, we can conclude that the difference between measured and modelled reactivity originates from: -the model does not consider long-range transported species. In this case we assume that the model represents well the reactivity of the BVOCs and the gap is only due to not having considered long-range transported species. To check this, we could include BVOCs in the boundary conditions and use a 3D transport chemical model as CHIMERE (Menut et al., 2015). -simplified chemical scheme of oxidation for

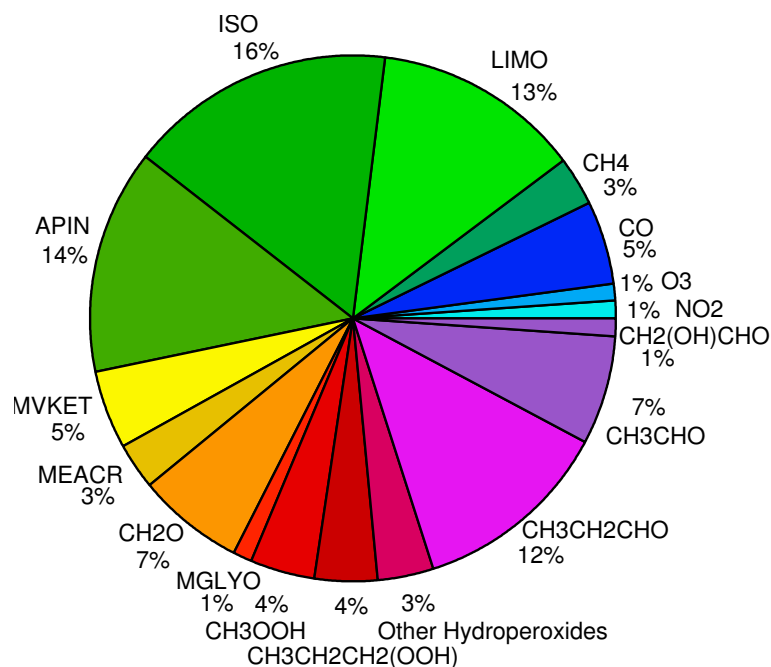


**Figure 5.14:** Modelled OH reactivity contributions predicted from the atmospheric mixing ratio of the BVOCs measured during 28/07/2013. The total OH reactivity obtained from the model amounted to  $11.5 \text{ s}^{-1}$ .

the BVOCs considered. In this case our model underestimates the reactivity because of an uncorrect reproduction of the chemistry. More advanced chemical schemes as MIM2 (Taraborrelli et al., 2009) or considering the primary biogenic compounds individually in the simulations might further reduce the missing OH reactivity gap. - Furthermore, no partitioning and particles formation was undertaken by the model. The high ambient temperature registered during the campaign might have released more semivolatiles in the gas phase that could have contributed to the measured OH reactivity. We would like therefore to explore these options in the future in order to better elucidate the missing OH reactivity observed during our field measurements.

## 5.5 Conclusions

Total OH reactivity was intensively measured during summertime at a coastal receptor site in the western Mediterranean basin for three weeks. It was on average  $5 \pm 4 \text{ s}^{-1}$  ( $1\sigma$  standard deviation of the data) and maximum  $17 \pm 6 \text{ s}^{-1}$  (35% uncertainty). We compared the total measured reactivity with the reactivity inferred from the concentration of the species measured at the site. Such comparison highlighted that during 23/07/2013-

30/07/2013, one week out of three of field measurements, a significant missing fraction (up to 59%) could not be explained by the measured compounds. Besides, we calculated that the biogenic species had the largest impact on the OH reactivity. This class of compounds had an average contribution during daytime of 45% on the whole reactivity calculated from the measures of our field work. We found out that a little part of the missing OH reactivity could be due to unmeasured monoterpenes emitted by the local vegetation. However, this finding adds only a little more information to our understanding. Interestingly, we noticed that some reference anthropogenic and biogenic tracers showed a different behavior during the period where a significant missing fraction was observed. The time series of CO and ethyne were used to assess the primary and secondary origin of the air masses received at the site in a companion study. A large difference between the concentrations of these two tracers, with larger concentration of CO, suggested that air masses were longer processed during this period. Similarly, by comparing acetone and CO, a stronger oxidation of biogenic precursors was pointed out. A two-layers box model describing the oxidation of biogenic compounds through a simple chemical scheme was used as tool to get more insights into the origin of the missing OH reactivity. The modelled OH reactivity due to the oxidation of all the measured BVOCs, following the chemistry of isoprene,  $\alpha$ -pinene and limonene, was  $11.5 \pm 2 \text{ s}^{-1}$ . This value was between the total measured reactivity ( $17 \pm 6 \text{ s}^{-1}$ ) and the calculated OH reactivity ( $7 \pm 1 \text{ s}^{-1}$ ) on 28/07/2013. Although the considered assumptions and the simplified chemical scheme we reduced the missing reactivity gap and found out that most of the missing reactivity is explained by two classes of compounds: aldehydes and hydroperoxides. We can conclude here that it is still challenging to capture all the secondary species formed from the oxidation of organic volatiles, even when many state of the art techniques are deployed simultaneously during an intensive field work. Simulations with more advanced chemical schemes of oxidation of the BVOCs, and simulations including long-range transport effects, would be of great help to our current understanding of the important reactive species in air. They would also be beneficial to assess the importance of some classes of compounds formed from the oxidation reactions of the BVOCs measured at this Mediterranean site.

## 5.6 Acknowledgments

This study was supported by European Commission's 7<sup>th</sup> Framework Programme under Grant Agreement Number 287382 "PIMMS", the programme ChArMEx, CEA and CNRS. The authors would like to thank F. Dulac and E. Hamonou for managing the ChArMEx project.





## Chapter 6

# Conclusion and future research

This thesis work has presented: (i) technical improvements of the Comparative Reactivity Method (CRM) for measuring the OH reactivity in ambient air and (ii) results of ambient measurements of OH reactivity at two sites in the Mediterranean basin exposed to different loadings of atmospheric reactants.

In order to measure the total OH reactivity in ambient air accurately it is important to have a robust instrument, easy to be used on the field, adaptable to different field constraints, whose data can be unambiguously processed. Scientists operating the Comparative Reactivity Method have showed, prior to this PhD project, promising results when deploying this technique in different environments. This PhD work has presented the method in detail, from its construction through its characterization to a detailed explanation on how the raw data are processed. The performance of the CRM device built during my PhD project was also compared through an intercomparison exercise to another CRM instrument built in another laboratory. The exercise served to investigate the performance of the two instruments through different tests to assess the corrections of the raw data and ambient measurements of reactivity. The main outcome of the intercomparison were: (i) novel method to measure the C1 reducing its time of acquisition, (ii) a detailed description for processing the raw data, (iii) different impact of such corrections for each instrument, (iv) excellent correlation among the data sets of ambient reactivity in the investigated range 0-300 s<sup>-1</sup>.

Ambient measurements of OH reactivity were conducted at two selected sites in the Mediterranean basin, as part of two intensive field campaigns, namely CANOPEE (Biosphere-atmosphere exchange of organic compounds: impact of intra-canopy processes) and ChArMEx (Chemistry-Aerosols in a Mediterranean Experiment). The site chosen for the field campaign CANOPEE is a Mediterranean forest composed mainly by downy oak trees, which are a species known to emit almost exclusively isoprene. Simultaneous measurements of

OH reactivity, BVOCs and main atmospheric constituents concentration were used to: (i) resolve our level of knowledge of the atmospheric composition inside and above this forest, (ii) determine the total loading of reactants above the forest. We found out that the measured and calculated reactivity were the same during daytime, when the OH reactivity is basically dominated only by isoprene (between 70-80%), to lesser extent by other BVOCs, OVOCs and inorganics. On the other hand, larger gaps between the measured and calculated reactivity were observed during the night, suggesting a larger contribution to the reactivity of the oxidation products of the primary BVOCs. We noticed that the two heights investigated (i.e. 2 m inside the canopy, 10 m above the canopy, mean canopy height 5 m) did not report any great difference in composition and measured reactivity, suggesting that most of the emissions released by vegetation were driven above the canopy without undergoing any significant chemical transformation. Finally, the OH reactivity measured on top of this forest of downy oaks reached  $69 \text{ s}^{-1}$  at its maximum. This result represents a large value of reactivity for a forest, so far as I know, only tropical forests reported such high values of reactivity.

The site chosen for the field campaign ChArMEX, on the other hand, presented different constraints. Ersa, in the northern cape of Corsica, is a receptor coastal site influenced by different air masses regimes with different footprints during summertime. We aimed at investigating the total loading and our level of knowledge of the composition of such air masses by measuring together the OH reactivity and the concentration of a broad suite of gaseous compounds. We observed a maximum OH reactivity of  $17 \text{ s}^{-1}$ , and a missing fraction of reactivity up to 50% during one week, out of three, of our measurements campaign. The contribution to the reactivity was mainly driven by the primary measured biogenic VOCs, followed by the inorganics, the oxygenated VOCs and finally the anthropogenic VOCs. Air masses back trajectories and gaseous profiles helped noticing that the missing reactivity could be explainable by unmeasured secondary-generated compounds. Preliminary results obtained from simple model simulations suggested that BVOCs oxidation played an important role on the field. With the measured concentrations of the primary biogenics the model reproduced a value of reactivity between the calculated and the measured one. Such results highlighted that modelling the oxidation of the biogenic precursors can add some valuable information to our measurements, and classes of unmeasured species such as aldehydes and hydroperoxides can have a larger, than estimated, contribution to the reactivity.

The OH reactivity tool demonstrated also in this thesis work its utility to better comprehend the atmospheric reactive composition and processes. In the Mediterranean region, large sinks of the OH radical were measured at two contrasted sites. Above the forest of OHP, the maximum value of reactivity was  $69 \text{ s}^{-1}$ . In Corsica, during summertime,

the peak of reactivity was  $17 \text{ s}^{-1}$ . Two large values if we consider these numbers in their context, i.e. temperate forest environment and receptor site. In both cases, the major drivers to such high values are the biogenic compounds, whose emissions are triggered by the higher values of ambient temperature and solar radiation encountered in the Mediterranean region during summertime. However, the Mediterranean region is very complex: its vegetation cover is highly variable within the region, it is rich in biodiversity and it is strongly influenced by the anthropogenic footprint. The OH reactivity tool has the great advantage of providing directly the total loading of atmospheric reactants. We saw with this thesis work that high loadings were measured during spring-summertime in the Mediterranean basin. However, in order to better characterize the atmospheric cleansing capacity over this region, more measurements of OH reactivity at other targeted sites are needed.

Forests can contribute largely to the OH reactivity, also in the Mediterranean. Our understanding of BVOCs oxidation processes, isoprene chemistry, and forests emission is, nevertheless, still limited. At OHP, we resolved the OH reactivity during daytime, when emissions were transported faster above the canopy structure, but nighttime chemical processes are left unclear. On the other hand, a receptor site in the Mediterranean, although being far from any source of pollution, was still affected by high loadings of reactants during summertime. The measured reactivity showed indeed a diurnal profile, average values above the background value and a larger than expected biogenic contribution. The combination of more effects as local oxidation processes and transported processed species made the understanding of our measurements at this site even more puzzling. Preliminary results, obtained with a model which considers a simple chemical scheme for the oxidation of the BVOCs, showed that unmeasured products of the oxidation of the measured BVOCs partly explain the observed missing OH reactivity.

The missing OH reactivity seems still to be a mixture of unmeasured primary and secondary generated compounds. At OHP, we observed an increasing level of oxygenated products during the nights of missing reactivity. Are these products leading to the missing reactivity or are there primary unmeasured precursors that lead together with their secondary products to the missing reactivity? This is still an open question. In Corsica, the missing reactivity was to a minor extent explained by the unmeasured monoterpenes. Unmeasured secondary products generated from the oxidation of BVOCs seem to have a larger contribution. Although the sites presented different influences, this thesis work confirms one common feature: BVOCs oxidation remains a major unknown in atmospheric chemistry. In this context, approaches as combining the OH reactivity measurements to other tools, and improving the current analytical techniques for measuring oxygenated larger semivolatile compounds on the field would be beneficial.

### Perspectives for further research

I underlined throughout the thesis the utility of measuring directly the total loading of reactants with only one parameter, as it is done by measuring the total OH reactivity. It is important that measurements of such parameter are extremely accurate and comparable when obtained from different instruments. The Comparative Reactivity Method reported a broader range of applications compared to other existing techniques but at the same time an exhausting data processing and instrumental interferences are also reported. This thesis work as well as the recent publication of Hansen et al., (2015) presented first comparison of two CRMs and a CRM and pump and probe instrument. A larger comparison among the three existing techniques, including more instruments for the same technique, will take place during October 2015 at the SAPHIR atmospheric chamber in Juelich Forschungszentrum. This exercise will help strengthen our confidence in these measurements techniques, further highlights the limitations and advantages of each of them and possibly starting to consider common operative procedures such as for calibrating the instrument and processing the raw data.

One of the major application of the OH reactivity, and the one discussed in this thesis project, is the comparison of the total reactivity measured with the one calculated from the measured species. This approach helps understanding the fraction not measured and why. It helped to stress so far that many unknowns are still associated to forests emissions and their chemical transformation. Understanding the missing reactivity is often more complicated than how it seems, since most of the times the unmeasured compounds are a mixture of primary emissions and secondary generated products. Additional tools are therefore needed in order to disentangle the two processes and better understand field results of OH reactivity, and more specifically, field observations at a biogenic dominated site. Some promising tools that can be combined to measurements of OH reactivity are: branch enclosure studies on the field, atmospheric chambers/environmental chambers laboratory studies and chemical models.

Branch enclosures permit to isolate a specific plant species and concentrate its emissions with regards to the background atmospheric compounds. Consequently, one can obtain: (i) information whether the unmeasured compounds are emitted by that specific plant species, (ii) information whether the unmeasured compounds are emitted or produced by oxidation processes. Kim et al., (2011) followed this approach, and by investigating the reactivity of the main plant species of a forest in Michigan they concluded that the unmeasured oxidation products generated from the primary emitted BVOCs at the site were indeed responsible for the missing reactivity. Another interesting result that can be obtained from plant cuvettes measurements is the fluxes of OH reactivity, or direct total flux of reactants.

Noelscher et al., (2013) measured the fluxes of OH reactivity from Norway Spruce by using a plant cuvette. Their main focus was to highlight the drivers of the missing reactivity when the primary species are the unmeasured compounds. They indeed confirmed that heat stress induced on plants trigger the emission of unknown/unmeasured compounds, therefore explaining the missing OH reactivity. An attempt in using a branch enclosure to measure the reactivity of a downy oak branch was also done during my PhD work (see poster in the appendix). However, our instrument needed more work to perform correctly measurements of such high values of reactivity and we aim at improving this aspect in the near future.

Laboratory studies with flow tubes and atmospheric chambers reported also promising results. Both Nakashima et al., (2012) and Noelscher et al., (2014) deployed the OH reactivity tool to investigate the oxidation of isoprene in the laboratory. Conversely to plant cuvettes, such combination helps to isolate oxidation processes from plants emissions and highlight possible not-considered before, oxidation pathways. Combining plant chambers to atmospheric chambers opens also new possibilities for studying the emissions and the oxidation of specific plants in a controlled environment. This might also be a possible outcome from the experiments of the intercomparison exercise planned in Juelich, due to the possibility of using their combined facility of the plant chamber SAPHIR+ and the atmospheric chamber SAPHIR.

Models resembling the chemistry of the oxidation of BVOCs to different details would be of great benefit when combined to measurements. Chapter 5 shows that preliminary attempts in modelling the chemistry of the biogenic species measured in Corsica provide important unmeasured reactive species as the classes of the hydroperoxides and aldehydes. We are interested in improving these attempts by using a model based on more recent and more detailed chemical scheme of reactions, and by considering the effects of long-range transport. This would be of benefit in order to: (i) understand the unmeasured reactive compounds contributing to the measured reactivity in Corsica, (ii) confirm the larger impact of local biogenic oxidation compared to long-range transported aged air masses.

Finally, the data of reactivity here provided could be used to determine the ozone formation potential and the aerosol yields at the investigated sites. This will be useful to assess the atmospheric impact of the loadings of reactive gases over the region and show potential applications of including measures of reactivity in regional monitoring networks.



## Appendix A

# Rate coefficients of reaction with OH for selected atmospheric compounds

**Table A.1:** Rate coefficients of reaction with OH for some atmospheric compounds discussed in this thesis work.

Compound name	$k_{i+OH}$ in $\text{cm}^3 \text{ molecules}^{-1} \text{ s}^{-1}$	Reference
$\alpha$ -terpinene	3.50E-10	Atkinson, 1986
$\gamma$ -terpinene	1.7E-10	Atkinson, 1986
limonene	1.69E-10	Atkinson, 1986
isoprene	1.00E-10	Atkinson, 1986
$\beta$ -pinene	7.81E-11	Atkinson, 1986
$\alpha$ -pinene	5.33E-11	Atkinson, 1986
camphene	5.33E-11	Atkinson, 1986
isobutylene	5.18E-11	Atkinson, 1986
hexene	3.70E-11	Grosjean and Williams, 1992
3-methyl-1-butene	3.17E-11	Atkinson, 1986
1-butene	3.11E-11	Atkinson, 1986
propene	2.60E-11	Atkinson, 1986
m-xylene	2.45E-11	Atkinson, 1986
NO	1E-11	Atkinson et al., 2004
p-xylene	1.52E-11	Atkinson, 1986
o-xylene	1.47E-11	Atkinson, 1986
NO <sub>2</sub>	3E-11	Atkinson et al., 1997
nonane	9.70E-12	Atkinson, 2003
HCHO	8.5E-12	Atkinson et al., 2001
cyclohexane	6.97E-12	Atkinson, 2003
heptane	6.76E-12	Atkinson, 2003
2-methylhexane	6.69E-12	Sprengnether et al., 2009
2,3,4-trimethylpentane	6.50E-12	Wilson et al., 2006
toluene	5.6E-12	Atkinson, 1986
3-methylpentane	5.85E-12	Wilson et al., 2006
2-methylpentane	5.20E-12	Atkinson, 2003
hexane	5.20E-12	Atkinson, 2003
pentane	3.84E-12	Atkinson, 2003
isopentane	3.60E-12	Atkinson, 2003
isobutane	2.14E-12	Atkinson, 2003
benzene	1.28E-12	Atkinson, 1986
propane	1.09E-12	Atkinson, 2003
acetylene	7.79E-13	Atkinson, 1986
ethane	2.41E-13	Atkinson et al., 2001
CO	1.44E-13	Atkinson et al., 2004
CH <sub>4</sub>	6.4E-15	Atkinson et al., 1997



Appendix B

## Selected Poster Presentations

## Intercomparison of two Comparative Reactivity Method instruments in the Mediterranean basin during summer 2013

Nora Zannoni<sup>1</sup>, Sébastien Dusanter<sup>2,3,4</sup>, Valérie Gros<sup>1</sup>, Roland Sarda Esteve<sup>1</sup>, Vincent Michoud<sup>5</sup>, Vinayak Sinha<sup>5</sup>, Bernard Bonsang<sup>1</sup>

(1) Laboratoire des Sciences du Climat et de l'Environnement (LSCE), CNRS-CEA-UVSQ, Gif sur Yvette, France (nora.zannoni@lscce.ipsl.fr), (2) Univ Lille Nord de France, F-59000, Lille, France, (3) Mines Douai, SAGE, F-59508 Douai, France, (4) School of Public and Environmental Affairs, Indiana University, Bloomington, IN, USA, (5) Department of Earth and Environmental Sciences, Indian Institute of Science Education and Research (IISER) Mohali, Punjab, India

### 1. Introduction

Measurements of total OH reactivity in the troposphere help to better constrain the OH chemistry and the burden of OH reactants in a specific environment. There are three existing methods capable to run these measurements: two of them are based on different variations of Laser Induced Fluorescence (LIF) technique [1,2], the third one is the recently developed Comparative Reactivity Method (CRM) [3]. The first two methods derive the total OH reactivity from the decay of artificially produced OH radicals when ambient air is sampled in a flow tube. The CRM relies on competitive kinetics with a reference molecule whose reactivity with OH is well known. Such method has been widely applied in recent field studies, showing a good applicability and fast response [4,5,6].

Herein we present preliminary results of one of the first intercomparison between two CRM instruments built in two different laboratories (CRM LSCE and CRM MD) by different research teams. We carried out measurements within the ChArMEx (Chemistry and Aerosols in a Mediterranean Experiment) project at a remote field site in the Mediterranean basin during summer 2013.

### 2. Methods

The CRM concept is to monitor a competition for artificially produced hydroxyl radicals between a reference molecule (i.e. pyrolyte), and reactive species in ambient air. Chemical reactions take place inside a glass flow reactor coupled to a detector, in our case a Proton Transfer Reaction-Mass Spectrometer (PTR-MS). Pyrolyte concentration is monitored at m/z 68 during several measurement stages (namely C0, C1, C2, C3) and total OH reactivity is determined by equation (1), with  $k_p$  the rate constant of reaction between pyrolyte and OH. The four experimental steps represent: (i) initial concentration of pyrolyte in absence of OH radicals and ambient air, (ii) initial concentration of pyrolyte in absence of OH radicals and ambient air, but after photolysis (C1), (iii) pyrolyte concentration after reaction with OH in zero air but in absence of ambient air (C2), (iv) pyrolyte concentration when zero air is replaced by ambient air (Fig. 1). C1 is always taken under dry conditions in the reactor, which is often time consuming. During the intercomparison we tried a faster way, that is to scavenge OH injecting a known amount of methane while the system was still wet (see results in Fig. 3). A simplified schematic of the experimental set up is shown in Fig. 2, characteristics and operational settings of CRM LSCE and CRM MD are reported in Table 1.

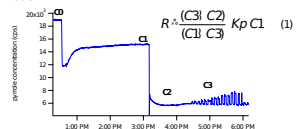


Figure 1. Pyrolyte concentrations during an OH reactivity experiment.

- [1] Kovacs and Brune, Total OH loss rate measurement, Atmos. Chem., 39, 105-122, 2001.
- [2] Solisag et al., Development of a measurement system of OH reactivity in the atmosphere by using a laser-induced pump and probe technique, Rev. Sci. Instrum., 75, 2648, 2004.
- [3] Sinha et al., The Comparative Reactivity Method (CRM) for measuring atmospheric OH reactivity in ambient air, Atmos. Chem. Phys., 8, 2213-2227, 2008.
- [4] Dolgrouky et al., Total OH reactivity measurements in Paris during the 2010 MEGAPOLI winter campaign, Atmos. Chem. Phys., 12, 9563-9612, 2012.
- [5] Nölscher et al., Seasonal measurements of total OH reactivity fluxes, total aerosol mass and mass concentrations in the wintertime in the Mediterranean basin, Biogeosciences Discuss., 9, 13497-13536, 2012.
- [6] Kinnel et al., Contributions of primary and secondary biogenic VOCs to total OH reactivity during the ChArMEx (Community Atmosphere Research Interactions Experiments) field campaign, Atmos. Chem. Phys., 11, 8613-8623, 2011.

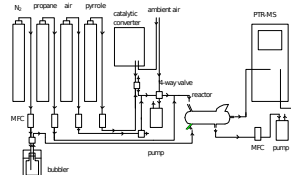


Figure 2. Simplified schematic of CRM LSCE. A different setup (not shown) was used for CRM MD.

Table 1- Characteristics of CRM LSCE and CRM MD.

Reactor	CRM LSCE	CRM MD
Reactor	Glass reactor from MPE	Glass reactor from MPE
Detection system	PTR-MS/Quadrupole from Veicon, Veicon, Austria	PTR-MS/RF from Kore Technology Ltd. By UK
Sampling line	1/4" ID Teflon line, 3.0m	1/4" ID Teflon line, 30m
Reactor volume (L)	11.7	8.4
Sampling flow rate (L/min)	~250	~2000
Sampling set up	No pump before sampling	Teflon pump before sampling
Total flow inside reactor (L/min)	~330	~355
Photolysis rate	~5%	~2%
C1 value (ppb)	Wet (pH=8.6)	From methanest (61.4± 0.6 (1σ))

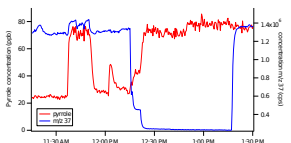


Figure 3. Pyrolyte concentration (ppb) during the methane test (time 11:40 AM) and dry C1 (12:25 PM). As comparison, the water cluster (m/z 37) counts are plotted as a reference of humidity changes in the system.

Table 2- Correction factors applied to raw data

Correction steps	CRM LSCE	CRM MD
Humidity	~20%	~8%
Pyrolyte	Correction factor = 1.7 ± 0.38x Pyr/OH (1 @ pyr/OH = 0.86)	Correction factor = 1.29 ± 0.38x Pyr/OH (1 @ pyr/OH = 1.56)
Dilution	1.36	1.31

### 3. Data processing

The reactivity obtained from Eq. (1) is corrected for the following:

- Humidity changes** in the system when consecutively sampling pyrolyte in zero air and pyrolyte in ambient air. Assessed by considering the difference between C3 and C2 in m/z 68 versus the difference between C3 and C2 in m/z 37 when dry air is injected in the reactor.
- Deviation from pseudo first order conditions** (assumed by Eq.1). Correction made as a function of [Pyrolyte]/[OH] changes due to OH field variation over time. Correction assessed through injection of a known reactivity with external gas standards (Fig. 4). CRM MD correction shows no dependency on the external gas standard used (Fig. 5), while CRM LSCE shows a larger scatter and this has to be further investigated and improved.
- Dilution** of ambient air inside the reactor

The correction factors employed by each team are reported in Table 2.

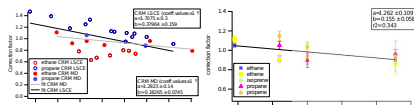


Figure 4. Correction factor dependency on pyrolyte/OH measured from the injection of known reactivity with propane and ethane for the two instruments (LSCE hollow circles, MD full circles).

### 4. Field site and tests

Measurements were carried out at a remote field site of Cape Corsica (42.97° N, 9.38° E altitude 533 m, Fig. 6), in the Mediterranean basin, within the ChArMEx (Chemistry-Aerosols Mediterranean Experiment) project. Table 3 indicates measurements performed to intercompare the two instruments.



Figure 6. Field site location.

Table 3- Experiments carried out during the intercomparison.

Date	Type of test
08/07/2013 09:07:2013	Enclosure experiment 1
10/07/2013 13:07:2013	Enclosure experiment 2
10/07/2013 13:07:2013	Enclosure experiment 2
07/2013-08/2013	Reactivity of standard gases
05/08/2013	Comparison of pyrolyte standards MD

### Acknowledgments

This work is supported by the European Commission's 7th Framework Programme under Grant Agreement Number 287382, 'FRIMMS' project, and number 293897, 'DERVOC' project. CNRS, CEA, ChArMEx, CARBOSOR are acknowledged. We are thankful to Max Planck Institute for providing the glass reactors.

### 5. Preliminary Results

**Total OH reactivity profiles measured by CRM LSCE and CRM MD from the plant enclosure (Fig. 7). Values peaked up to 300 s<sup>-1</sup> when we induced stress on the plant.**

**Correlation found between the two instruments: CRM LSCE=1.3(CRM MD)-2.2. Instruments uncertainty ~30% see Fig. 8.**

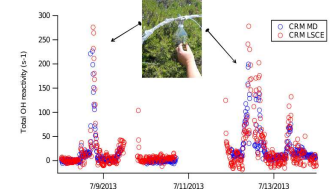


Figure 7. Total OH reactivity profiles from a rosemary plant enclosure measured by CRM LSCE and CRM MD for the whole time period of the test. Data points refer to branch enclosure experiment part 1 and part 2 and ambient measurements (reactivity <math>\le 5 s^{-1}</math>), refer to Table 3 for more details.

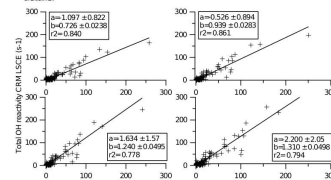


Figure 8. Correlations of CRM LSCE versus CRM MD among from top left to bottom right: (1) raw data, (2) humidity correction, (3) humidity and pseudo first order deviation correction, (4) humidity, kinetics and dilution correction. Data are averaged over 30 minutes and coefficient values include one standard deviation.

### 6. Conclusions

Preliminary results suggest a good agreement between the two CRM instruments for OH reactivity values up to 300 s<sup>-1</sup>, with differences within measurement uncertainty. Though the two CRM systems had significant differences in configuration (used different PTR-MS detectors (Quad vs ToF) and sampling methods), the generally good agreement demonstrates the robust reproducibility of the CRM technique. Moreover a new way to reduce the conditioning between wet and dry stages using methane is demonstrated.



Figure B.1: Poster presented at the European Geosciences Union General Assembly, Vienna, Austria, April 2013.

## Impact of Biogenic Volatile Organic Compounds on Total OH reactivity at a remote site in the Mediterranean basin during summer 2013

Zannoni N.<sup>1</sup>, Gros V.<sup>1</sup>, Sarla R.<sup>1</sup>, Bonsang B.<sup>1</sup>, Sinha V.<sup>2</sup>, Kalogridis C.<sup>1</sup>, Michoud V.<sup>3</sup>, Dusanter S.<sup>3,4,5</sup>, Locoge N.<sup>3</sup>, Sauvage S.<sup>3</sup>, Leonardi T.<sup>3</sup>, Kukui A.<sup>6</sup>, Colomb A.<sup>7</sup>, Cazaunau M.<sup>8</sup>, Borbon A.<sup>8</sup>

(1) LSCE-CNRS-GEA-UVSQ, Gif sur Yvette, France (norazannoni@lsce.jpl.fr), (2) Department of Earth and Environmental Sciences, IISER, Mohali, Punjab, India, (3) Mines Douai, SAGE, F-59508 Douai, France, (4) School of Public and Environmental Affairs, Indiana University, Bloomington, IN, USA, (5) Univ Lille Nord de France, F-59000, Lille, France, (6) LPC2E, Orléans, France, (7) LaMP, Aubière, France, (8) ISA, CNRS-LUPEC-UPD, Orfèl, France

### 1. Total OH reactivity

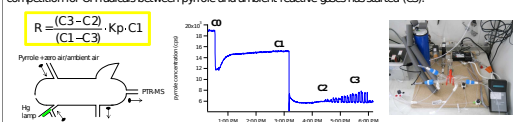
The hydroxyl radical reacts with most of the atmospheric species, and leads ultimately to the formation of ozone and Secondary Organic Aerosols which impact human health, air quality and climate [1]. Total OH reactivity is the total loss of OH due to atmospheric reactive gases. Measurements of total OH reactivity help to quantify the actual OH budget and the total loading of reactants in ambient air. Moreover, the comparison between total OH reactivity and the sum of reactivity obtained from gas phase measurements reveals whether unmeasured or unknown compounds are present in the atmosphere.

BVOCs are key compounds in atmospheric processes for their high abundance and high reactivity towards OH [2]. Previous studies highlighted the need to investigate OH reactivity processes close to biogenic sources.

In the following we show preliminary results of a measurement campaign run during three weeks (16/07/2013- 05/08/2013) in summer 2013 at a remote site in the Mediterranean basin, within the ChArMEx-CARBOSOR project. We measured the total OH reactivity with the Comparative Reactivity Method (CRM, [2,3,4]), and we compared the results with the calculated reactivity obtained from gas measurements run with complementary techniques.

### 2. Comparative Reactivity Method (CRM)

Pyrrrole is diluted in a glass flow reactor and its concentration is monitored with a PTR-MS after injection (C1), photolysis (C1), after OH radicals are artificially produced (C2) and when ambient air is sampled and the competition for OH radicals between pyrrrole and ambient reactive gases has started (C3).



### 3. ChArMEx-CARBOSOR campaign at Cape Corsica (42.97° N, 9.38° E, altitude 533 m)

Chemistry- Aerosols in a Mediterranean Experiment- Source and Reactivity of gaseous Organic Carbon (hydrocarbons, OVOC's of both anthropogenic and biogenic origin)



### 4. Preliminary Results

#### 4.1 Total OH reactivity

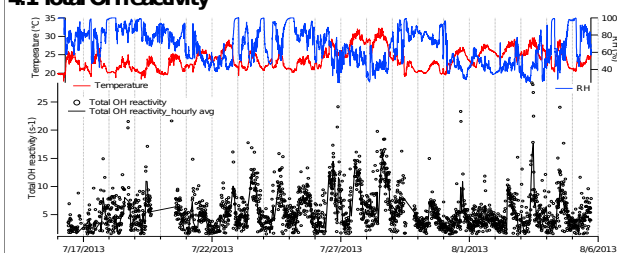
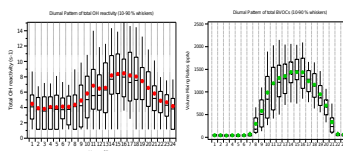


Figure 1, 2, 3. Time series of total OH reactivity, its diurnal pattern (upper left panel) and diurnal pattern of total measured BVOC's (upper right panel).



Measured total OH reactivity during the three weeks of campaign ranged from the method LOD ( $2-3 \text{ s}^{-1}$ ) to a maximum of  $20 \text{ s}^{-1}$ , on average  $\sim 5 \text{ s}^{-1}$ . Total OH reactivity shows a clear diurnal pattern. Diurnal pattern of total OH reactivity increased at 10 am and reached a maximum at 3 pm. It suggests that the largest contribution to the OH reactivity came from biogenics and photo-oxidation products. The profile agrees well with the total biogenics mixing ratio profiles (sum of m/z 69 and 137 from a PTR-MS).

#### 4.2 OH reactivity from gas-phase measurements and BVOCs impact

Reactivity from ancillary gas phase measurements at the same site is calculated as the sum of the products between concentration and rate constant of reaction of each measured species. Total OH reactivity measured and calculated are then compared and their difference corresponds to the missing fraction. We used backward trajectories and meteo data to investigate the missing fraction.

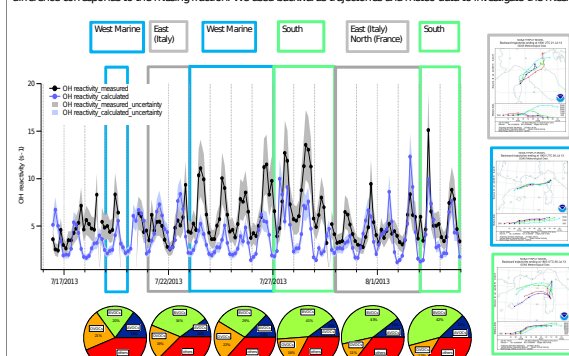


Figure 4. Measured vs calculated reactivity from gas phase measurements. Time series are classified according to air masses backtrajectories and pies indicate the relative contributions between BVOCs, OVOCs and others (NO<sub>x</sub> and CO).

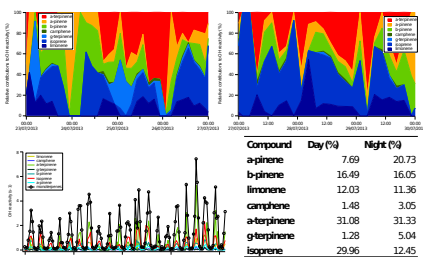


Figure 5a,b. 6. Relative contributions of reactivity among measured BVOCs during periods of highest missing reactivity; absolute reactivity values of BVOCs for the whole campaign. Values reported in the table refer to BVOCs contributions during the whole campaign.

BVOCs contribution to OH reactivity is high during the whole campaign (higher during the second part of the campaign due to higher temperature). This suggests that local vegetation and meteorological conditions had a large impact on the reactivity. Among the measured biogenic species, isoprene, alpha-terpinene and beta-pinene were the species contributing more to the reactivity.

### Conclusions

Total OH reactivity at Cape Corsica during 16/07/2013-05/08/2013 ranged between our instrument LOD and  $20 \text{ s}^{-1}$ , on average  $5 \text{ s}^{-1}$ . Correlations with gas phase measurements showed that BVOCs had a large impact on the OH reactivity and that during 23-30/07/2013 there was a significant missing reactivity. We believe that unmeasured monoterpenes and air masses enriched of OVOCs (longer processed air masses coming from west) can explain the missing fraction.

### Acknowledgments

This work is supported by the European Commission's 7th Framework Programme under Grant Agreement Number 287382, "PIMMS" project. CNRS, CEA, ChArMEx PRIMEQUAL-CARBOSOR are also acknowledged.

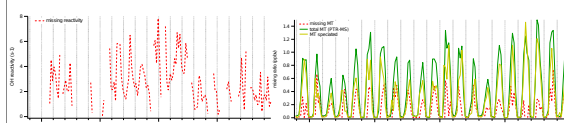


Figure 7, 8. Absolute missing reactivity and missing monoterpenes concentration from the difference between total monoterpenes (m/z 137 PTR-MS) and spated ones from sampling tubes.

- [1] Seinfeld and Pandis, Atmospheric Chemistry and Physics: From Air Pollution to Climate Change, Wiley, 2006.  
 [2] Atkinson and Arey, Gas-phase tropospheric chemistry of biogenic volatile organic compounds: a review, Atmos. Environ., 37, 5307-5210, 2003.  
 [3] Sinha et al., The Comparative Reactivity Method: a new tool to measure total OH reactivity in ambient air, Atmos. Chem. Phys., 8, 2213-2227, 2008.  
 [4] Doljopoury et al., Total OH reactivity measurements in Paris during the 2010 MEGACAP winter campaign, Atmos. Chem. Phys., 12, 9563-9612, 2012.  
 [5] Nölscher et al., Seasonal measurements of total OH reactivity fluxes, total ozone loss rates and missing emissions from Norway spruce in 2011, Biogeosciences, 10, 4241-4257, 2013.



Figure B.2: Poster presented at the Gordon Research Conference on Biogenic Hydrocarbons and the Atmosphere, Girona, Spain, July 2014.

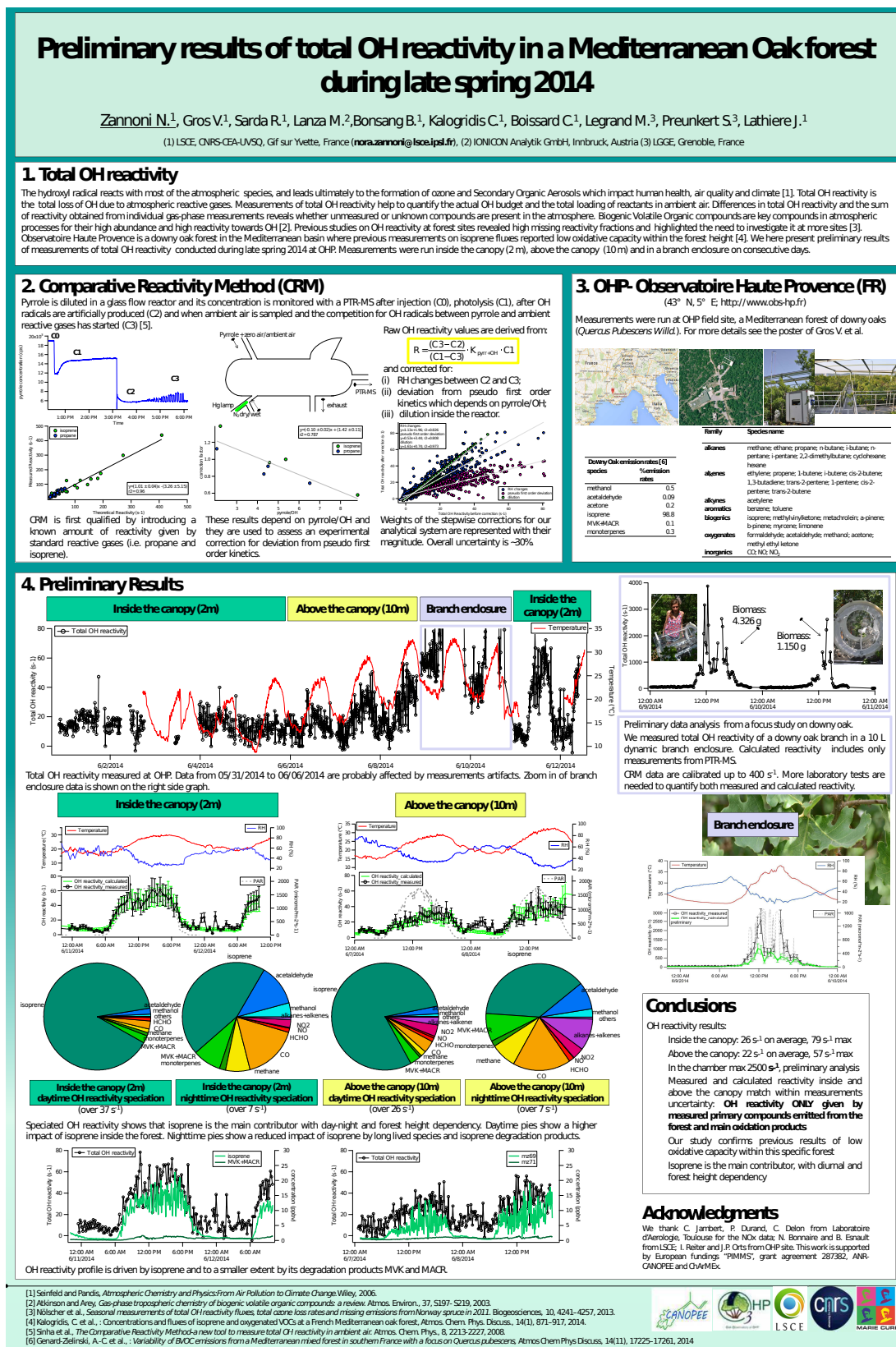


Figure B.3: Poster presented at International Global Atmospheric Chemistry Conference, Natal, Brazil, September 2014

# List of Tables

1.1	Global tropospheric NO <sub>x</sub> emissions . . . . .	5
1.2	Sources of anthropogenic VOCs . . . . .	7
1.3	Estimated global emissions of biogenic VOCs . . . . .	10
1.4	Atmospheric lifetimes of BVOCs . . . . .	12
1.5	Atmospheric lifetimes of AVOCs . . . . .	13
1.6	Performance of existing OH reactivity measuring methods . . . . .	19
1.7	Measured anthropogenic VOCs concentration during 2009 . . . . .	28
2.1	CRM comparison . . . . .	59
3.1	Technical parts and operational settings of CRM LSCE and CRM MD during the intercomparison exercise. . . . .	72
3.2	Summary of correction stages applied to raw reactivity data for CRM-LSCE and CRM-MD . . . . .	80
4.1	Measured species used for calculating OH reactivity. . . . .	98
4.2	Name and mass of VOCs included in the standard mixture used for calibrating the PTR-MS . . . . .	99
4.3	Volume mixing ratios inside and above the canopy of targeted molecules sampled with the PTR-MS. . . . .	104
5.1	Quality check controls run on the CRM . . . . .	122
5.2	Measured compounds and group of reference to indicate the compounds concentration . . . . .	124
5.3	Summary of the experimental methods deployed during the field work . . .	128

5.4	Air masses regime modeled with Hysplit . . . . .	131
5.5	Relative contributions of speciated BVOCs to the total calculated OH reactivity BVOCs fraction . . . . .	136
5.6	Sensitivity study of the model for a base case of modelled OH reactivity of $12 \text{ s}^{-1}$ . . . . .	144
A.1	Rate coefficients of reaction with OH for selected atmospheric compounds .	156

# List of Figures

1.1	IPCC total radiative forcing . . . . .	2
1.2	Chemical structures of some anthropogenic VOCs . . . . .	8
1.3	Tree's emissions . . . . .	8
1.4	Chemical structures of some biogenic VOCs . . . . .	9
1.5	Oxidation scheme of VOCs . . . . .	14
1.6	Carbon mass balance of BVOCs oxidation . . . . .	15
1.7	OH reactivity world map . . . . .	22
1.8	Monoterpenes and isoprene European emissions . . . . .	26
1.9	Mixing ratio of biogenic VOCs and estimated OH reactivity . . . . .	27
1.10	Concentration of ozone reduced due to emissions reduction . . . . .	29
2.1	Schematic of the Proton Transfer Reaction-Mass Spectrometer . . . . .	35
2.2	Example of experiment with the CRM instrument . . . . .	38
2.3	flow reactor in the CRM instrument . . . . .	40
2.4	Measured OH reactivity vs Calculated OH reactivity . . . . .	43
2.5	Pyrrrole signal measured by the PTR-MS . . . . .	45
2.6	Detailed empirical investigations on NO interference . . . . .	46
2.7	Weights of consecutive corrections applied to OH reactivity raw data . . . . .	48
2.8	Automatic alternated switches between C2 and C3 . . . . .	51
2.9	Linearity range of OH reactivity for CRM-LSCE . . . . .	54
2.10	Humidity dependency on the C2 level . . . . .	54
2.11	wef . . . . .	55

2.12	Correction factor . . . . .	55
2.13	ABCDFEF . . . . .	56
3.1	Pyrrole concentration detected by the PTR-MS during typical CRM OH reactivity test . . . . .	66
3.2	Linear least squares fit of $m/z$ 68 during C2 vs. $m_{37}/m_{19}$ . . . . .	70
3.3	Simplified not-to-scale schematic of CRM-LSCE . . . . .	71
3.4	Top view of the field site at Cape Corsica . . . . .	76
3.5	Comparison between C1 acquired with the OH scavenger approach and with the original approach . . . . .	77
3.6	Correction factor of reactivity for the kinetics regime . . . . .	81
3.7	Linear least squares fits of total OH reactivity measured by CRM-LSCE vs. Total OH reactivity measured by CRM-MD . . . . .	82
3.8	Time series of enclosure and ambient kOH . . . . .	85
4.1	Site of Observatoire de Haute Provence (OHP) in the European map . . . . .	94
4.2	Diurnal profile of $m/z$ 69, $m/z$ 71, HCHO, temperature and PAR . . . . .	103
4.3	Time series of $m/z$ 69 (isoprene), $m/z$ 71 (ISOP.OXs=MVK+MACR+ISOPOOH), HCHO and ISOP.OXs / isoprene . . . . .	104
4.4	Time series of $m/z$ 33, $m/z$ 45, $m/z$ 59, $m/z$ 73, $m/z$ 137 . . . . .	105
4.5	Total OH reactivity measured with CRM and calculated OH reactivity . . . . .	106
4.6	Total OH reactivity measured and OH reactivity calculated above the canopy . . . . .	107
4.7	Total OH reactivity speciation inside the canopy . . . . .	109
4.8	Total OH reactivity speciation above the canopy . . . . .	109
4.9	Total OH reactivity, calculated reactivity and ISOP.OXs / isoprene ratio at 2m height . . . . .	111
4.10	Total OH reactivity, calculated reactivity and ISOP.OXs / isoprene ratio at 10m height . . . . .	111
4.11	Total OH reactivity results from all the published experiments conducted worldwide at forested sites . . . . .	113
5.1	Location of Ersa windfarm field site . . . . .	121



---

5.2	Total OH reactivity profile measured at Ersa, Corsica, France . . . . .	132
5.3	Diurnal pattern of measured OH reactivity at Ersa . . . . .	133
5.4	Total biogenic volatile organic compounds volume mixing ratio measured at Ersa . . . . .	134
5.5	Total measured OH reactivity and calculated OH reactivity from the measured compounds in ambient air . . . . .	134
5.6	Daytime and nighttime contributions to the calculated OH reactivity . . .	135
5.7	Absolute OH reactivity calculated for the measured biogenic compounds at Ersa . . . . .	138
5.8	Total monoterpenes measured by PTR-MS compared to speciated monoterpenes measured off-line by GC-MS . . . . .	139
5.9	Calculated OH reactivity for different monoterpenes emitted by typical Mediterranean plants . . . . .	140
5.10	Ethyne and CO variability along the time of the field work . . . . .	141
5.11	Acetone and CO variability along the time of the field work. . . . .	141
5.12	Relative contributions to the calculated OH reactivity among the measured BVOCs . . . . .	142
5.13	Observed and imposed atmospheric mixing ratios for isoprene, sum of pinenes and camphene, sum of limonene and terpinenes . . . . .	143
5.14	Modelled OH reactivity contributions predicted from the atmospheric mixing ratio of the BVOCs measured during 28/07/2013. . . . .	146
B.1	EGU 2014 poster . . . . .	158
B.2	GRC 2014 poster . . . . .	159
B.3	IGAC 2014 poster . . . . .	160



# Bibliography

- [1] ACTRIS Measurement Guidelines VOC, WP4-NA4: Trace gases networking: Volatile organic carbon and nitrogen oxides Deliverable D4.1: Draft for standardized operating procedures (SOPs) for VOC measurements, [http://ebas-submit.nilu.no/Portals/117/media/SOPs/MG\\_VOC\\_draft\\_20120718.pdf](http://ebas-submit.nilu.no/Portals/117/media/SOPs/MG_VOC_draft_20120718.pdf), p:24-32, 2012
- [2] Ait-Helal, W., Borbon, A., Sauvage, S., de Gouw, J. A., Colomb, A., Gros, V., Freutel, F., Crippa, M., Afif, C., Baltensperger, U., Beekmann, M., Doussin, J.-F., Durand-Jolibois, R., Fronval, I., Grand, N., Leonardis, T., Lopez, M., Michoud, V., Miet, K., Perrier, S., Prévôt, A. S. H., Schneider, J., Siour, G., Zapf, P., and Locoge, N.: Volatile and intermediate volatility organic compounds in suburban Paris: variability, origin and importance for SOA formation, *Atmos. Chem. Phys.*, 14, 10439-10464, doi:10.5194/acp-14-10439-2014, 2014
- [3] Ammann, C., Brunner, A., Spirig, C., and Neftel, A.: Technical note: Water vapour concentration and flux measurements with PTR-MS, *Atmos. Chem. Phys.*, 6, 4643–4651, doi:10.5194/acp-6-4643-2006, 2006.
- [4] Archibald, A. T., Petit, A. S., Percival, C. J., Harvey, J. N., and Shallcross, D. E.: On the importance of the reaction between OH and RO<sub>2</sub> radicals, *Atmos. Sci. Lett.*, 10, 102–108, doi:10.1002/asl.216, 2009.
- [5] Atkinson, R., Aschmann, S. M., Winer, A. M., and Carter, W. P. L.: Rate constants for the gas phase reactions of OH radicals and O<sub>3</sub> with pyrrole at 295 ± 1 K and atmospheric pressure, *Atmos. Environ.*, 18, 2105–2107, doi:10.1016/0004-6981(84)90196-3, 1984.
- [6] Atkinson, R., Baulch, D. L., Cox, R. A., Crowley, J. N., Hampson, R. F., Hynes, R. G., Jenkin, M. E., Rossi, M. J., and Troe, J.: Evaluated kinetic and photochemical data for atmospheric chemistry: Volume III – gas phase reactions of inorganic halogens, *Atmos. Chem. Phys.*, 7, 981–1191, doi:10.5194/acp-7-981-2007, 2007.

- [7] Atkinson, R.: Kinetics and mechanisms of the gas-phase reactions of the hydroxyl radical with organic compounds under atmospheric conditions, *Chem. Rev.*, 86, 69–201, doi:10.1021/cr00071a004, 1986.
- [8] Atkinson, R.: Atmospheric chemistry of VOCs and NO<sub>x</sub>, *Atmos. Environ.*, 34, 2063–2101, doi:10.1016/S1352-2310(99)00460-4, 2000.
- [9] Atkinson, R. and Arey, J.: Atmospheric Chemistry of Biogenic Organic Compounds, *Acc. Chem. Res.*, 31, 574–583, doi:10.1021/ar970143z, 1998.
- [10] Atkinson, R. and Arey, J.: Gas-phase tropospheric chemistry of biogenic volatile organic compounds: a review, *Atmos. Environ.*, 37, 197–219, doi:10.1016/S1352-2310(03)00391-1, 2003.
- [11] Atkinson, R., Baulch, D. L., Cox, R. A., Hampson Jr., R. F., Kerr, J. A., Rossi, M. J., and Troe, J.: Evaluated Kinetic and Photochemical Data for Atmospheric Chemistry: Supplement VI. IUPAC Subcommittee on Gas Kinetic Data Evaluation for Atmospheric Chemistry, *J. Phys. Chem. Ref. Data*, 26, 1329–1499, doi:10.1063/1.556010, 1997.
- [12] Badol, C., Borbon, A., Locoge, N., Leonardis, T., Galloo, J.C.: An automated monitoring system for VOC ozone precursors in ambient air: development, implementation and data analysis. *Anal. Bioanal. Chem.*, 378, 7, 1815–1827, 2004
- [13] Baghi, R., Durand, P., Jambert, C., Jarnot, C., Delon, C., Serça, D., Striebig, N., Ferlicoq, M., and Keravec, P.: A new disjunct eddy-covariance system for BVOC flux measurements – validation on CO<sub>2</sub> and H<sub>2</sub>O fluxes, *Atmos. Meas. Tech.*, 5, 3119–3132, doi:10.5194/amt-5-3119-2012, 2012.
- [14] Berresheim, H., Plass-Dülmer, C., Elste, T., Mihalopoulos, N., and Rohrer, F.: OH in the coastal boundary layer of Crete during MINOS: Measurements and relationship with ozone photolysis, *Atmos. Chem. Phys.*, 3, 639–649, doi:10.5194/acp-3-639-2003, 2003.
- [15] Blake, Robert S., Monks, Paul S., and Ellis Andrew M.: Proton-Transfer Reaction Mass Spectrometry, *Chemical Reviews*, 109 (3), 861–896 DOI: 10.1021/cr800364q, 2009.
- [16] Bonsang, B., Polle, C., and Lambert, G.: Evidence for marine production of isoprene, *Geophys. Res. Lett.*, 19, 1129–1132, doi:10.1029/92GL00083, 1992.

- [17] Bracho-Nunez, A., Welter, S., Staudt, M., and Kesselmeier, J.: Plant-specific volatile organic compound emission rates from young and mature leaves of Mediterranean vegetation, *J. Geophys. Res.-Atmos.*, 116, D16304, doi:10.1029/2010JD015521, 2011.
- [18] Calpini, B., Jeanneret, F., Bourqui, M., Clappier, A., Vajtai, R., and van den Bergh, H.: Direct measurement of the total reaction rate of OH in the atmosphere, *Analisis*, 27, 328–336, doi:10.1051/analisis:1999270328, 1999.
- [19] Cazorla, M. and Brune, W. H.: Measurement of Ozone Production Sensor, *Atmos Meas Tech*, 3(3), 545–555, doi:10.5194/amt-3-545-2010, 2010.
- [20] Claeys, M., Graham, B., Vas, G., Wang, W., Vermeylen, R., Pashynska, V., Cafmeyer, J., Guyon, P., Andreae, M. O., Artaxo, P., and Maenhaut, W.: Formation of Secondary Organic Aerosols Through Photooxidation of Isoprene, *Science*, 303, 1173–1176, doi:10.1126/science.1092805, 2004.
- [21] Dasgupta, P. K., Dong, S., Hwang, H., Yang, H.-C., and Genfa, Z.: Continuous liquid-phase fluorometry coupled to a diffusion scrubber for the real-time determination of atmospheric formaldehyde, hydrogen peroxide and sulfur dioxide, *Atmos. Environ.* 1967, 22, 949–963, doi:10.1016/0004-6981(88)90273-9, 1988.
- [22] Davison, B., Taipale, R., Langford, B., Misztal, P., Fares, S., Matteucci, G., Loreto, F., Cape, J. N., Rinne, J., and Hewitt, C. N.: Concentrations and fluxes of biogenic volatile organic compounds above a Mediterranean macchia ecosystem in western Italy, *Biogeosciences*, 6, 1655-1670, doi:10.5194/bg-6-1655-2009, 2009.
- [23] De Gouw, J. and Warneke, C.: Measurements of volatile organic compounds in the earth's atmosphere using proton-transfer-reaction mass spectrometry, *Mass Spectrom. Rev.*, 26, 223–257, doi:10.1002/mas.20119, 2007.
- [24] Detournay, A., Sauvage, S., Locoge, N., Gaudion, V., Leonardis, T., Fronval, I., Kaluzny, P., and Galloo, J.-C.: Development of a sampling method for the simultaneous monitoring of straightchain alkanes, straight-chain saturated carbonyl compounds and monoterpenes in remote areas. *J. Environ. Monitor.*, 13, 983–990, 2011.
- [25] Di Carlo, P. D., Brune, W. H., Martinez, M., Harder, H., Leshner, R., Ren, X., Thornberry, T., Carroll, M. A., Young, V., Shepson, P. B., Riemer, D., Apel, E., and Campbell, C.: Missing OH Reactivity in a Forest: Evidence for Unknown Reactive Biogenic VOCs, *Science*, 304, 722–725, doi:10.1126/science.1094392, 2004.

- [26] Dillon, T. J., Tucceri, M. E., Dulitz, K., Horowitz, A., Vereecken, L., and Crowley, J. N.: Reaction of Hydroxyl Radicals with C<sub>4</sub>H<sub>5</sub>N (Pyrrole): Temperature and Pressure Dependent Rate Coefficients, *J. Phys. Chem. A*, 116, 6051–6058, doi:10.1021/jp211241x, 2012.
- [27] Dolgorouky, C., Gros, V., Sarda-Esteve, R., Sinha, V., Williams, J., Marchand, N., Sauvage, S., Poulain, L., Sciare, J., and Bonsang, B.: Total OH reactivity measurements in Paris during the 2010 MEGAPOLI winter campaign, *Atmos. Chem. Phys.*, 12, 9593–9612, doi:10.5194/acp-12-9593-2012, 2012.
- [28] Draxler, R.R. and Rolph, G.D. HYSPLIT (HYbrid Single-Particle Lagrangian Integrated Trajectory) Model access via NOAA ARL READY Website (<http://www.arl.noaa.gov/HYSPLIT.php>). NOAA Air Resources Laboratory, College Park, MD.
- [29] Dusanter, S., Vimal, D., Stevens, P. S., Volkamer, R., and Molina, L. T.: Measurements of OH and HO<sub>2</sub> concentrations during the MCMA-2006 field campaign – Part 1: Deployment of the Indiana University laser-induced fluorescence instrument, *Atmos. Chem. Phys.*, 9, 1665–1685, doi:10.5194/acp-9-1665-2009, 2009.
- [30] Edwards, P. M., Evans, M. J., Furneaux, K. L., Hopkins, J., Ingham, T., Jones, C., Lee, J. D., Lewis, A. C., Moller, S. J., Stone, D., Whalley, L. K., and Heard, D. E.: OH reactivity in a South East Asian tropical rainforest during the Oxidant and Particle Photochemical Processes (OP3) project, *Atmos. Chem. Phys.*, 13, 9497–9514, doi:10.5194/acp-13-9497-2013, 2013.
- [31] Eichler, P., Müller, M., D’Anna, B., and Wisthaler, A.: A novel inlet system for online chemical analysis of semi-volatile submicron particulate matter, *Atmos. Meas. Tech.*, 8, 1353–1360, doi:10.5194/amt-8-1353-2015, 2015.
- [32] Fall R.: (1999) Biogenic emissions of VOCs from higher plants. In: *Reactive Hydrocarbons in the Atmosphere*, C.N. Hewitt (ed.), pp. 43–96, Academic Press, San Diego.
- [33] Faloon, I. C., Tan, D., Leshner, R. L., Hazen, N. L., Frame, C. L., Simpas, J. B., Harder, H., Martinez, M., Carlo, P. D., Ren, X., and Brune, W. H.: A Laser-induced Fluorescence Instrument for Detecting Tropospheric OH and HO<sub>2</sub>: Characteristics and Calibration, *J. Atmos. Chem.*, 47, 139–167, doi:10.1023/B:JOCH.0000021036.53185.0e, 2004.

- [34] Fittschen, C., Whalley, L. K., and Heard, D. E.: The Reaction of CH<sub>3</sub>O<sub>2</sub> Radicals with OH Radicals: A Neglected Sink for CH<sub>3</sub>O<sub>2</sub> in the Remote Atmosphere, *Environ. Sci. Technol.*, 48, 7700–7701, doi:10.1021/es502481q, 2014.
- [35] Fuchs, H., Hofzumahaus, A., Rohrer, F., Bohn, B., Brauers, T., Dorn, H.-P., Häsel, R., Holland, F., Kaminski, M., Li, X., Lu, K., Nehr, S., Tillmann, R., Wegener, R., and Wahner, A.: Experimental evidence for efficient hydroxyl radical regeneration in isoprene oxidation, *Nat. Geosci.*, 6, 1023–1026, doi:10.1038/ngeo1964, 2013.
- [36] Fuentes, J. D., Gu, L., Lerdau, M., Atkinson, R., Baldocchi, D., Bottenheim, J. W., Ciccioli, P., Lamb, B., Geron, C., Guenther, A., Sharkey, T. D., and Stockwell, W.: Biogenic Hydrocarbons in the Atmospheric Boundary Layer: A Review, *B. Am. Meteorol. Soc.*, 81, 1537–1575, doi:10.1175/1520-0477(2000)081<1537:BHITAB>2.3.CO;2, 2000.
- [37] Genard-Zielinski, A.-C., Boissard, C., Fernandez, C., Kalogridis, C., Lathièrre, J., Gros, V., Bonnaire, N., and Ormeño, E.: Variability of BVOC emissions from a Mediterranean mixed forest in southern France with a focus on *Quercus pubescens*, *Atmos. Chem. Phys.*, 15, 431–446, doi:10.5194/acp-15-431-2015, 2015.
- [38] Giorgi, F.: Climate change hot-spots, *Geophys. Res. Lett.*, 33, L08707, doi:10.1029/2006GL025734, 2006.
- [39] Giorgi, F. and Lionello, P.: Climate change projections for the Mediterranean region, *Glob. Planet. Change*, 63, 90–104, doi:10.1016/j.gloplacha.2007.09.005, 2008.
- [40] Giorgi, F., Im, E.-S., Coppola, E., Diffenbaugh, N. S., Gao, X. J., Mariotti, L., and Shi, Y.: Higher Hydroclimatic Intensity with Global Warming, *J. Clim.*, 24, 5309–5324, doi:10.1175/2011JCLI3979.1, 2011.
- [41] Goldstein, A. H. and Galbally, I. E.: Known and Unexplored Organic Constituents in the Earth's Atmosphere, *Environ. Sci. Technol.*, 41, 1514–1521, doi:10.1021/es072476p, 2007.
- [42] Guenther, A., Hewitt, C. N., Erickson, D., Fall, R., Geron, C., Graedel, T., Harley, P., Klinger, L., Lerdau, M., McKay, W. A., Pierce, T., Scholes, B., Steinbrecher, R., Tallamraju, R., Taylor, J., and Zimmerman, P.: A global model of natural volatile organic compound emissions, *J. Geophys. Res.-Atmos.*, 100, 8873–8892, doi:10.1029/94JD02950, 1995.

- [43] Guenther, A., Karl, T., Harley, P., Wiedinmyer, C., Palmer, P. I., and Geron, C.: Estimates of global terrestrial isoprene emissions using MEGAN (Model of Emissions of Gases and Aerosols from Nature), *Atmos. Chem. Phys.*, 6, 3181–3210, doi:10.5194/acp-6-3181-2006, 2006.
- [44] Guenther, A. B., Jiang, X., Heald, C. L., Sakulyanontvittaya, T., Duhl, T., Emmons, L. K. and Wang, X.: The Model of Emissions of Gases and Aerosols from Nature version 2.1 (MEGAN2.1): an extended and updated framework for modeling biogenic emissions, *Geosci Model Dev*, 5(6), 1471–1492, doi:10.5194/gmd-5-1471-2012, 2012.
- [45] Hansen, R. F., Griffith, S. M., Dusanter, S., Rickly, P. S., Stevens, P. S., Bertman, S. B., Carroll, M. A., Erickson, M. H., Flynn, J. H., Grossberg, N., Jobson, B. T., Lefer, B. L., and Wallace, H. W.: Measurements of total hydroxyl radical reactivity during CABINEX 2009 – Part 1: field measurements, *Atmos. Chem. Phys.*, 14, 2923–2937, doi:10.5194/acp-14-2923-2014, 2014.
- [46] Hansen, R. F., Blocquet, M., Schoemaeker, C., Léonardis, T., Locoge, N., Fittschen, C., Hanoune, B., Stevens, P. S., Sinha, V., and Dusanter, S.: Intercomparison of the comparative reactivity method (CRM) and pump-probe technique for measuring total OH reactivity in an urban environment, *Atmos. Meas. Tech. Discuss.*, 8, 6119–6178, doi:10.5194/amtd-8-6119-2015, 2015.
- [47] Hens, K., Novelli, A., Martinez, M., Auld, J., Axinte, R., Bohn, B., Fischer, H., Keronen, P., Kubistin, D., Nölscher, A. C., Oswald, R., Paasonen, P., Petäjä, T., Regelin, E., Sander, R., Sinha, V., Sipilä, M., Taraborrelli, D., Tatum Ernest, C., Williams, J., Lelieveld, J., and Harder, H.: Observation and modelling of HO<sub>x</sub> radicals in a boreal forest, *Atmos. Chem. Phys.*, 14, 8723–8747, doi:10.5194/acp-14-8723-2014, 2014.
- [48] Hirsch, A. I., Munger, J. W., Jacob, D. J., Horowitz, L. W., and Goldstein, A. H.: Seasonal variation of the ozone production efficiency per unit NO<sub>x</sub> at Harvard Forest, Massachusetts, *J. Geophys. Res.-Atmos.*, 101, 12659–12666, doi:10.1029/96JD00557, 1996.
- [49] Holzinger, R., Sanhueza, E., von Kuhlmann, R., Kleiss, B., Donoso, L., and Crutzen, P. J.: Diurnal cycles and seasonal variation of isoprene and its oxidation products in the tropical savanna atmosphere, *Glob. Biogeochem. Cy.*, 16, 1074, doi:10.1029/2001GB001421, 2002.



- [50] Holzinger, R., Lee, A., Paw, K. T., and Goldstein, U. A. H.: Observations of oxidation products above a forest imply biogenic emissions of very reactive compounds, *Atmos. Chem. Phys.*, 5, 67–75, doi:10.5194/acp-5-67-2005, 2005.
- [51] Holzinger, R., Williams, J., Herrmann, F., Lelieveld, J., Donahue, N. M., and Röckmann, T.: Aerosol analysis using a Thermal-Desorption Proton-Transfer-Reaction Mass Spectrometer (TD-PTR-MS): a new approach to study processing of organic aerosols, *Atmos. Chem. Phys.*, 10, 2257-2267, doi:10.5194/acp-10-2257-2010, 2010.
- [52] Hofzumahaus, A., Rohrer, F., Lu, K., Bohn, B., Brauers, T., Chang, C.-C., Fuchs, H., Holland, F., Kita, K., Kondo, Y., Li, X., Lou, S., Shao, M., Zeng, L., Wahner, A., and Zhang, Y.: Amplified Trace Gas Removal in the Troposphere, *Science*, 324, 1702–1704, doi:10.1126/science.1164566, 2009.
- [53] Ingham, T., Goddard, A., Whalley, L. K., Furneaux, K. L., Edwards, P. M., Seal, C. P., Self, D. E., Johnson, G. P., Read, K. A., Lee, J. D., and Heard, D. E.: A flow-tube based laser-induced fluorescence instrument to measure OH reactivity in the troposphere, *Atmos. Meas. Tech.*, 2, 465–477, doi:10.5194/amt-2-465-2009, 2009.
- [54] IPCC, 2013: Climate Change 2013: The Physical Science Basis. Contribution of Working Group I to the Fifth Assessment Report of the Intergovernmental Panel on Climate Change [Stocker, T.F., D. Qin, G.-K. Plattner, M. Tignor, S.K. Allen, J. Boschung, A. Nauels, Y. Xia, V. Bex and P.M. Midgley (eds.)]. Cambridge University Press, Cambridge, United Kingdom and New York, NY, USA, 1535 pp, doi:10.1017/CBO9781107415324
- [55] Jacob, D. J., Field, B. D., Jin, E. M., Bey, I., Li, Q., Logan, J. A., Yantosca, R. M., and Singh, H. B.: Atmospheric budget of acetone, *J. Geophys. Res.-Atmos.*, 107, ACH 5–1, doi:10.1029/2001JD000694, 2002.
- [56] Jacob, D. J., Field, B. D., Li, Q., Blake, D. R., de Gouw, J., Warneke, C., Hansel, A., Wisthaler, A., Singh, H. B., and Guenther, A.: Global budget of methanol: Constraints from atmospheric observations, *J. Geophys. Res.-Atmos.*, 110, D08303, doi:10.1029/2004JD005172, 2005.
- [57] Jeanneret, F., Kirchner, F., Clappier, A., van den Bergh, H., and Calpini, B.: Total VOC reactivity in the planetary boundary layer: 1. Estimation by a pump and probe OH experiment, *J. Geophys. Res.-Atmos.*, 106, 3083–3093, doi:10.1029/2000JD900602, 2001.

- [58] Jenkin, M. E., Boyd, A. A., and Lesclaux, R.: Peroxy Radical Kinetics Resulting from the OH-Initiated Oxidation of 1,3-Butadiene, 2,3-Dimethyl-1,3-Butadiene and Isoprene, *J. Atmos. Chem.*, 29, 267–298, doi:10.1023/A:1005940332441, 1998.
- [59] Jud, W., Fischer, L., Canaval, E., Wohlfahrt, G., Tissier, A., and Hansel, A.: Plant surface reactions: an ozone defence mechanism impacting atmospheric chemistry, *Atmos. Chem. Phys. Discuss.*, 15, 19873–19902, doi:10.5194/acpd-15-19873-2015, 2015.
- [60] Junkermann, W.: On the distribution of formaldehyde in the western Po-Valley, Italy, during FORMAT 2002/2003, *Atmospheric Chem. Phys.*, 9(23), 9187–9196, 2009.
- [61] Kalogridis, C., Gros, V., Sarda-Esteve, R., Langford, B., Loubet, B., Bonsang, B., Bonnaire, N., Nemitz, E., Genard, A.-C., Boissard, C., Fernandez, C., Ormeño, E., Baisnée, D., Reiter, I., and Lathièrre, J.: Concentrations and fluxes of isoprene and oxygenated VOCs at a French Mediterranean oak forest, *Atmos. Chem. Phys.*, 14, 10085–10102, doi:10.5194/acp-14-10085-2014, 2014.
- [62] Kang, E., Root, M. J., Toohey, D. W. and Brune, W. H.: Introducing the concept of Potential Aerosol Mass (PAM), *Atmos Chem Phys*, 7(22), 5727–5744, doi:10.5194/acp-7-5727-2007, 2007.
- [63] Karl, T., Harley, P., Guenther, A., Rasmussen, R., Baker, B., Jardine, K., and Nemitz, E.: The bi-directional exchange of oxygenated VOCs between a loblolly pine (*Pinus taeda*) plantation and the atmosphere, *Atmos. Chem. Phys.*, 5, 3015–3031, doi:10.5194/acp-5-3015-2005, 2005.
- [64] Karl, T., Guenther, A., Yokelson, R. J., Greenberg, J., Potosnak, M., Blake, D. R., and Artaxo, P.: The tropical forest and fire emissions experiment: Emission, chemistry, and transport of biogenic volatile organic compounds in the lower atmosphere over Amazonia, *J. Geophys. Res.-Atmos.*, 112, D18302, doi:10.1029/2007JD008539, 2007.
- [65] Karl, T., Apel, E., Hodzic, A., Riemer, D. D., Blake, D. R., and Wiedinmyer, C.: Emissions of volatile organic compounds inferred from airborne flux measurements over a megacity, *Atmos. Chem. Phys.*, 9, 271–285, doi:10.5194/acp-9-271-2009, 2009.
- [66] Kesselmeier, J., Bode, K., Schäfer, L., Schebeske, G., Wolf, A., Brancaleoni, E., Cecinato, A., Ciccioli, P., Frattoni, M., Dutaur, L., Fugit, J. L., Simon, V., and Torres, L.: Simultaneous field measurements of terpene and isoprene emissions from two dominant mediterranean oak species in relation to a North American species, *Atmos. Environ.*, 32, 1947–1953, doi:10.1016/S1352-2310(97)00500-1, 1998.

- [67] Kesselmeier, J. and Staudt, M.: Biogenic Volatile Organic Compounds (VOC): An Overview on Emission, Physiology and Ecology, *J. Atmos. Chem.*, **33**, 23–88, doi:10.1023/A:1006127516791, 1999.
- [68] Kesselmeier, J., Ciccioli, P., Kuhn, U., Stefani, P., Biesenthal, T., Rottenberger, S., Wolf, A., Vitullo, M., Valentini, R., Nobre, A., Kabat, P., and Andreae, M. O.: Volatile organic compound emissions in relation to plant carbon fixation and the terrestrial carbon budget, *Global Biogeochem. Cycles*, **16**, 73-1–73-9, doi:10.1029/2001GB001813, 2002a.
- [69] Kim, S., Guenther, A., Karl, T., and Greenberg, J.: Contributions of primary and secondary biogenic VOC to total OH reactivity during the CABINEX (Community Atmosphere-Biosphere Interactions Experiments)-09 field campaign, *Atmos. Chem. Phys.*, **11**, 8613–8623, doi:10.5194/acp-11-8613-2011, 2011.
- [70] Kovacs, T. A. and Brune, W. H.: Total OH Loss Rate Measurement, *J. Atmos. Chem.*, **39**, 105–122, doi:10.1023/A:1010614113786, 2001.
- [71] Kumar, V. and Sinha, V.: VOC–OHM: A new technique for rapid measurements of ambient total OH reactivity and volatile organic compounds using a single proton transfer reaction mass spectrometer, *Int. J. Mass Spectrom.*, **374**, 55–63, doi:10.1016/j.ijms.2014.10.012, 2014.
- [72] Laohawornkitkul, J., Taylor, J. E., Paul, N. D., and Hewitt, C. N.: Biogenic volatile organic compounds in the Earth system, *New Phytol.*, **183**, 27–51, doi:10.1111/j.1469-8137.2009.02859.x, 2009.
- [73] Lappalainen, H. K., Sevanto, S., Bäck, J., Ruuskanen, T. M., Kolari, P., Taipale, R., Rinne, J., Kulmala, M., and Hari, P.: Day-time concentrations of biogenic volatile organic compounds in a boreal forest canopy and their relation to environmental and biological factors, *Atmos. Chem. Phys.*, **9**, 5447–5459, doi:10.5194/acp-9-5447-2009, 2009.
- [74] Lee, J., Young, J., Read, K., Hamilton, J., Hopkins, J., Lewis, A., Bandy, B., Davey, J., Edwards, P., Ingham, T., Self, D., Smith, S., Pilling, M., and Heard, D.: Measurement and calculation of OH reactivity at a United Kingdom coastal site, *J. Atmos. Chem.*, **64**, 53–76, doi:10.1007/s10874-010-9171-0, 2009.
- [75] Lelieveld, J.: Global Air Pollution Crossroads over the Mediterranean, *Science*, **298**(5594), 794–799, doi:10.1126/science.1075457, 2002.

- [76] Lindinger, W. and Jordan, A.: Proton-transfer-reaction mass spectrometry (PTR-MS): on-line monitoring of volatile organic compounds at pptv levels, *Chem. Soc. Rev.*, 27, 347–375, doi:10.1039/A827347Z, 1998.
- [77] Liu, Y. J., Herdinger-Blatt, I., McKinney, K. A., and Martin, S. T.: Production of methyl vinyl ketone and methacrolein via the hydroperoxyl pathway of isoprene oxidation, *Atmos. Chem. Phys.*, 13, 5715–5730, doi:10.5194/acp-13-5715-2013, 2013.
- [78] Lou, S., Holland, F., Rohrer, F., Lu, K., Bohn, B., Brauers, T., Chang, C.C., Fuchs, H., Häsel, R., Kita, K., Kondo, Y., Li, X., Shao, M., Zeng, L., Wahner, A., Zhang, Y., Wang, W., and Hofzumahaus, A.: Atmospheric OH reactivities in the Pearl River Delta – China in summer 2006: measurement and model results, *Atmos. Chem. Phys.*, 10, 11243–11260, doi:10.5194/acp-10-11243-2010, 2010.
- [79] Lu, K. D., Hofzumahaus, A., Holland, F., Bohn, B., Brauers, T., Fuchs, H., Hu, M., Häsel, R., Kita, K., Kondo, Y., Li, X., Lou, S. R., Oebel, A., Shao, M., Zeng, L. M., Wahner, A., Zhu, T., Zhang, Y. H., and Rohrer, F.: Missing OH source in a suburban environment near Beijing: observed and modelled OH and HO<sub>2</sub> concentrations in summer 2006, *Atmos. Chem. Phys.*, 13, 1057–1080, doi:10.5194/acp-13-1057-2013, 2013.
- [80] Mao, J., Ren, X., Brune, W. H., Olson, J. R., Crawford, J. H., Fried, A., Huey, L. G., Cohen, R. C., Heikes, B., Singh, H. B., Blake, D. R., Sachse, G. W., Diskin, G. S., Hall, S. R., and Shetter, R. E.: Airborne measurement of OH reactivity during INTEX-B, *Atmos. Chem. Phys.*, 9, 163–173, doi:10.5194/acp-9-163-2009, 2009.
- [81] Mao, J., Ren, X., Zhang, L., Van Duin, D. M., Cohen, R. C., Park, J.-H., Goldstein, A. H., Paulot, F., Beaver, M. R., Crouse, J. D., Wennberg, P. O., DiGangi, J. P., Henry, S. B., Keutsch, F. N., Park, C., Schade, G. W., Wolfe, G. M., Thornton, J. A., and Brune, W. H.: Insights into hydroxyl measurements and atmospheric oxidation in a California forest, *Atmos. Chem. Phys.*, 12, 8009–8020, doi:10.5194/acp-12-8009-2012, 2012.
- [82] Martinez, M., Harder, H., Kovacs, T. A., Simpas, J. B., Bassis, J., Leshner, R., Brune, W. H., Frost, G. J., Williams, E. J., Stroud, C. A., Jobson, B. T., Roberts, J. M., Hall, S. R., Shetter, R. E., Wert, B., Fried, A., Alicke, B., Stutz, J., Young, V. L., White, A. B., and Zamora, R. J.: OH and HO<sub>2</sub> concentrations, sources, and loss rates during the Southern Oxidants Study in Nashville, Tennessee, summer 1999, *J. Geophys. Res.*, 108, 4617, , doi:10.1029/2003JD003551, 2003.

- [83] Mellouki, A. and Ravishankara, A. R.: Regional Climate Variability and its Impacts in the Mediterranean Area, Springer Science & Business Media., 2007.
- [84] Menut, L., Mailler, S., Siour, G., Bessagnet, B., Turquety, S., Rea, G., Briant, R., Mallet, M., Sciare, J., Formenti, P., and Meleux, F.: Ozone and aerosol tropospheric concentrations variability analyzed using the ADRIMED measurements and the WRF and CHIMERE models, *Atmos. Chem. Phys.*, 15, 6159-6182, doi:10.5194/acp-15-6159-2015, 2015.
- [85] Messina, P., J. Lathière, D. Hauglustaine, K. Sindelarova, N. Vuichard, N. Viovy, S. Szopa, A. Cozic, J. Ghattas, "Biogenic volatile organic compound emissions in ORCHIDEE: future evolution and impact on atmospheric composition", ÉCLAIRE Open Science Conference: Integrating Impacts of Air Pollution and Climate Change on Ecosystems, 1st-2nd October 2014, Budapest, Hungary
- [86] Michoud, V., Hansen, R. F., Locoge, N., Stevens, P. S., and Dusanter, S.: Detailed characterizations of the new Mines Douai comparative reactivity method instrument via laboratory experiments and modeling, *Atmos. Meas. Tech.*, 8, 3537–3553, doi:10.5194/amt-8-3537-2015, 2015.
- [87] Middleton P., 1995: Sources of air pollutants. In Singh, H. B. (ed.) *Composition Chemistry, and Climate of the Atmosphere*. John Wiley & Sons, Inc., USA
- [88] Millet, D. B., Guenther, A., Siegel, D. A., Nelson, N. B., Singh, H. B., de Gouw, J. A., Warneke, C., Williams, J., Eerdekens, G., Sinha, V., Karl, T., Flocke, F., Apel, E., Riemer, D. D., Palmer, P. I., and Barkley, M.: Global atmospheric budget of acetaldehyde: 3-D model analysis and constraints from in-situ and satellite observations, *Atmos. Chem. Phys.*, 10, 3405–3425, doi:10.5194/acp-10-3405-2010, 2010.
- [89] Mochizuki, T., Miyazaki, Y., Ono, K., Wada, R., Takahashi, Y., Saigusa, N., Kawamura, K., and Tani, A.: Emissions of biogenic volatile organic compounds and subsequent formation of secondary organic aerosols in a *Larix kaempferi* forest, *Atmos. Chem. Phys. Discuss.*, 15, 10739-10771, doi:10.5194/acpd-15-10739-2015, 2015.
- [90] Mogensen, D., Smolander, S., Sogachev, A., Zhou, L., Sinha, V., Guenther, A., Williams, J., Nieminen, T., Kajos, M. K., Rinne, J., Kulmala, M., and Boy, M.: Modelling atmospheric OH-reactivity in a boreal forest ecosystem, *Atmos. Chem. Phys.*, 11, 9709–9719, doi:10.5194/acp-11-9709-2011, 2011.
- [91] Mogensen, D., Gierens, R., Crowley, J. N., Keronen, P., Smolander, S., Sogachev, A., Nölscher, A. C., Zhou, L., Kulmala, M., Tang, M. J., Williams, J. and Boy, M.:

- Simulations of atmospheric OH, O<sub>3</sub> and NO<sub>3</sub> reactivities within and above the boreal forest, *Atmos Chem Phys*, 15(7), 3909–3932, doi:10.5194/acp-15-3909-2015, 2015.
- [92] Nakashima, Y., Tsurumaru, H., Imamura, T., Bejan, I., Wenger, J. C., and Kajii, Y.: Total OH reactivity measurements in laboratory studies of the photooxidation of isoprene, *Atmos. Environ.*, 62, 243–247, doi:10.1016/j.atmosenv.2012.08.033, 2012.
- [93] Nakashima, Y., Kato, S., Greenberg, J., Harley, P., Karl, T., Turnipseed, A., Apel, E., Guenther, A., Smith, J., and Kajii, Y.: Total OH reactivity measurements in ambient air in a southern Rocky mountain ponderosa pine forest during BEACHON-SRM08 summer campaign, *Atmos. Environ.*, 85, 1–8, doi:10.1016/j.atmosenv.2013.11.042, 2014.
- [94] Nash, T.: The colorimetric estimation of formaldehyde by means of the Hantzsch reaction, *Biochem. J.*, 55(3), 416–421, 1953.
- [95] Nölscher, A. C., Sinha, V., Bockisch, S., Klüpfel, T., and Williams, J.: Total OH reactivity measurements using a new fast Gas Chromatographic Photo-Ionization Detector (GC-PID), *Atmos. Meas. Tech.*, 5, 2981–2992, doi:10.5194/amt-5-2981-2012, 2012a.
- [96] Nölscher, A. C., Williams, J., Sinha, V., Custer, T., Song, W., Johnson, A. M., Axinte, R., Bozem, H., Fischer, H., Pouvesle, N., Phillips, G., Crowley, J. N., Rantala, P., Rinne, J., Kulmala, M., Gonzales, D., Valverde-Canossa, J., Vogel, A., Hoffmann, T., Ouwersloot, H. G., Vilà-Guerau de Arellano, J., and Lelieveld, J.: Summertime total OH reactivity measurements from boreal forest during HUMPPA-COPEC 2010, *Atmos. Chem. Phys.*, 12, 8257–8270, doi:10.5194/acp-12-8257-2012, 2012b.
- [97] Nölscher, A. C., Bourtsoukidis, E., Bonn, B., Kesselmeier, J., Lelieveld, J., and Williams, J.: Seasonal measurements of total OH reactivity emission rates from Norway spruce in 2011, *Biogeosciences*, 10, 4241–4257, doi:10.5194/bg-10-4241-2013, 2013.
- [98] Nölscher, A. C., Butler, T., Auld, J., Veres, P., Muñoz, A., Taraborrelli, D., Vereecken, L., Lelieveld, J., and Williams, J.: Using total OH reactivity to assess isoprene photooxidation via measurement and model, *Atmos. Environ.*, 89, 453–463, doi:10.1016/j.atmosenv.2014.02.024, 2014.
- [99] Ormeño E., Fernandez C., Mévy J.P.: Plant coexistence alters terpene emission and content of Mediterranean species, *Phytochemistry*, 68(6):840-52, 2007.
- [100] Owen SM, Boissard C, Hewitt CN. Volatile organic compounds (VOCs) emitted from 40 Mediterranean plant species: VOC speciation and extrapolation to habitat scale. *Atmospheric Environment*. 35(32):5393-5409, 10.1016/S1352-2310(01)00302-8, 2001.

- [101] Paulson, S. E., Chung, M. Y., and Hasson, A. S.: OH Radical Formation from the Gas-Phase Reaction of Ozone with Terminal Alkenes and the Relationship between Structure and Mechanism, *J. Phys. Chem. A*, 103, 8125–8138, doi:10.1021/jp991995e, 1999.
- [102] Preunkert, S. and Legrand, M.: Towards a quasi-complete reconstruction of past atmospheric aerosol load and composition (organic and inorganic) over Europe since 1920 inferred from Alpine ice cores, *Clim. Past*, 9, 1403–1416, doi:10.5194/cp-9-1403-2013, 2013.
- [103] Preunkert, S., Legrand, M., Frey, M. M., Kukui, A., Savarino, J., Gallée, H., King, M., Jourdain, B., Vicars, W., and Helmig, D.: Formaldehyde (HCHO) in air, snow, and interstitial air at Concordia (East Antarctic Plateau) in summer, *Atmos. Chem. Phys.*, 15, 6689–6705, doi:10.5194/acp-15-6689-2015, 2015.
- [104] PTR-TOF community wiki, <https://sites.google.com/site/ptrtof/home>, last access 27/09/2015
- [105] Rainer Steinbrecher, G. S.: Intra- and inter-annual variability of VOC emissions from natural and semi-natural vegetation in Europe and neighbouring countries, *Atmos. Environ.*, 7, 1380–1391, doi:10.1016/j.atmosenv.2008.09.072, 2009.
- [106] Ren, X.: HO<sub>x</sub> concentrations and OH reactivity observations in New York City during PMTACS-NY2001, *Atmos. Environ.*, 37, 3627–3637, doi:10.1016/S1352-2310(03)00460-6, 2003.
- [107] Ren, X., Brune, W. H., Oliger, A., Metcalf, A. R., Simpas, J. B., Shirley, T., Schwab, J. J., Bai, C., Roychowdhury, U., Li, Y., Cai, C., Demerjian, K. L., He, Y., Zhou, X., Gao, H., and Hou, J.: OH, HO<sub>2</sub>, and OH reactivity during the PMTACS–NY Whiteface Mountain 2002 campaign: Observations and model comparison, *J. Geophys. Res.-Atmos.*, 111, D10S03, doi:10.1029/2005JD006126, 2006.
- [108] Richards, N. A. D., Arnold, S. R., Chipperfield, M. P., Miles, G., Rap, A., Siddans, R., Monks, S. A., and Hollaway, M. J.: The Mediterranean summertime ozone maximum: global emission sensitivities and radiative impacts, *Atmos. Chem. Phys.*, 13, 2331–2345, doi:10.5194/acp-13-2331-2013, 2013.
- [109] Rinne, H. J. I., Guenther, A. B., Greenberg, J. P., and Harley, P. C.: Isoprene and monoterpene fluxes measured above Amazonian rainforest and their dependence on light and temperature, *Atmos. Environ.*, 36, 2421–2426, doi:10.1016/S1352-2310(01)00523-4, 2002.

- [110] Rivera-Rios, J. C., Nguyen, T. B., Crouse, J. D., Jud, W., St. Clair, J. M., Mikoviny, T., Gilman, J. B., Lerner, B. M., Kaiser, J. B., de Gouw, J., Wisthaler, A., Hansel, A., Wennberg, P. O., Seinfeld, J. H., and Keutsch, F. N.: Conversion of hydroperoxides to carbonyls in field and laboratory instrumentation: Observational bias in diagnosing pristine versus anthropogenically controlled atmospheric chemistry, *Geophys. Res. Lett.*, 41, GL061919, doi:10.1002/2014GL061919, 2014.
- [111] Rolph, G.D. Real-time Environmental Applications and Display sYstem (READY) Website (<http://www.ready.noaa.gov>). NOAA Air Resources Laboratory, College Park, MD.
- [112] Roukos, J., Plaisance, H., Leonardis, T., Bates, M., and Locoge, N.: Development and validation of an automated monitoring system for oxygenated volatile organic compounds and nitrile compounds in ambient air, *J. Chroma. A*, 1216, 8642–8651, doi:10.1016/j.chroma.2009.10.018, 2009.
- [113] Sadanaga, Y., Yoshino, A., Watanabe, K., Yoshioka, A., Wakazono, Y., Kanaya, Y., and Kajii, Y.: Development of a measurement system of OH reactivity in the atmosphere by using a laser-induced pump and probe technique, *Rev. Sci. Instrum.*, 75, 2648–2655, doi:10.1063/1.1775311, 2004.
- [114] SAPRC-99 CHEMICAL MECHANISM AND UPDATED VOC REACTIVITY SCALES, <http://www.engr.ucr.edu/~carter/reactdat.htm>. Consulted on 14/09/2015.
- [115] SAPRC Atmospheric Chemical Mechanisms and VOC Reactivity Scales, <http://www.engr.ucr.edu/~carter/SAPRC/>. Consulted on 14/09/2015.
- [116] Schade, G. W. and Goldstein, A. H.: Fluxes of oxygenated volatile organic compounds from a ponderosa pine plantation, *J. Geophys. Res.-Atmos.*, 106, 3111–3123, doi:10.1029/2000JD900592, 2001.
- [117] Seco, R., Peñuelas, J., Filella, I., Llusia, J., Molowny-Horas, R., Schallhart, S., Metzger, A., Müller, M., and Hansel, A.: Contrasting winter and summer VOC mixing ratios at a forest site in the Western Mediterranean Basin: the effect of local biogenic emissions, *Atmos. Chem. Phys.*, 11, 13161–13179, doi:10.5194/acp-11-13161-2011, 2011.
- [118] Seco, R., Peñuelas, J., Filella, I., Llusia, J., Schallhart, S., Metzger, A., Müller, M., and Hansel, A.: Volatile organic compounds in the western Mediterranean basin: urban and rural winter measurements during the DAURE campaign, *Atmos. Chem. Phys.*, 13, 4291–4306, doi:10.5194/acp-13-4291-2013, 2013.



- [119] Seinfeld J. H. and Pandis S. N. (2006) *Atmospheric Chemistry and Physics: From Air Pollution to Climate Change*, 2nd edition, J. Wiley, New York.
- [120] Shirley, T. R., Brune, W. H., Ren, X., Mao, J., Leshner, R., Cardenas, B., Volkamer, R., Molina, L. T., Molina, M. J., Lamb, B., Velasco, E., Jobson, T., and Alexander, M.: Atmospheric oxidation in the Mexico City Metropolitan Area (MCMA) during April 2003, *Atmos. Chem. Phys.*, 6, 2753–2765, doi:10.5194/acp-6-2753-2006, 2006.
- [121] Simpson, D., et al. (1999), Inventorying emissions from nature in Europe, *J. Geophys. Res.*, 104(D7), 8113–8152, doi:10.1029/98JD02747.
- [122] Sindelarova, K., Granier, C., Bouarar, I., Guenther, A., Tilmes, S., Stavrakou, T., Müller, J.-F., Kuhn, U., Stefani, P., and Knorr, W.: Global data set of biogenic VOC emissions calculated by the MEGAN model over the last 30 years, *Atmos. Chem. Phys.*, 14, 9317–9341, doi:10.5194/acp-14-9317-2014, 2014.
- [123] Singh, H.B., and P.B. Zimmerman (1992) *Atmospheric distributions and sources of nonmethane hydrocarbons Gaseous Pollutants. Characterization and Cycling*, J. Wiley, New York.
- [124] Sinha, V., Williams, J., Crowley, J. N., and Lelieveld, J.: The Comparative Reactivity Method – a new tool to measure total OH Reactivity in ambient air, *Atmos. Chem. Phys.*, 8, 2213–2227, doi:10.5194/acp-8-2213-2008, 2008.
- [125] Sinha, V., Custer, T. G., Kluepfel, T., and Williams, J.: The effect of relative humidity on the detection of pyrrole by PTR-MS for OH reactivity measurements, *Int. J. Mass Spectrom.*, 282, 108–111, doi:10.1016/j.ijms.2009.02.019, 2009.
- [126] Sinha, V., Williams, J., Lelieveld, J., Ruuskanen, T. M., Kajos, M. K., Patokoski, J., Hellen, H., Hakola, H., Mogensen, D., Boy, M., Rinne, J., and Kulmala, M.: OH Reactivity Measurements within a Boreal Forest: Evidence for Unknown Reactive Emissions, *Environ. Sci. Technol.*, 44, 6614–6620, doi:10.1021/es101780b, 2010.
- [127] Sinha, V., Williams, J., Diesch, J. M., Drewnick, F., Martinez, M., Harder, H., Regelin, E., Kubistin, D., Bozem, H., Hosaynali-Beygi, Z., Fischer, H., Andrés-Hernández, M. D., Kartal, D., Adame, J. A., and Lelieveld, J.: Constraints on instantaneous ozone production rates and regimes during DOMINO derived using in-situ OH reactivity measurements, *Atmos. Chem. Phys.*, 12, 7269–7283, doi:10.5194/acp-12-7269-2012, 2012.
- [128] Steiner, A. H. and Goldstein, A. L.: Biogenic VOCs, in *Volatile Organic Compounds in the Atmosphere*, edited by R. Koppmann, 82–128, Blackwell Publishing Ltd., 2007.

- [129] Szopa S., Aumont B., Madronich S.: Assessment of the reduction methods used to develop chemical schemes: building of a new chemical scheme for VOC oxidation suited to three dimensional multiscale HO<sub>x</sub>-NO<sub>x</sub>-VOC chemistry simulations, *Atmos. Chem. Phys.*, 5, 2519–2538, 2005.
- [130] Taraborrelli, D., Lawrence, M. G., Butler, T. M., Sander, R., and Lelieveld, J.: Mainz Isoprene Mechanism 2 (MIM2): an isoprene oxidation mechanism for regional and global atmospheric modelling, *Atmos. Chem. Phys.*, 9, 2751-2777, doi:10.5194/acp-9-2751-2009, 2009.
- [131] Tsigaridis, K. and Kanakidou, M.: Importance of volatile organic compounds photochemistry over a forested area in central Greece, *Atmos. Environ.*, 36, 3137–3146, doi:10.1016/S1352-2310(02)00234-0, 2002.
- [132] Wallington, T. J.: Kinetics of the gas phase reaction of OH radicals with pyrrole and thiophene, *Int. J. Chem. Kinet.*, 18(4), 487–496, doi:10.1002/kin.550180407, 1986.
- [133] Warneke, C., Holzinger, R., Hansel, A., Jordan, A., Lindinger, W., Pöschl, U., Williams, J., Hoor, P., Fischer, H., Crutzen, P. J., Scheeren, H. A., and Lelieveld, J.: Isoprene and Its Oxidation Products Methyl Vinyl Ketone, Methacrolein, and Isoprene Related Peroxides Measured Online over the Tropical Rain Forest of Surinam in March 1998, *J. Atmos. Chem.*, 38, 167–185, doi:10.1023/A:1006326802432, 2001.
- [134] Weinstock B., (1969), Carbon Monoxide: Residence Time in the Atmosphere , Science New Series, Vol. 166, No. 3902, pp. 224-225
- [135] Wesely, M. L.: Parameterization of surface resistances to gaseous dry deposition in regional-scale numerical models, *Atmos. Environ.*, 23, 1293–1304, 1989.
- [136] Whalley, L., Stone, D., and Heard, D.: New insights into the tropospheric oxidation of isoprene: combining field measurements, laboratory studies, chemical modelling and quantum theory, *Top. Curr. Chem.*, 339, 55–95, doi:10.1007/128\_2012\_359, 2014.
- [137] Wiedinmyer, C., Guenther, A. B., Harley, P., Hewitt, N., Geron, C., Artaxo, P., Steinbrecher, R., and Rasmussen, R. M.: Global organic emissions from vegetation. Emissions of Atmospheric Trace Compounds (Advances in Global Change Research), edited by: Granier, C., Artaxo, P., and Reeves, C., Kluwer Academic Publishers, 115–170, 2004.
- [138] Williams, J., Holzinger, R., Gros, V., Xu, X., Atlas, E., and Wallace, D. W. R.: Measurements of organic species in air and seawater from the tropical Atlantic, *Geophys. Res. Lett.*, 31, L23S06, doi:10.1029/2004GL020012, 2004.

- [139] Yáñez-Serrano, A. M., Nölscher, A. C., Williams, J., Wolff, S., Alves, E., Martins, G. A., Bourtsoukidis, E., Brito, J., Jardine, K., Artaxo, P., and Kesselmeier, J.: Diel and seasonal changes of biogenic volatile organic compounds within and above an Amazonian rainforest, *Atmos. Chem. Phys.*, 15, 3359–3378, doi:10.5194/acp-15-3359-2015, 2015.
- [140] Yoshino, A., Sadanaga, Y., Watanabe, K., Kato, S., Miyakawa, Y., Matsumoto, J., and Kajii, Y.: Measurement of total OH reactivity by laser-induced pump and probe technique—comprehensive observations in the urban atmosphere of Tokyo, *Atmos. Environ.*, 40, 7869–7881, doi:10.1016/j.atmosenv.2006.07.023, 2006.
- [141] Zannoni, N., Dusanter, S., Gros, V., Sarda Esteve, R., Michoud, V., Sinha, V., Locoge, N., and Bonsang, B.: Intercomparison of two Comparative Reactivity Method instruments in the Mediterranean basin during summer 2013, *Atmos. Meas. Tech. Discuss.*, 8, 5065–5104, doi:10.5194/amtd-8-5065-2015, 2015.
- [142] Zannoni, N., Gros, V., Lanza, M., Sarda, R., Bonsang, B., Kalogridis, C., Preunkert, S., Legrand, M., Jambert, C., Boissard, C., and Lathiere, J.: OH reactivity and concentrations of Biogenic Volatile Organic Compounds in a Mediterranean forest of downy oak trees, *Atmos. Chem. Phys. Discuss.*, 15, 22047–22095, doi:10.5194/acpd-15-22047-2015, 2015.



# Acknowledgements

This thesis is the result of the help and support of many people that I would like to acknowledge here.

First of all, I would like to thank my supervisors, Valerie Gros and Bernard Bonsang for choosing me for this PhD position . I received many opportunities as a PIMM, enjoyed a lot studying the OH reactivity and doing field measurements. Especially when we went to Corsica and I could see every morning my coast on the other side of our van. You constantly supervised my work and improved its quality with advices and suggestions during these years. I am thankful also to Roland Sarda for spending a lot of time in the lab with me during my first year and Francois Truong for his help now.

I would like to thank Sebastien Dusanter for teaching me a lot on the field as well as during our meetings, emails and calls, about the reactivity and helping for improving the quality of the article on the intercomparison. I would like to thank Vincent Michoud for his help on everything, but especially for answering always so quick to my emails and his data and the calculations and the reactivity...too many things...!Thanks! I thank Christophe Boissard for letting me use his branch enclosure and Sophie Szopa for working on the modeling part of the data from Corsica. Thanks to Nicolas Bonnaire for his help in the analysis of the cartridges from OHP and the filters from Juelich. I am thankful also to Francois Dulac, Eric Hamanou and Juliette Lathiere for organizing the projects Charmex and Canopee.

I am thankful to Vinayak Sinha, Chimnoy and Vinod for teaching me about the CRM and being very nice hosts in India. I would like to thank Lukas Maerk, Philipp Sulzer and Simone Jurschik for letting me use their instruments at Ionicon. I thank Astrid Kiendler-Scharr and Ralf Tilmann for letting me participate to the Pimms campaign at Saphir.

I am thankful to Chris Mayhew and Nigel Mason for giving shape to the PIMMS network and working so hard to organize every meeting and write every report and make every course extremely useful. I am also thankful to all the PIMMS supervisors to select the

right students and gather together an incredible group of PhD students. Of course, I am extremely thankful to all the PIMMS, for all the funny times and immeasurable support in our hard PIMMS times. We should all find a nursing home in the valley of Innsbruck for spending our old age, finishing all the networking undone and sharing our leftovers of knowledge about PTR-MS.

I would like to thank also my Master's studies supervisor and professors of atmospheric chemistry at the University of Copenhagen, Merete Bilde, Ole John Nielsen and Matthew Johnson for letting me love this discipline and convincing me in doing a PhD.

I am grateful to my best colleague and friend Cherry, for the wonderful times spent together in conferences and campaigns, our fruitful conversations on sciences and politics in the worst piano bars of Paris, and the wild dances in the even worse bars of Paris. I am thankful also to my other colleagues at LSCE for welcoming here especially the first times, and the nice times in Corsica: Vincent, Alexia, A.C., Jose, Jean Eudes and Jason.

A big thanks goes to all my other colleagues, somewhere at LSCE, somewhere in CEA, an unspecified number of loud people ...mates of adventures in all this crazy up and down in trains buses and metros to reach the *last columns of Hercules* of Saclay every day from Paris despite all strikes, trains victims and many many many...too many, suspicious bags. I thank Johannes, a lot! For all the nice breaks at work and after work and for creating a monster of latex in only 3 days. Thank you for all your work, and sharing with me the nightmares of all these  $s^{-1}$  and of writing a second PhD thesis. Thanks to Jonathan for his comfortable bed and nice apartment! Thanks to all my friends of tous chez Norà, Danilo, Marco, Valox, Kobra, David, Fox, Alienor, Angiu, Mathy, Scianna, for being great friends and making me happy every day like if it was my birthday! Of course, a special, huuuge thanks goes to la Pedersen! I still wonder how would have been these 3 years here if I had not met you on that rainy night! I am sorry but this looks like destiny.

I would like to thank all my friends dispersed all over the world, starting from that wild woman living in the jungle, together from Scandinavia to the tropics, la Skia, all my friends of Erasmus, of Copenhagen, my ex flatmates, Pitt and Todsén, my ex colleagues from CCAR.

A big thanks to all my friends at home for still supporting me and hoping that I will come back throughout all these years, Babsi, Frenki, Zappi, Wex, la kane, piccionz e piccionz, lortite e tanti altri.

Finally, the greatest of all thanks is for my family for always supporting my choices and encouraging me all the times.

# Curriculum Vitae

Nora Zannoni

born on 22 August 1985 in Prato, Italy

## *Education:*

- 2012 - 2015 PhD student in atmospheric chemistry,  
at Laboratoire Scientifique du Climat et de l'Environnement (LSCE- CNRS)  
and University Paris sud  
Marie Curie Early Stage Researcher in  
*Proton Ionization Molecular Mass Spectrometry*
- 2009 - 2011 Master degree in Chemistry, University of Copenhagen, Denmark  
Thesis: *A volatility study on organic compounds in atmospheric aerosols* (12/12)
- 2004 - 2009 Bachelor degree in Chemistry, University of Florence, Italy  
Thesis: *Spectroscopic study of sigillate ceramic* (101/110).

## *Work experience:*

- 2011 - 2012 Research assistant,  
Copenhagen Centre for Atmospheric Research, University of Copenhagen, Denmark
- 2010 - 2011 Laboratory technician assistant,  
Centre for Ice and Climate, University of Copenhagen, Denmark

## *Field campaigns:*

- summer 2015 PISA (PImms-SAphir), Saphir atmospheric simulation chamber, Germany  
spring 2014 CANOPEE 2014, Observatoire de Haute Provence, France  
summer 2013 ChArMEx, Corsica, France

## *Languages:*

- Italian (native), English (excellent), Spanish (excellent)  
French (medium), German (basics), Danish (basics)

## *Publications:*

- Zannoni, N., Dusanter, S., Gros, V., Sarda Esteve, R., Michoud, V., Sinha, V., Locoge, N., and Bonsang, B.: Intercomparison of two comparative reactivity method instruments in the Mediterranean basin during summer 2013, *Atmos. Meas. Tech.*, **8**, 3851-3865, doi:10.5194/amt-8-3851-2015, 2015.
- Zannoni, N., Gros, V., Lanza, M., Sarda, R., Bonsang, B., Kalogridis, C., Preunkert, S., Legrand, M., Jambert, C., Boissard, C., and Lathiere, J.: OH reactivity and concentrations of Biogenic Volatile Organic Compounds in a Mediterranean forest of downy oak trees, *Atmos. Chem. Phys. Discuss.*, **15**, 22047-22095, doi:10.5194/acpd-15-22047-2015, 2015.



**Titre :** OH reactivity measurements in the Mediterranean region

**Mots clés :** Volatile organic compounds, Comparative reactivity method, mass spectrometry

**Résumé :** La réactivité totale OH est la perte totale du radical hydroxyle (le principal oxydant de l'atmosphère) avec les gaz réactifs dans l'air ambiant. Elle représente la mesure de la quantité totale des réactifs dans un environnement donné. Nous présentons ici un travail expérimental se concentrant sur les améliorations techniques d'une méthode appelée "Comparative Reactivity Method" pour mesurer la réactivité OH sur le terrain ainsi que sur des résultats obtenus sur deux sites ciblés dans le bassin méditerranéen. La réactivité OH mesurée était élevée dans les deux sites. Sur le site récepteur en Corse (France) au cours de l'été 2013, nous avons observé que la réactivité OH était en moyenne de 5,5 s<sup>-1</sup> (avec un maximum de 17 s<sup>-1</sup>). Ces mesures ont été comparées avec les observations de composés en phase gazeuse réalisées pendant la campagne. Il a été noté que pendant une période de la campagne, seulement 50% de la réactivité était expliqué par les mesures complémentaires.

Lors de mesures dans une forêt de chênes pubescents, émetteurs isoprène, dans le sud de la France, nous avons observé que la réactivité OH maximale était très élevée (69 s<sup>-1</sup>), en accord avec la réactivité calculée à partir des mesures des gaz réactifs. Ce travail de thèse met en évidence que: (i) le bassin méditerranéen est un fort émetteur de gaz réactifs, (ii) la réactivité mesurée dans ces deux sites de la Méditerranée a été fortement impactée par les émissions biogéniques, (iii) il reste encore beaucoup de composés inconnus associés aux émissions biogéniques primaires et secondaires. A l'avenir, plusieurs approches pourraient être utilisées pour identifier ces composés inconnus: en couplant la mesure de la réactivité OH avec des mesures de plantes dans des enceintes fermées (composés primaires), études en chambre de vieillissement (composés primaires et secondaires), ainsi que des approches de modélisation.

**Title :** OH reactivity measurements in the Mediterranean region

**Keywords :** Volatile organic compounds, Comparative reactivity method, mass spectrometry

**Summary:**

The total OH reactivity is the total loss frequency of the hydroxyl radical due to reactive gases in ambient air. It represents a top down measure of the total loading of reactants in a given environment. Here we present an experimental work focusing on the technical improvements of the Comparative Reactivity Method to measure the OH reactivity on the field and field measurements of OH reactivity at two targeted sites in the Mediterranean basin. The measured OH reactivity was high at both sites. At a receptor site in Corsica (France) during summer 2013, we observed that the OH reactivity was maximum 17 s<sup>-1</sup>, on average 5.5 s<sup>-1</sup> and during one week only 50% was explained by the complementary measurements in the gas phase. At a forest of downy oak trees, high isoprene emitters, in the south of France, we observed that the OH reactivity was maximum 69 s<sup>-1</sup>, in agreement with the

reactivity calculated from the measurements of reactive gases only during daytime.

This thesis work highlights that: (i) the Mediterranean basin is a strong emitter of reactive gases, (ii) the reactivity measured in these two sites in the Mediterranean was strongly impacted by biogenic emissions, (iii) there are still many unknowns associated to measures of biogenic volatiles primary emitted and secondary produced. Such unknowns might be reduced in the future by coupling the measurement of the OH reactivity with plants enclosures and chambers studies as well as experiments with models.

